The strange quantum physics of the high temperature superconductors

University of Maryland
September 29, 2020
Subir Sachdev

PHYSICS
HARVARD

Talk online: sachdev.physics.harvard.edu

High temperature superconductors

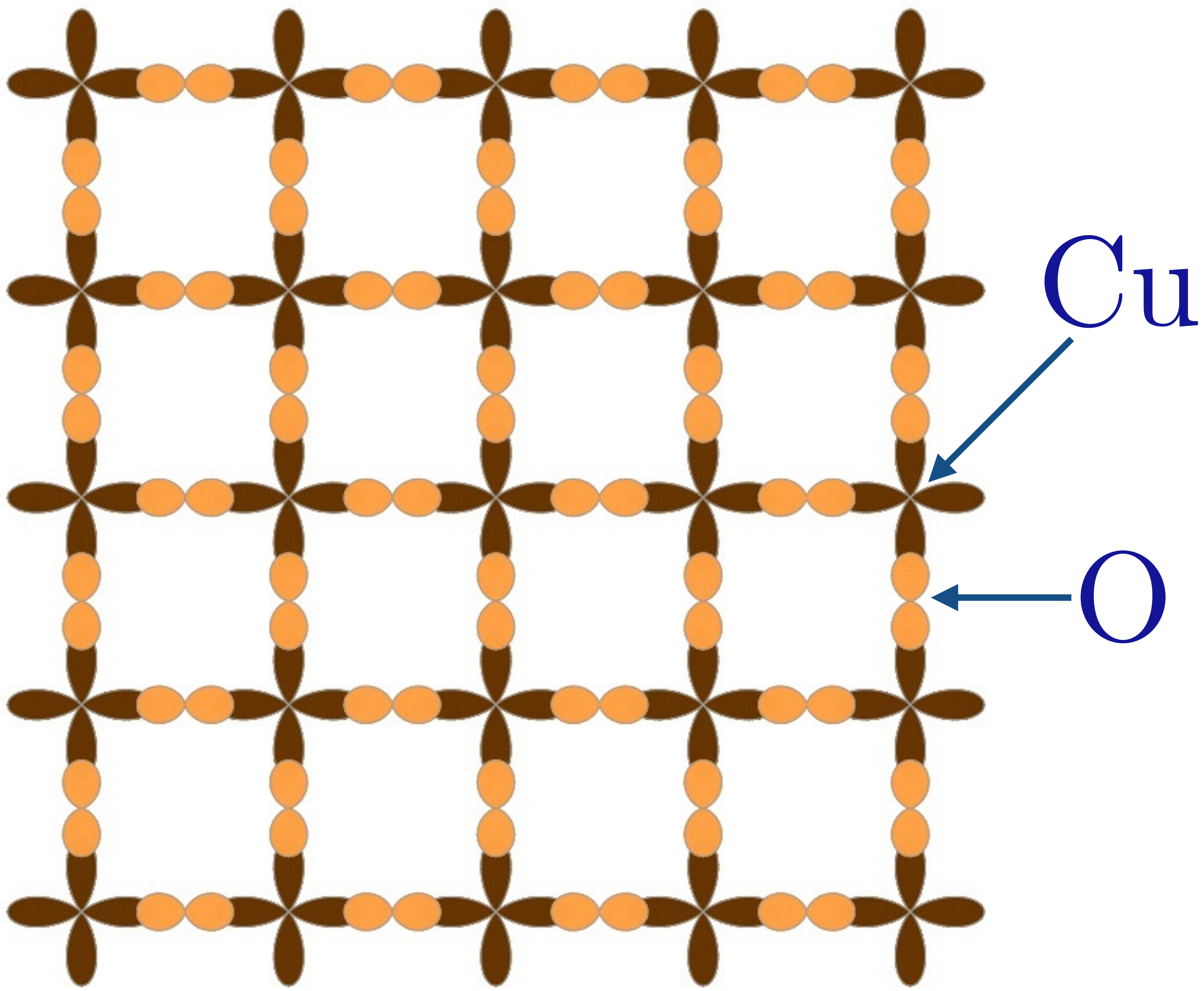

CuO_2 plane

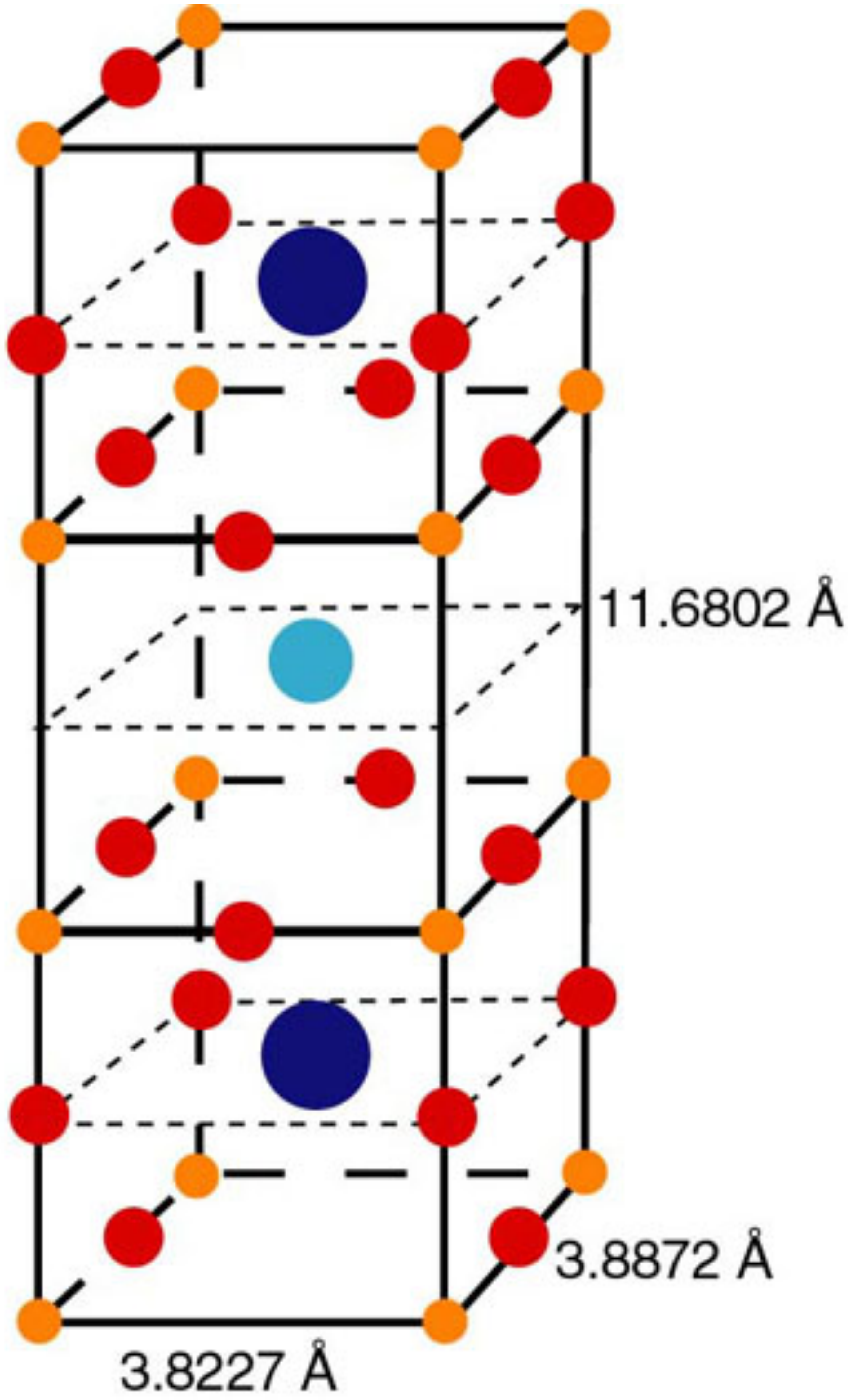

$YBa_2Cu_3O_{6+x}$

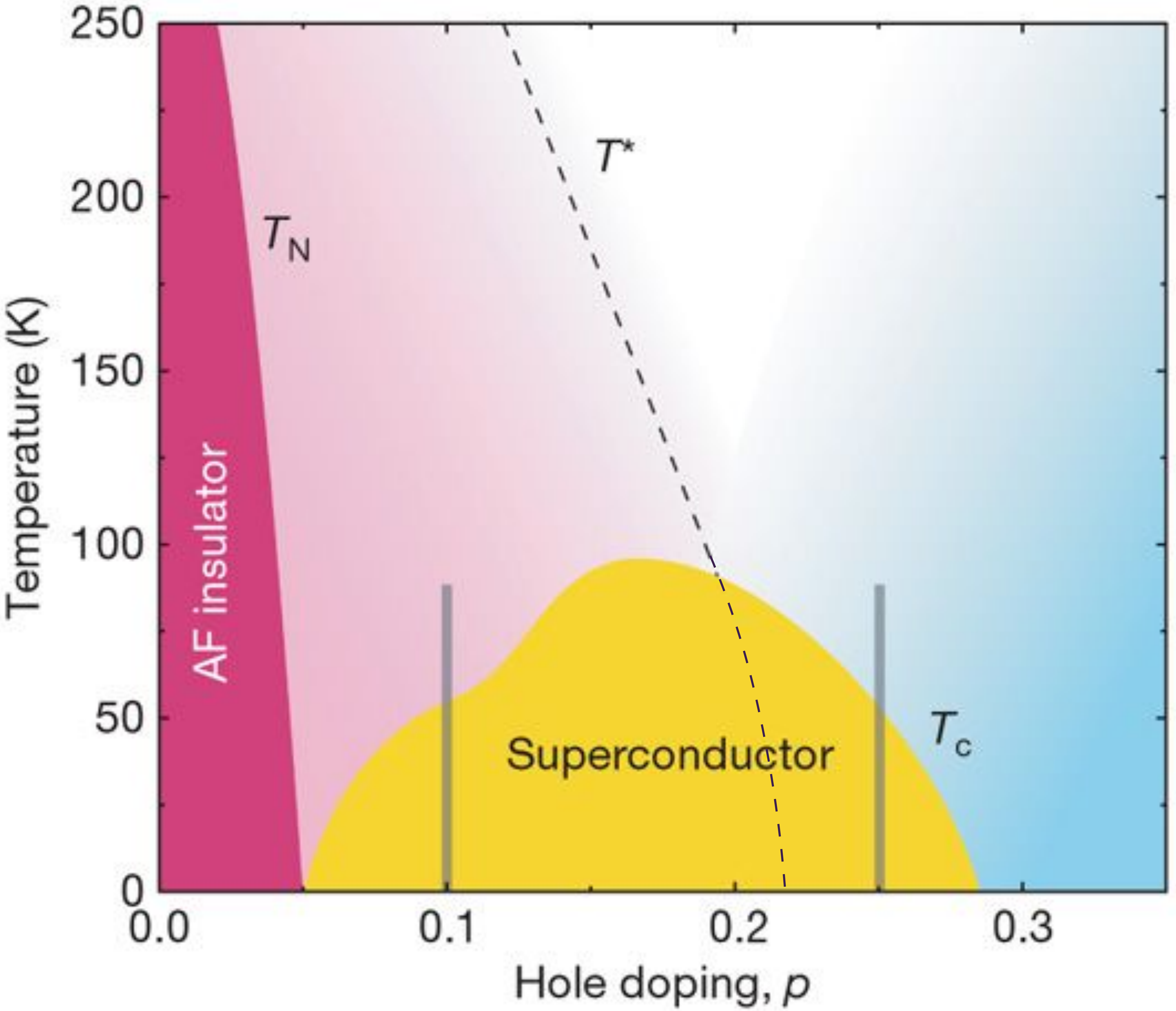
250
200
150
100
50
0
0.0
0.1
0.2
0.3
Temperature (K)
Hole doping, p
AF insulator
T_N
T*
T_c
Superconductor

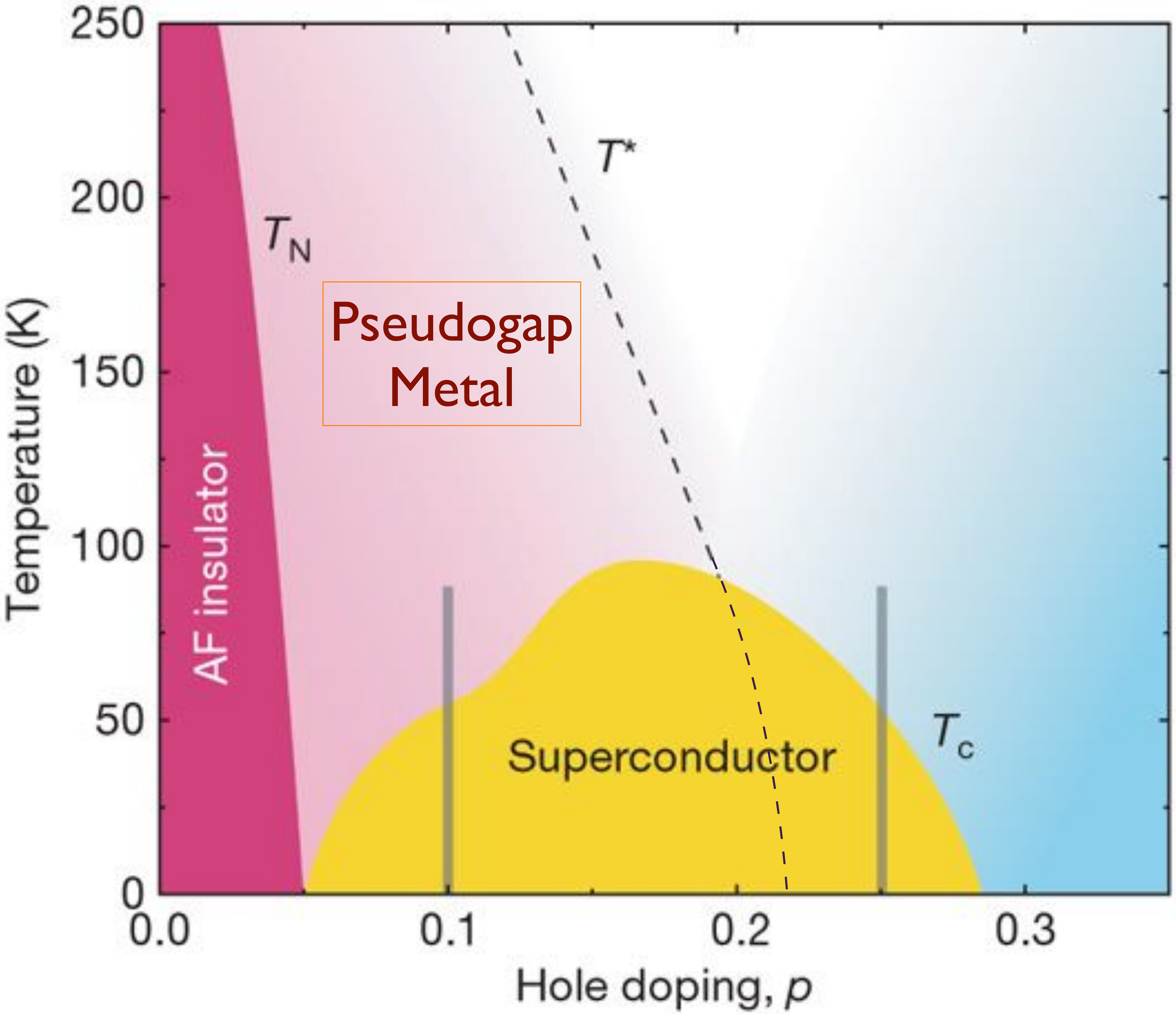

Pseudogap
Metal
AF insulator
T_N
T^*
T_c
Superconductor
Temperature (K)
Hole doping, p
250
200
150
100
50
0
0.0
0.1
0.2
0.3

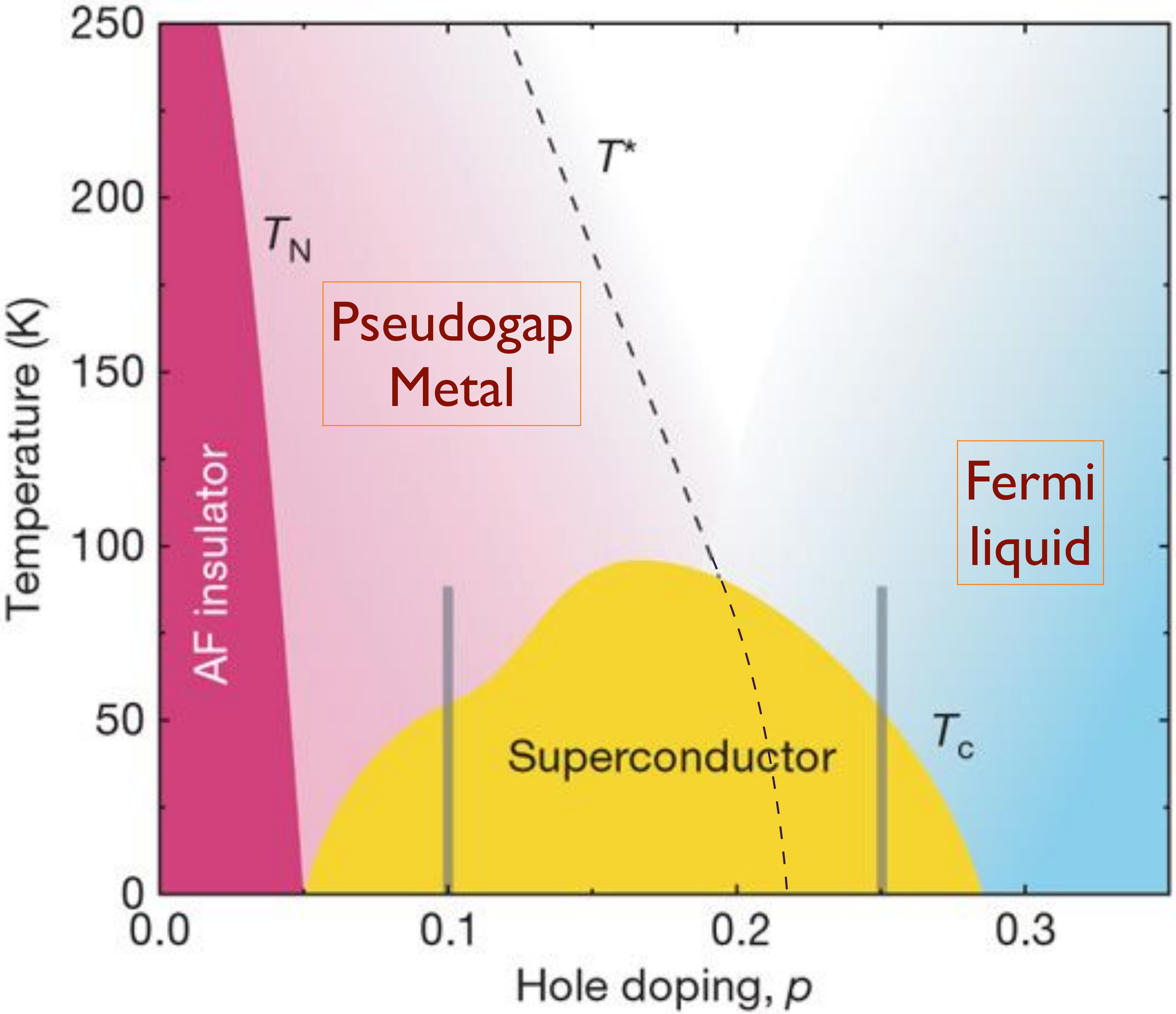

250
200
150
100
50
0
0.0
0.1
0.2
0.3
Temperature (K)
Hole doping, p
AF insulator
T_N
T*
Pseudogap Metal
Fermi liquid
Superconductor
T_c

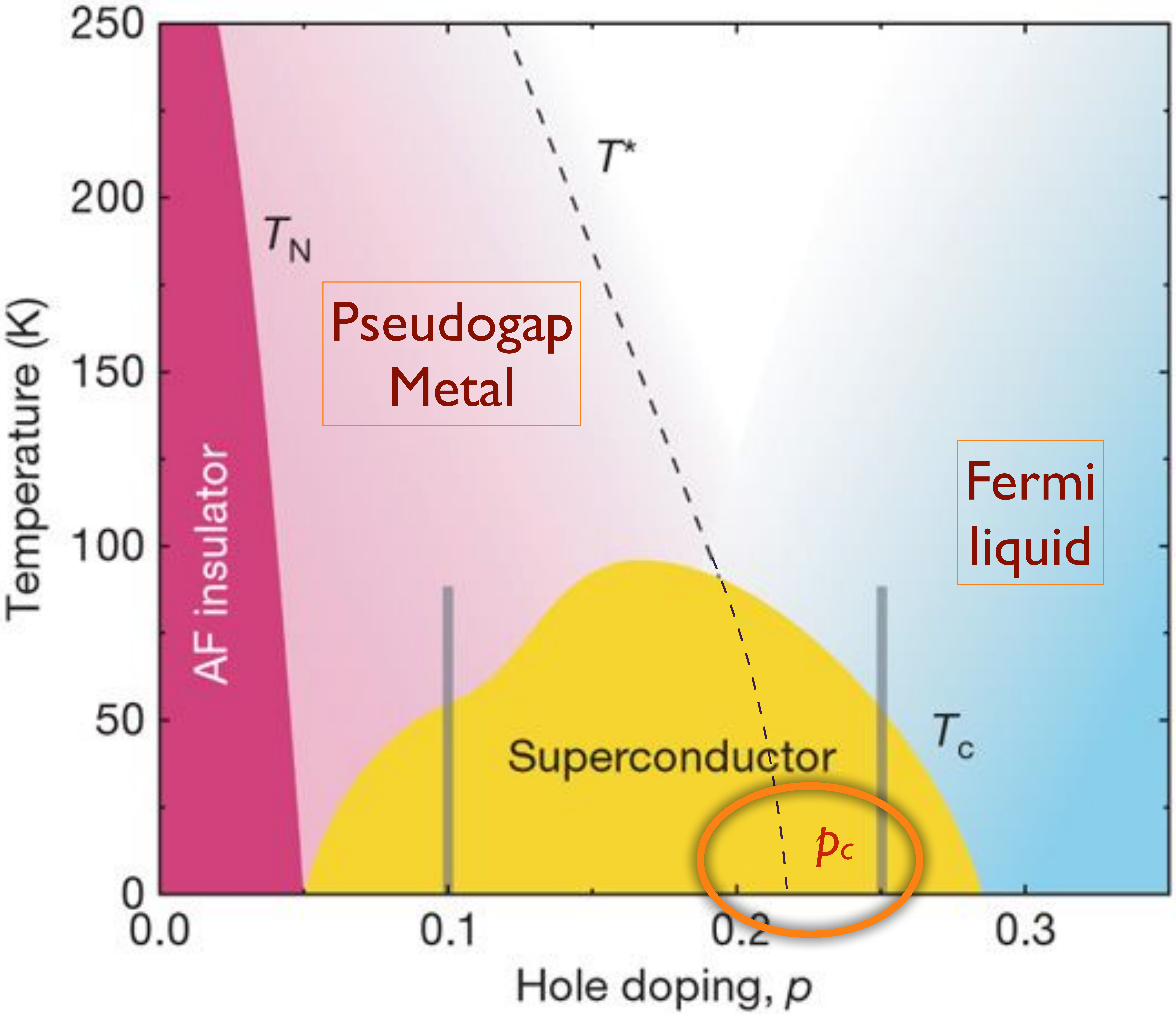

250
200
150
100
50
0
0.0
0.1
0.2
0.3
Temperature (K)
Hole doping, p
AF insulator
T_N
Pseudogap
Metal
T*
Fermi
liquid
Superconductor
T_c
p_c

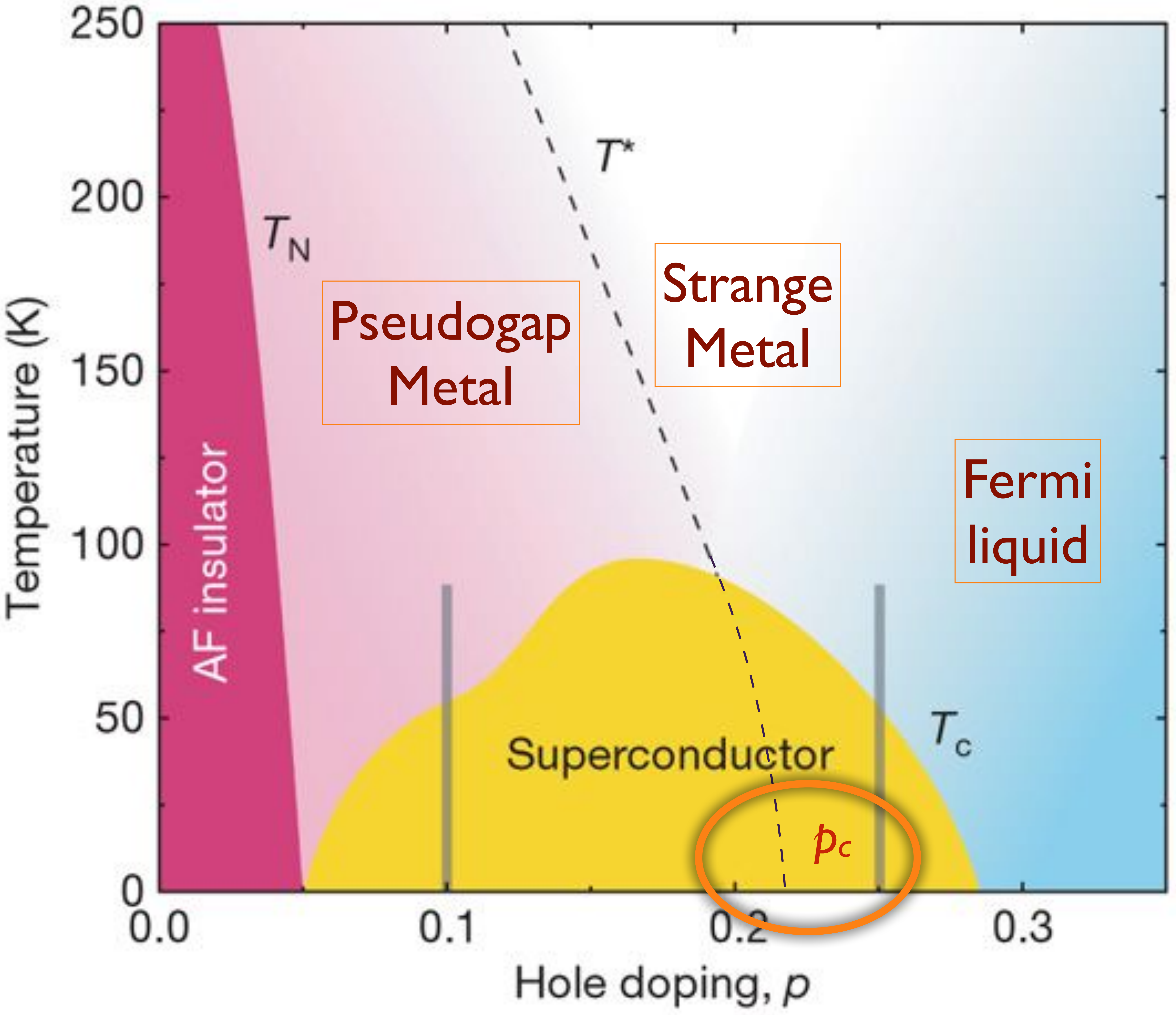

250
200
150
100
50
0
0.0
0.1
0.2
0.3
Temperature (K)
Hole doping, p
AF insulator
T_N
Pseudogap Metal
T*
Strange Metal
Fermi liquid
Superconductor
T_c
p_c

Insulating antiferromagnet

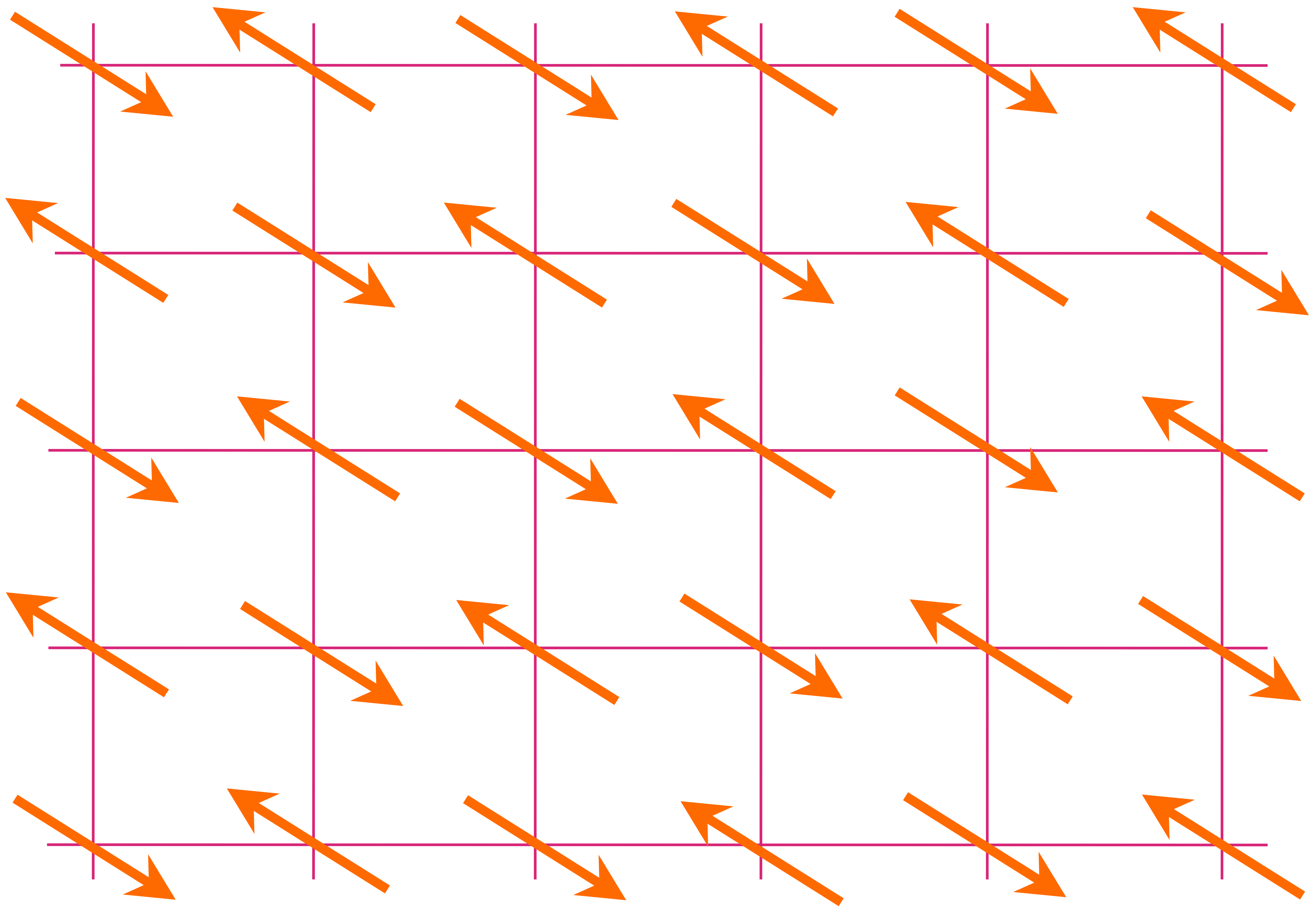

Insulating antiferromagnet

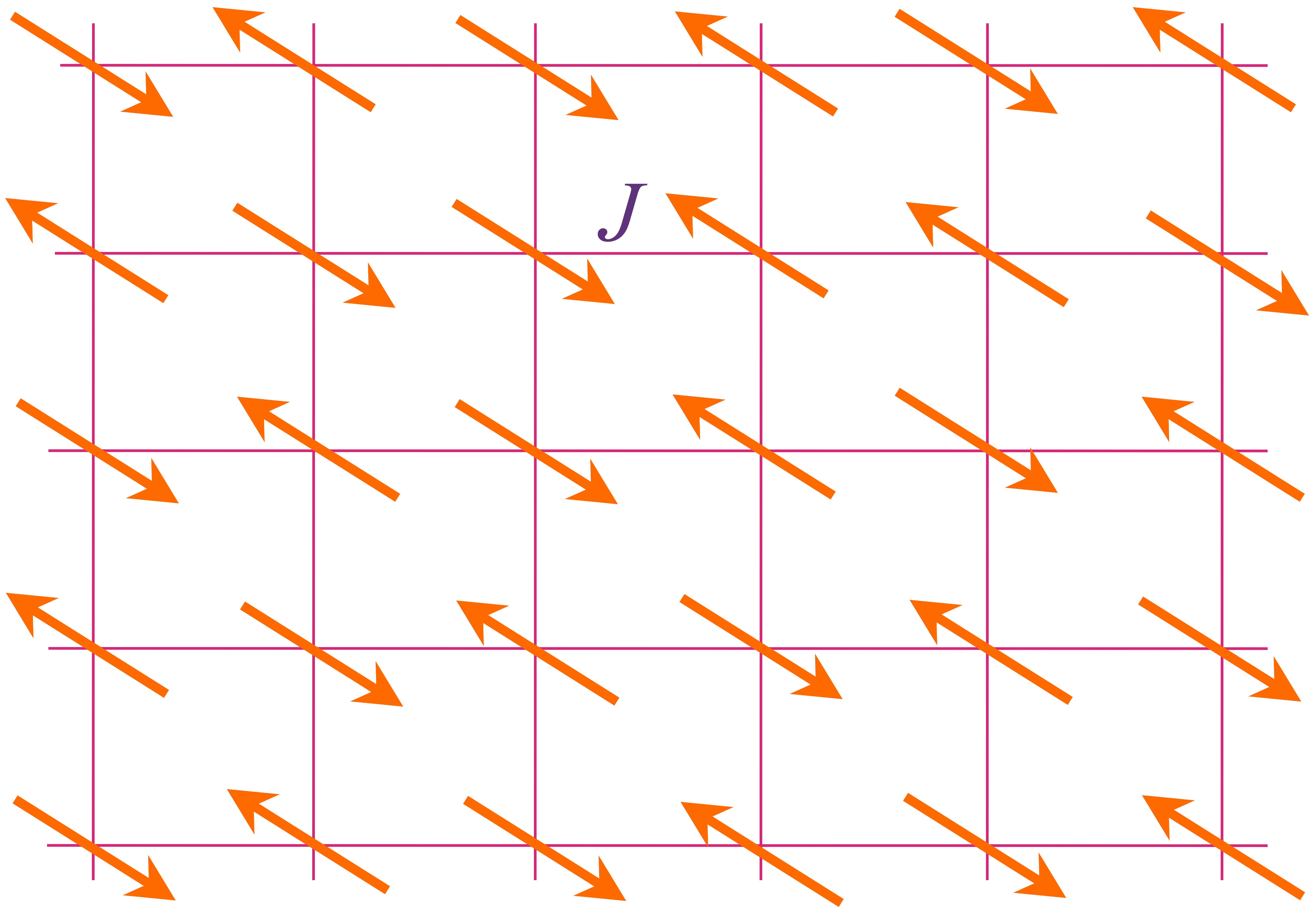

Insulating antiferromagnet

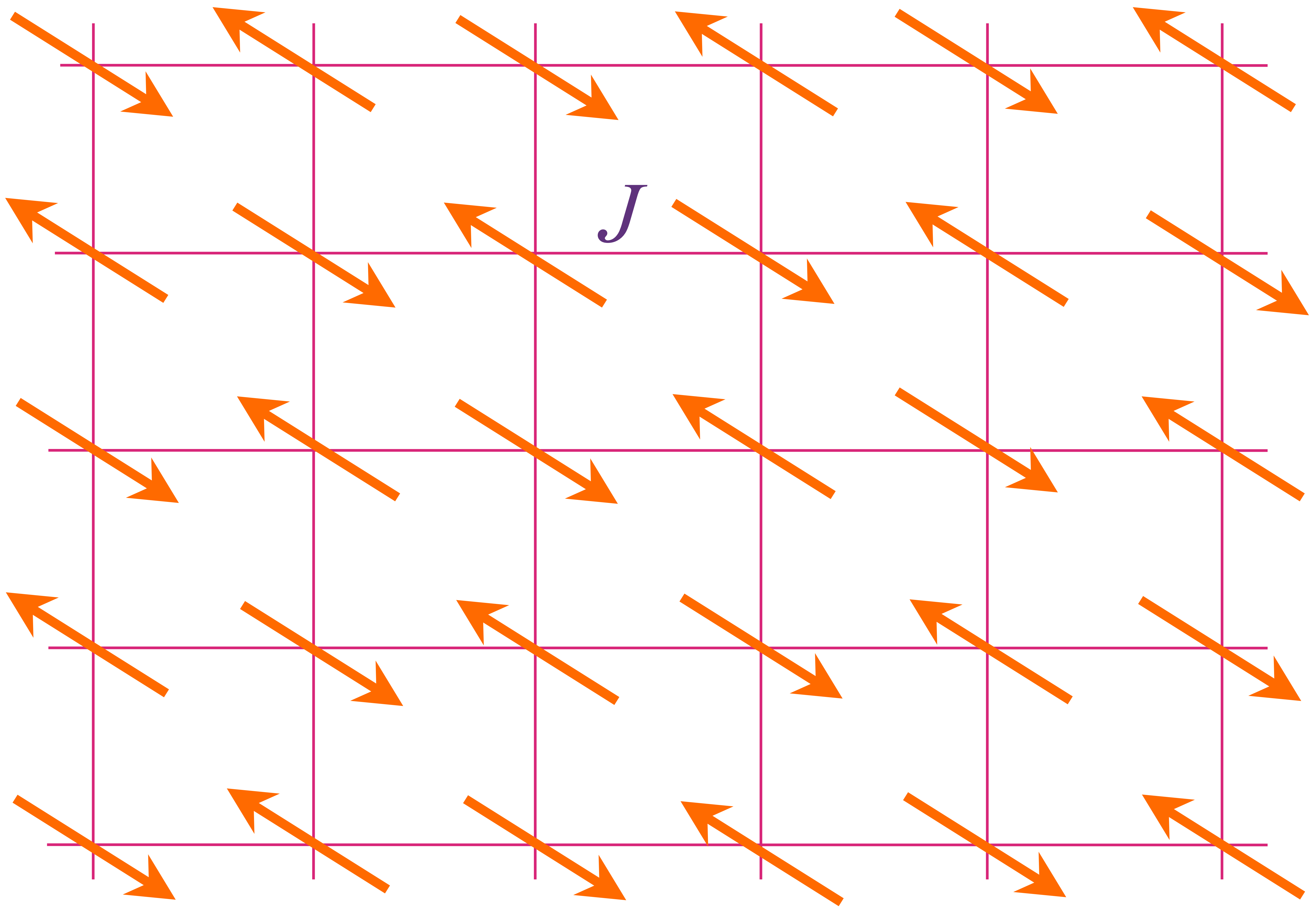

Antiferromagnet doped with hole density p

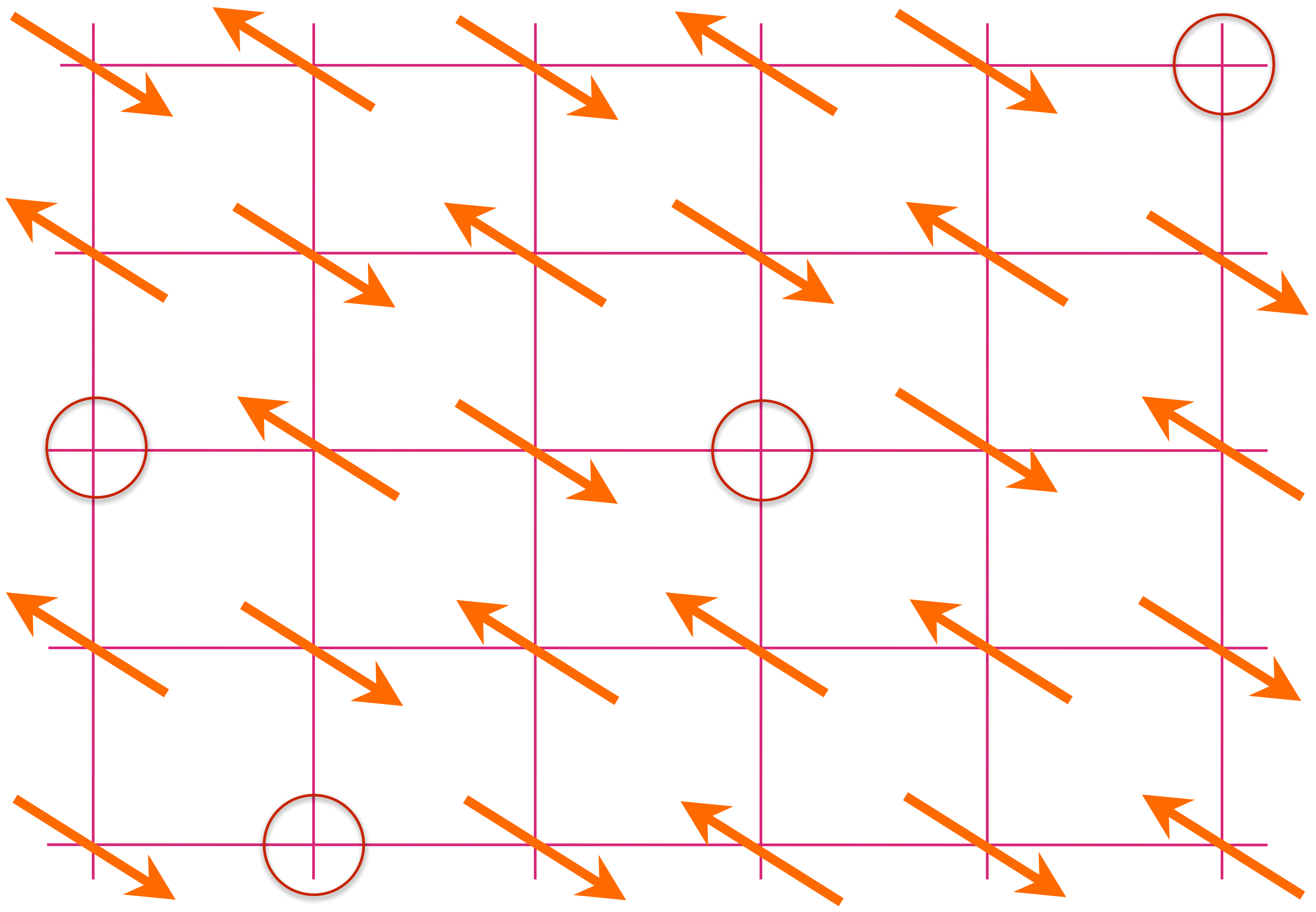

Antiferromagnet doped with hole density p

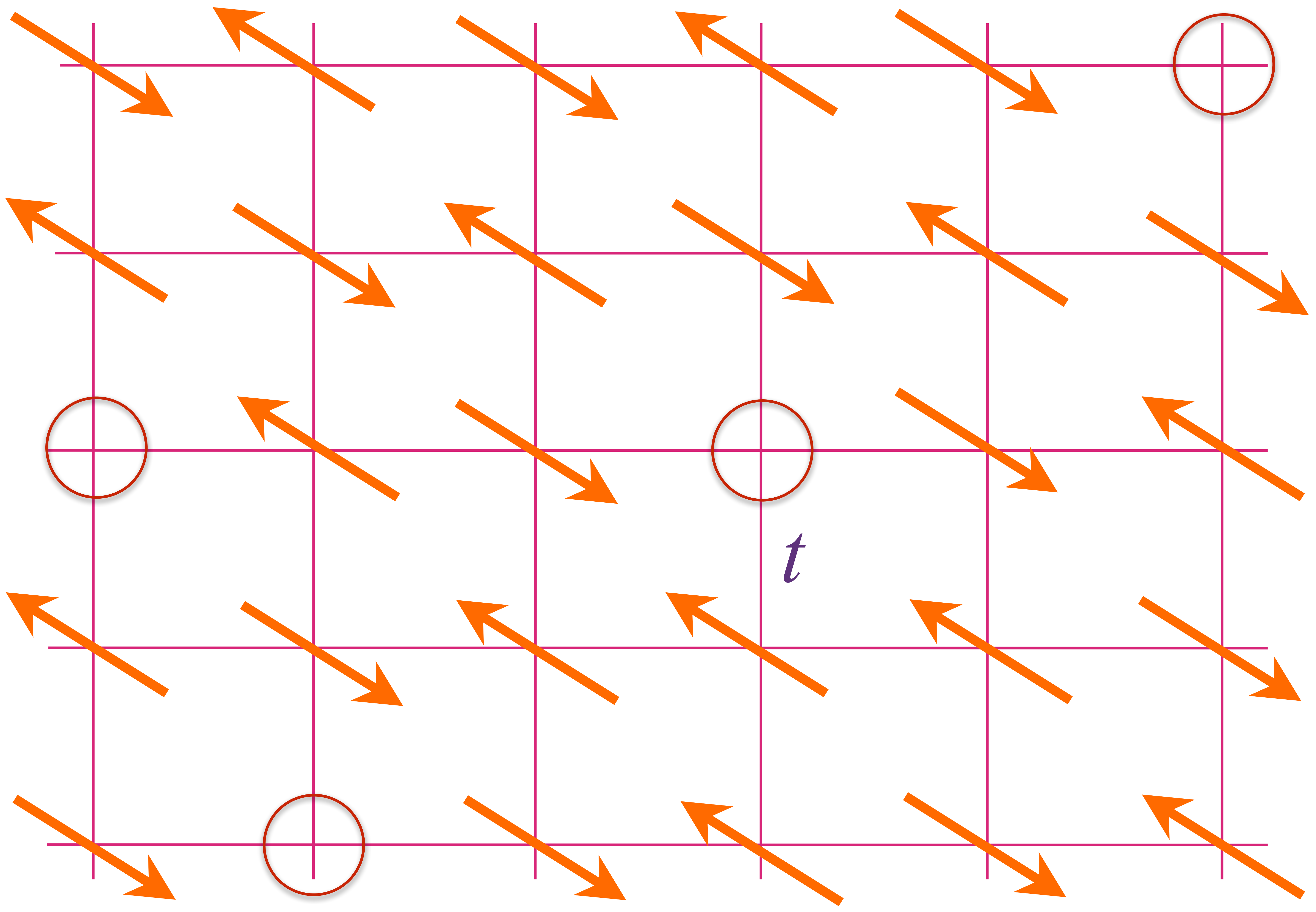

Antiferromagnet doped with hole density p

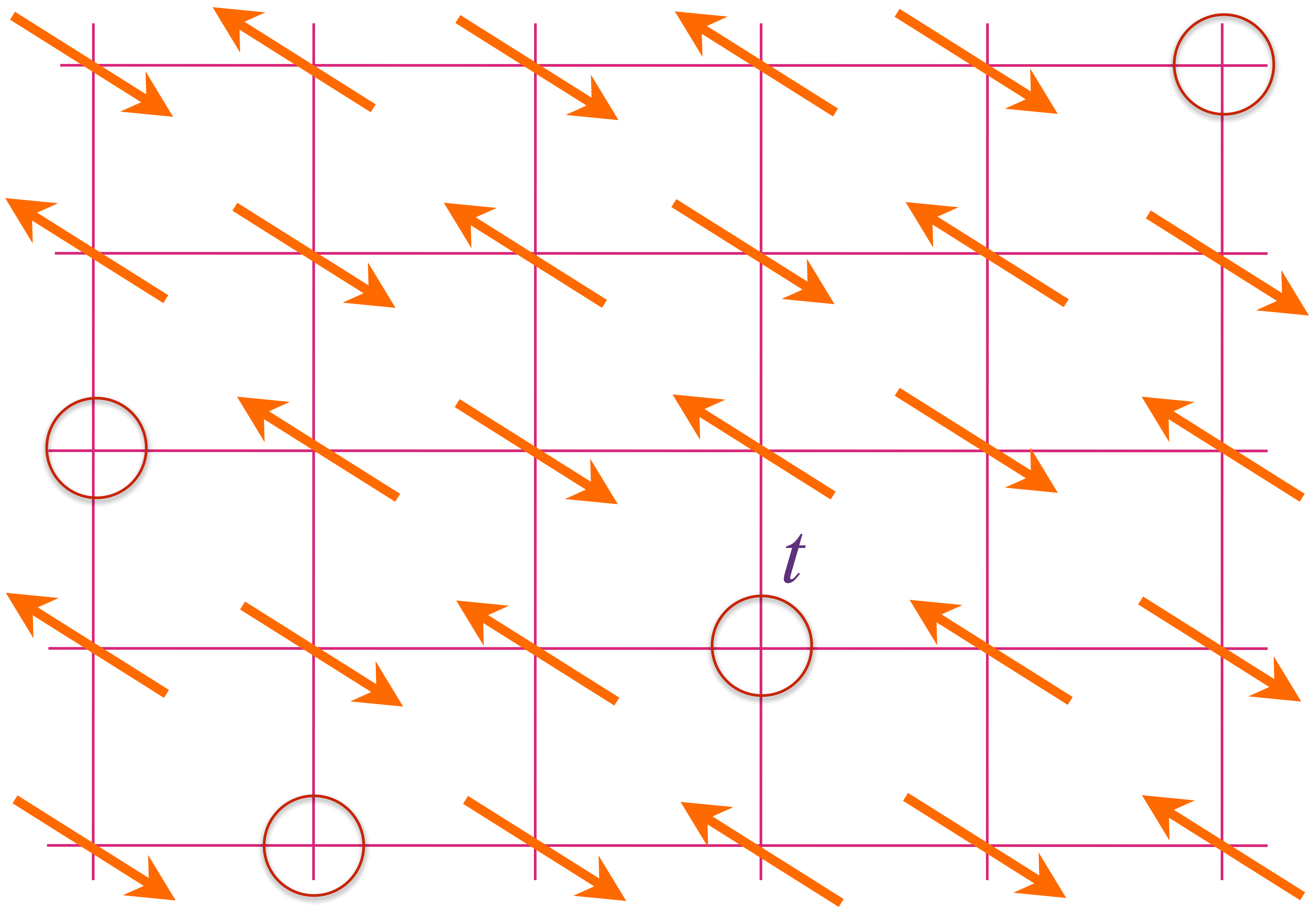

Real-space view at small p

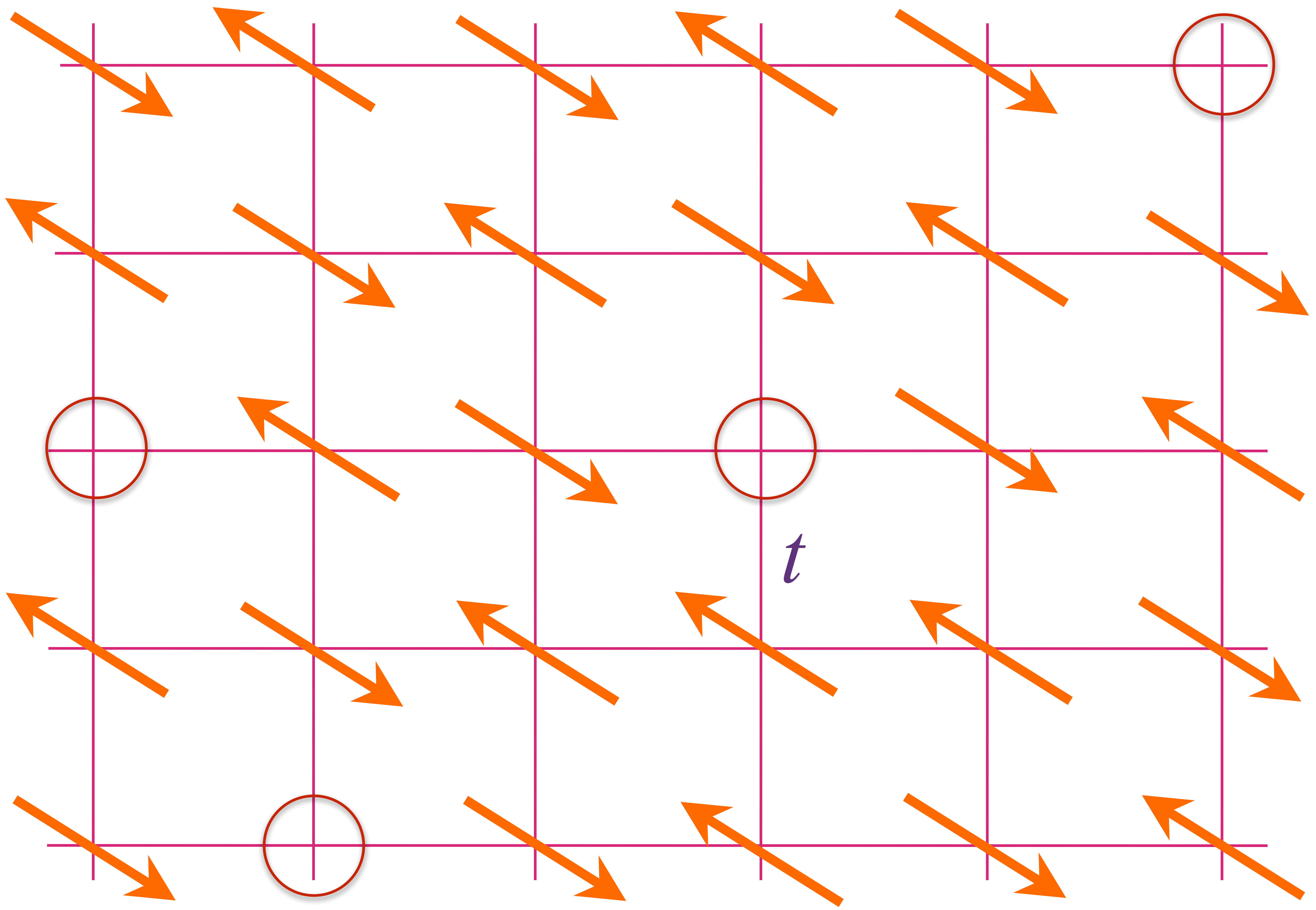

p mobile holes in a background of fluctuating spins

Real-space view at small p

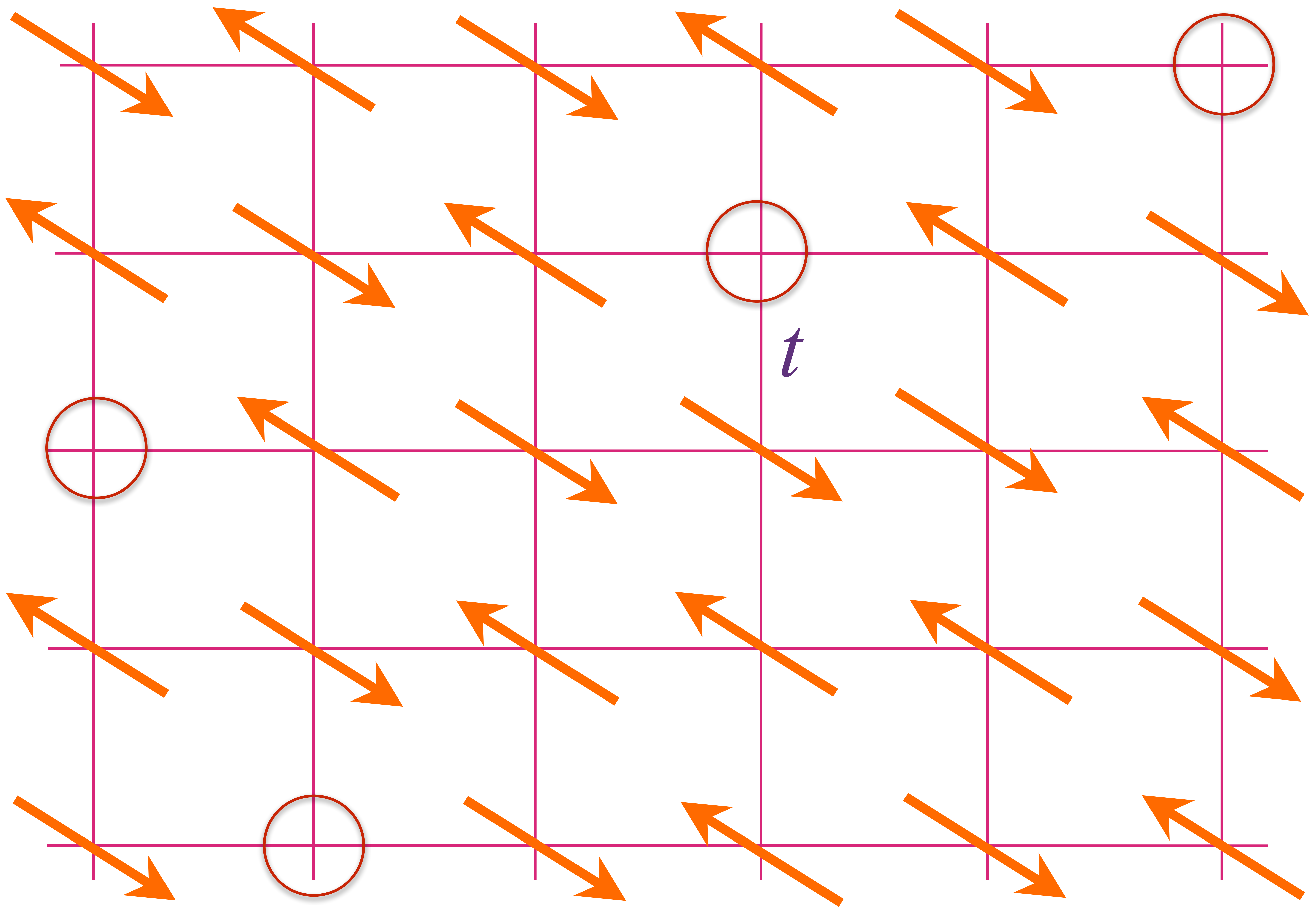

p mobile holes in a background of fluctuating spins

Real-space view at small p

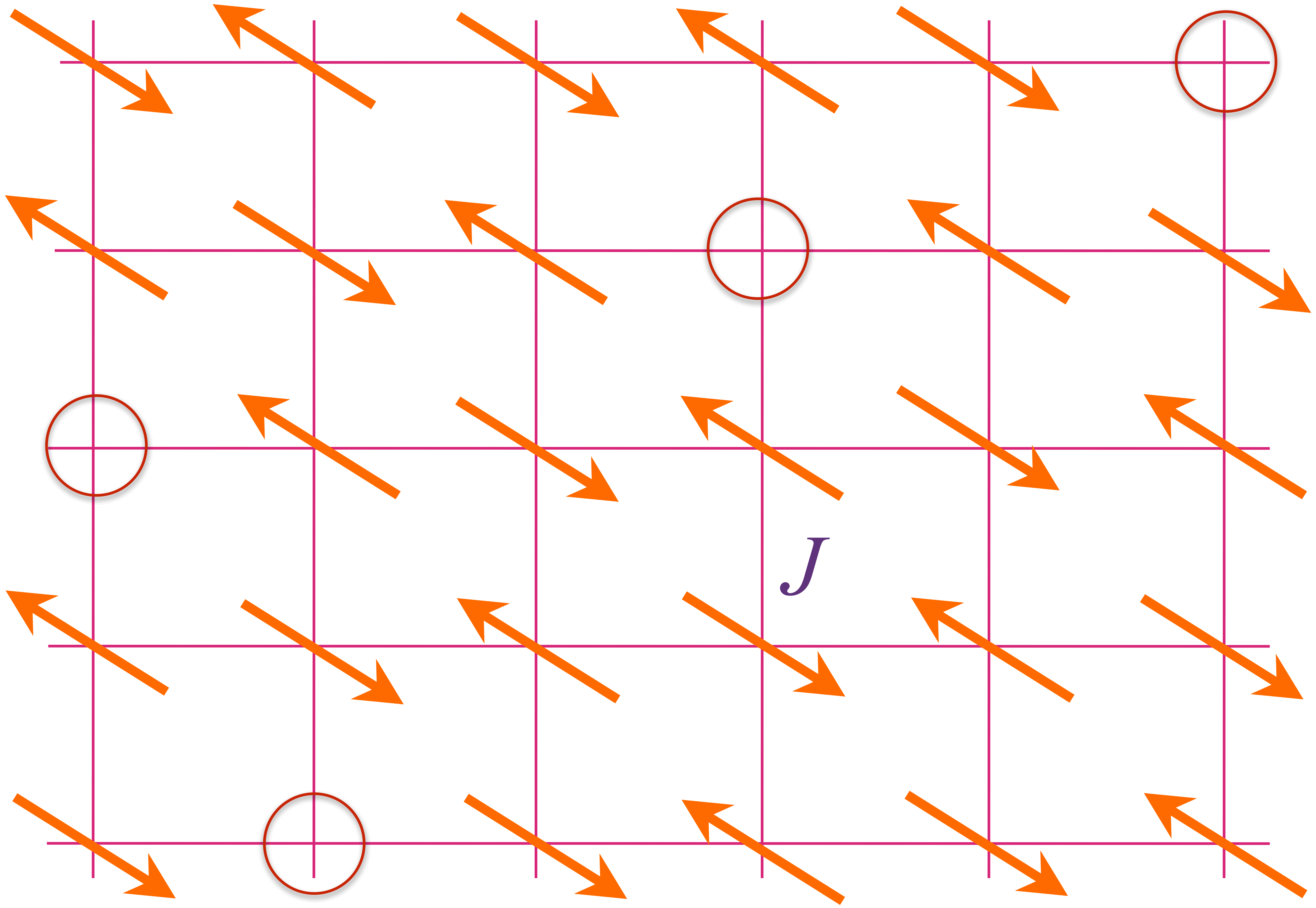

p mobile holes in a background of fluctuating spins

Real-space view at small p

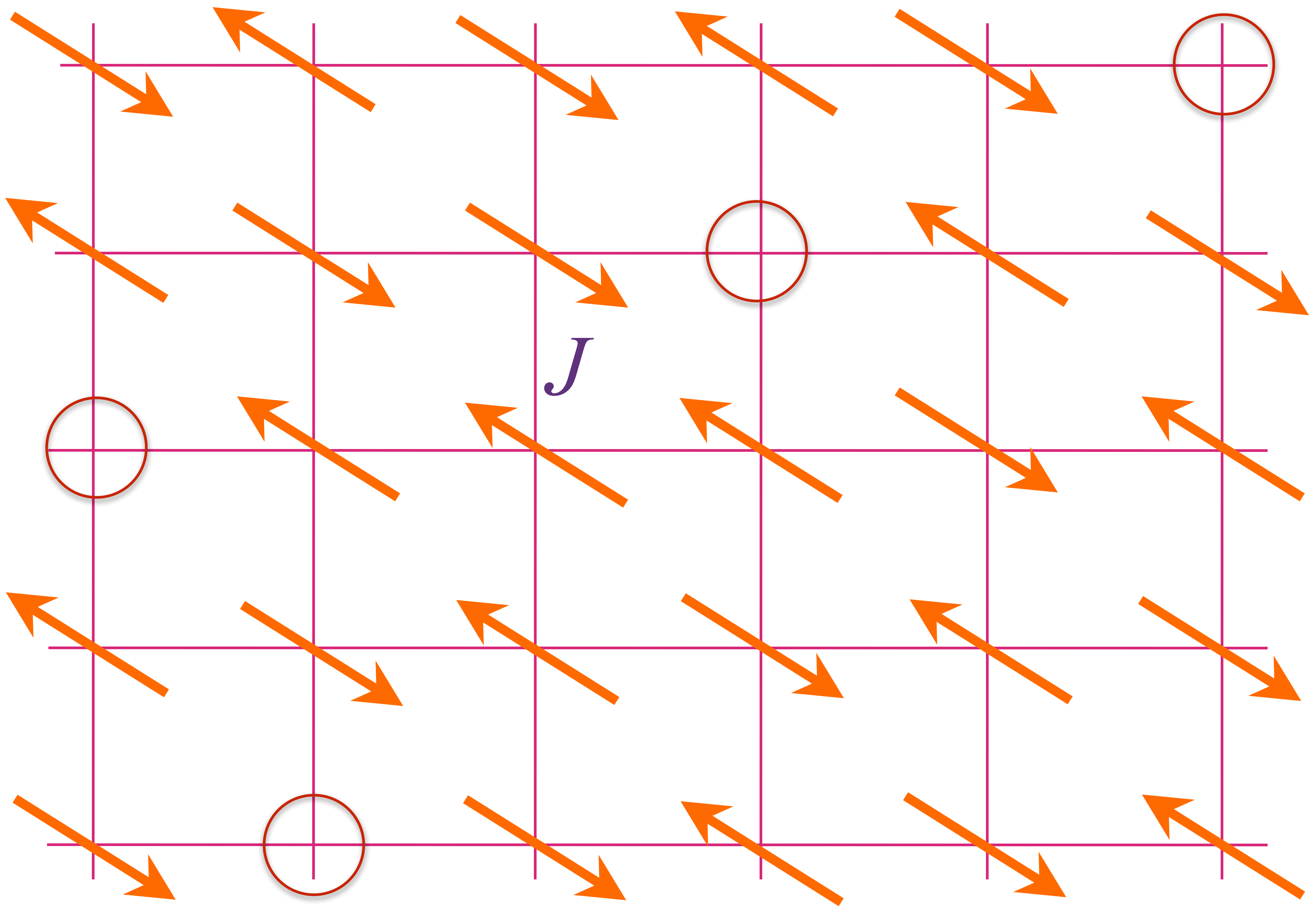

p mobile holes in a background of fluctuating spins

Real-space view at small p

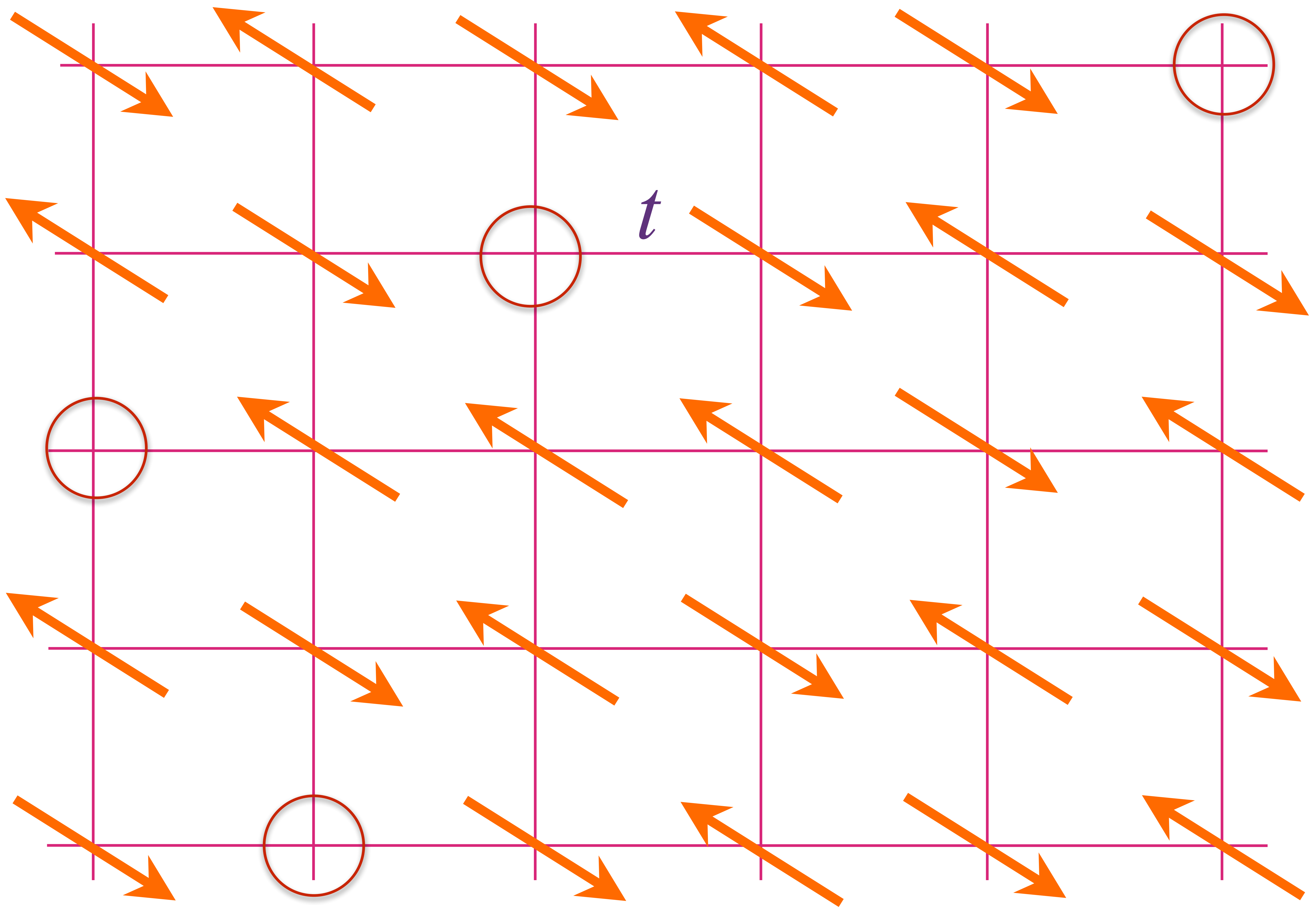

p mobile holes in a background of fluctuating spins

Real-space view at small p

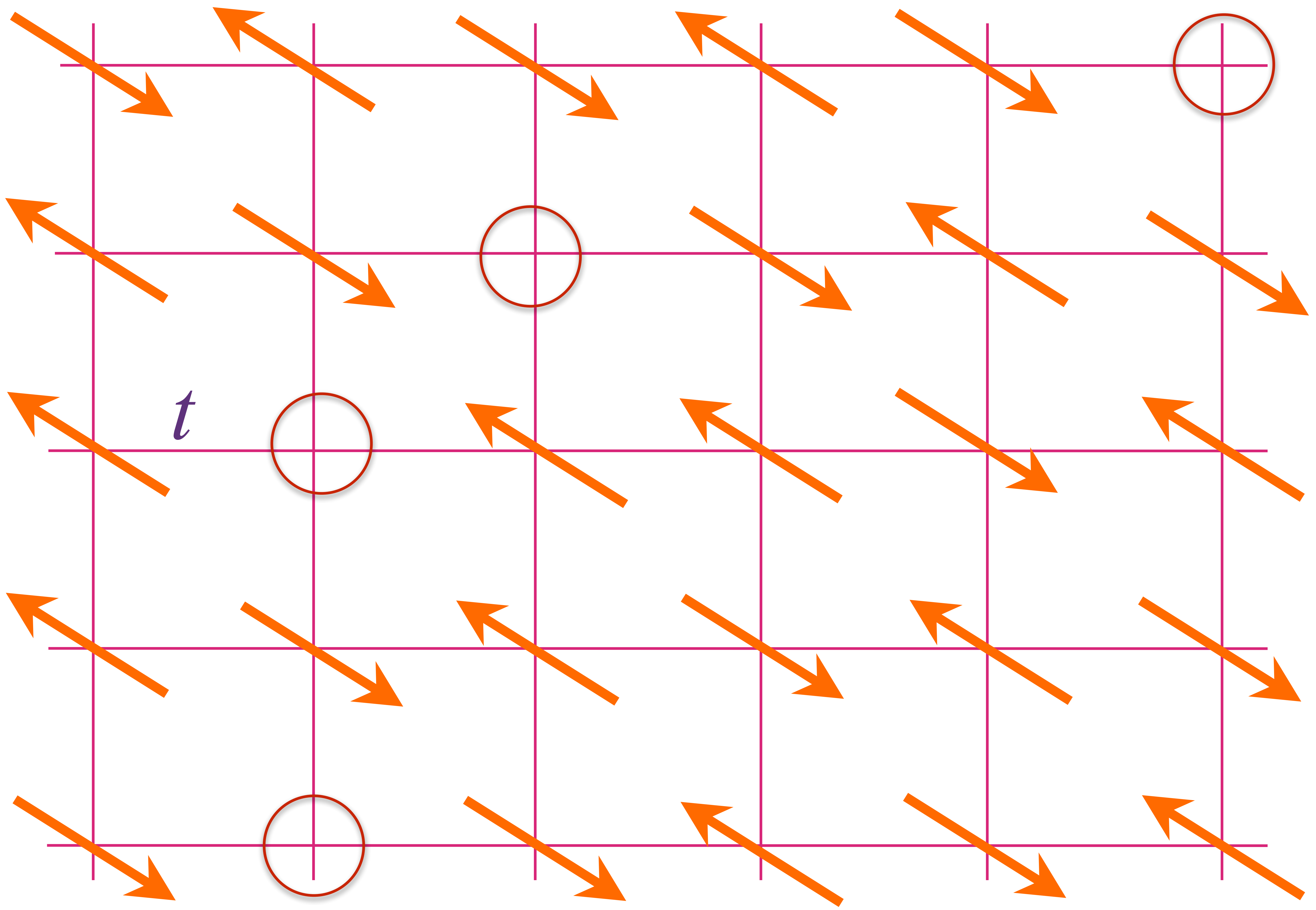

p mobile holes in a background of fluctuating spins

Real-space view at small p

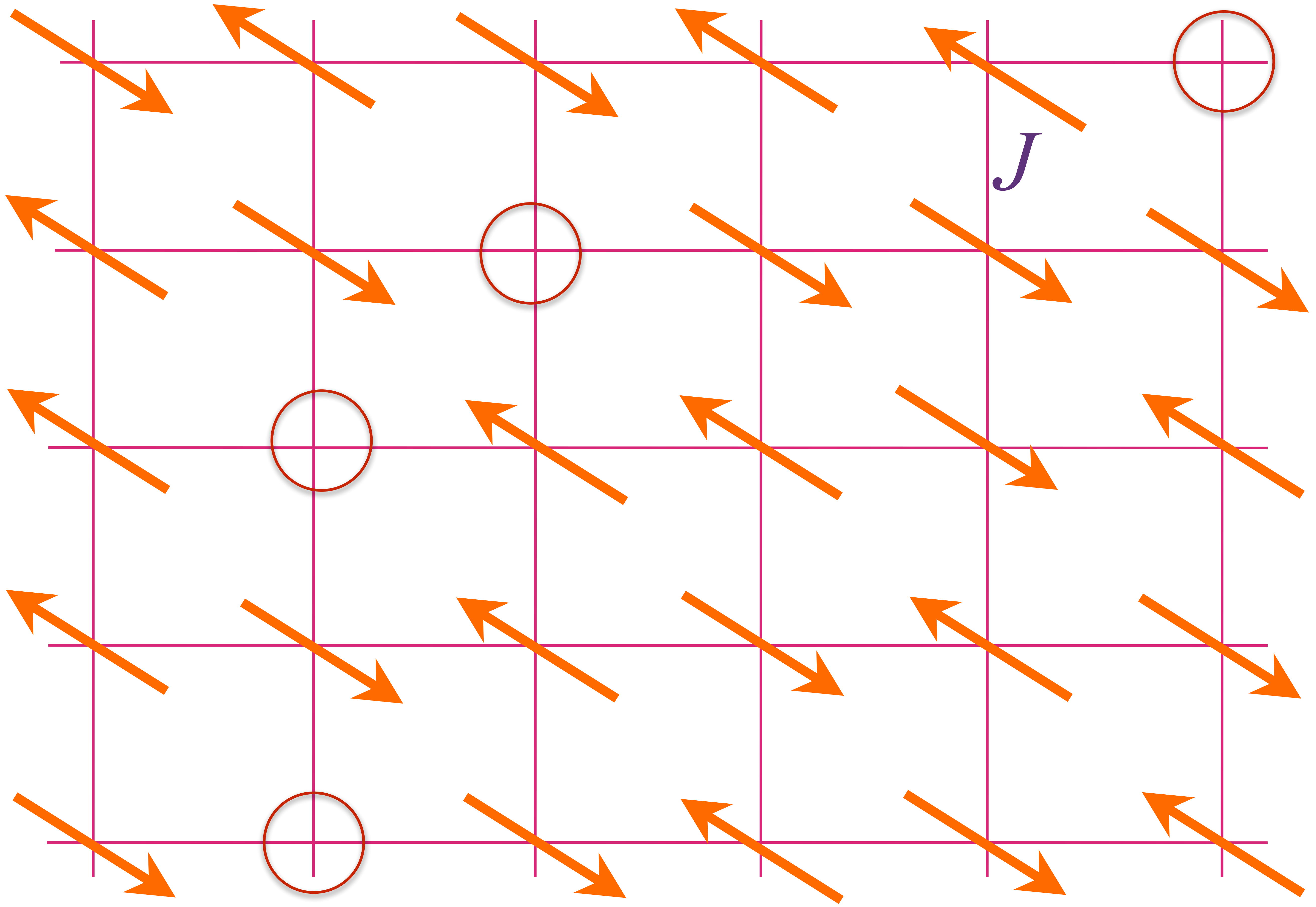

p mobile holes in a background of fluctuating spins

Real-space view at small p

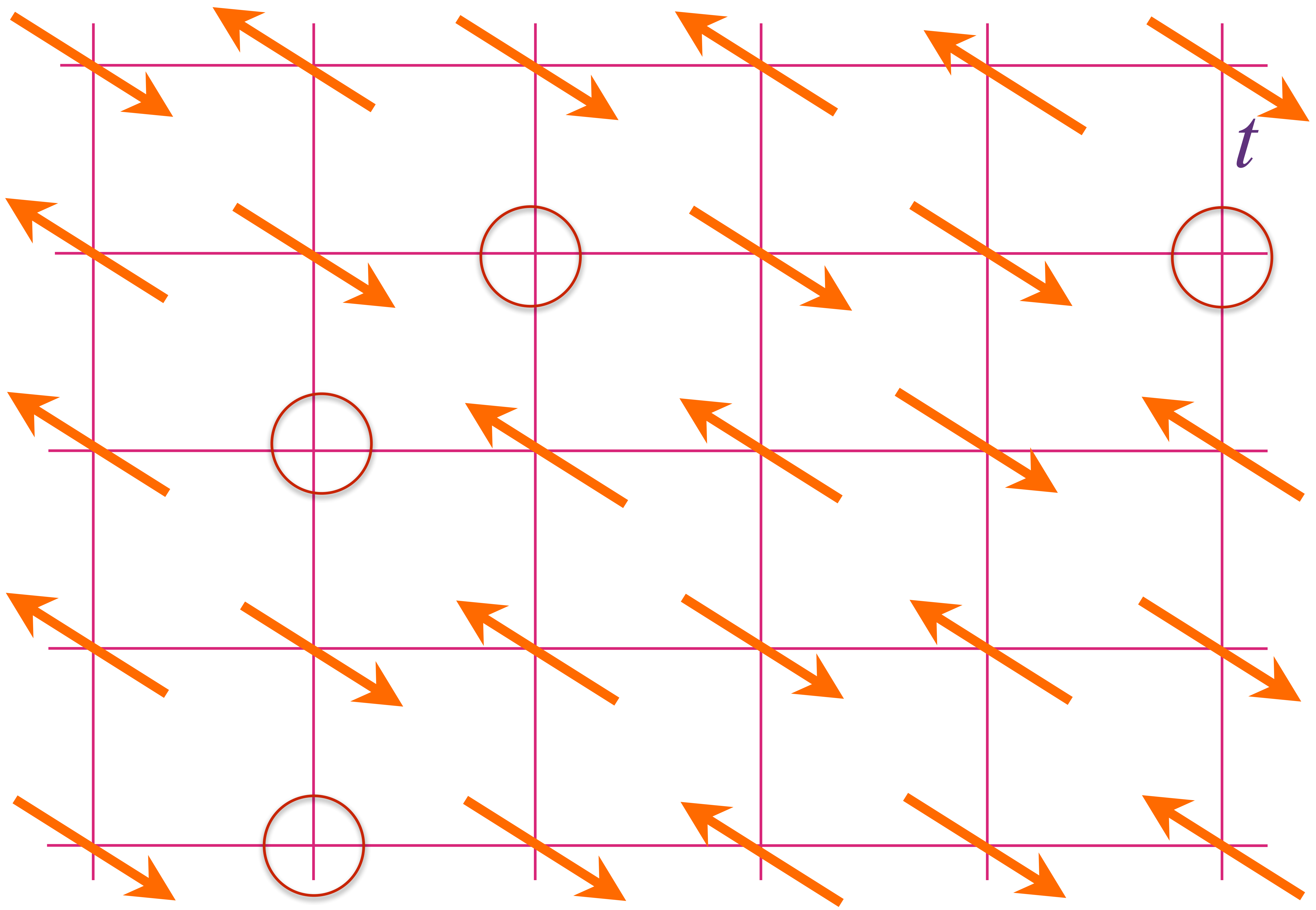

p mobile holes in a background of fluctuating spins

Momentum-space view at large p

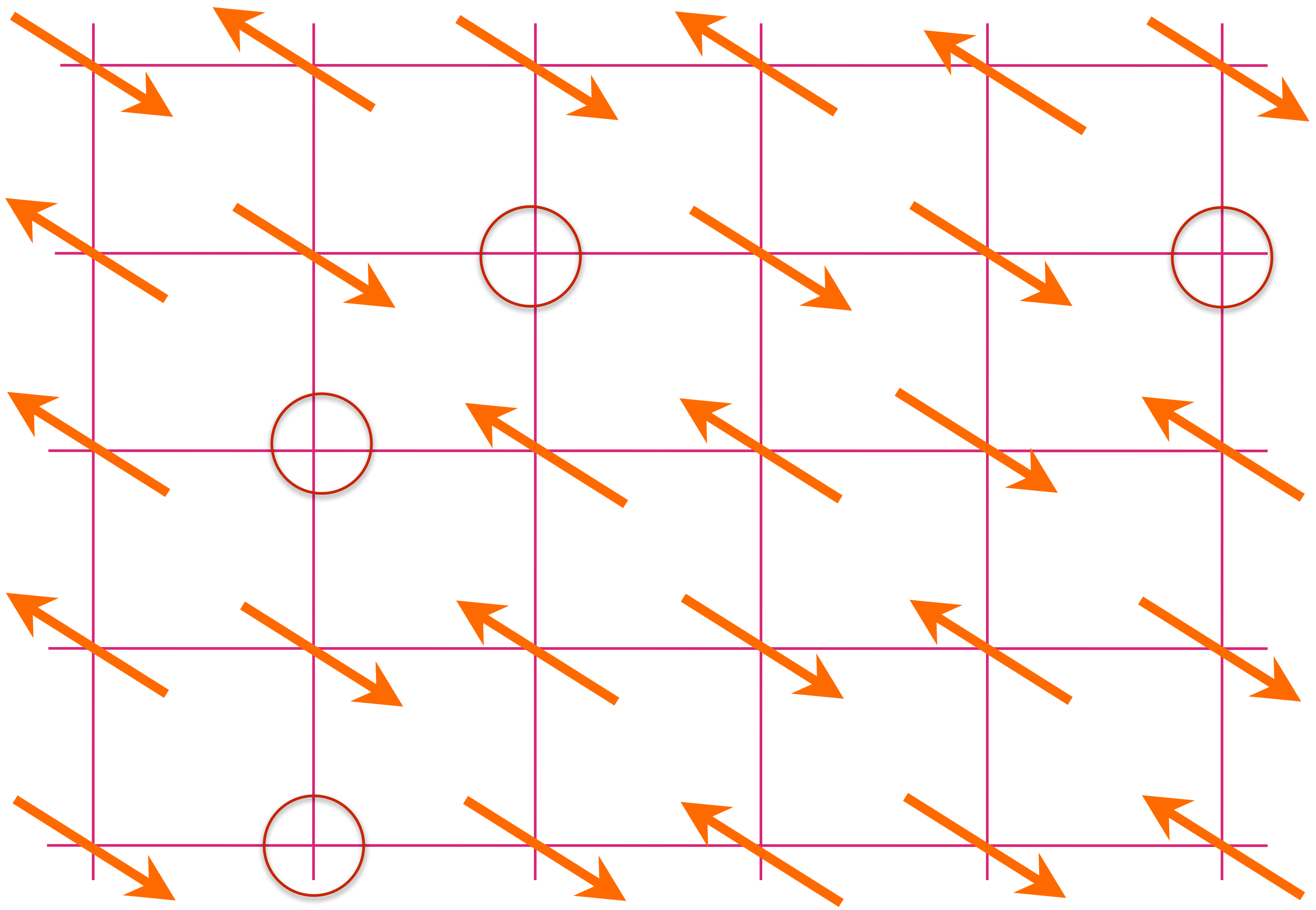

1-p mobile electrons =
$1+p$ mobile holes in a filled band

Momentum-space view at large p

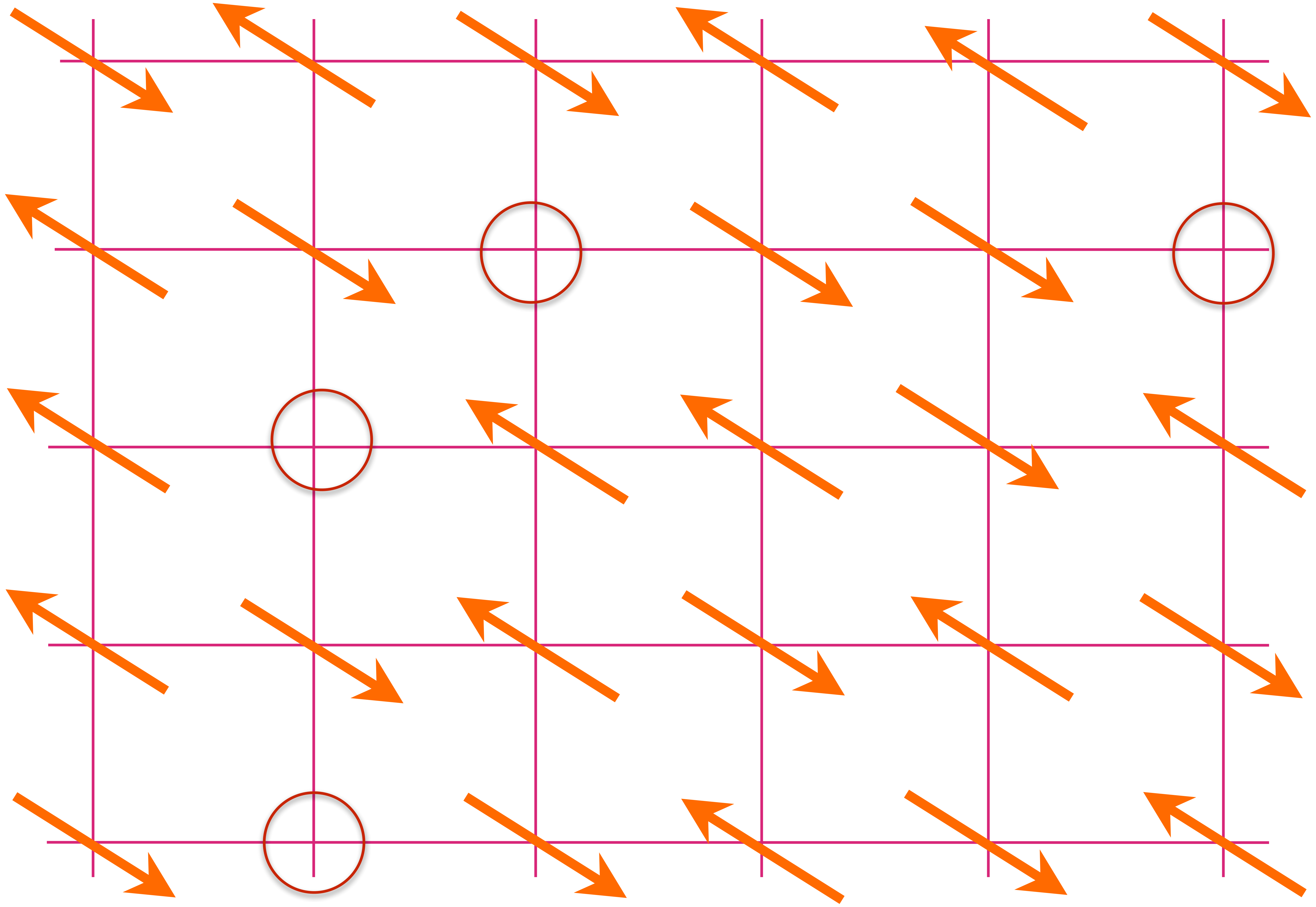

1-p mobile electrons =
$1+p$ mobile holes in a filled band

Momentum-space view at large p

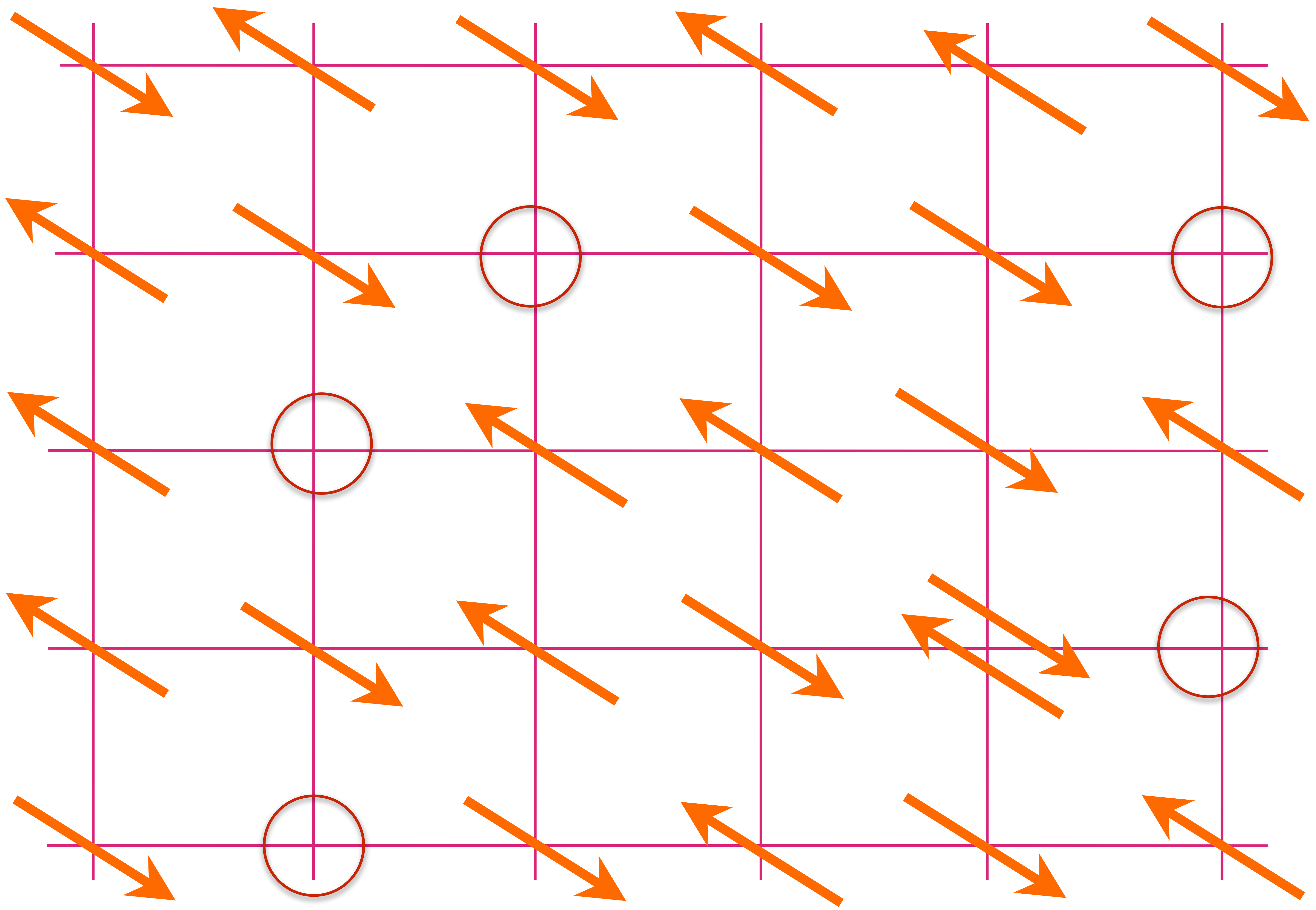

$1\text{-}p$ mobile electrons =
$1+p$ mobile holes in a filled band

Momentum-space view at large p

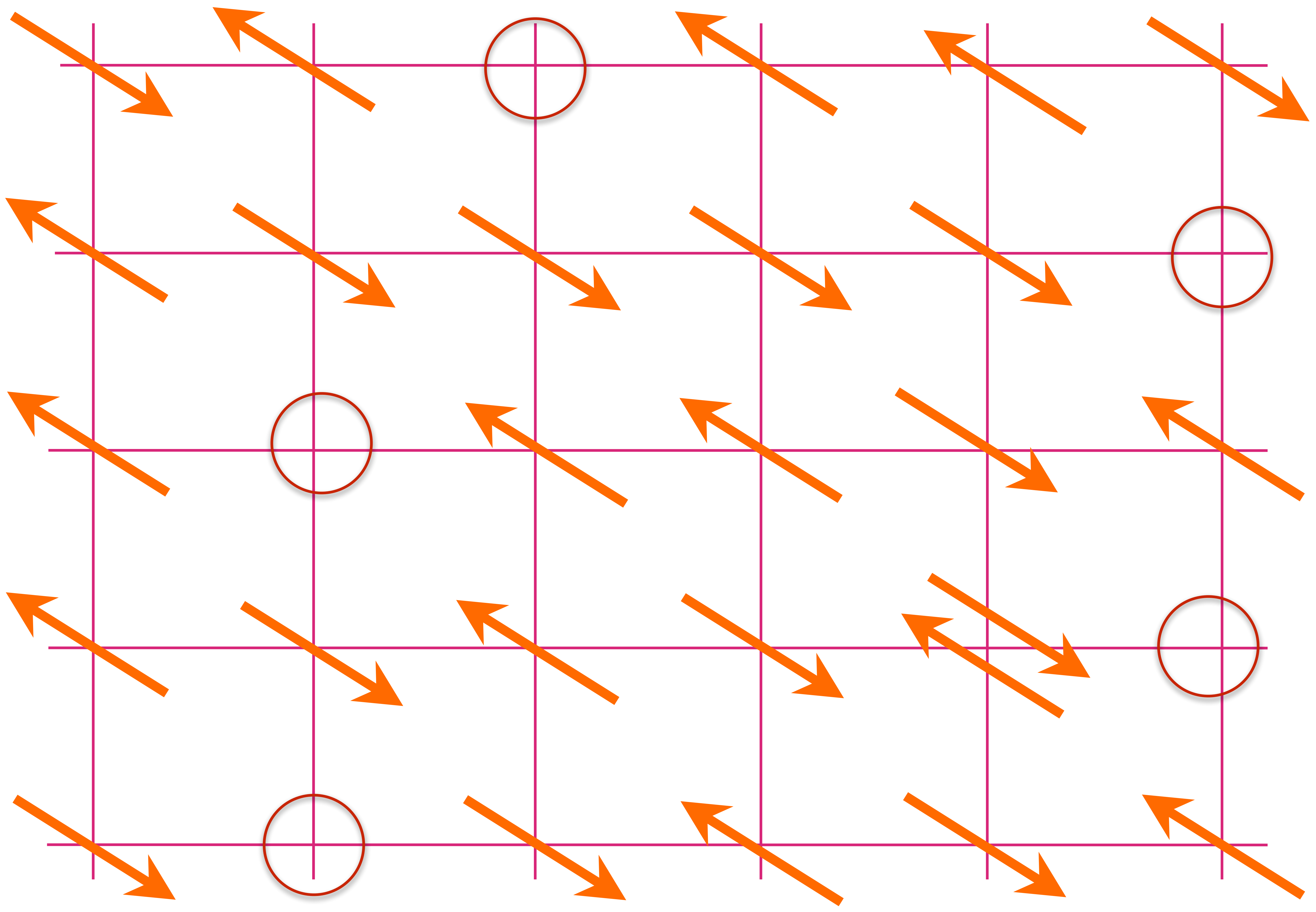

$1\text{-}p$ mobile electrons =
$1+p$ mobile holes in a filled band

Momentum-space view at large p

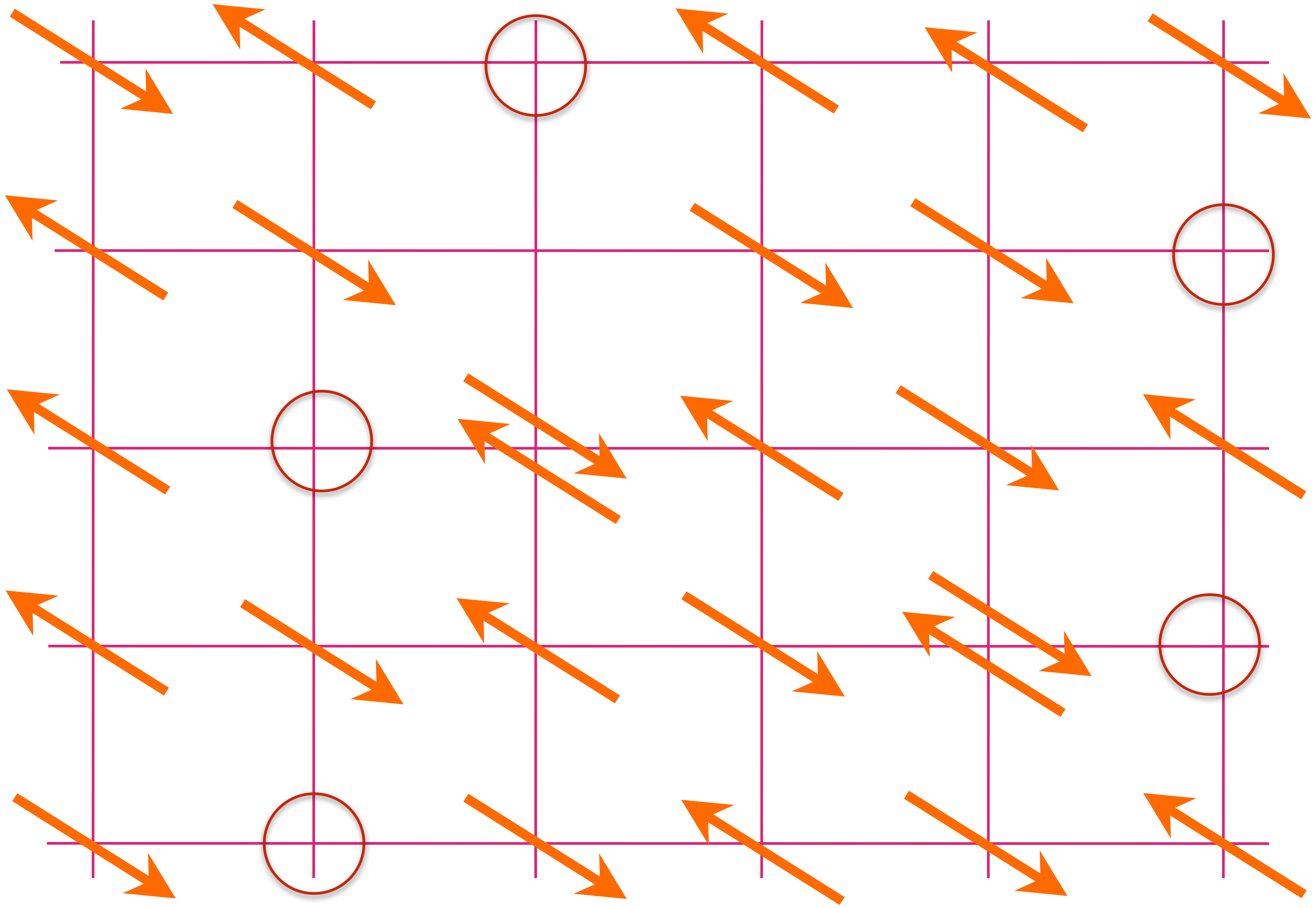

$1\text{-}p$ mobile electrons =
$1+p$ mobile holes in a filled band

Momentum-space view at large p

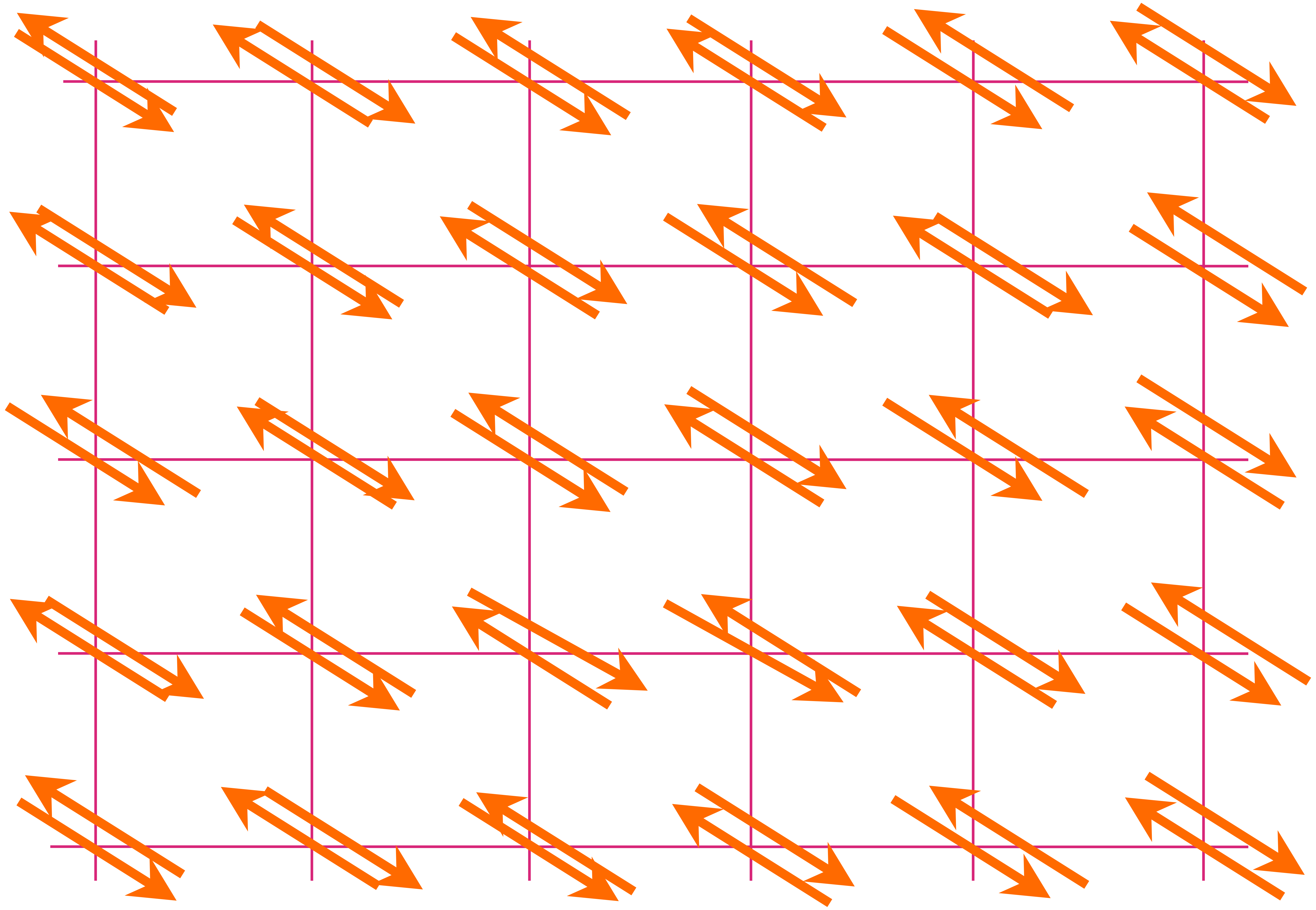

Filled Band

Momentum-space view at large p

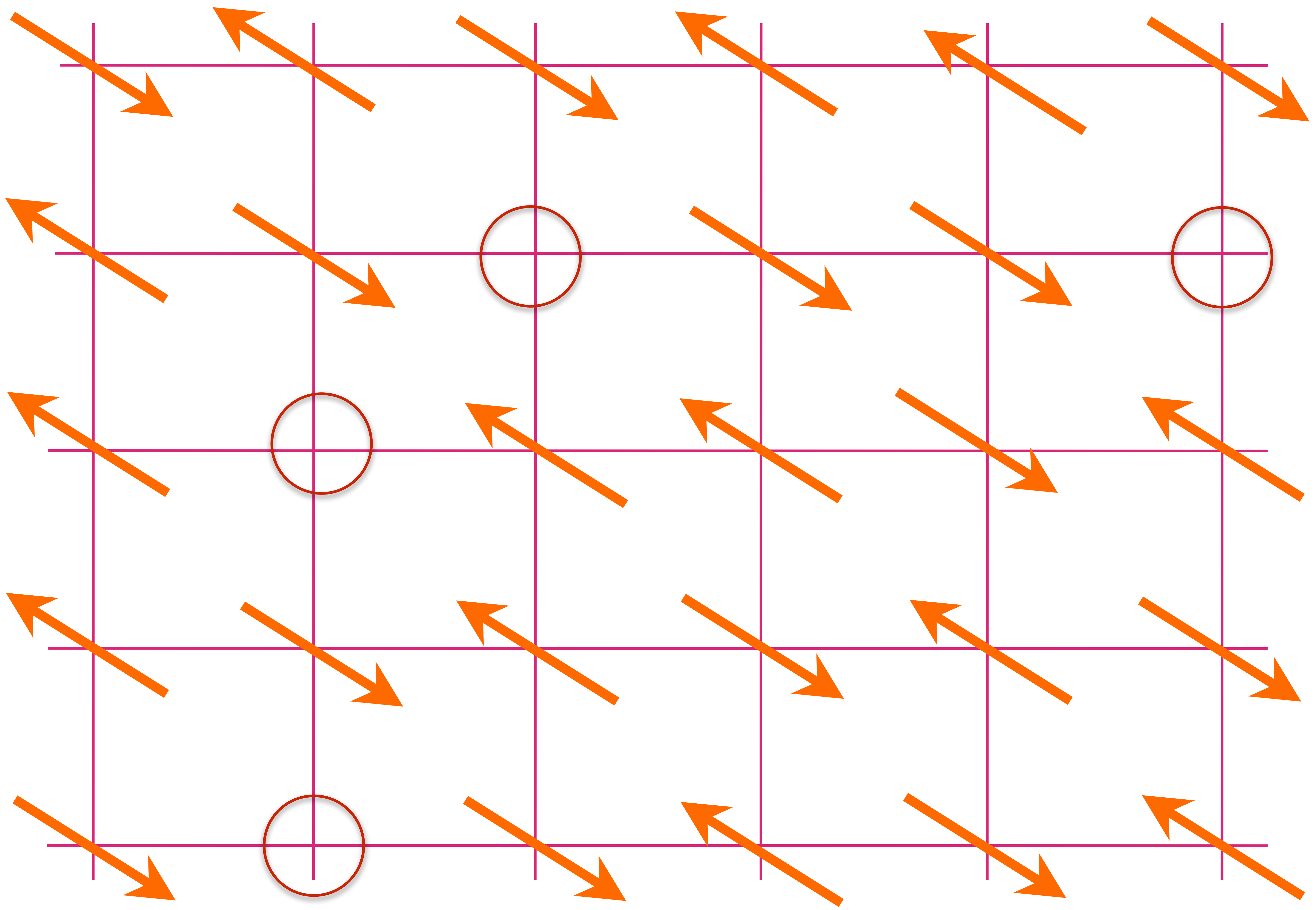

$1-p$ mobile electrons =
$1+p$ mobile holes in a filled band

Momentum-space view at large p

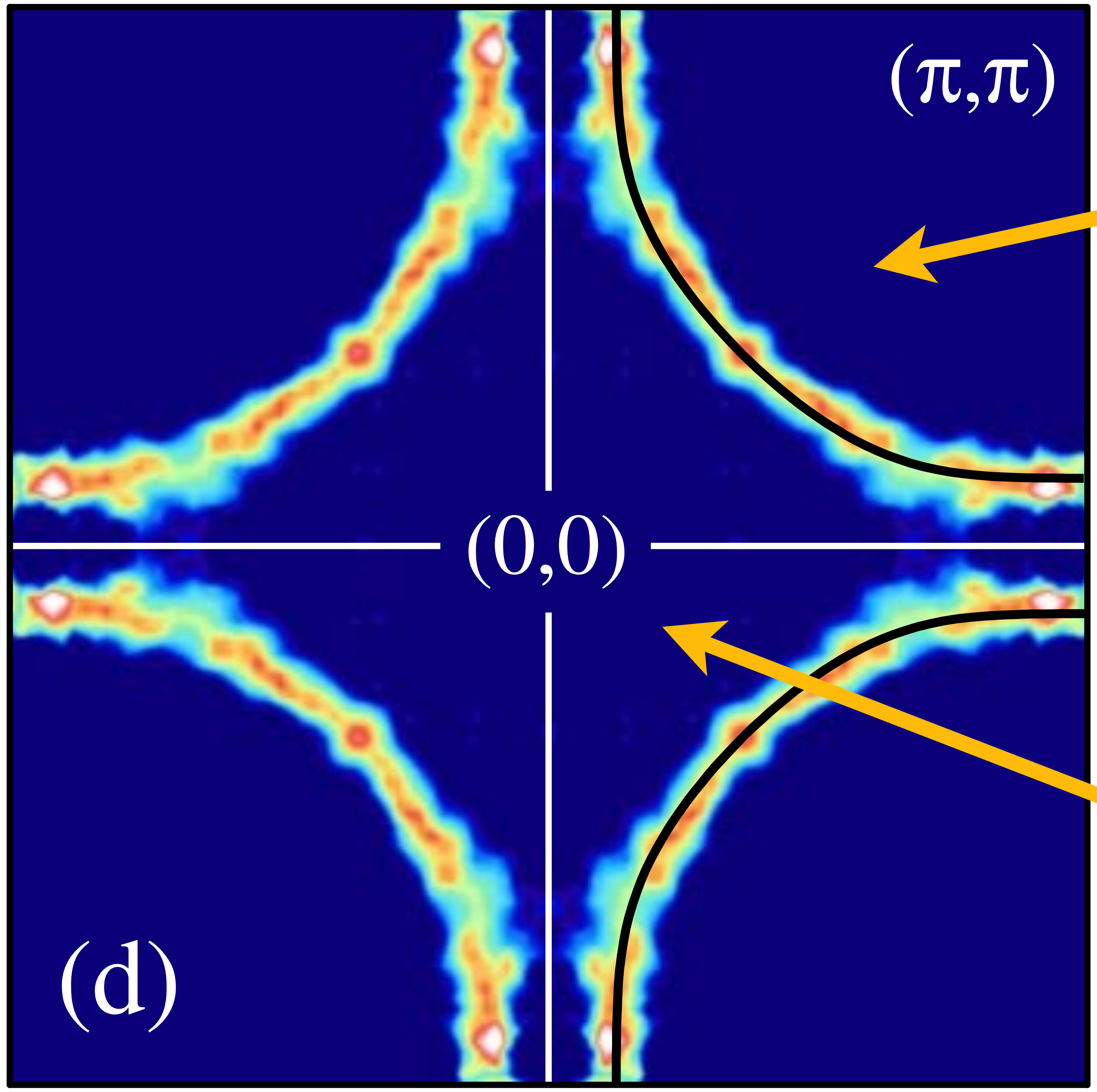

$1+p$ holes

1-p electrons

Overdoped $Tl_2Ba_2CuO_{6+\delta}$
$T_c = 30K$

$1+p$ mobile holes in a filled band

M. Platé, J. D. F. Mottershead, I. S. Elfimov, D. C. Peets, Ruixing Liang, D. A. Bonn, W. N. Hardy, S. Chiuzbaian, M. Falub, M. Shi, L. Patthey, and A. Damascelli, Phys. Rev. Lett. **95**, 077001 (2005)

Momentum-space view at small p

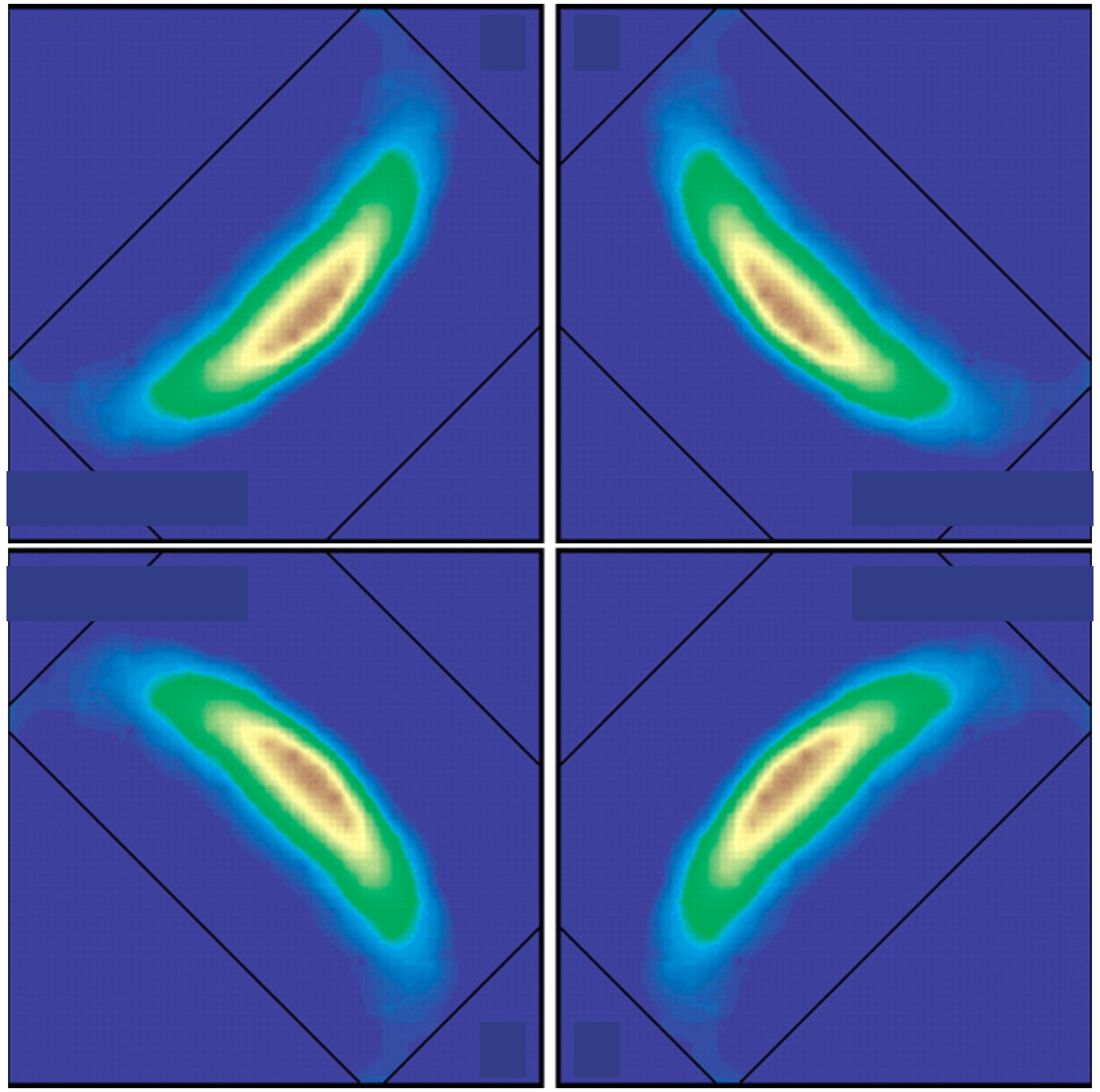

$Ca_{2-x}Na_xCuO_2Cl_2$
at $x = 0.10$

"Fermi arcs"

Kyle M. Shen, F. Ronning, D. H. Lu, F. Baumberger, N. J. C. Ingle, W. S. Lee, W. Meevasana, Y. Kohsaka, M. Azuma, M. Takano, H. Takagi, Z.-X. Shen, Science **307**, 901 (2005)

Fermi surface transformation at the pseudogap critical point of a cuprate superconductor

Yawen Fang, Gaël Grissonnanche, Anaëlle Legros, Simon Verret, Francis Laliberté, Clément Collignon, Amirreza Ataei, Maxime Dion, Jianshi Zhou, David Graf, M. J. Lawler, Paul Goddard, Louis Taillefer, and B. J. Ramshaw, arXiv:2004.01725

We use angle-dependent magnetoresistance (ADMR) to measure the Fermi surface of the cuprate $La_{1.6-x}Nd_{0.4}Sr_xCuO_4$. Above the critical doping p*—outside of the pseudogap phase—we find a Fermi surface that is in quantitative agreement with angle-resolved photoemission. Below p*, however, the ADMR is qualitatively different, revealing a clear change in Fermi surface topology. We find that our data is most consistent with a Fermi surface that has been reconstructed by a Q = (π,π) wavevector. While static Q = (π,π) antiferromagnetism is not found at these dopings, our results suggest that this wavevector is a fundamental organizing principle of the pseudogap phase.

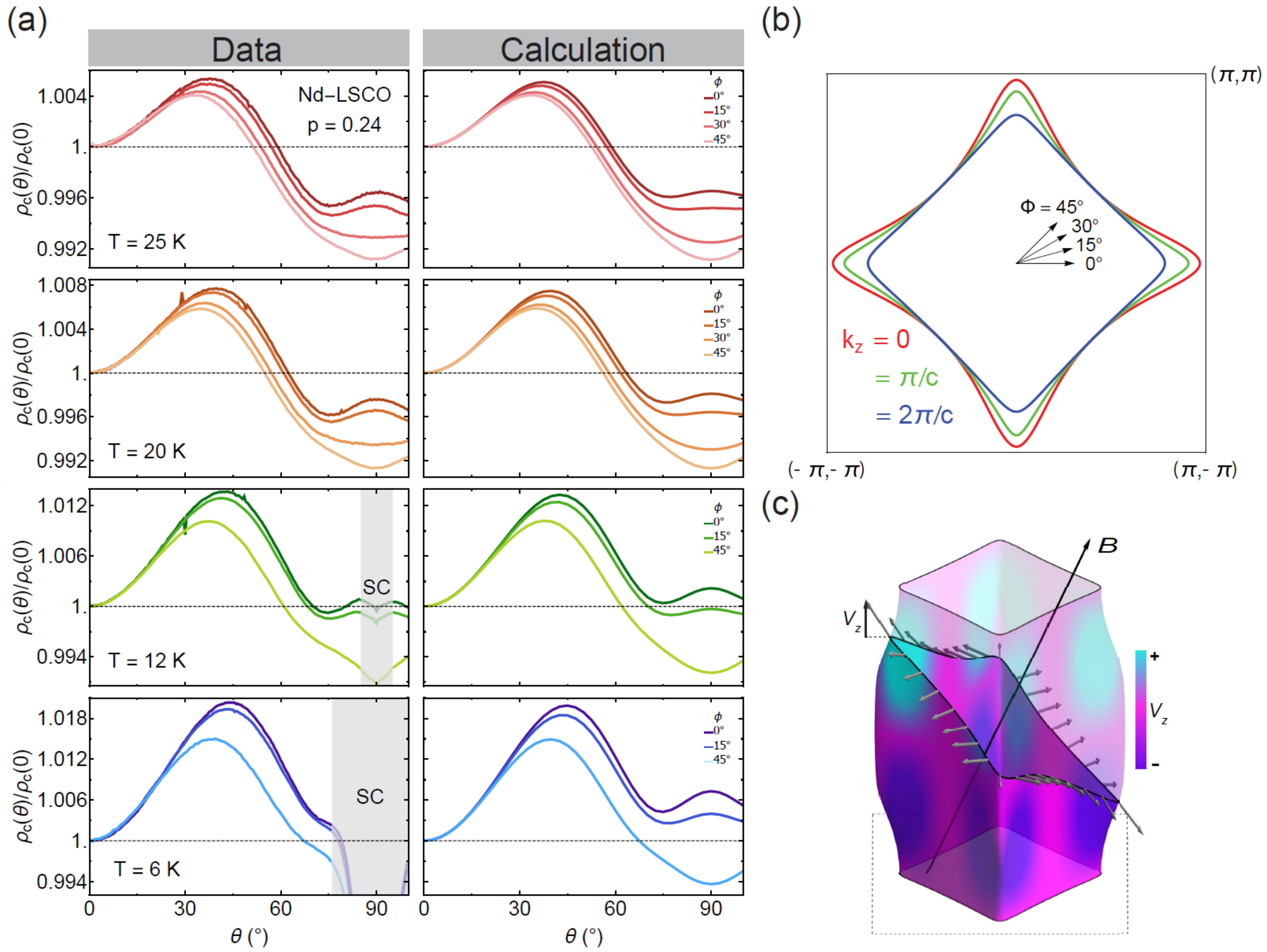

$p > p_c$ Large Fermi surface

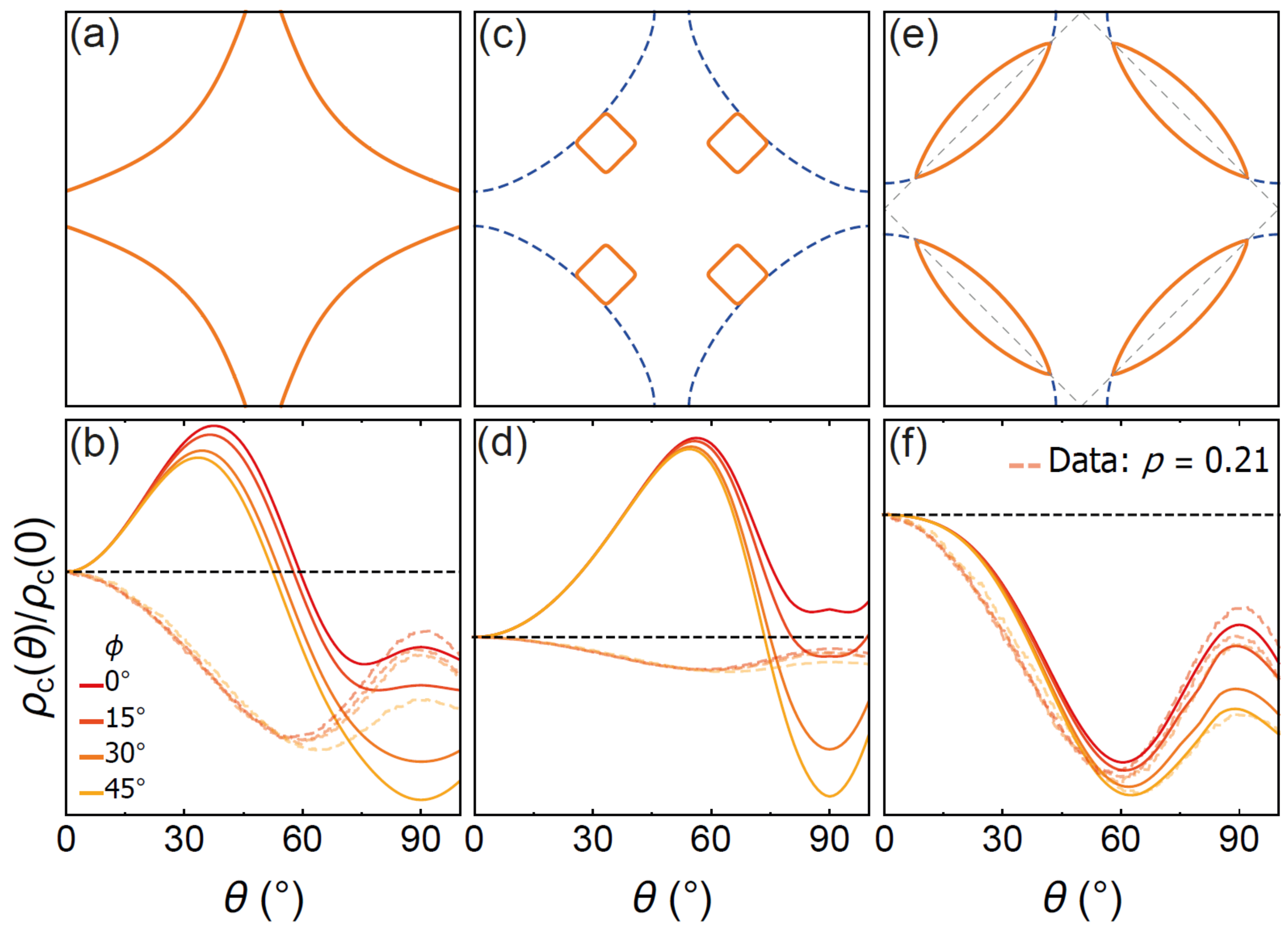

$p < p_c$ Reconstructed Fermi surface

Hole doped cuprates

The remarkable underlying ground states of cuprate superconductors

Cyril Proust and Louis Taillefer, Annual Review Condensed Matter Physics **10,** 409 (2019)

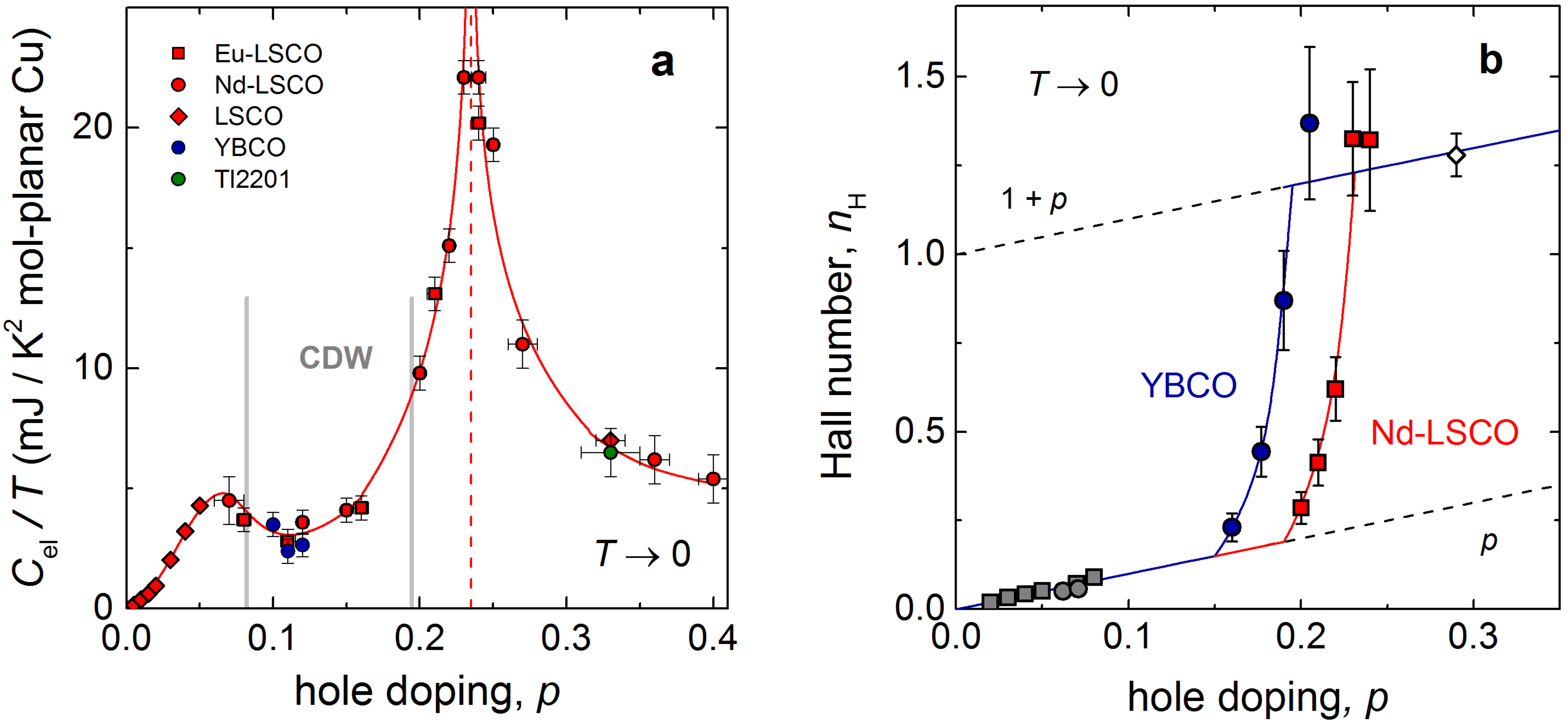

1. Metal-metal transition in the Kondo Lattice

2. Metal-metal transition in a one-band model

   A. *FL* model of the pseudogap*

   B. *Ancilla qubits and ghost Fermi surfaces*

3. Random t-*J* model

   SYK criticality and Numerics

1. Metal-metal transition in the Kondo Lattice

2. Metal-metal transition in a one-band model
   A. *FL* model of the pseudogap*
   B. *Ancilla qubits and ghost Fermi surfaces*

3. Random t-*J* model
   SYK criticality and Numerics

Kondo model

$$J_K \left(c^\dagger_{0\alpha} \vec{\sigma}_{\alpha\beta} c_{0\beta} \right) \cdot \vec{S}_f$$

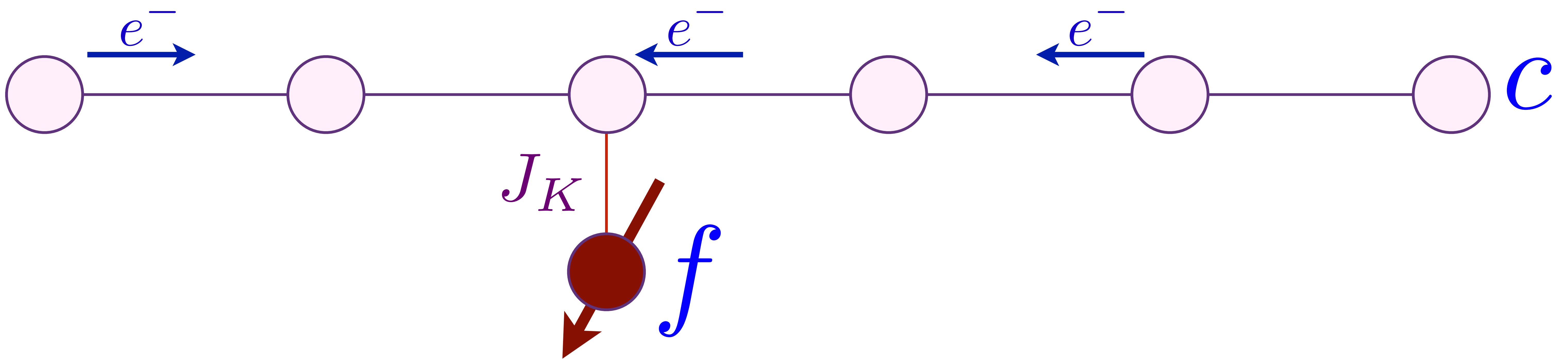

Kondo model

$J_K \left(c^\dagger_{0\alpha} \vec{\sigma}_{\alpha\beta} c_{0\beta} \right) \cdot \vec{S}_f$

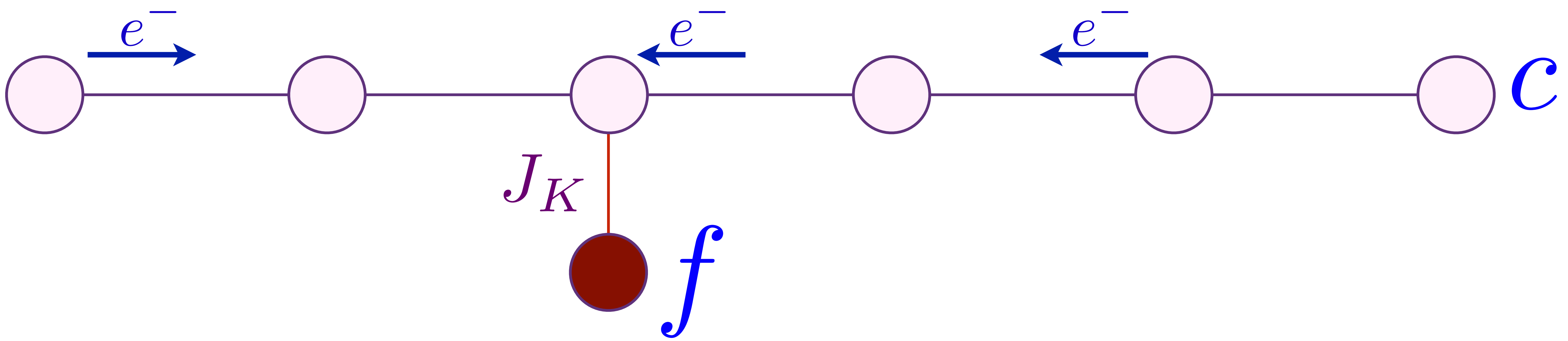

The c electrons ‘Kondo screen’ the f spin at low energies:
The f electron ‘dissolves’ into the Fermi sea.

Metal-metal transitions in ***Kondo lattice*** models

Kondo lattice of f electron spins coupled
to a conduction band of c electrons of density p.

$$J_K \sum_i \left(c_{i\alpha}^\dagger \vec{\sigma}_{\alpha\beta} c_{i\beta} \right) \cdot \vec{S}_{fi}$$

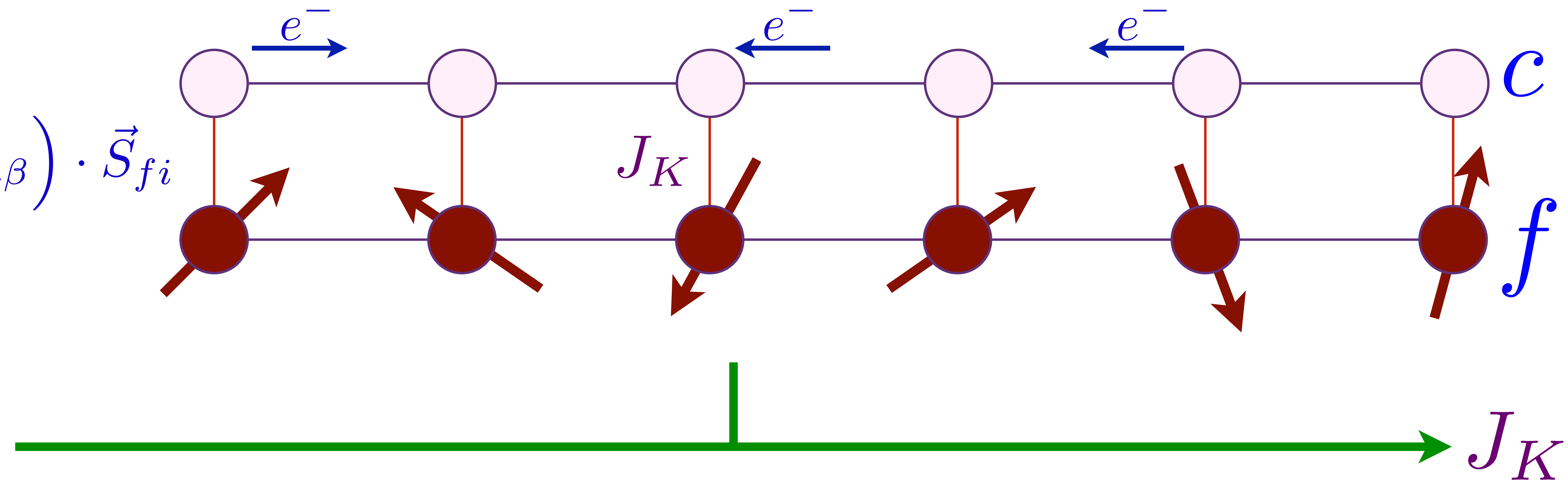

Metal-metal transitions in ***Kondo lattice*** models

Kondo lattice of f electron spins coupled
to a conduction band of c electrons of density p.

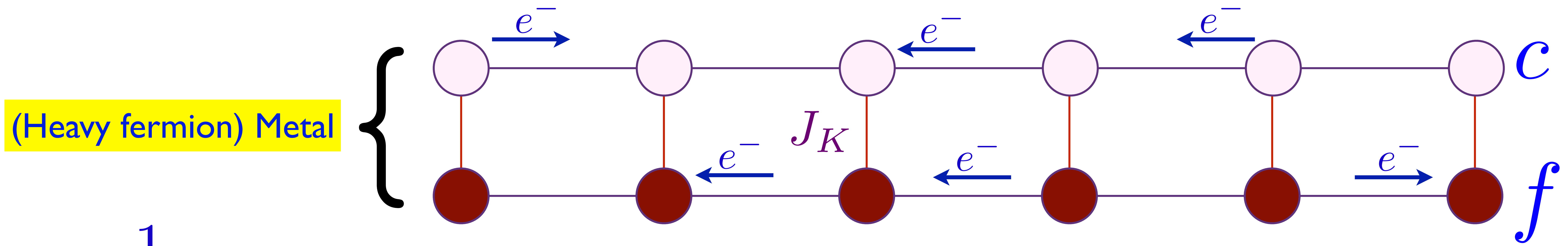

$$\vec{S}_{fi} = \frac{1}{2} f^\dagger_{i\alpha} \vec{\sigma}_{\alpha\beta} f_{i\beta}$$

$$\langle c^\dagger_\alpha f_\alpha \rangle \neq 0$$

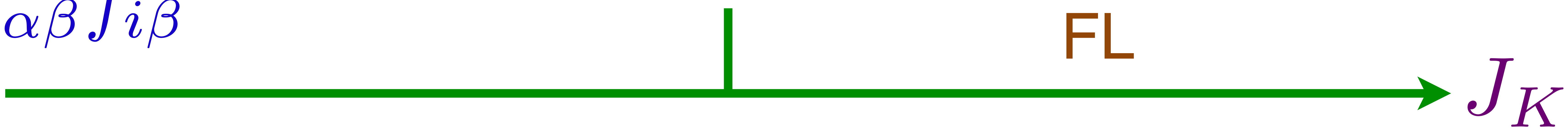

The c electrons 'Kondo screen' the f spins in the FL phase:
The f electrons 'dissolve' into the Fermi sea.

Varma, Coleman, Millis, P.A. Lee, Q. Si, Auerbach, Levin….

Metal-metal transitions in ***Kondo lattice*** models

Kondo lattice of f electron spins coupled
to a conduction band of c electrons of density p.

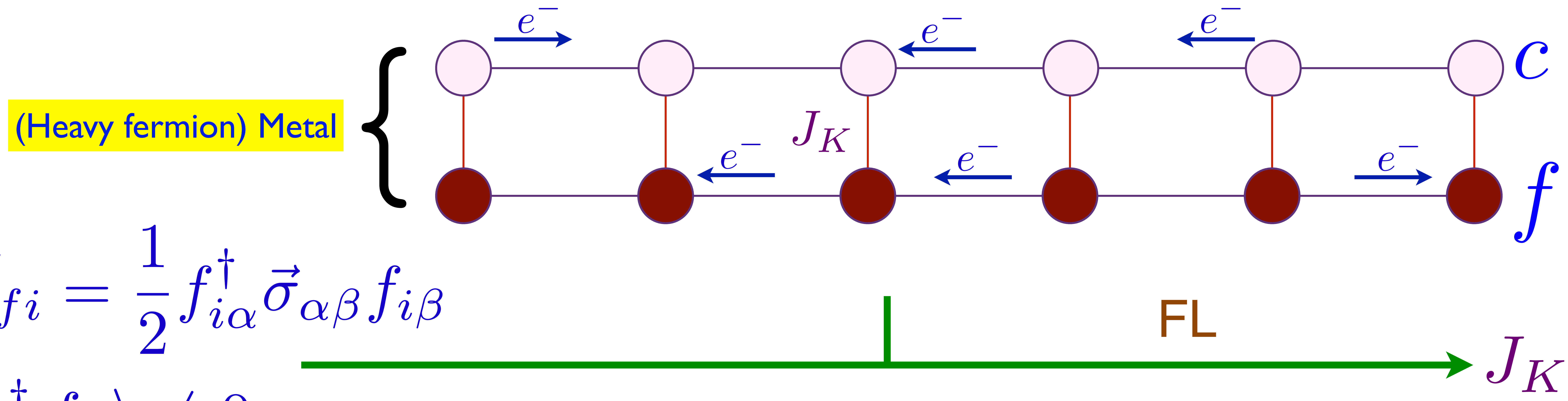

$$\vec{S}_{fi} = \frac{1}{2} f^\dagger_{i\alpha} \vec{\sigma}_{\alpha\beta} f_{i\beta}$$

$$\langle c^\dagger_\alpha f_\alpha \rangle \neq 0$$

The Kondo lattice model has a gauge symmetry: $f_{i\alpha} \to e^{i\theta_i} f_{i\alpha}$
This gauge symmetry is fully broken by a Higgs condensate $\langle c^\dagger_\alpha f_\alpha \rangle$ in the FL phase.

Metal-metal transitions in ***Kondo lattice*** models

Kondo lattice of f electron spins coupled
to a conduction band of c electrons of density p.

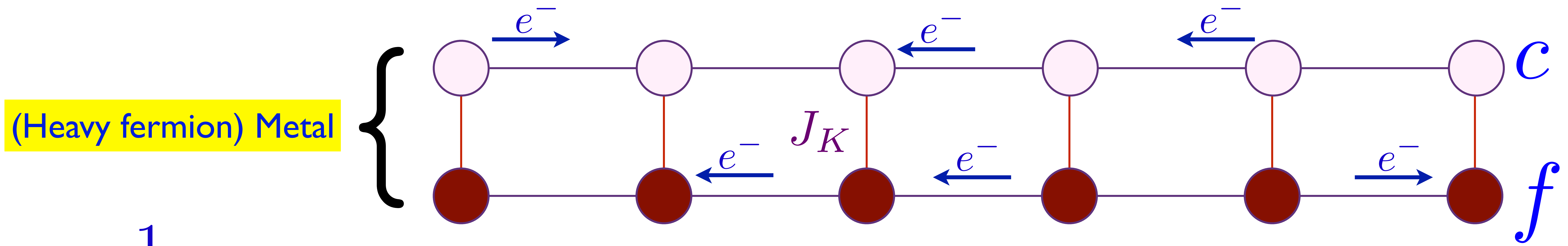

$$\vec{S}_{fi} = \frac{1}{2} f^\dagger_{i\alpha} \vec{\sigma}_{\alpha\beta} f_{i\beta}$$

$$\langle c^\dagger_\alpha f_\alpha \rangle \neq 0$$

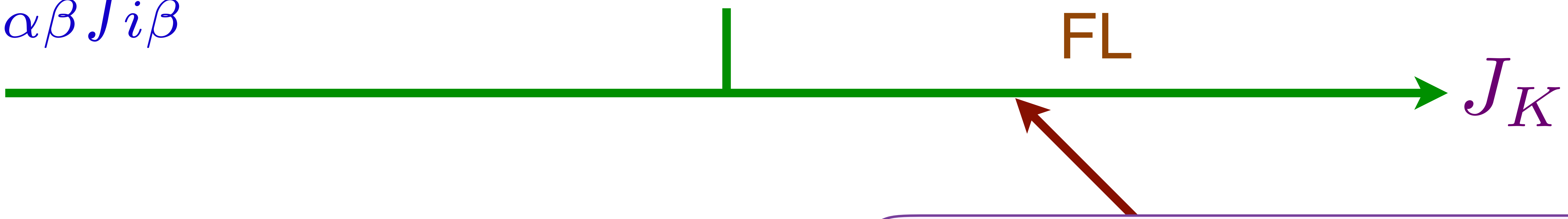

Large Fermi surface of size $1 + p$

$$|\Phi\rangle = [\text{Projection onto one } f \text{ per site}] \bowtie |\text{Slater determinant of } (c, f)\rangle$$

Varma, Coleman, Millis, P.A. Lee, Q. Si, Auerbach, Levin….

Metal-metal transitions in ***Kondo lattice*** models

Kondo lattice of f electron spins coupled
to a conduction band of c electrons of density p.

(Heavy fermion) Metal

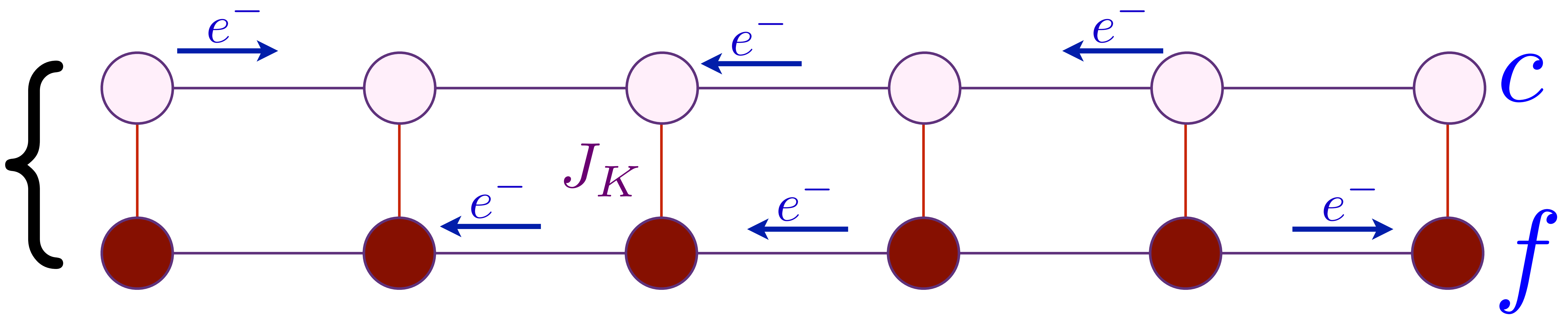

$$\vec{S}_{fi} = \frac{1}{2} f^\dagger_{i\alpha} \vec{\sigma}_{\alpha\beta} f_{i\beta}$$

$$\langle c^\dagger_\alpha f_\alpha \rangle \neq 0$$

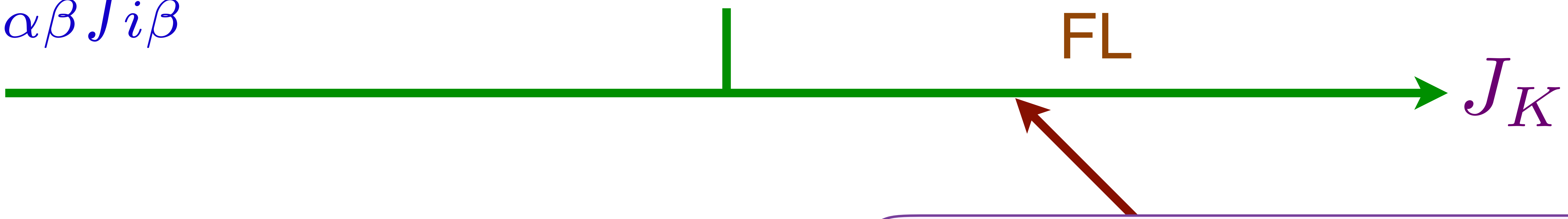

Luttinger Theorem obeyed

Large Fermi surface of size $1 + p$

$$|\Phi\rangle = [\text{Projection onto one } f \text{ per site}] \bowtie |\text{Slater determinant of } (c, f)\rangle$$

Varma, Coleman, Millis, P.A. Lee, Q. Si, Auerbach, Levin….

Metal-metal transitions in ***Kondo lattice*** models

Kondo lattice of f electron spins coupled
to a conduction band of c electrons of density p.

Kondo-breakdown or 'selective Mott' transition

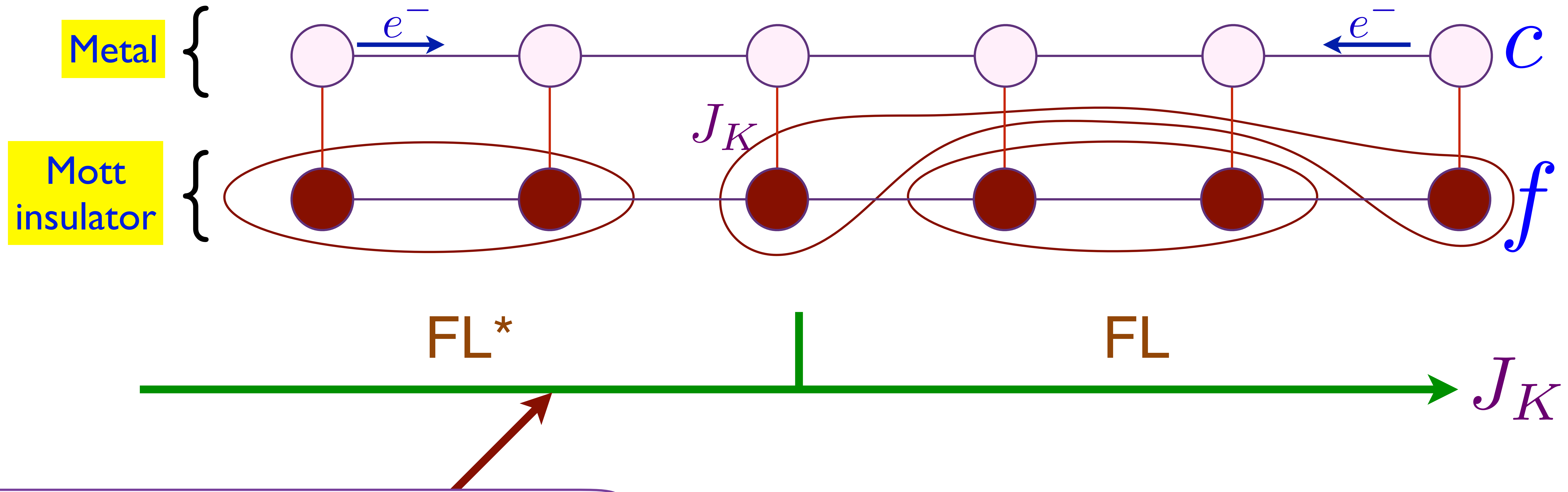

Small Fermi surface of size p

$$|\Phi\rangle = |\text{Spin liquid insulator of } f\rangle \otimes |\text{Slater determinant of } c\rangle$$

S. Burdin, D. R. Grempel, and A. Georges, PRB **66**, 045111 (2002)
T. Senthil, M. Vojta, and S. Sachdev, PRB **69**, 035111 (2004)

Metal-metal transitions in ***Kondo lattice*** models

Kondo lattice of f electron spins coupled
to a conduction band of c electrons of density p.

Kondo-breakdown or 'selective Mott' transition

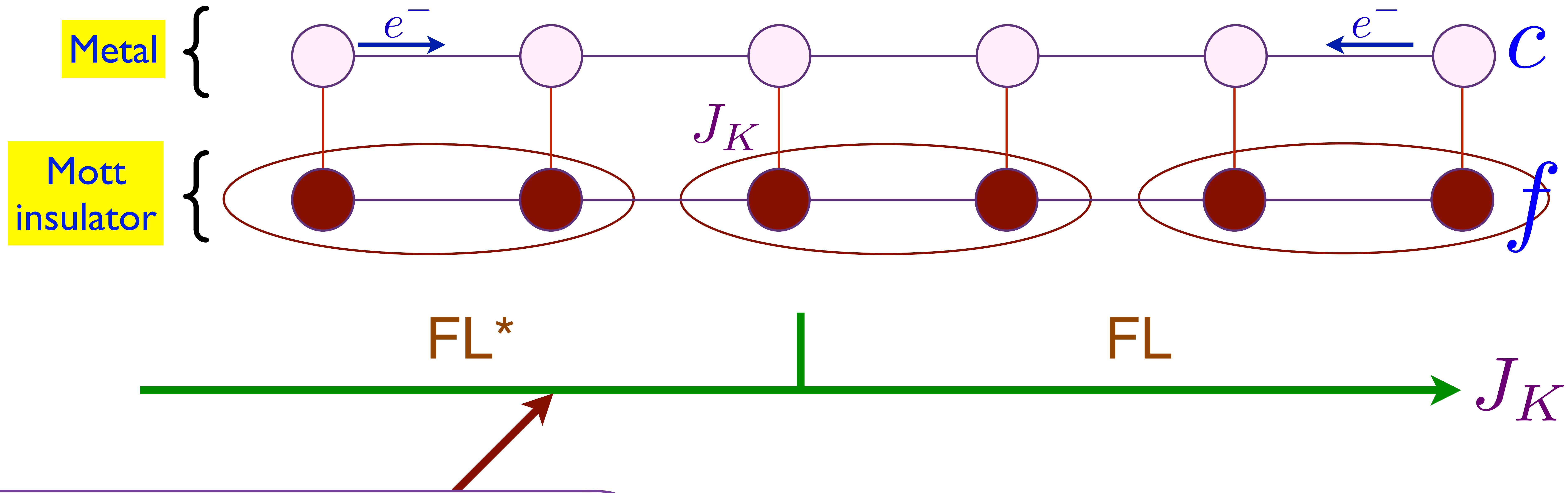

Small Fermi surface of size p

$$|\Phi\rangle = |\text{Spin liquid insulator of } f\rangle \otimes |\text{Slater determinant of } c\rangle$$

S. Burdin, D. R. Grempel, and A. Georges, PRB **66**, 045111 (2002)
T. Senthil, M. Vojta, and S. Sachdev, PRB **69**, 035111 (2004)

Metal-metal transitions in ***Kondo lattice*** models

Kondo lattice of f electron spins coupled
to a conduction band of c electrons of density p.

Kondo-breakdown or 'selective Mott' transition

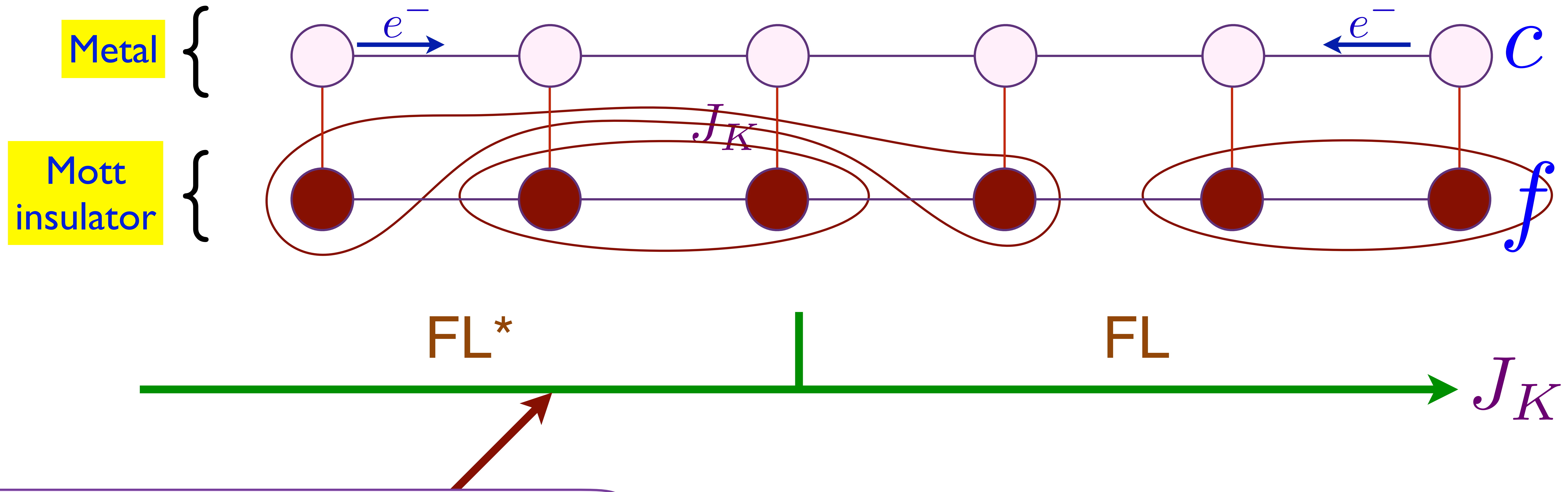

Small Fermi surface of size p

$$|\Phi\rangle = |\text{Spin liquid insulator of } f\rangle \otimes |\text{Slater determinant of } c\rangle$$

S. Burdin, D. R. Grempel, and A. Georges, PRB **66**, 045111 (2002)
T. Senthil, M. Vojta, and S. Sachdev, PRB **69**, 035111 (2004)

Metal-metal transitions in ***Kondo lattice*** models

Kondo lattice of f electron spins coupled
to a conduction band of c electrons of density p.

Kondo-breakdown or 'selective Mott' transition

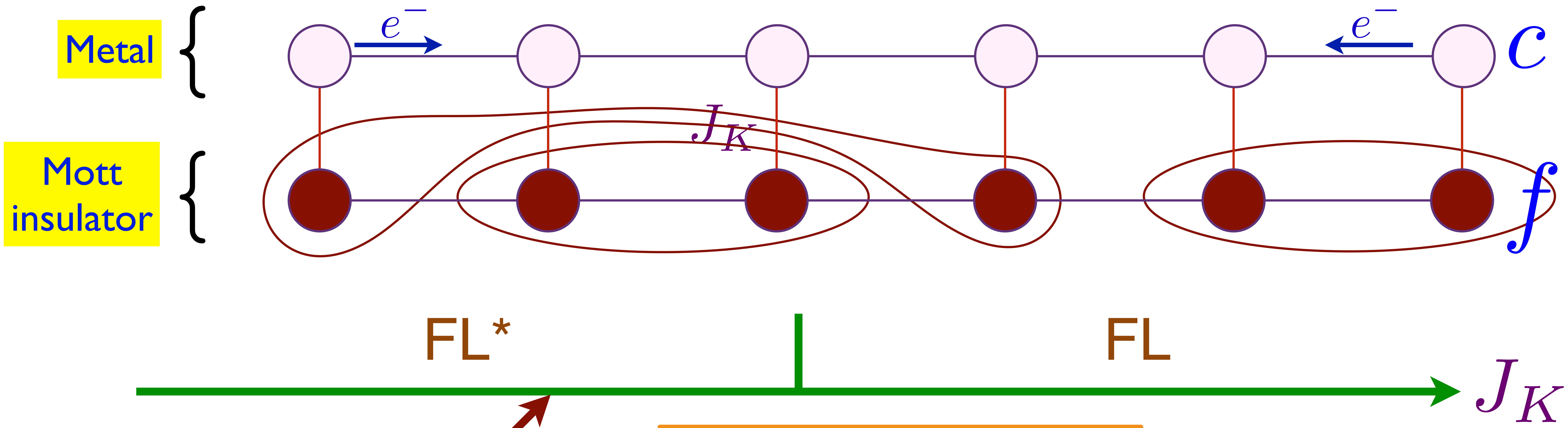

Small Fermi surface of size p

$$|\Phi\rangle = |\text{Spin liquid insulator of } f\rangle \otimes |\text{Slater determinant of } c\rangle$$

Luttinger Theorem violated; OK, because of topological order of *f* spins

T. Senthil, M. Vojta, and S. Sachdev, PRB **69**, 035111 (2004)

Metal-metal transitions in ***Kondo lattice*** models

Kondo lattice of f electron spins coupled
to a conduction band of c electrons of density p.

Kondo-breakdown or 'selective Mott' transition

U(1) gauge theory of a
'hybridization-Higgs' boson $b \sim f_\alpha^\dagger c_\alpha$
which condenses on the
'Large Fermi surface' side.

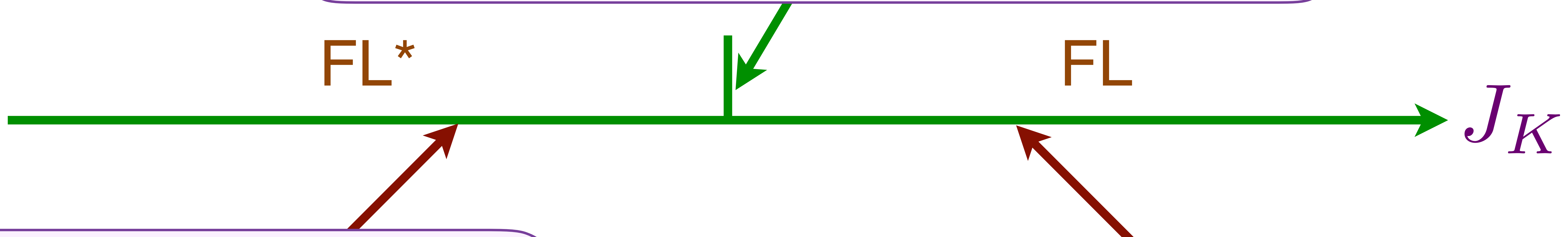

Small Fermi surface of size p

$|\Phi\rangle = |\text{Spin liquid insulator of } f\rangle$
$\otimes\, |\text{Slater determinant of } c\rangle$

Large Fermi surface of size $1 + p$

$|\Phi\rangle = [\text{Projection onto one } f \text{ per site}]$
$\bowtie\, |\text{Slater determinant of } (c, f)\rangle$

T. Senthil, M. Vojta, and S. Sachdev, PRB **69**, 035111 (2004)

Metal-metal transitions in ***Kondo lattice*** models

Kondo lattice of f electron spins coupled
to a conduction band of c electrons of density p.

Kondo-breakdown or 'selective Mott' transition

Shortcomings:

- Only works well for a particular spin liquid in the f band: the spinon Fermi surface with a trivial PSG.

Metal-metal transitions in ***Kondo lattice*** models

Kondo lattice of f electron spins coupled
to a conduction band of c electrons of density p.

Kondo-breakdown or 'selective Mott' transition

Shortcomings:

- Only works well for a particular spin liquid in the f band: the spinon Fermi surface with a trivial PSG.
- No natural extension to the case where the non-FL state has magnetic order.

Metal-metal transitions in ***Kondo lattice*** models

Kondo lattice of f electron spins coupled
to a conduction band of c electrons of density p.

Kondo-breakdown or 'selective Mott' transition

Shortcomings:

- Only works well for a particular spin liquid in the f band: the spinon Fermi surface with a trivial PSG.
- No natural extension to the case where the non-FL state has magnetic order.
- No simple extension to one-band model.

1. Metal-metal transition in the Kondo Lattice

2. Metal-metal transition in a one-band model
   A. *FL* model of the pseudogap*
   B. *Ancilla qubits and ghost Fermi surfaces*

3. Random t-*J* model
   SYK criticality and Numerics

1. Metal-metal transition in the Kondo Lattice

2. Metal-metal transition in a one-band model

   A. FL model of the pseudogap*

   B. Ancilla qubits and ghost Fermi surfaces

3. Random t-J model

   SYK criticality and Numerics

Metal-metal transitions in a ***one-band*** model

- Can realize the FL* state as a doped spin liquid in which spinons and holons bind to form 'electrons', which then form a small Fermi surface (X.-G. Wen and P. A. Lee, PRL **76**, 503 (1996)); but there is no complete description of this process, except in the very strong binding limit of dimer 'electrons' (M. Punk, A. Allais, and S. Sachdev,PNAS **112**, 9552 (2015)). This approach does not yield a theory of the transition to the FL state.

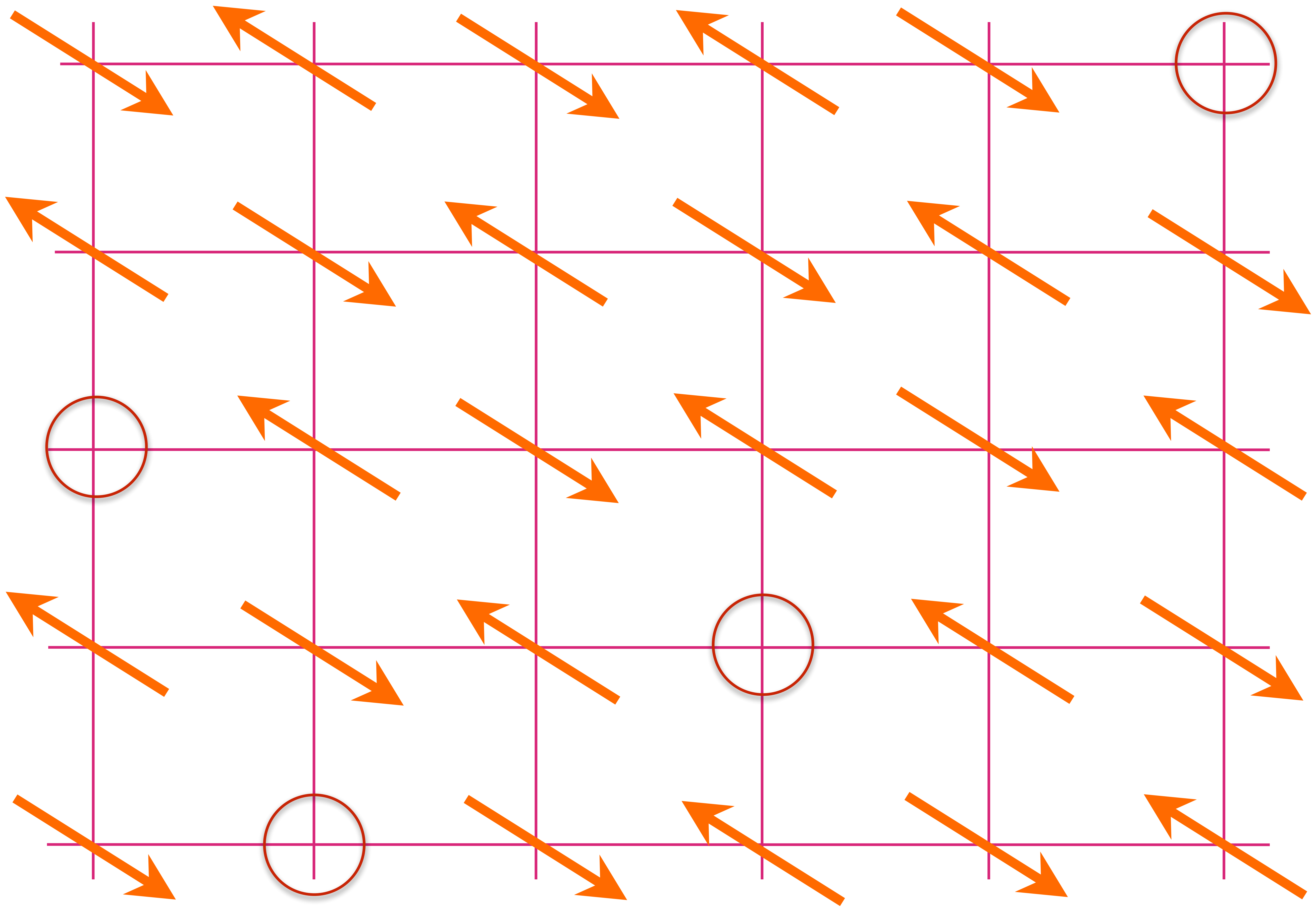

Anti-ferromagnet with p holes per square

Holon metal

S.A. Kivelson, D.S. Rokhsar and J.P. Sethna, PRB **35**, 8865 (1987)
D. Rokhsar and S.A. Kivelson, PRL **61**, 2376 (1988)

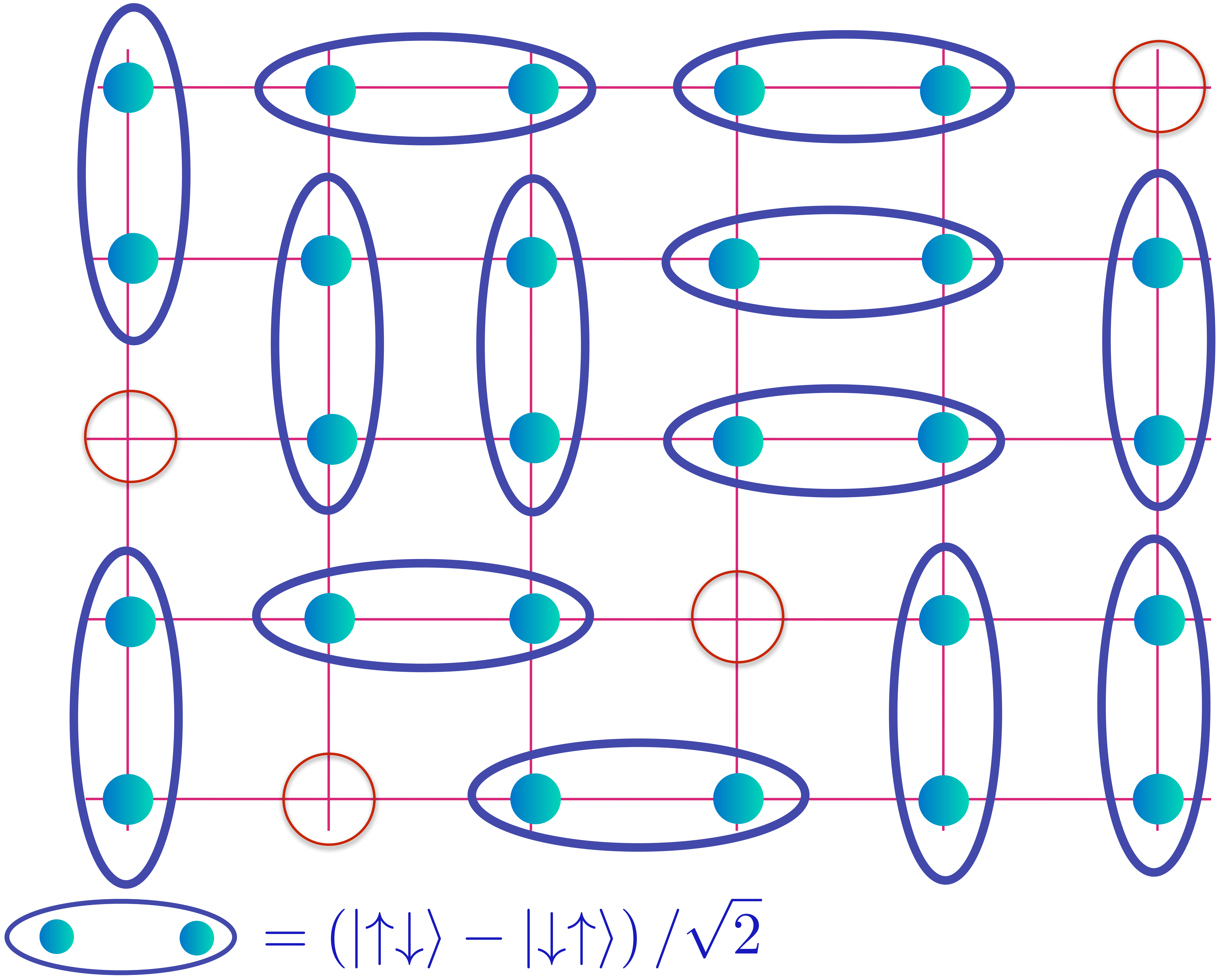

$$= \left(|\uparrow\downarrow\rangle - |\downarrow\uparrow\rangle\right)/\sqrt{2}$$

Spin liquid with density p of spinless, charge +e "holons".

Holon metal

S.A. Kivelson, D.S. Rokhsar and J.P. Sethna, PRB **35**, 8865 (1987)
D. Rokhsar and S.A. Kivelson, PRL **61**, 2376 (1988)

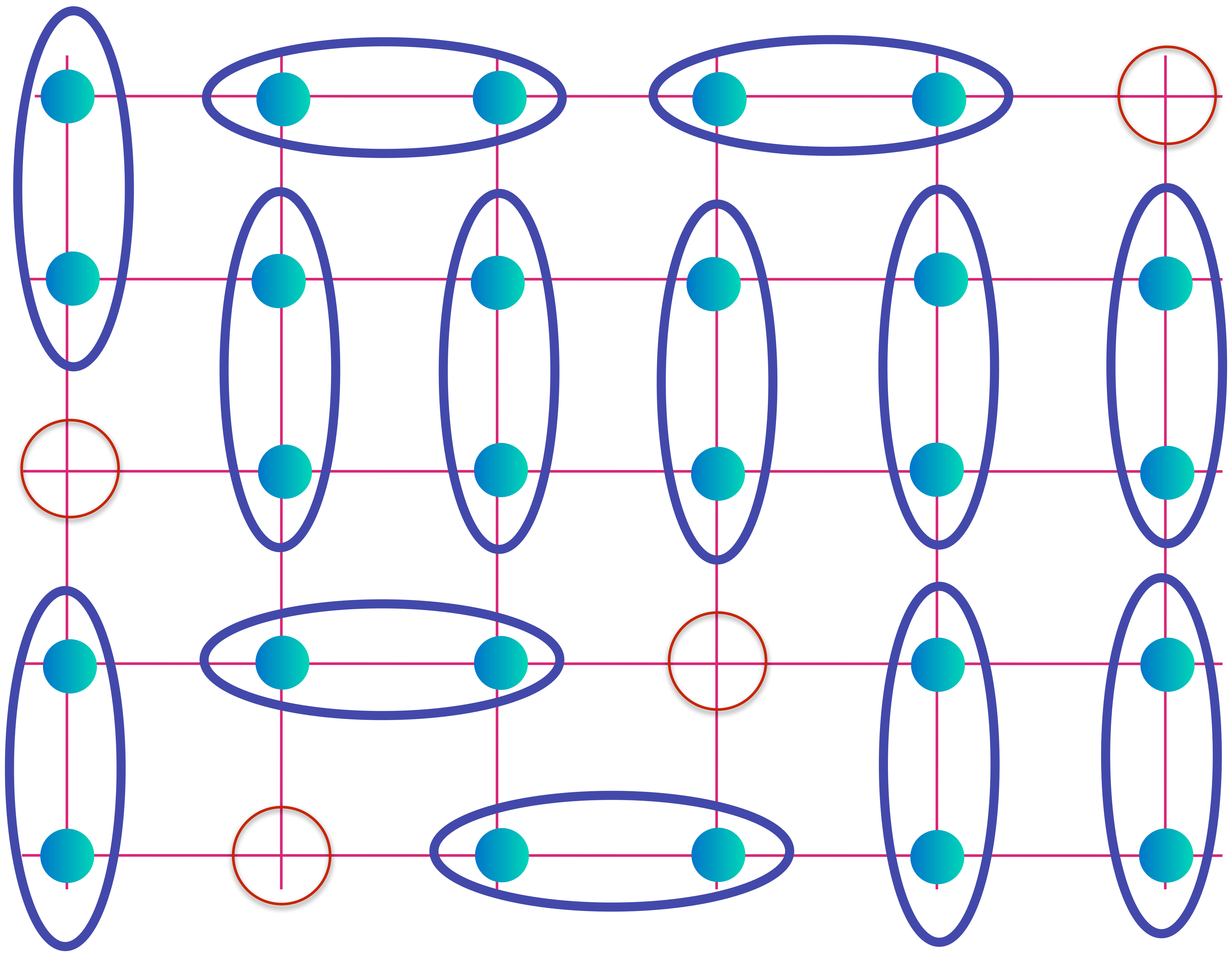

Spin liquid with density p of spinless, charge +e "holons".

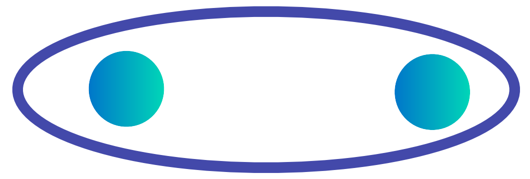

$$= \left(|\uparrow\downarrow\rangle - |\downarrow\uparrow\rangle \right) / \sqrt{2}$$

Holon metal

S.A. Kivelson, D.S. Rokhsar and J.P. Sethna, PRB **35**, 8865 (1987)
D. Rokhsar and S.A. Kivelson, PRL **61**, 2376 (1988)

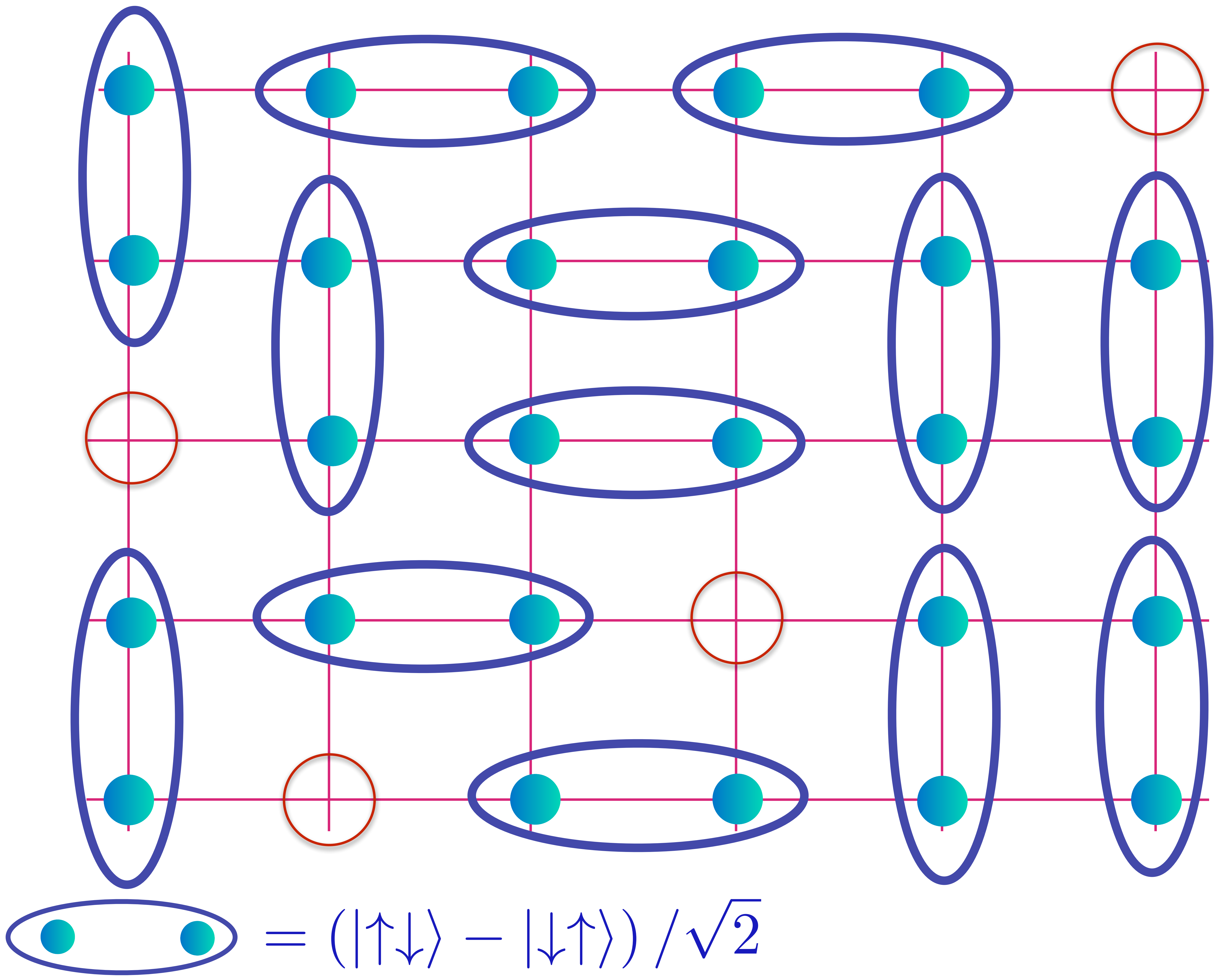

$$= \left(|\uparrow\downarrow\rangle - |\downarrow\uparrow\rangle\right)/\sqrt{2}$$

Spin liquid with density p of spinless, charge +e “holons”.

Holon metal

S.A. Kivelson, D.S. Rokhsar and J.P. Sethna, PRB **35**, 8865 (1987)
D. Rokhsar and S.A. Kivelson, PRL **61**, 2376 (1988)

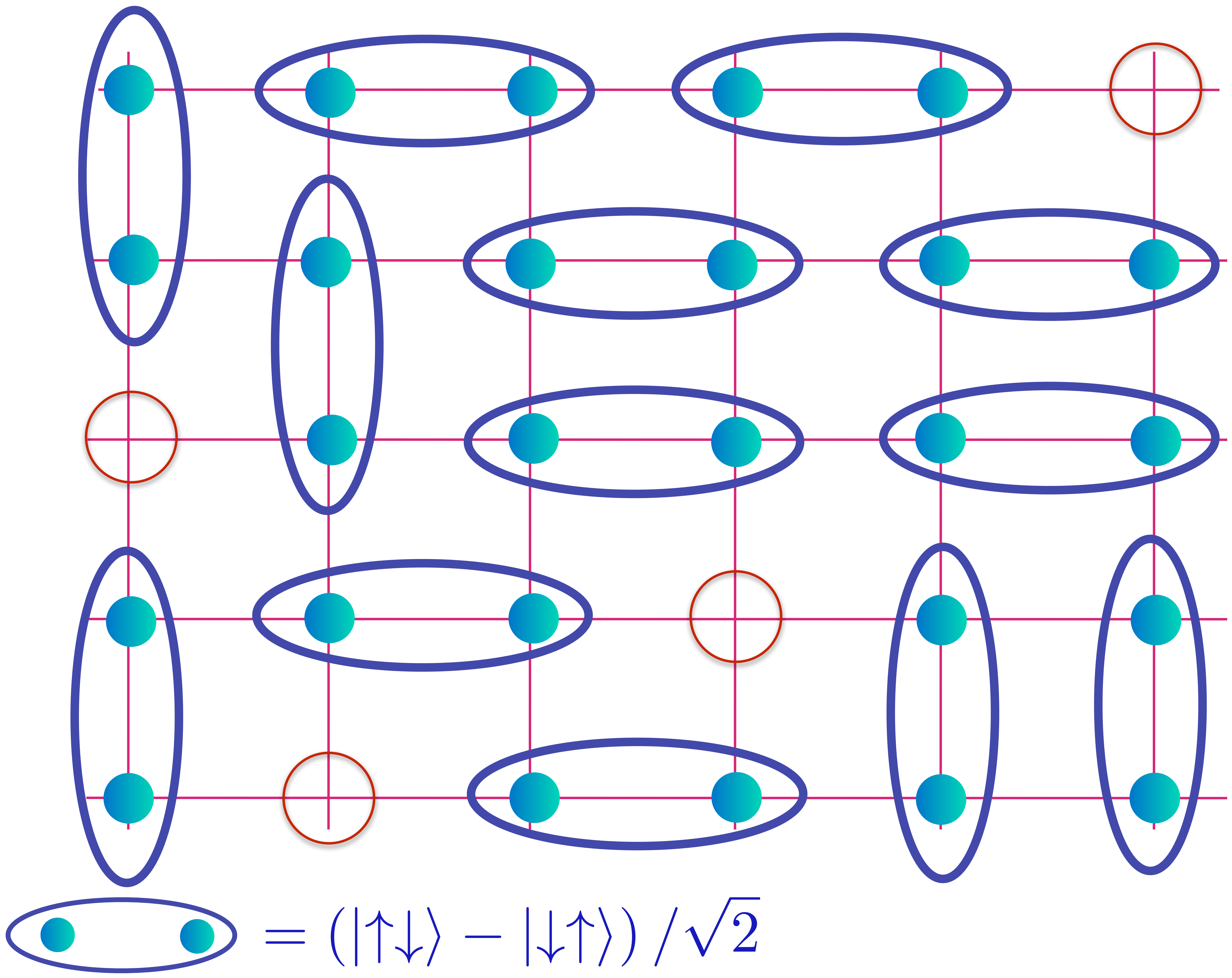

$$= \left(|\uparrow\downarrow\rangle - |\downarrow\uparrow\rangle\right)/\sqrt{2}$$

Spin liquid with density p of spinless, charge +e "holons".

Holon metal

S.A. Kivelson, D.S. Rokhsar and J.P. Sethna, PRB **35**, 8865 (1987)
D. Rokhsar and S.A. Kivelson, PRL **61**, 2376 (1988)

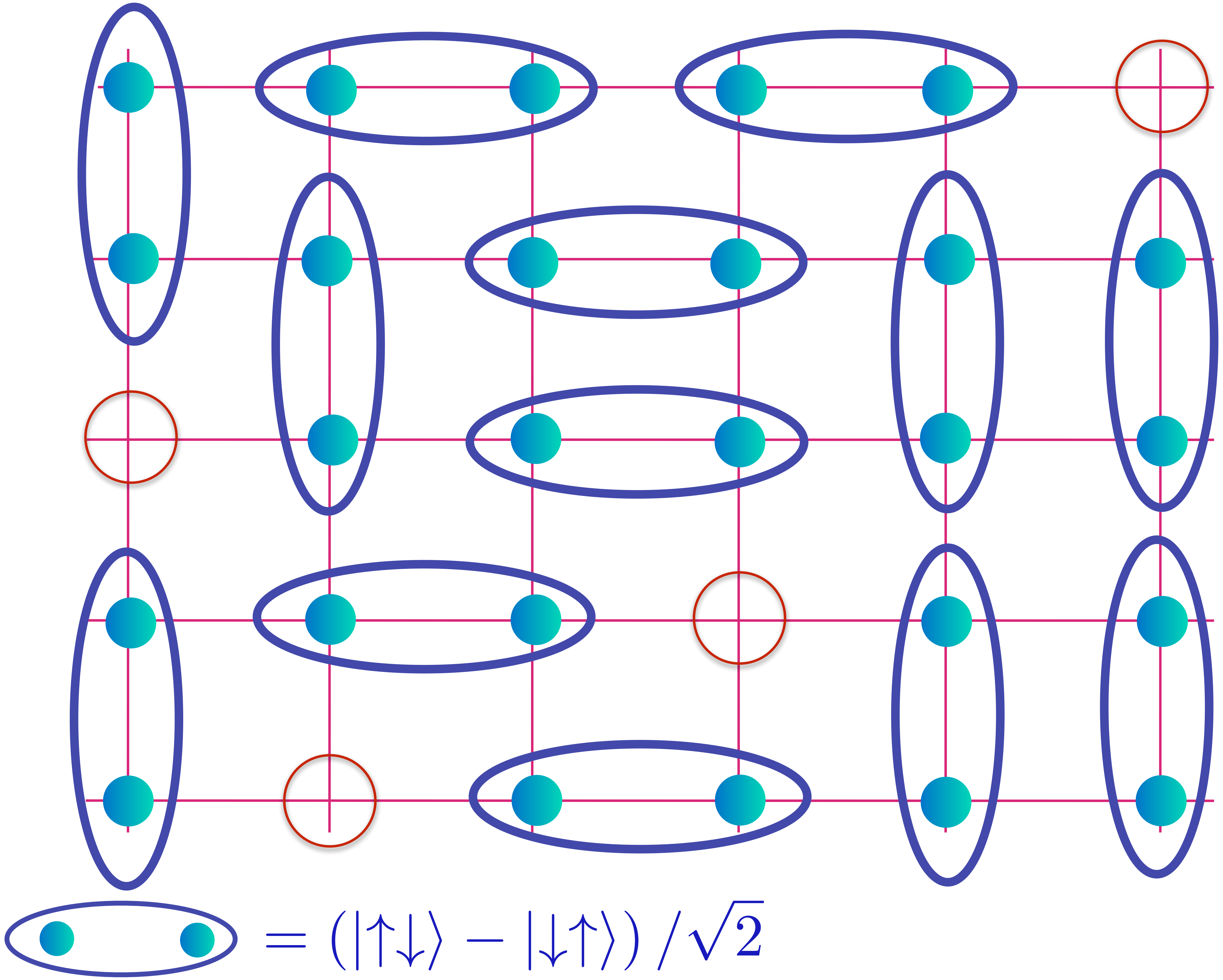

$= (|\uparrow\downarrow\rangle - |\downarrow\uparrow\rangle) / \sqrt{2}$

Spin liquid with density p of spinless, charge +e "holons".

Holon metal

S.A. Kivelson, D.S. Rokhsar and J.P. Sethna, PRB **35**, 8865 (1987)
D. Rokhsar and S.A. Kivelson, PRL **61**, 2376 (1988)

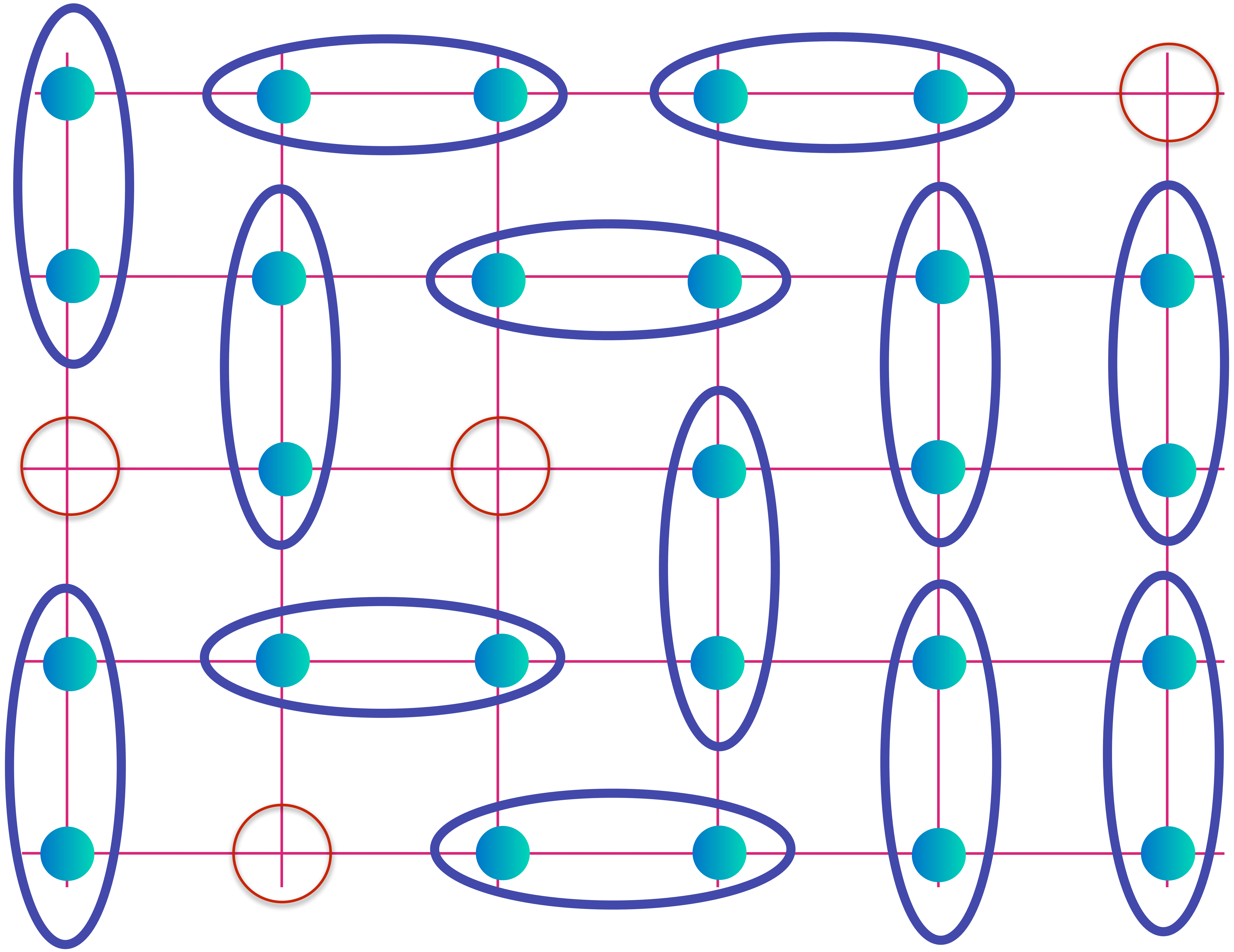

Spin liquid with density p of spinless, charge +e "holons".

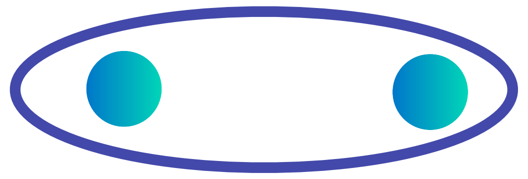

$$= \left(|\uparrow\downarrow\rangle - |\downarrow\uparrow\rangle\right)/\sqrt{2}$$

Holon metal

S.A. Kivelson, D.S. Rokhsar and J.P. Sethna, PRB **35**, 8865 (1987)
D. Rokhsar and S.A. Kivelson, PRL **61**, 2376 (1988)

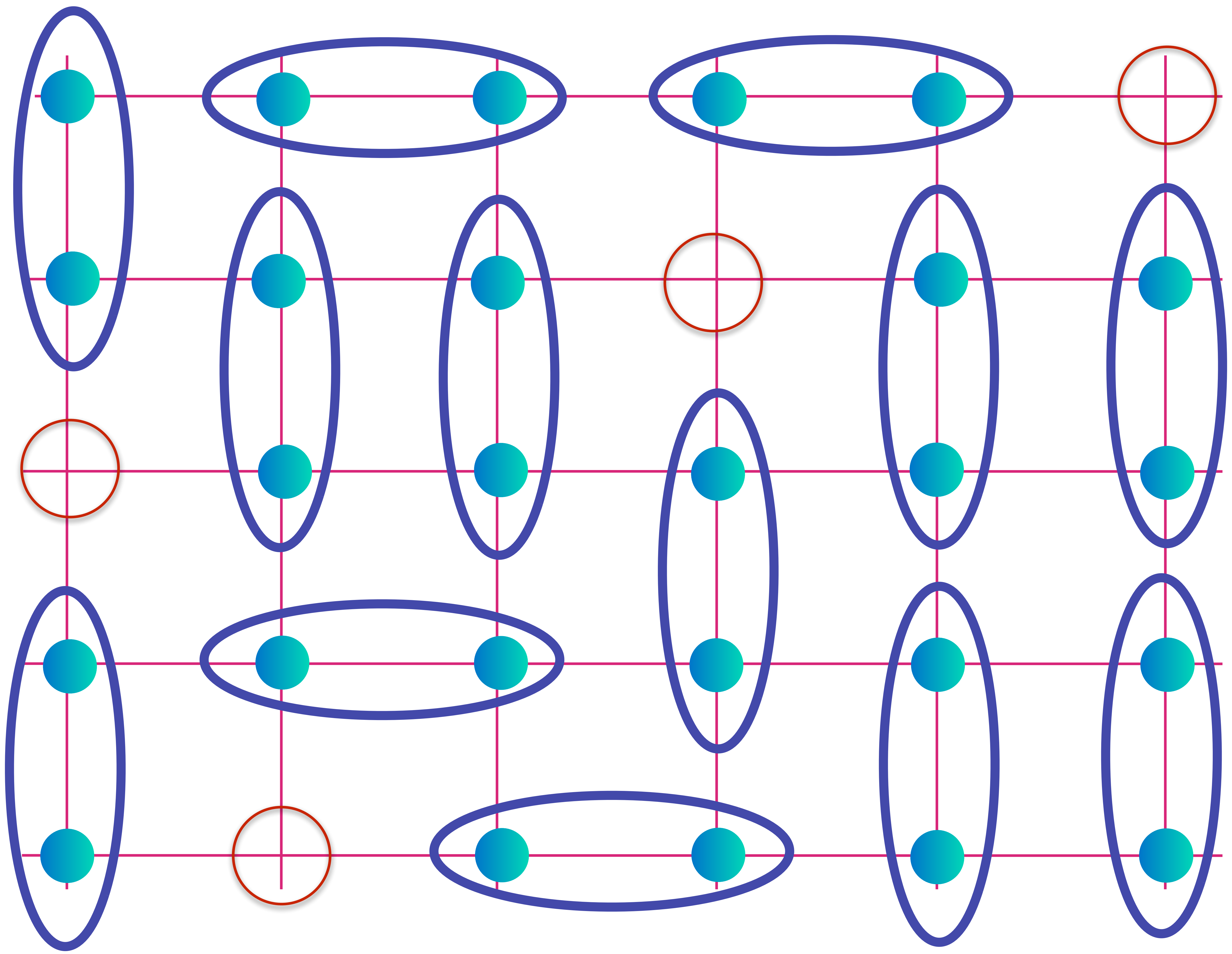

Spin liquid with density p of spinless, charge +e "holons".

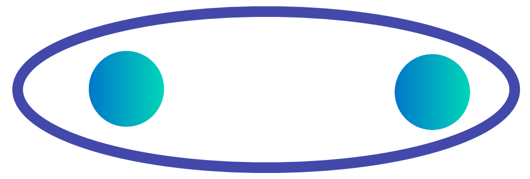

$$= \left(|\uparrow\downarrow\rangle - |\downarrow\uparrow\rangle\right)/\sqrt{2}$$

Holon metal

S.A. Kivelson, D.S. Rokhsar and J.P. Sethna, PRB **35**, 8865 (1987)
D. Rokhsar and S.A. Kivelson, PRL **61**, 2376 (1988)

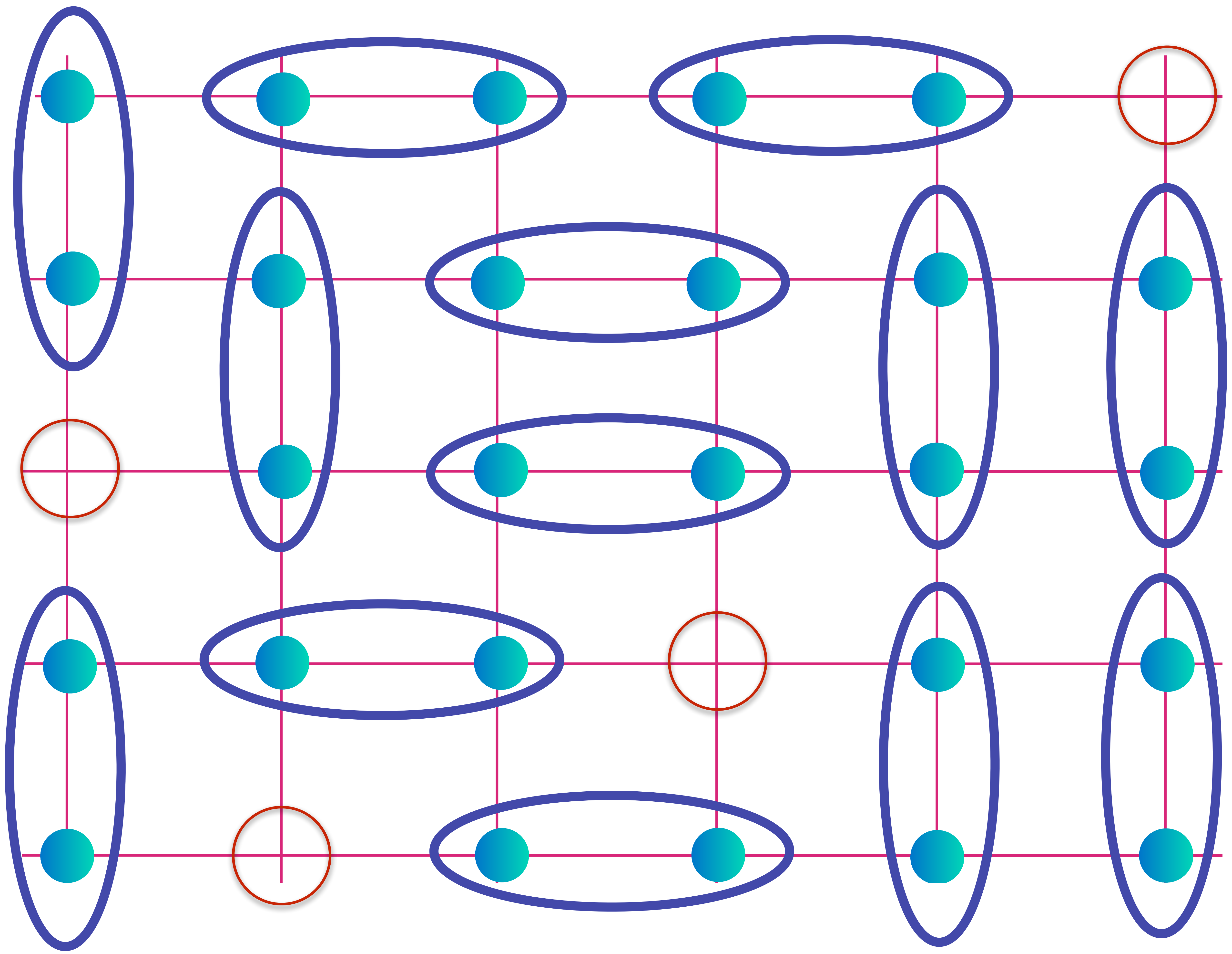

Spin liquid
with density
p of spinless,
charge +e
“holons”.

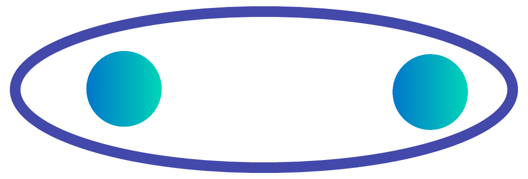 $= \left(|\uparrow\downarrow\rangle - |\downarrow\uparrow\rangle \right) / \sqrt{2}$

Holon metal

S.A. Kivelson, D.S. Rokhsar and J.P. Sethna, PRB **35**, 8865 (1987)
D. Rokhsar and S.A. Kivelson, PRL **61**, 2376 (1988)

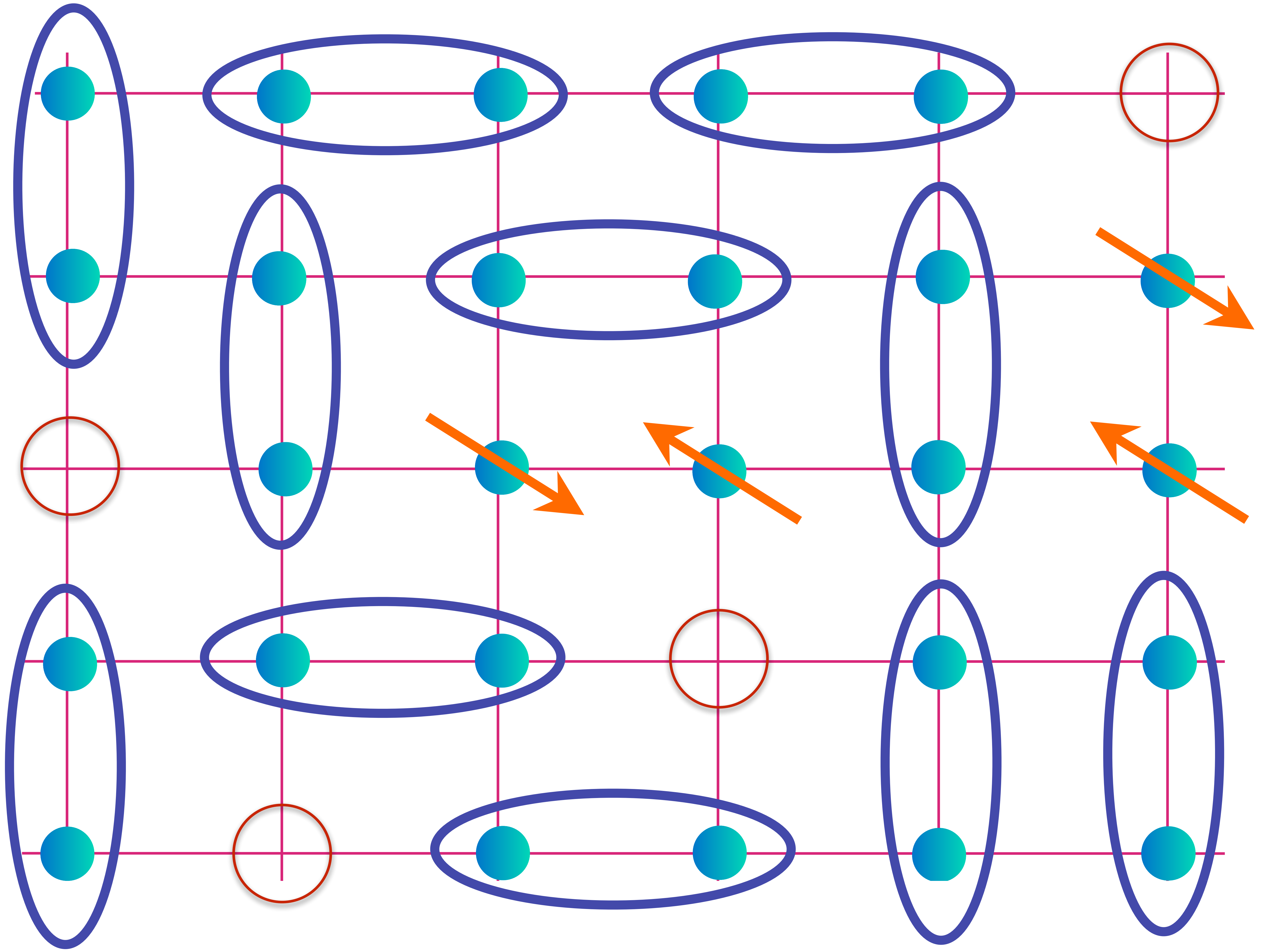

Spin liquid with density p of spinless, charge +e "holons" and charge 0, spin-1/2 "spinons".

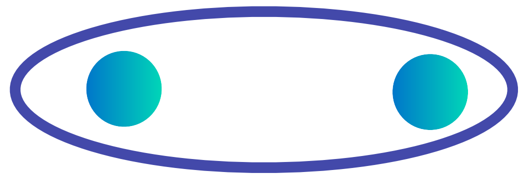 $= (|\uparrow\downarrow\rangle - |\downarrow\uparrow\rangle)/\sqrt{2}$

Holon metal

S.A. Kivelson, D.S. Rokhsar and J.P. Sethna, PRB **35**, 8865 (1987)
D. Rokhsar and S.A. Kivelson, PRL **61**, 2376 (1988)

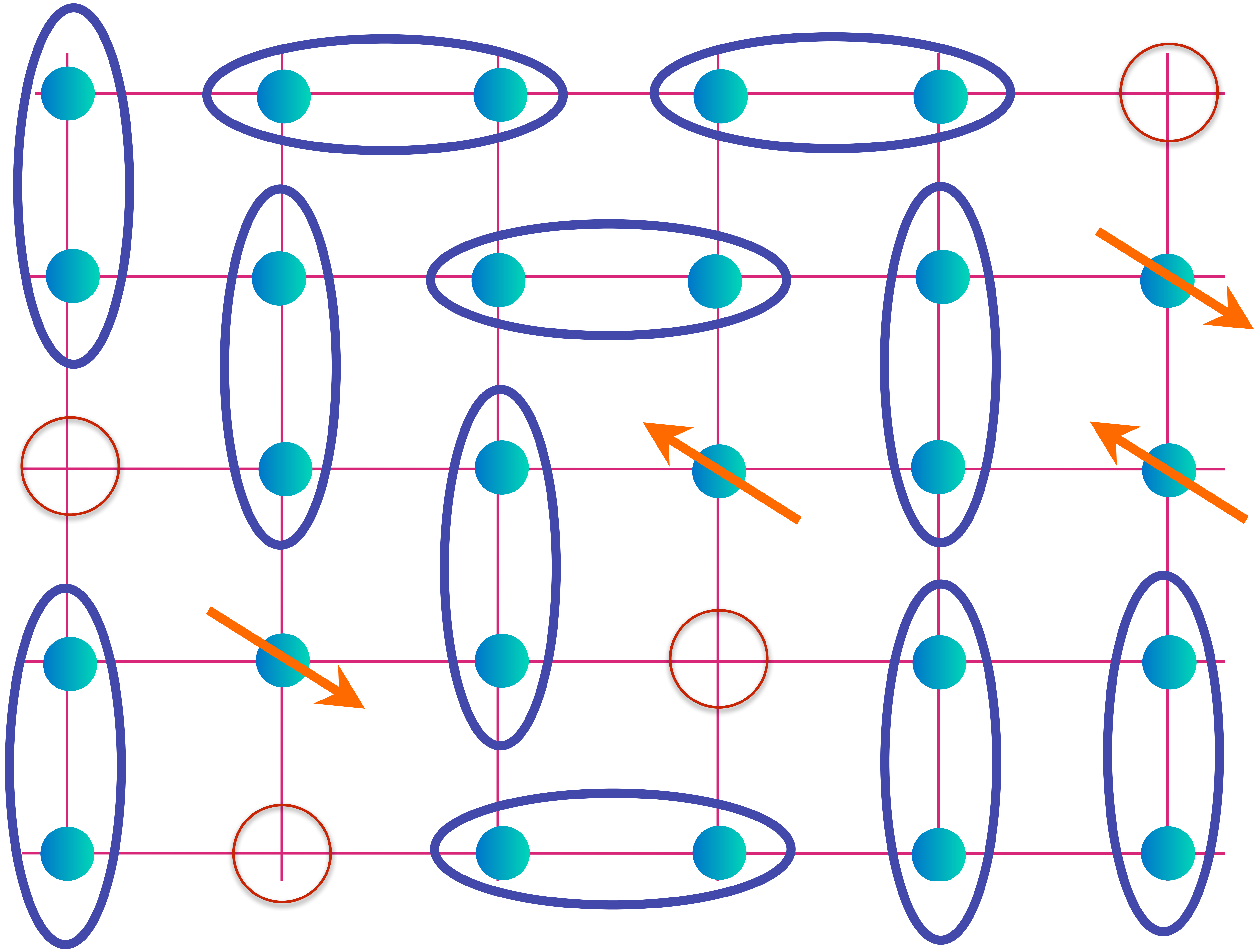

Spin liquid with density p of spinless, charge +e "holons" and charge 0, spin-1/2 "spinons".

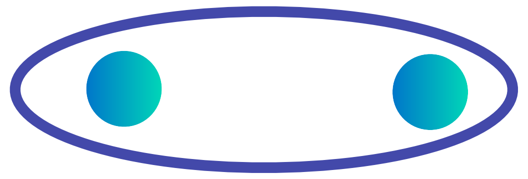 $= \left(|\uparrow\downarrow\rangle - |\downarrow\uparrow\rangle\right)/\sqrt{2}$

Holon metal

S.A. Kivelson, D.S. Rokhsar and J.P. Sethna, PRB **35**, 8865 (1987)
D. Rokhsar and S.A. Kivelson, PRL **61**, 2376 (1988)

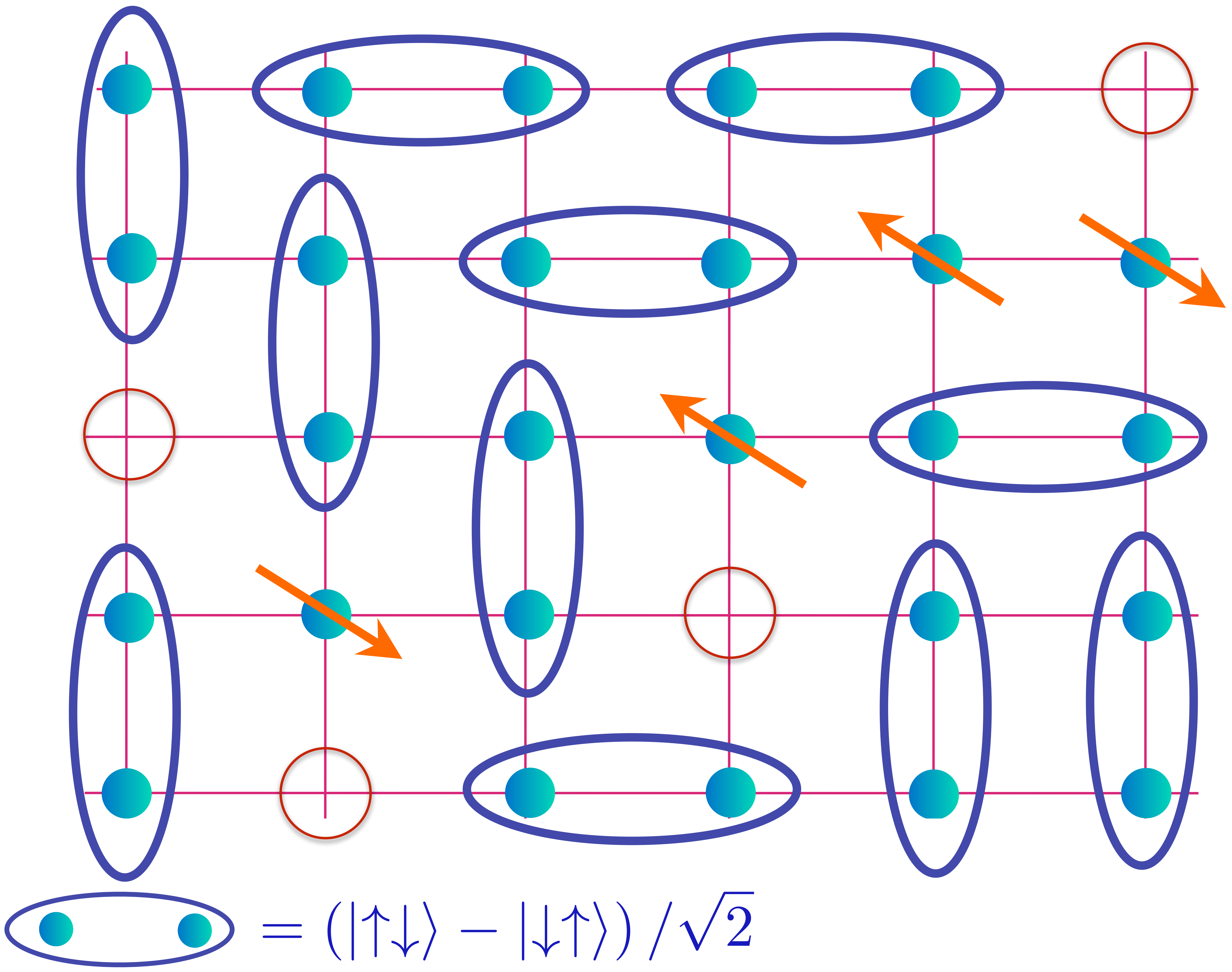

$$= \left(|\uparrow\downarrow\rangle - |\downarrow\uparrow\rangle\right)/\sqrt{2}$$

Spin liquid with density p of spinless, charge +e "holons" and charge 0, spin-1/2 "spinons".

Holon metal

S.A. Kivelson, D.S. Rokhsar and J.P. Sethna, PRB **35**, 8865 (1987)
D. Rokhsar and S.A. Kivelson, PRL **61**, 2376 (1988)

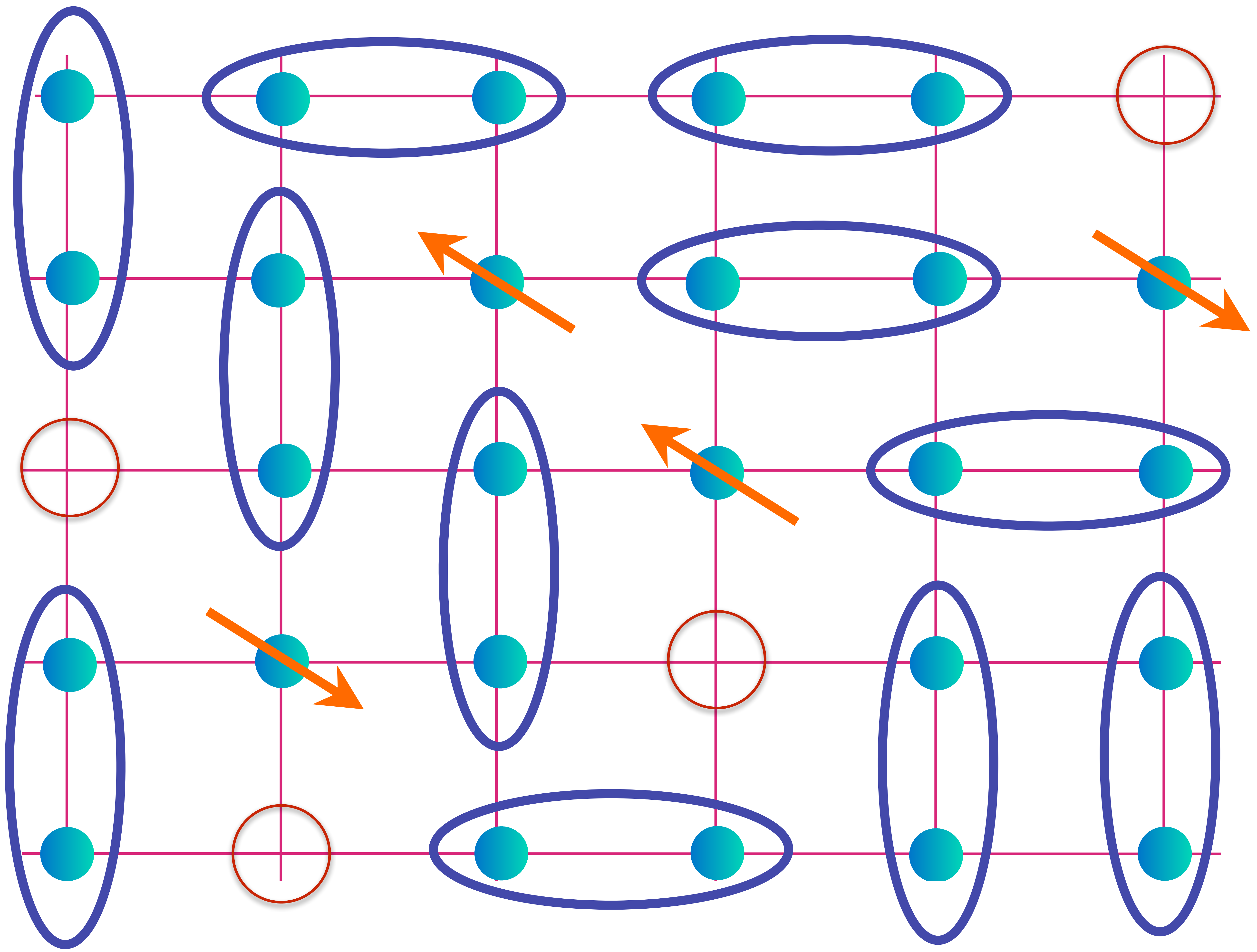

Spin liquid with density p of spinless, charge +e "holons" and charge 0, spin-1/2 "spinons".

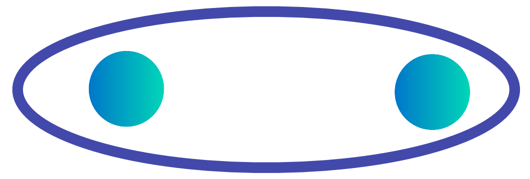

$$= \left(|\uparrow\downarrow\rangle - |\downarrow\uparrow\rangle \right) / \sqrt{2}$$

Holon metal

S.A. Kivelson, D.S. Rokhsar and J.P. Sethna, PRB **35**, 8865 (1987)
D. Rokhsar and S.A. Kivelson, PRL **61**, 2376 (1988)

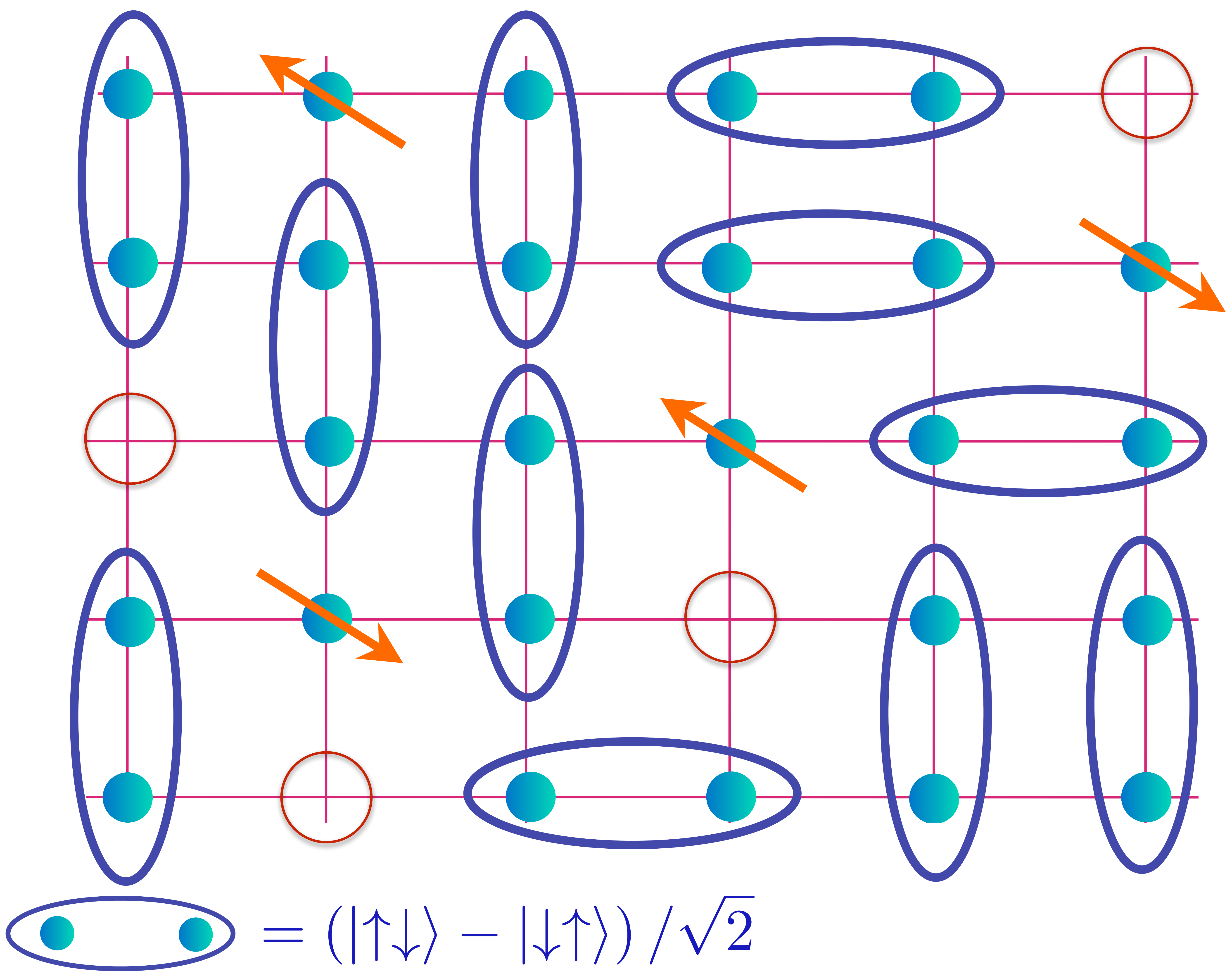

Spin liquid with density p of spinless, charge +e "holons" and charge 0, spin-1/2 "spinons".

$$= \left(|\uparrow\downarrow\rangle - |\downarrow\uparrow\rangle\right)/\sqrt{2}$$

Holon metal

S.A. Kivelson, D.S. Rokhsar and J.P. Sethna, PRB **35**, 8865 (1987)
D. Rokhsar and S.A. Kivelson, PRL **61**, 2376 (1988)

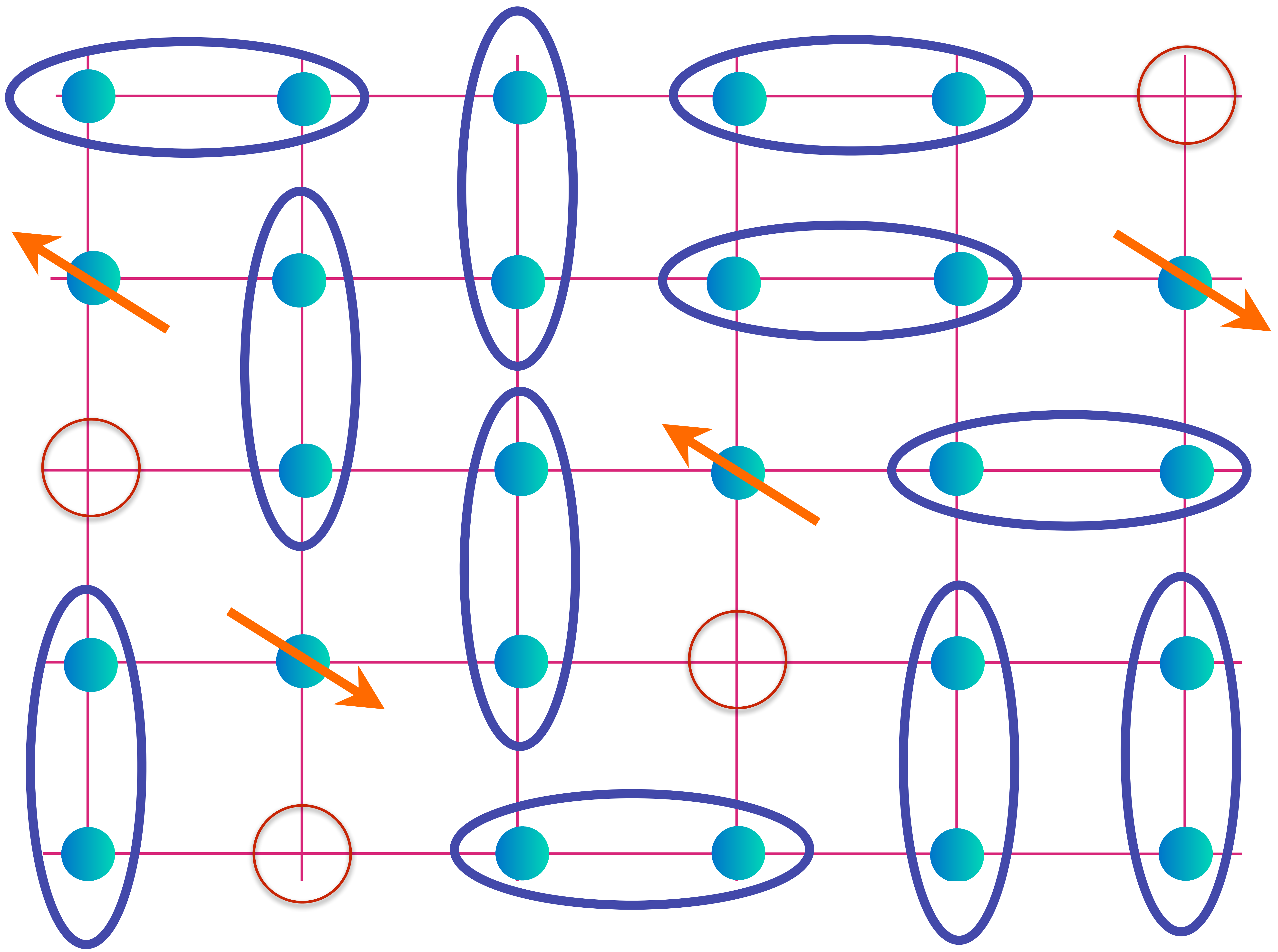

Spin liquid with density p of spinless, charge +e "holons" and charge 0, spin-1/2 "spinons".

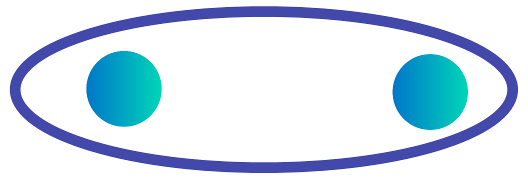

$$= \left(|\uparrow\downarrow\rangle - |\downarrow\uparrow\rangle\right)/\sqrt{2}$$

Holon metal

S.A. Kivelson, D.S. Rokhsar and J.P. Sethna, PRB **35**, 8865 (1987)
D. Rokhsar and S.A. Kivelson, PRL **61**, 2376 (1988)

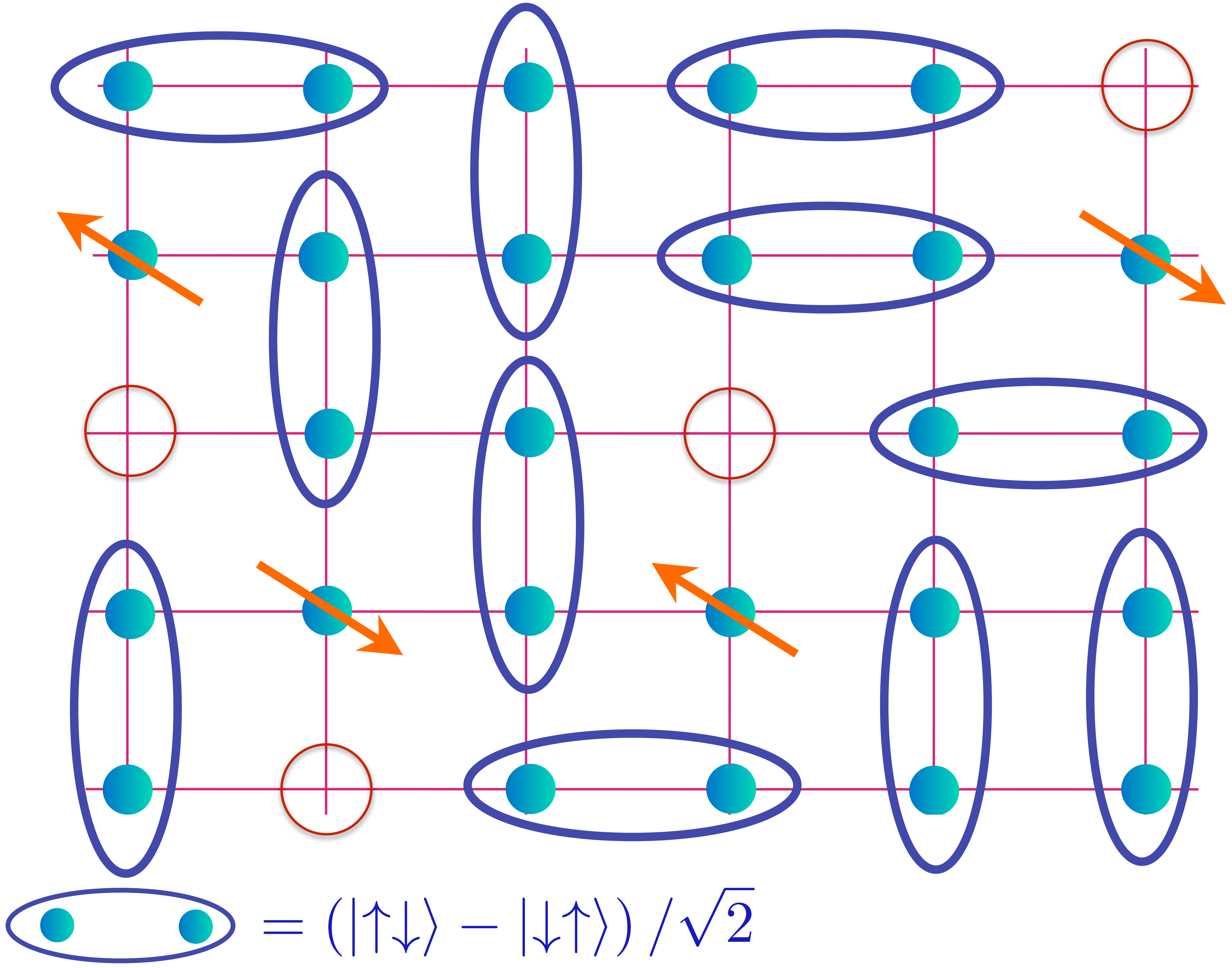

$$= \left(|\uparrow\downarrow\rangle - |\downarrow\uparrow\rangle \right) / \sqrt{2}$$

Spin liquid with density p of spinless, charge +e "holons" and charge 0, spin-1/2 "spinons".

Holon metal

S.A. Kivelson, D.S. Rokhsar and J.P. Sethna, PRB **35**, 8865 (1987)
D. Rokhsar and S.A. Kivelson, PRL **61**, 2376 (1988)

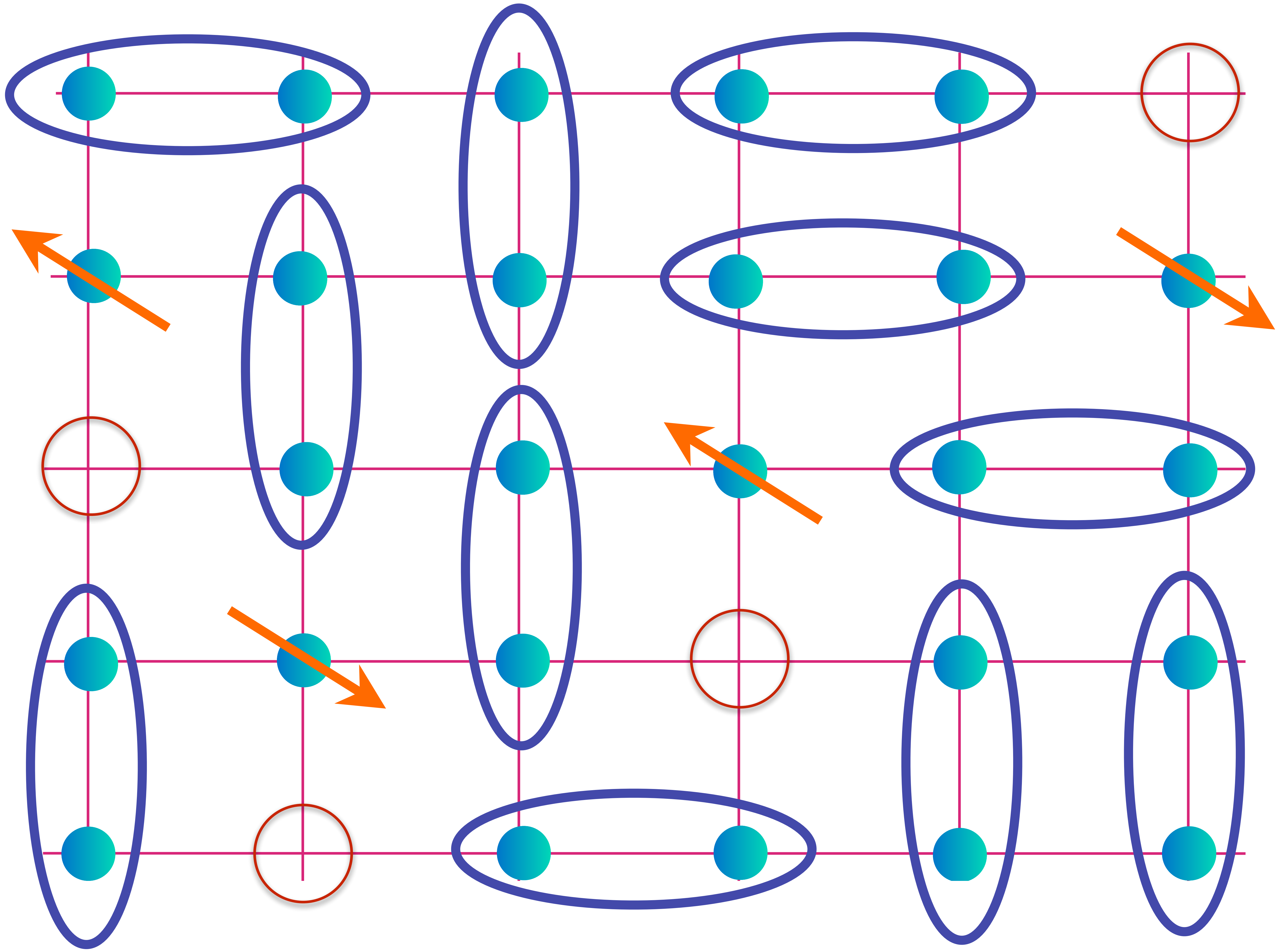

Spin liquid with density p of spinless, charge +e "holons" and charge 0, spin-1/2 "spinons".

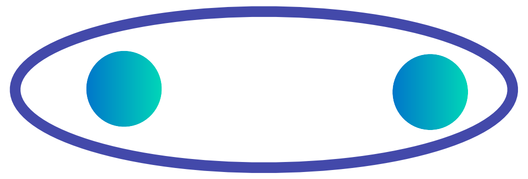

$$= \left(|\uparrow\downarrow\rangle - |\downarrow\uparrow\rangle\right)/\sqrt{2}$$

FL*

S. Sachdev PRB **49**, 6770 (1994); X.-G. Wen and P.A. Lee PRL **76**, 503 (1996)
R. K. Kaul, A. Kolezhuk, M. Levin, S. Sachdev, and T. Senthil, PRB **75**, 235122 (2007)

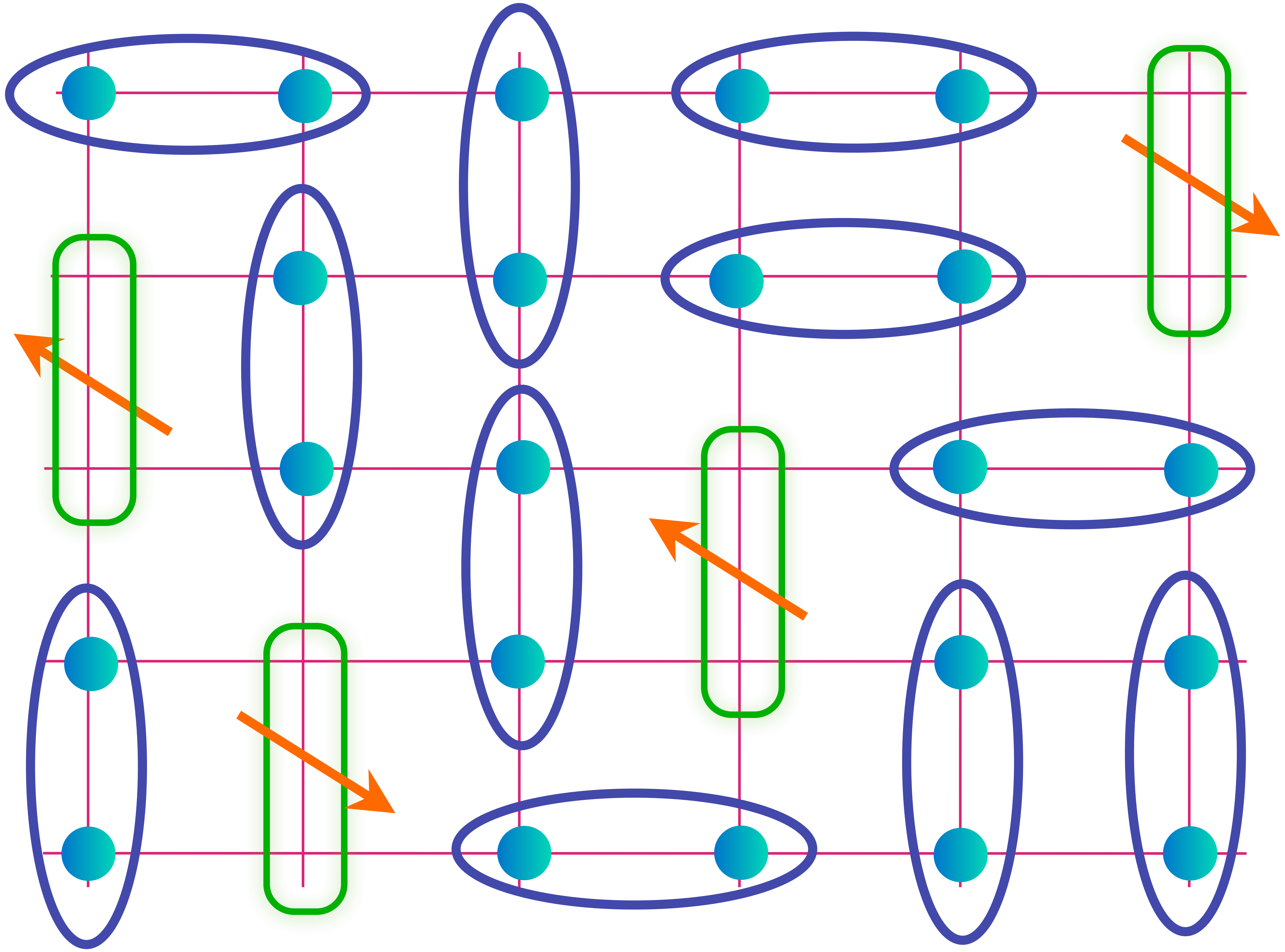

Each green "dimer" is a "bound state" of a vacancy and a free spin

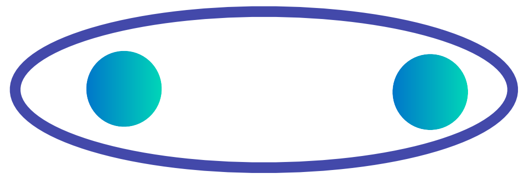 $= \left(|\uparrow\downarrow\rangle - |\downarrow\uparrow\rangle\right)/\sqrt{2}$

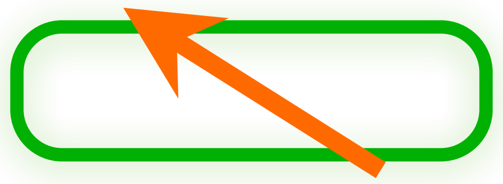 $= \left(|\uparrow\circ\rangle + |\circ\uparrow\rangle\right)/\sqrt{2}$

M. Punk, A. Allais, and S. Sachdev, PNAS **112**, 9552 (2015)

FL*

S. Sachdev PRB **49**, 6770 (1994); X.-G. Wen and P.A. Lee PRL **76**, 503 (1996)
R. K. Kaul, A. Kolezhuk, M. Levin, S. Sachdev, and T. Senthil, PRB **75**, 235122 (2007)

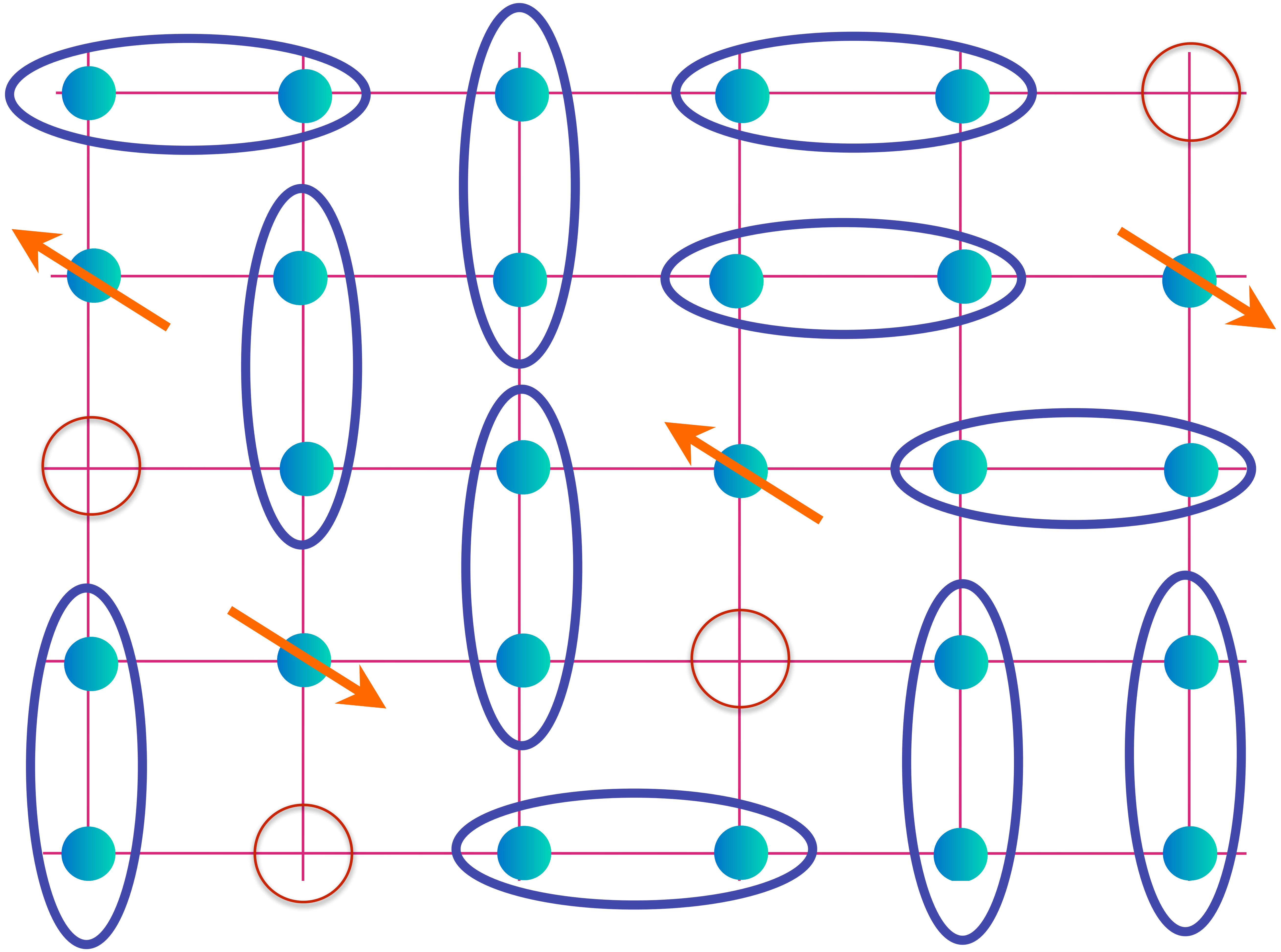

Each green "dimer" is a "bound state" of a vacancy and a free spin

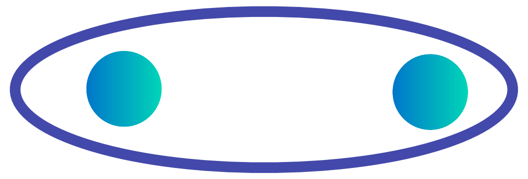 $= \left(|\uparrow\downarrow\rangle - |\downarrow\uparrow\rangle\right)/\sqrt{2}$

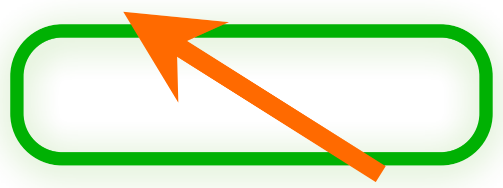 $= \left(|\uparrow\circ\rangle + |\circ\uparrow\rangle\right)/\sqrt{2}$

M. Punk, A. Allais, and S. Sachdev, PNAS **112**, 9552 (2015)

FL*

S. Sachdev PRB **49**, 6770 (1994); X.-G. Wen and P.A. Lee PRL **76**, 503 (1996)
R. K. Kaul, A. Kolezhuk, M. Levin, S. Sachdev, and T. Senthil, PRB **75**, 235122 (2007)

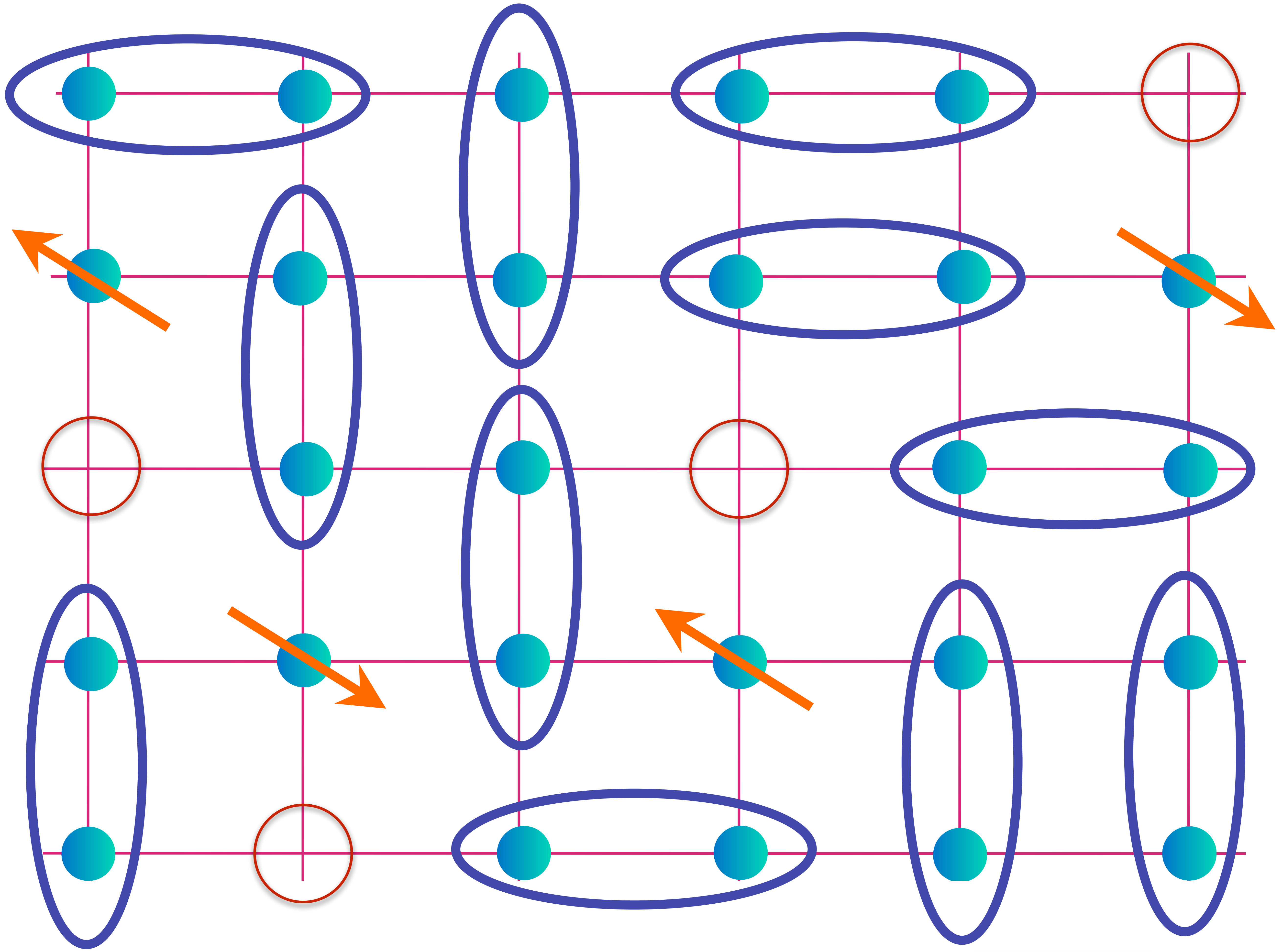

Each green "dimer" is a "bound state" of a vacancy and a free spin

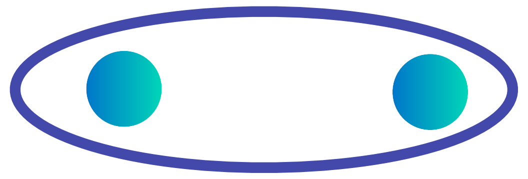
$= \left(|\uparrow\downarrow\rangle - |\downarrow\uparrow\rangle\right)/\sqrt{2}$

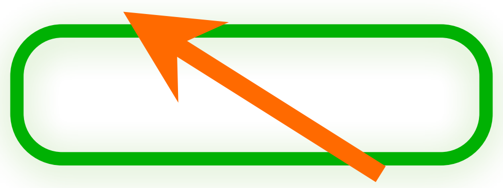
$= \left(|\uparrow \circ\rangle + |\circ \uparrow\rangle\right)/\sqrt{2}$

M. Punk, A. Allais, and S. Sachdev, PNAS **112**, 9552 (2015)

FL*

S. Sachdev PRB **49**, 6770 (1994); X.-G. Wen and P.A. Lee PRL **76**, 503 (1996)
R. K. Kaul, A. Kolezhuk, M. Levin, S. Sachdev, and T. Senthil, PRB **75**, 235122 (2007)

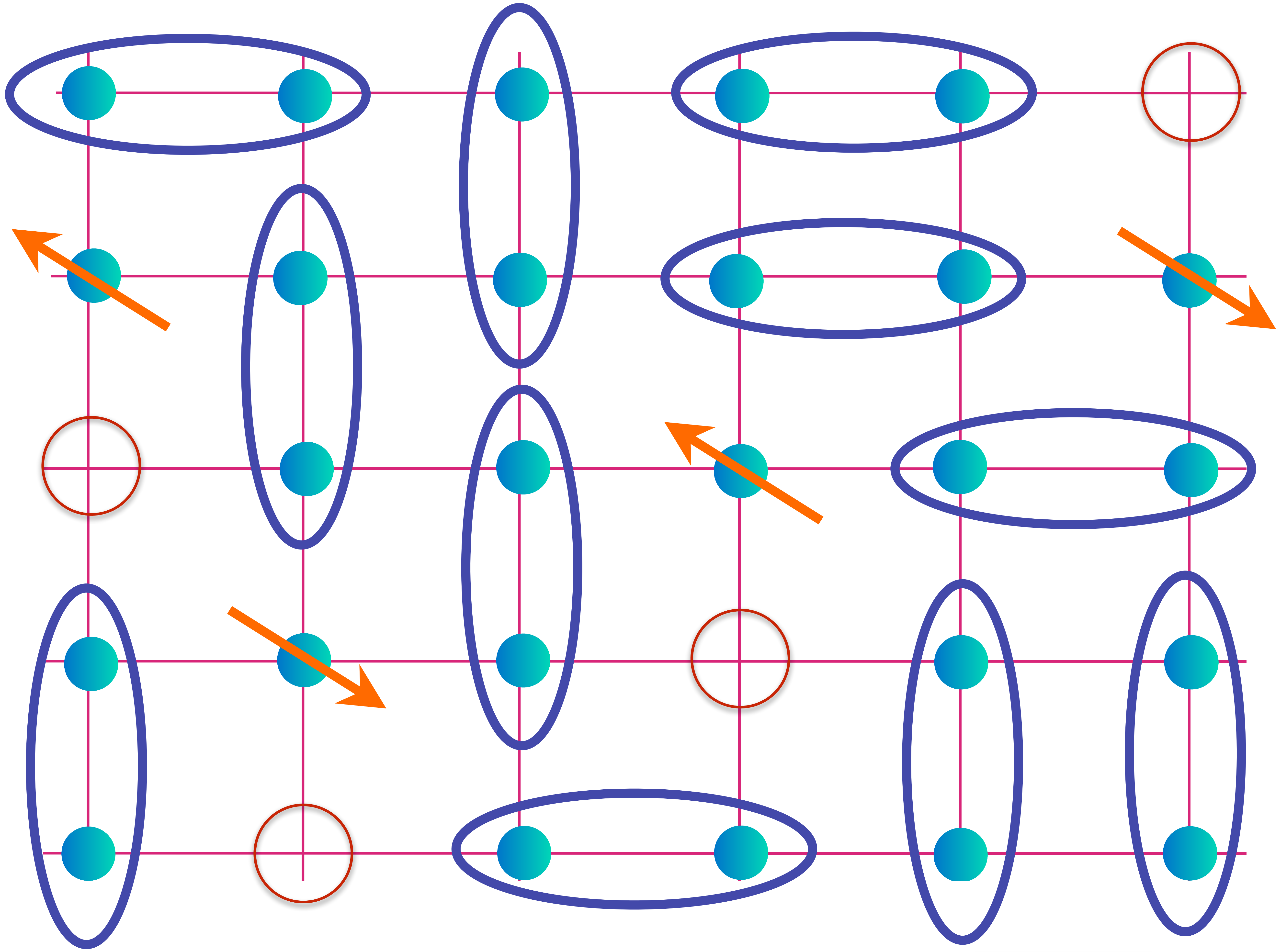

Each green “dimer” is a “bound state” of a vacancy and a free spin

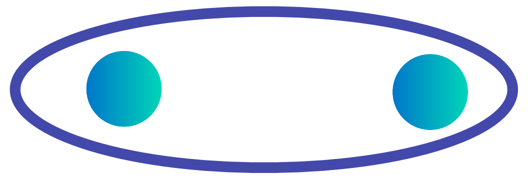 $= \left(|\uparrow\downarrow\rangle - |\downarrow\uparrow\rangle\right)/\sqrt{2}$

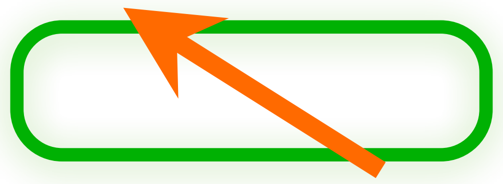 $= \left(|\uparrow \circ\rangle + |\circ \uparrow\rangle\right)/\sqrt{2}$

M. Punk, A. Allais, and S. Sachdev, PNAS **112**, 9552 (2015)

FL*

S. Sachdev PRB **49**, 6770 (1994); X.-G. Wen and P.A. Lee PRL **76**, 503 (1996)
R. K. Kaul, A. Kolezhuk, M. Levin, S. Sachdev, and T. Senthil, PRB **75**, 235122 (2007)

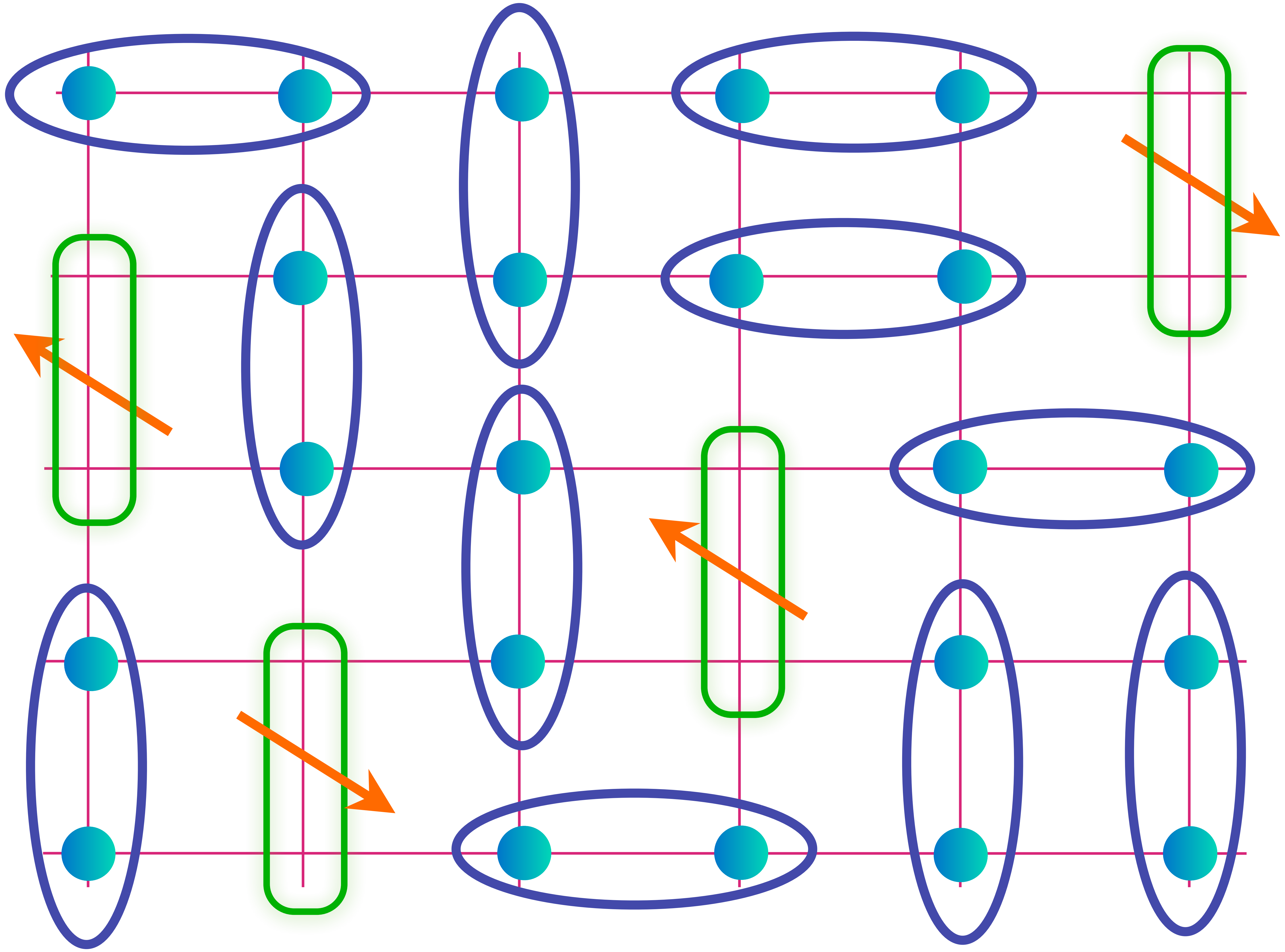

Metal with electron-like quasiparticles on a Fermi surface of size p, and emergent gauge fields

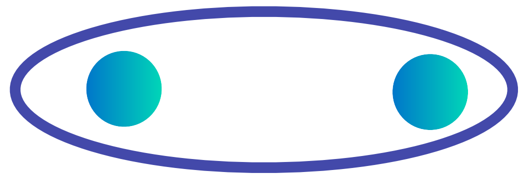 $= \left(|\uparrow\downarrow\rangle - |\downarrow\uparrow\rangle\right)/\sqrt{2}$

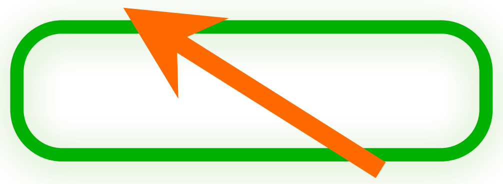 $= \left(|\uparrow\circ\rangle + |\circ\uparrow\rangle\right)/\sqrt{2}$

M. Punk, A. Allais, and S. Sachdev, PNAS **112**, 9552 (2015)

FL*

S. Sachdev PRB **49**, 6770 (1994); X.-G. Wen and P.A. Lee PRL **76**, 503 (1996)

R. K. Kaul, A. Kolezhuk, M. Levin, S. Sachdev, and T. Senthil, PRB **75**, 235122 (2007)

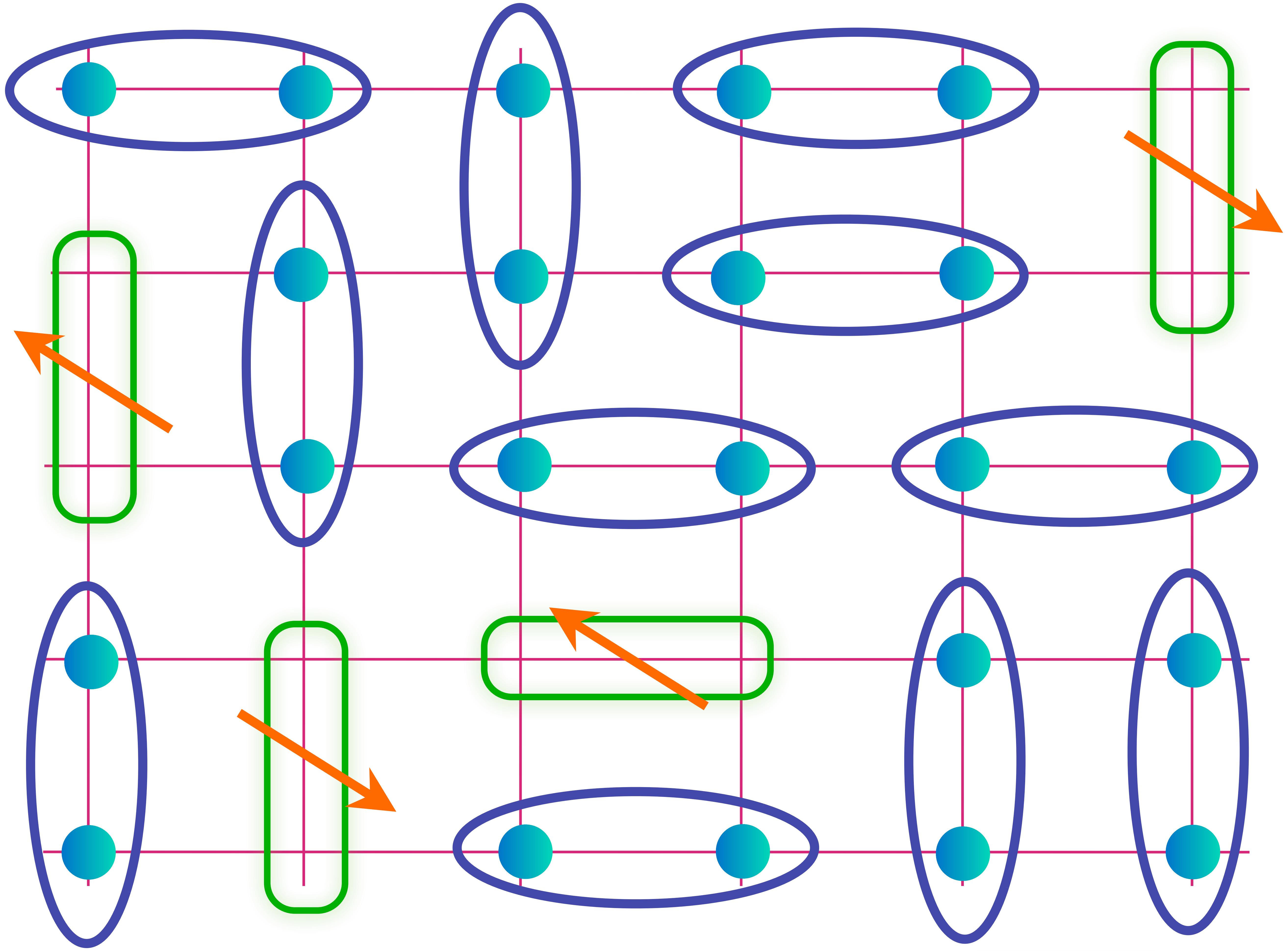

Metal with electron-like quasiparticles on a Fermi surface of size p, and emergent gauge fields

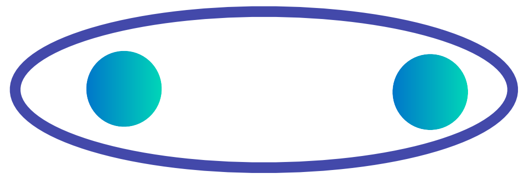

$= (|\uparrow\downarrow\rangle - |\downarrow\uparrow\rangle) / \sqrt{2}$

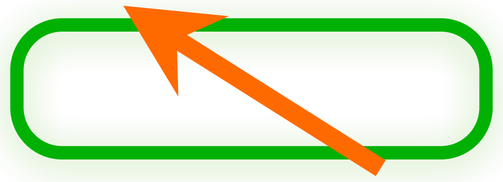

$= (|\uparrow \circ\rangle + |\circ \uparrow\rangle) / \sqrt{2}$

M. Punk, A. Allais, and S. Sachdev, PNAS **112**, 9552 (2015)

FL*

S. Sachdev PRB **49**, 6770 (1994); X.-G. Wen and P.A. Lee PRL **76**, 503 (1996)
R. K. Kaul, A. Kolezhuk, M. Levin, S. Sachdev, and T. Senthil, PRB **75**, 235122 (2007)

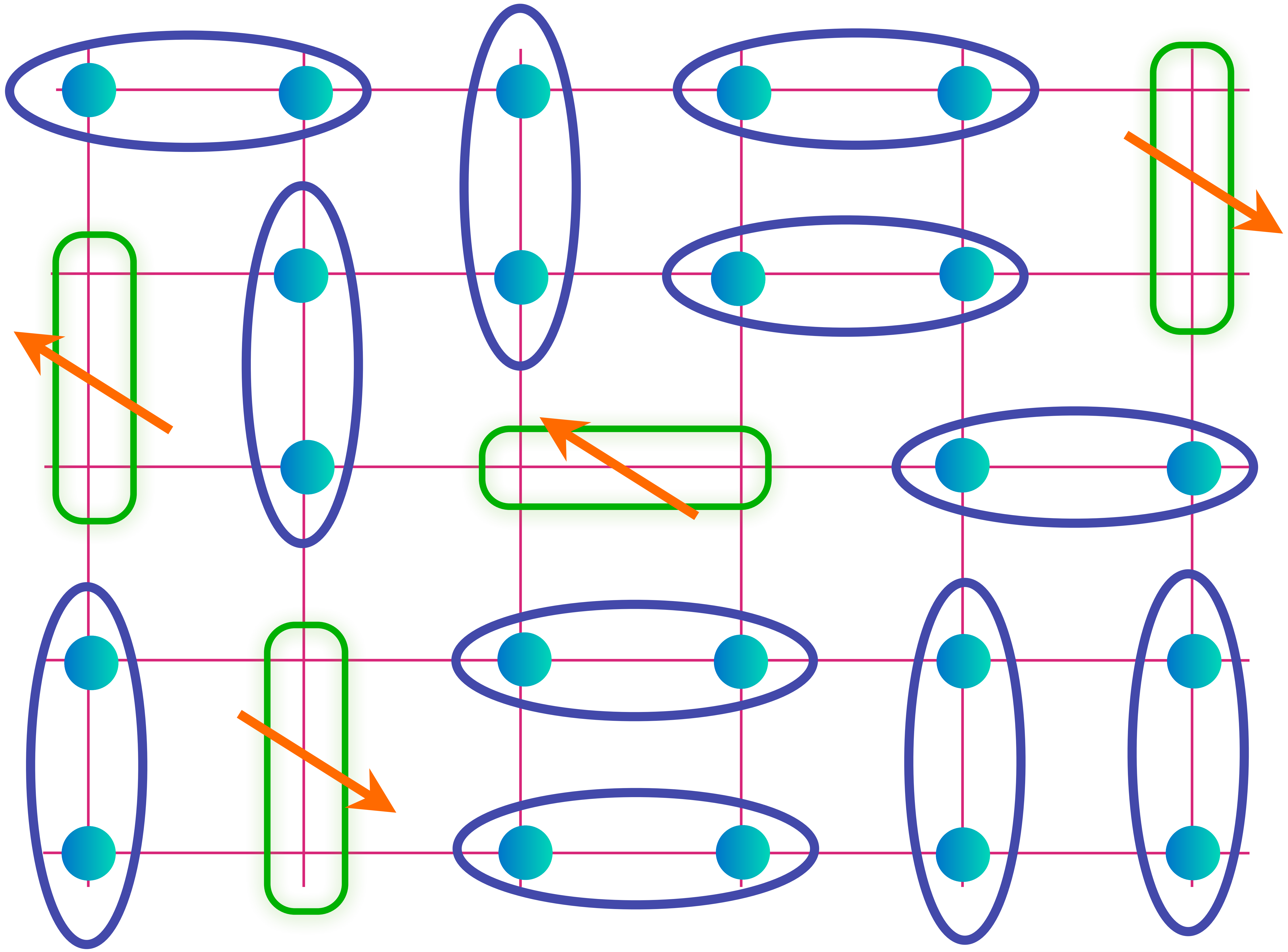

Metal with electron-like quasiparticles on a Fermi surface of size p, and emergent gauge fields

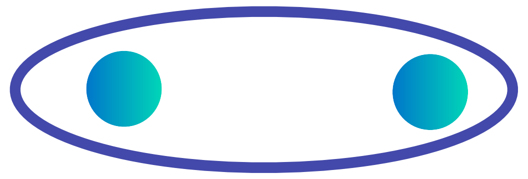

$= \left(|\uparrow\downarrow\rangle - |\downarrow\uparrow\rangle\right)/\sqrt{2}$

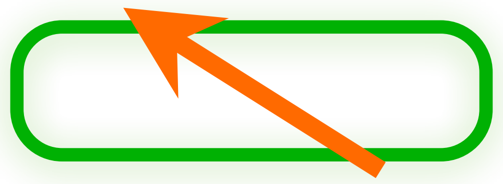

$= \left(|\uparrow\circ\rangle + |\circ\uparrow\rangle\right)/\sqrt{2}$

M. Punk, A. Allais, and S. Sachdev, PNAS **112**, 9552 (2015)

FL*

S. Sachdev PRB **49**, 6770 (1994); X.-G. Wen and P.A. Lee PRL **76**, 503 (1996)

R. K. Kaul, A. Kolezhuk, M. Levin, S. Sachdev, and T. Senthil, PRB **75**, 235122 (2007)

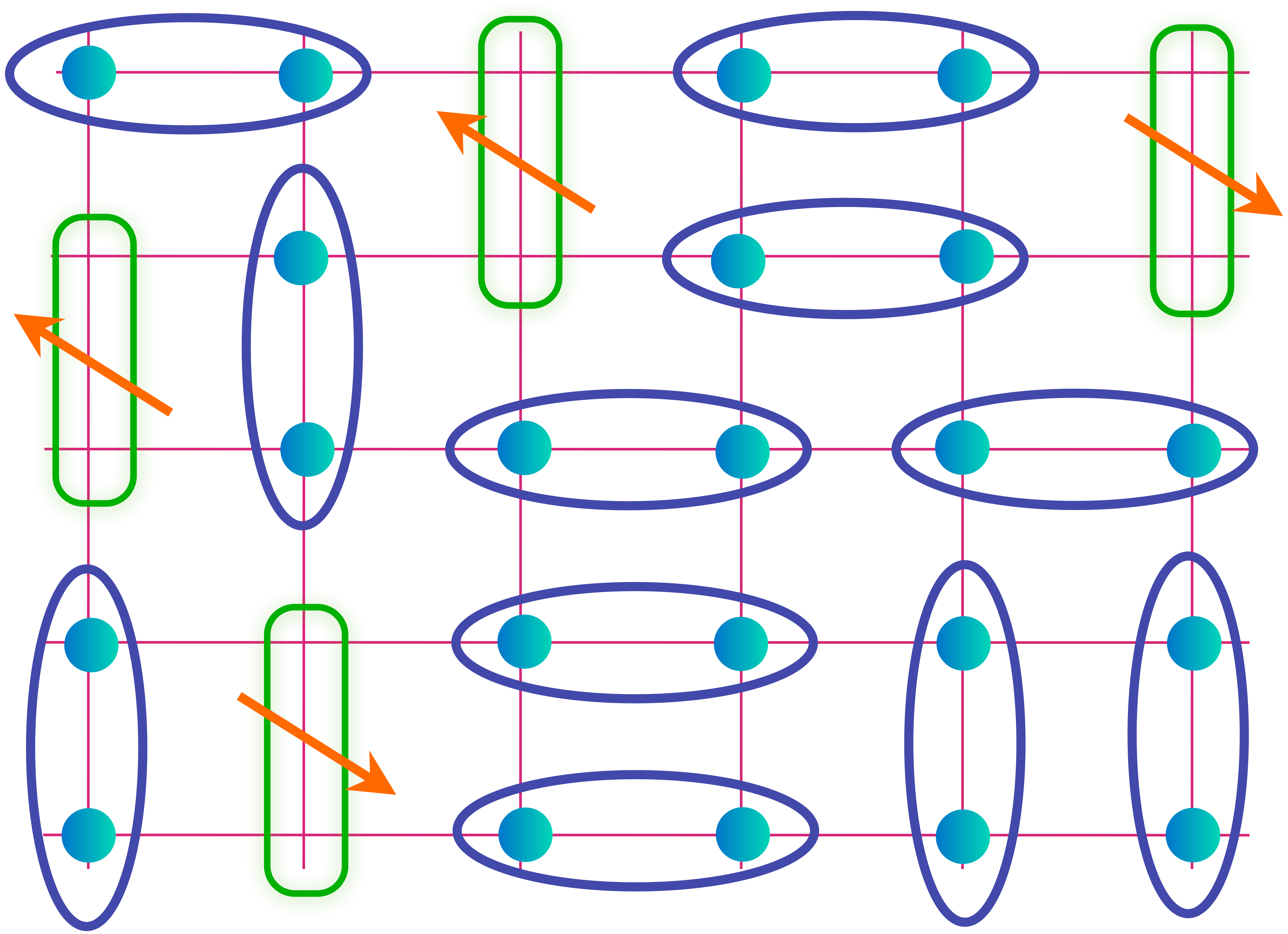

Metal with electron-like quasiparticles on a Fermi surface of size p, and emergent gauge fields

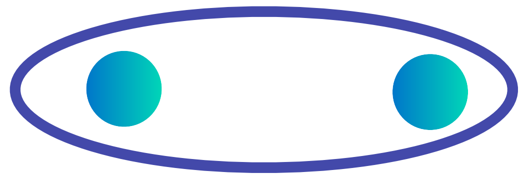 $= \left(|\uparrow\downarrow\rangle - |\downarrow\uparrow\rangle\right)/\sqrt{2}$

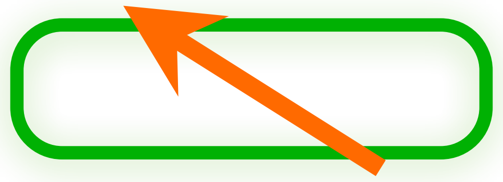 $= \left(|\uparrow \circ\rangle + |\circ \uparrow\rangle\right)/\sqrt{2}$

M. Punk, A. Allais, and S. Sachdev, PNAS **112**, 9552 (2015)

FL*

S. Sachdev PRB **49**, 6770 (1994); X.-G. Wen and P.A. Lee PRL **76**, 503 (1996)
R. K. Kaul, A. Kolezhuk, M. Levin, S. Sachdev, and T. Senthil, PRB **75**, 235122 (2007)

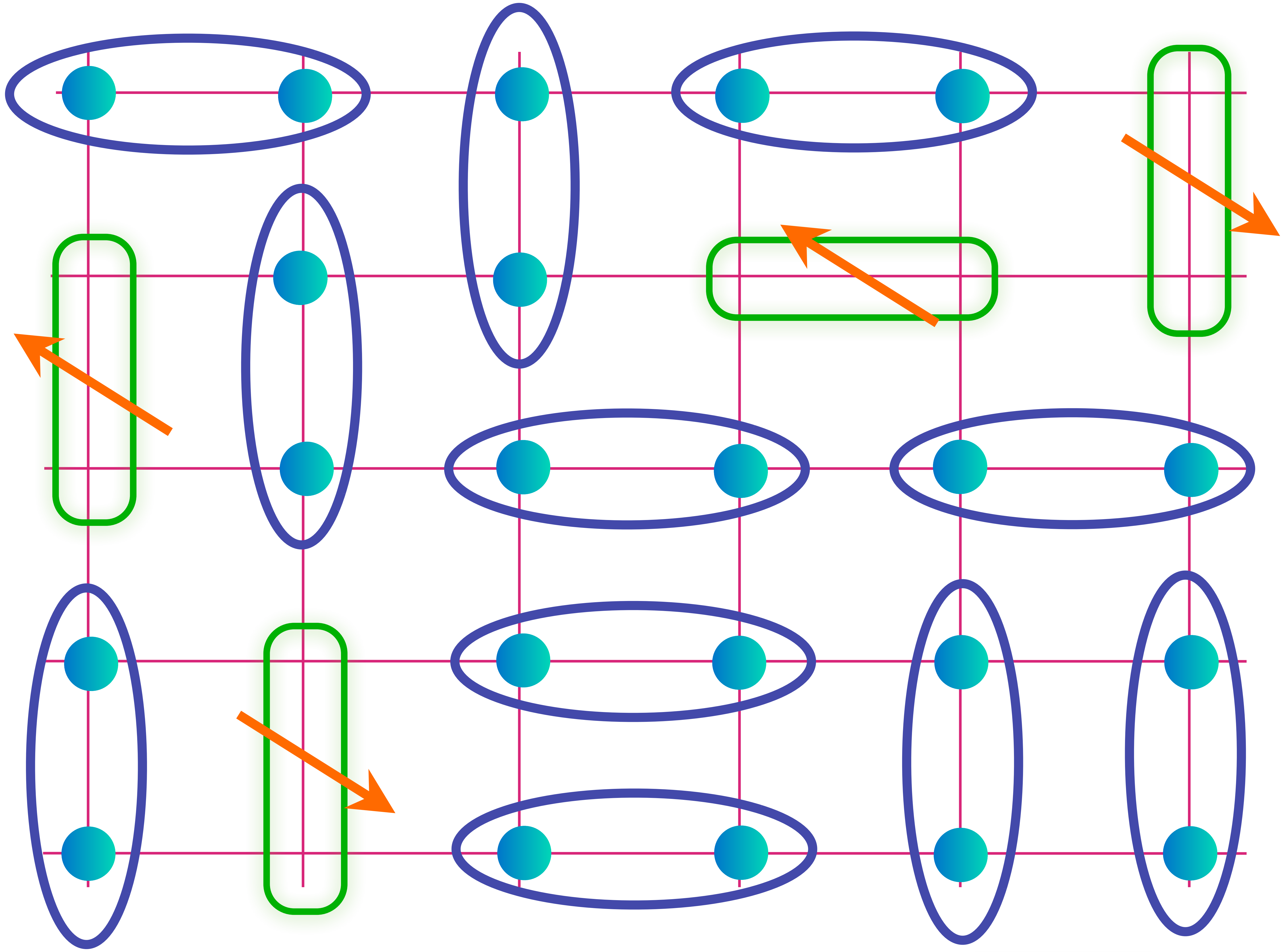

Metal with electron-like quasiparticles on a Fermi surface of size p, and emergent gauge fields

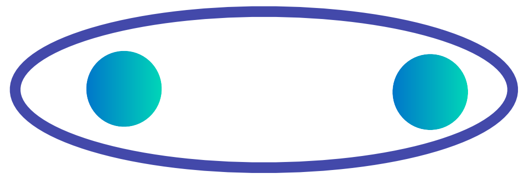

$= \left(|\uparrow\downarrow\rangle - |\downarrow\uparrow\rangle \right) / \sqrt{2}$

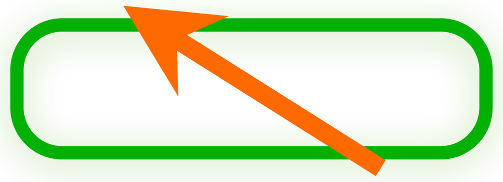

$= \left(|\uparrow \circ\rangle + |\circ \uparrow\rangle \right) / \sqrt{2}$

M. Punk, A. Allais, and S. Sachdev, PNAS **112**, 9552 (2015)

FL*

S. Sachdev PRB **49**, 6770 (1994); X.-G. Wen and P.A. Lee PRL **76**, 503 (1996)
R. K. Kaul, A. Kolezhuk, M. Levin, S. Sachdev, and T. Senthil, PRB **75**, 235122 (2007)

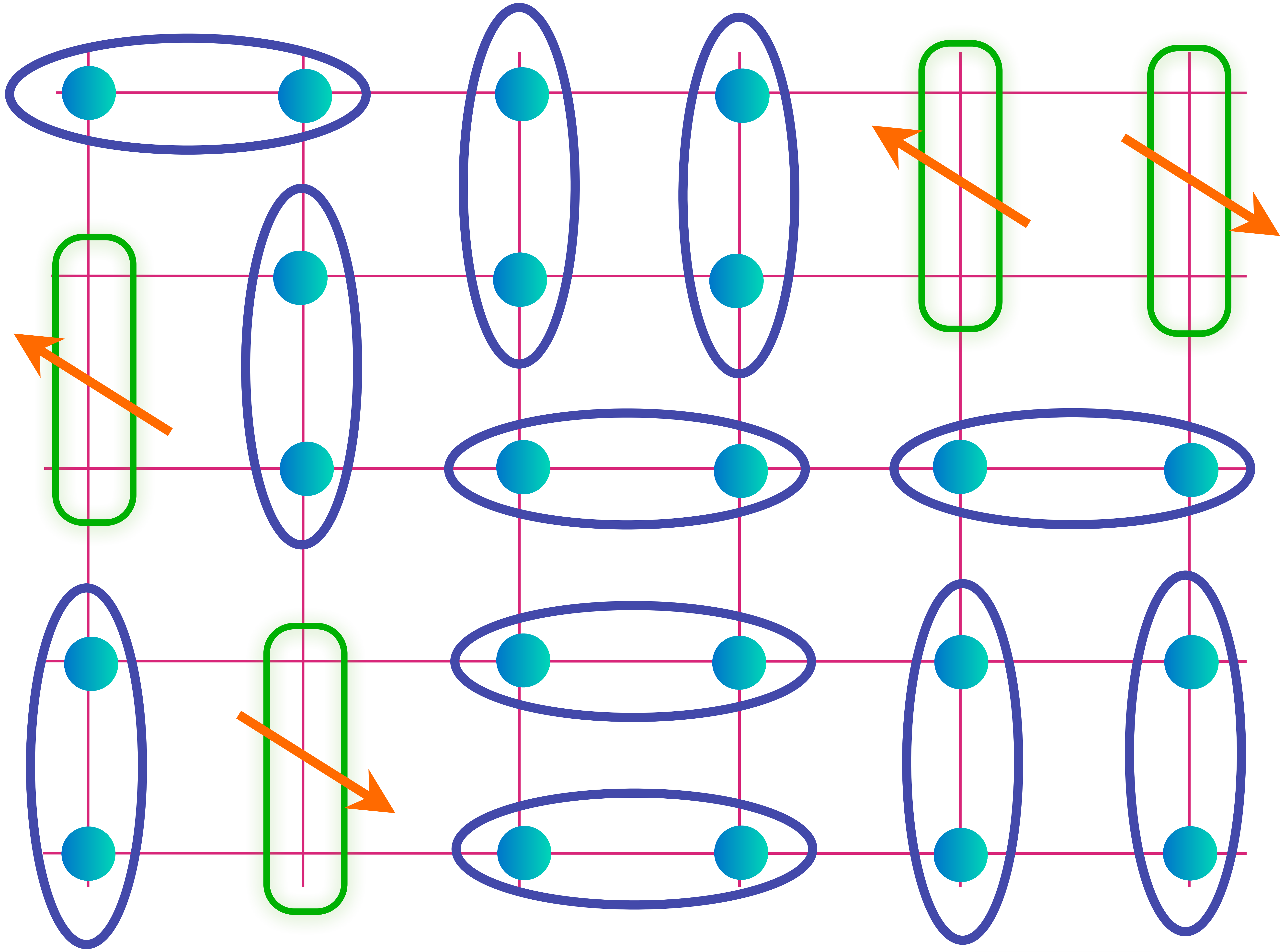

Metal with electron-like quasiparticles on a Fermi surface of size p, and emergent gauge fields

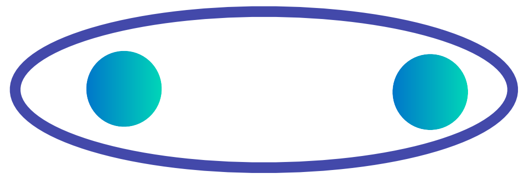 $= \left(|\uparrow\downarrow\rangle - |\downarrow\uparrow\rangle\right)/\sqrt{2}$

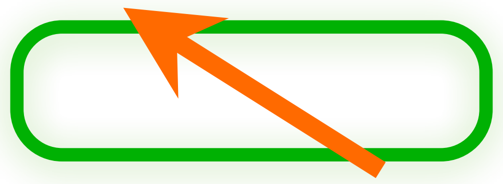 $= \left(|\uparrow\circ\rangle + |\circ\uparrow\rangle\right)/\sqrt{2}$

M. Punk, A. Allais, and S. Sachdev, PNAS **112**, 9552 (2015)

FL*

S. Sachdev PRB **49**, 6770 (1994); X.-G. Wen and P.A. Lee PRL **76**, 503 (1996)
R. K. Kaul, A. Kolezhuk, M. Levin, S. Sachdev, and T. Senthil, PRB **75**, 235122 (2007)

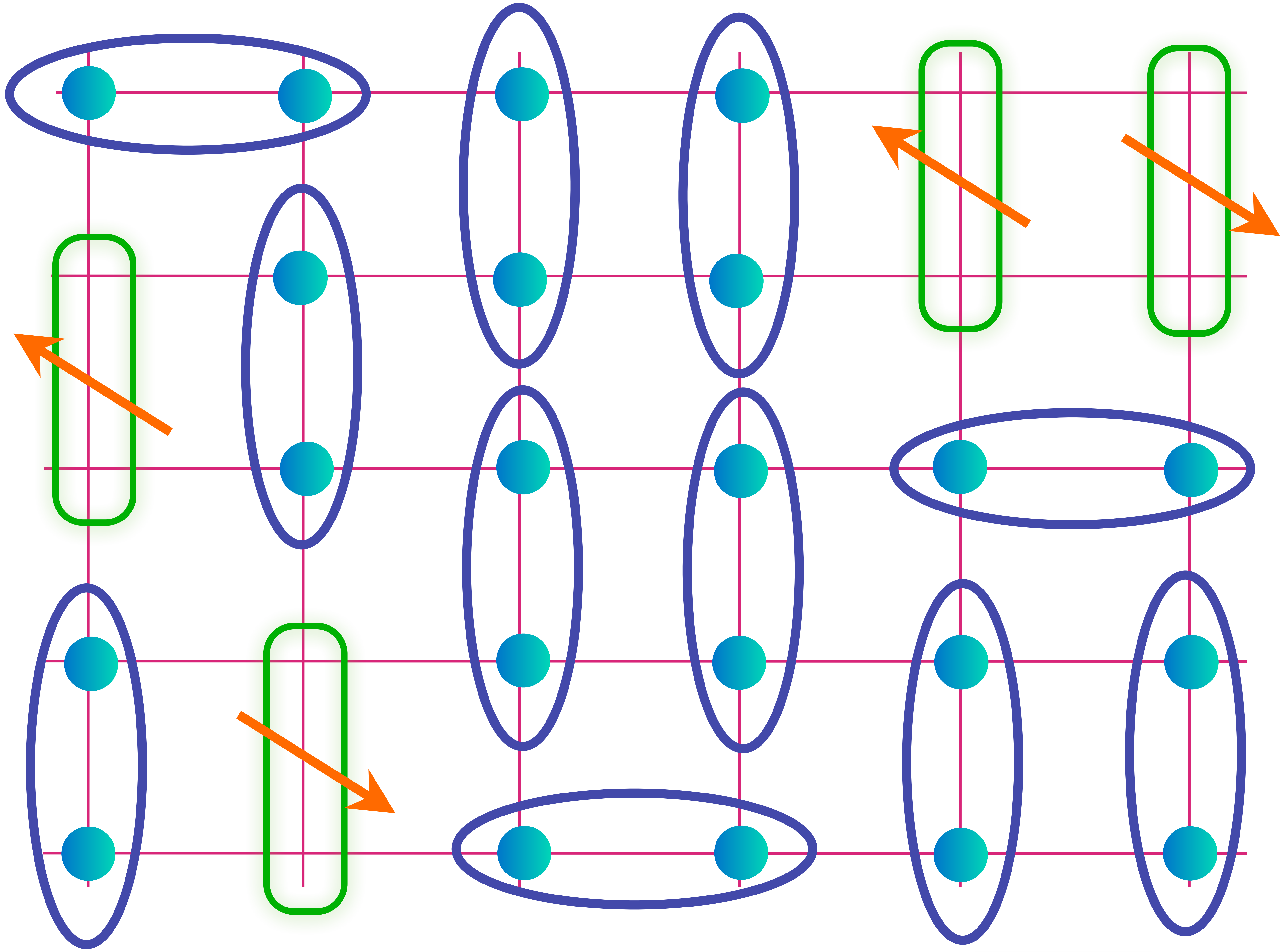

Metal with electron-like quasiparticles on a Fermi surface of size p, and emergent gauge fields

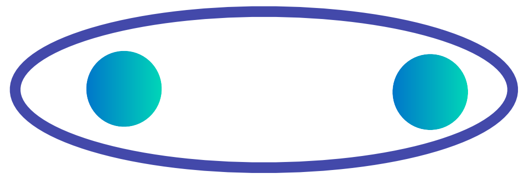 $= \left(|\uparrow\downarrow\rangle - |\downarrow\uparrow\rangle \right) / \sqrt{2}$

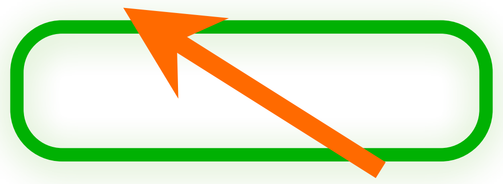 $= \left(|\uparrow \circ\rangle + |\circ \uparrow\rangle \right) / \sqrt{2}$

M. Punk, A. Allais, and S. Sachdev, PNAS **112**, 9552 (2015)

FL*

S. Sachdev PRB **49**, 6770 (1994); X.-G. Wen and P.A. Lee PRL **76**, 503 (1996)
R. K. Kaul, A. Kolezhuk, M. Levin, S. Sachdev, and T. Senthil, PRB **75**, 235122 (2007)

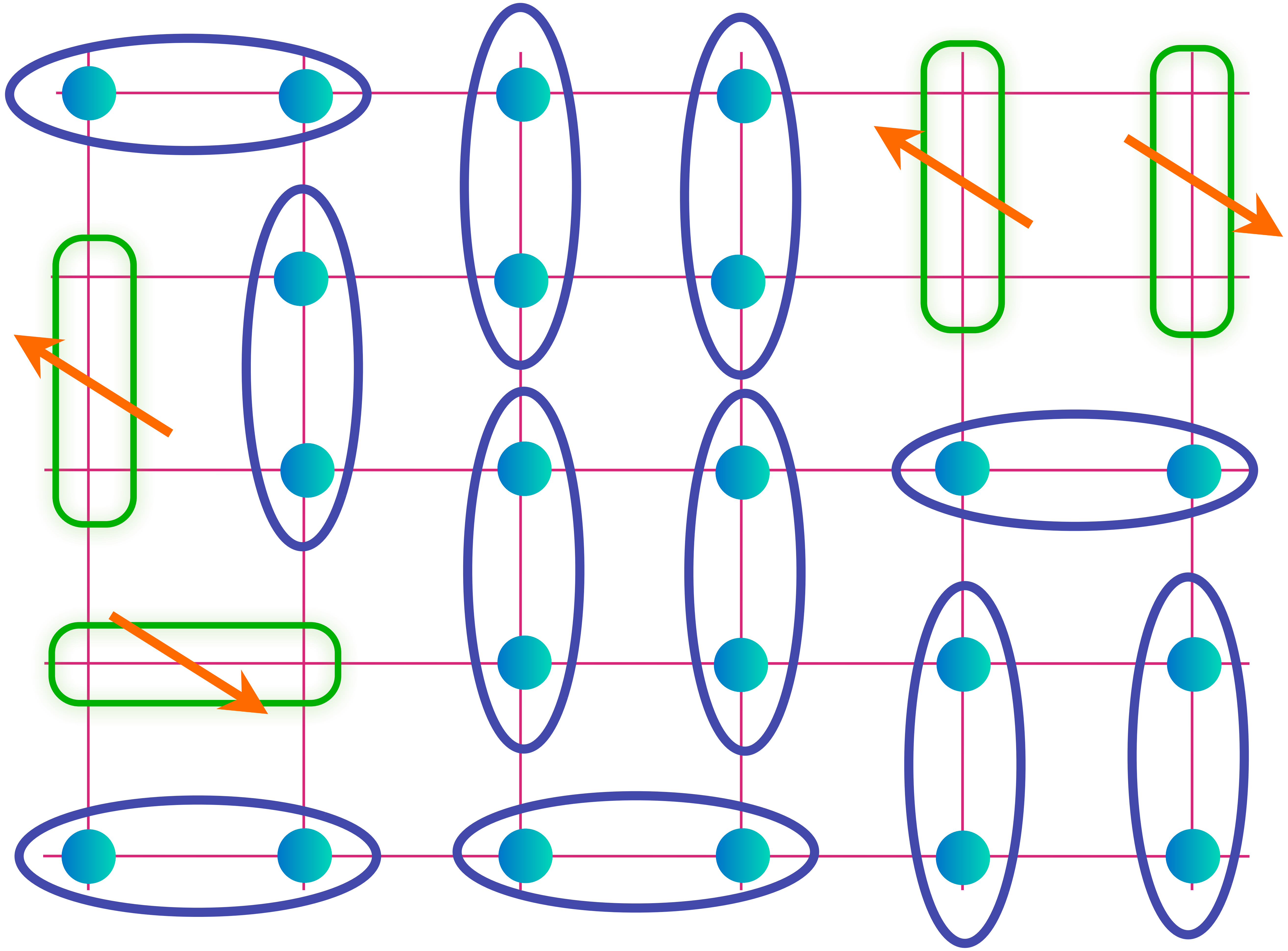

Metal with electron-like quasiparticles on a Fermi surface of size p, and emergent gauge fields

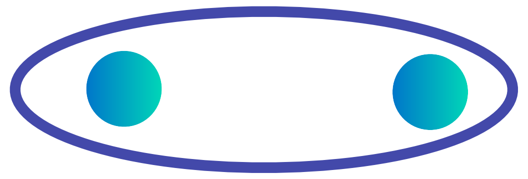

$= (|\uparrow\downarrow\rangle - |\downarrow\uparrow\rangle)/\sqrt{2}$

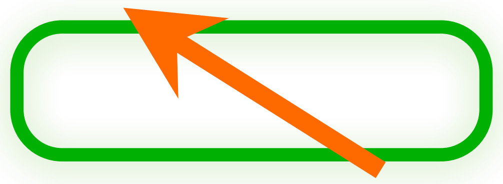

$= (|\uparrow\circ\rangle + |\circ\uparrow\rangle)/\sqrt{2}$

M. Punk, A. Allais, and S. Sachdev, PNAS **112**, 9552 (2015)

Metal-metal transitions in a ***one-band*** model

- Can realize the FL* state as a doped spin liquid in which spinons and holons bind to form 'electrons', which then form a small Fermi surface (X.-G. Wen and P. A. Lee, PRL **76**, 503 (1996)); but there is no complete description of this process, except in the very strong binding limit of dimer 'electrons' (M. Punk, A. Allais, and S. Sachdev,PNAS **112**, 9552 (2015)). This approach does not yield a theory of the transition to the FL state.

Metal-metal transitions in a ***one-band*** model

- Can realize the FL* state as a doped spin liquid in which spinons and holons bind to form 'electrons', which then form a small Fermi surface (X.-G. Wen and P. A. Lee, PRL **76**, 503 (1996)); but there is no complete description of this process, except in the very strong binding limit of dimer 'electrons' (M. Punk, A. Allais, and S. Sachdev,PNAS **112**, 9552 (2015)). This approach does not yield a theory of the transition to the FL state.

- There is a proposal (S. Sachdev, H. D. Scammell, M. S. Scheurer, and G. Tarnopolsky, PRB **99**, 054516 (2019)) for a transition from FL* to FL using a $SU(2)_S$ gauge theory, but some 'hand-waving' is required to produce the FL* Fermi surface.

1. Metal-metal transition in the Kondo Lattice

2. Metal-metal transition in a one-band model

   A. FL model of the pseudogap*

   B. Ancilla qubits and ghost Fermi surfaces

3. Random t-*J* model

   SYK criticality and Numerics

Metal-metal transitions in a ***one-band*** model

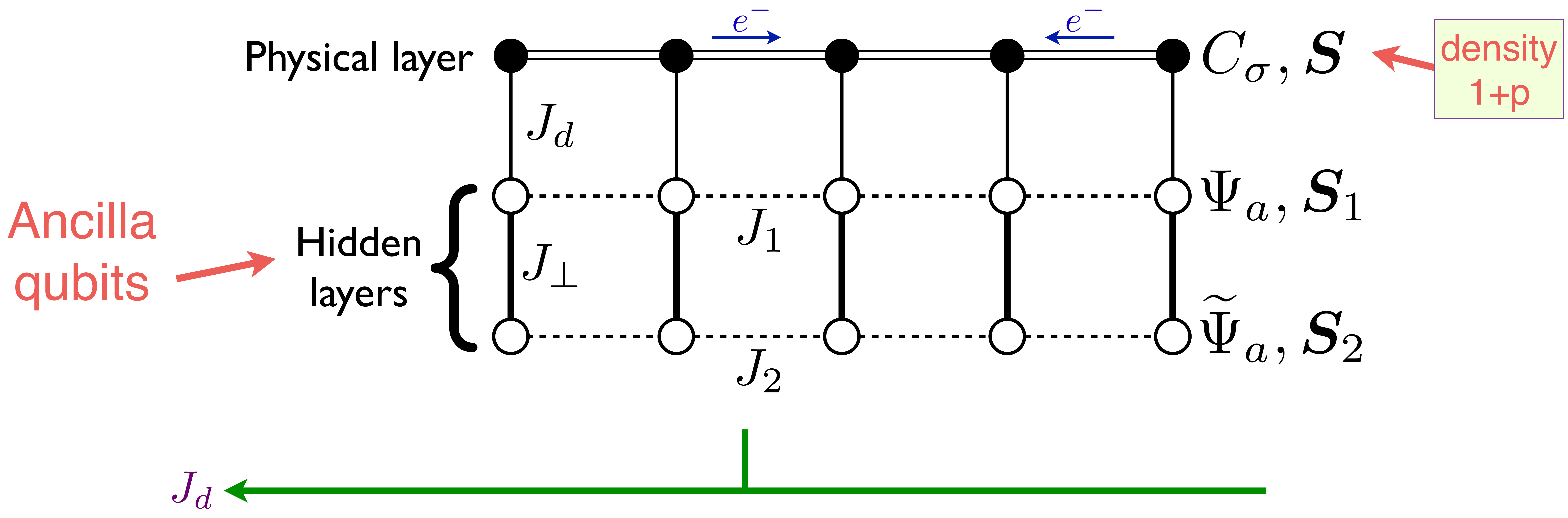

Ya-Hui Zhang

Ya-Hui Zhang, S. Sachdev, PRR **2**, 023172 (2020); arXiv:2006.01140.

Metal-metal transitions in a ***one-band*** model

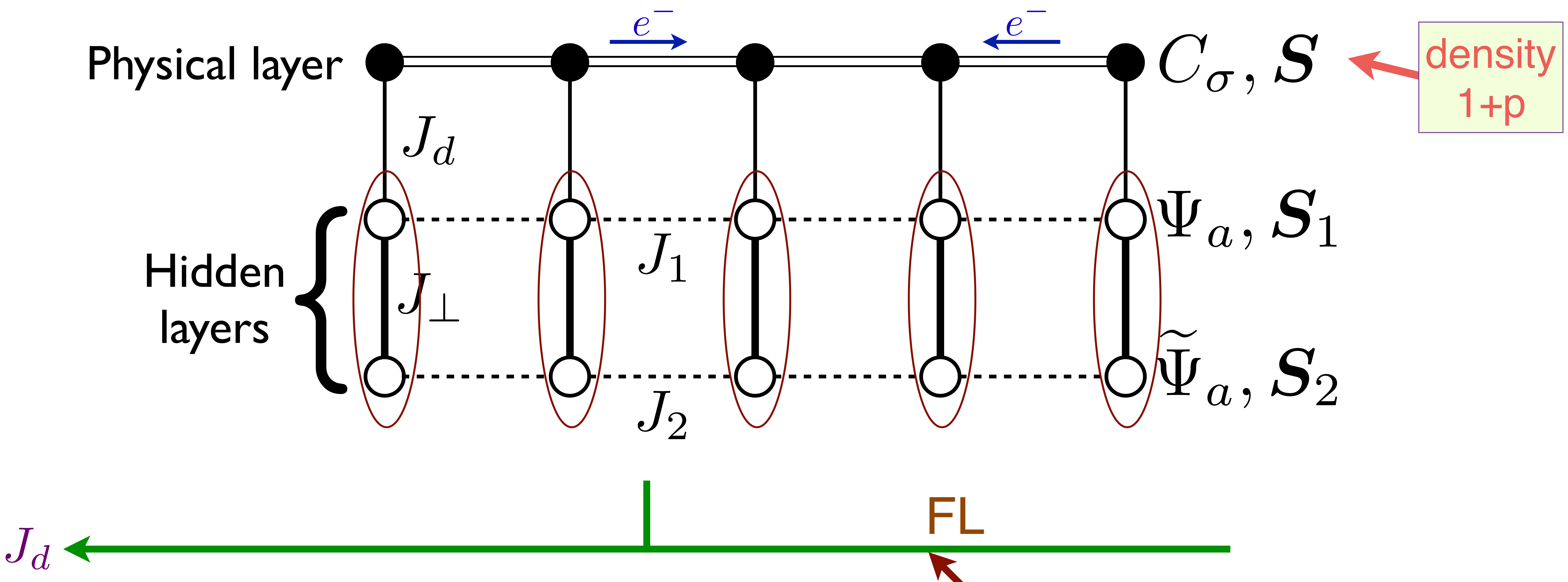

Large Fermi surface of size $1 + p$

$$|\Phi\rangle = \left|\text{Rung singlets of } \Psi, \widetilde{\Psi}\right\rangle \otimes |\text{Slater determinant of } C\rangle$$

Ya-Hui Zhang

Ya-Hui Zhang, S. Sachdev, PRR **2**, 023172 (2020); arXiv:2006.01140.

Metal-metal transitions in a ***one-band*** model

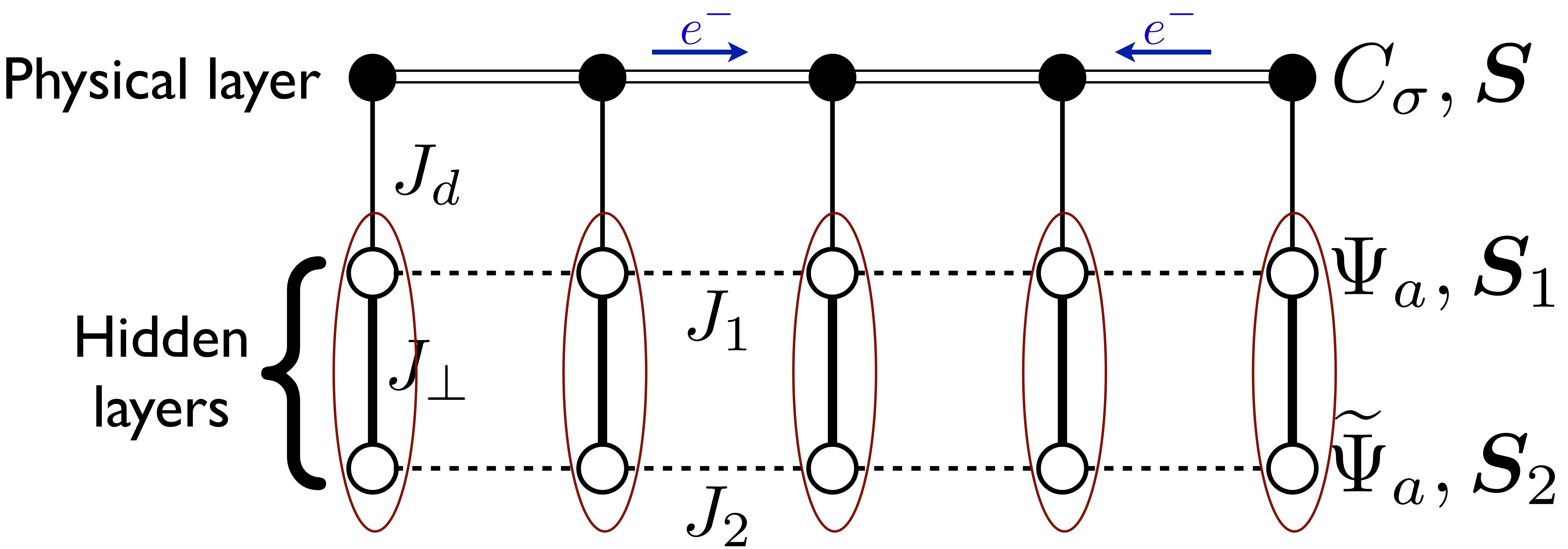

density 1+p

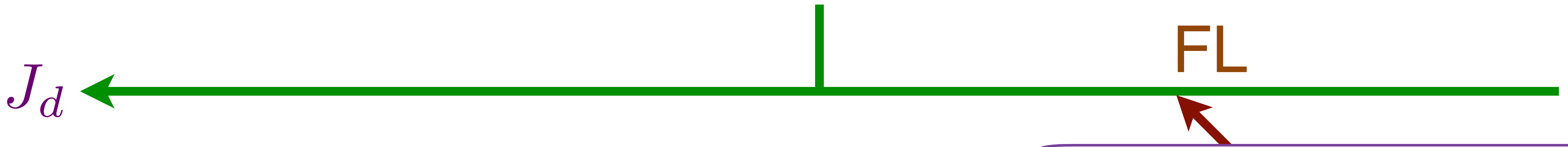

Luttinger Theorem obeyed

Large Fermi surface of size $1+p$

$$|\Phi\rangle = \left|\text{Rung singlets of } \Psi, \widetilde{\Psi}\right\rangle \otimes |\text{Slater determinant of } C\rangle$$

Ya-Hui Zhang

Ya-Hui Zhang, S. Sachdev, PRR **2**, 023172 (2020); arXiv:2006.01140.

Metal-metal transitions in a ***one-band*** model

Metal.
Density
$2 + p \cong p$

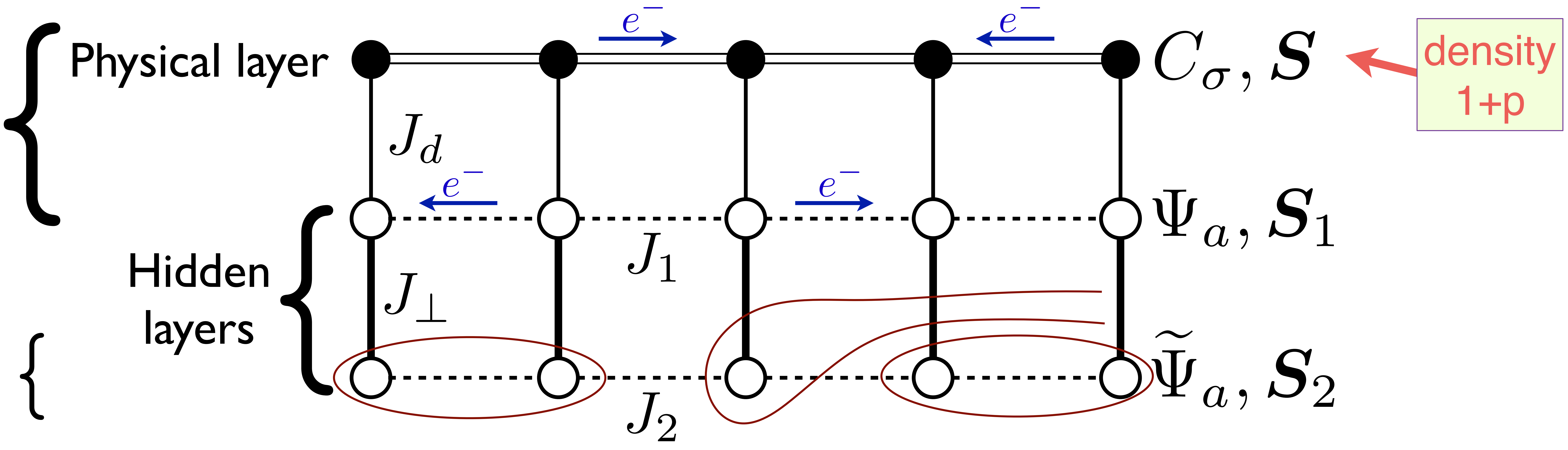

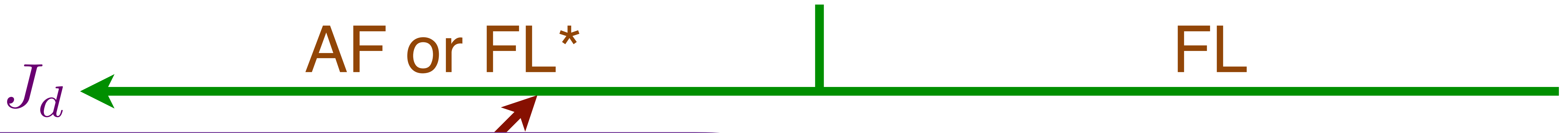

Small Fermi surface of size p

$$|\Phi\rangle = \Big[\text{Projection onto rung singlets of } \Psi, \widetilde{\Psi}\Big] \bowtie |\text{Slater determinant of } (C, \Psi)\rangle \otimes \Big|\text{Spin liquid of } \widetilde{\Psi}\Big\rangle$$

Ya-Hui Zhang

Ya-Hui Zhang, S. Sachdev, PRR **2**, 023172 (2020); arXiv:2006.01140.

Metal-metal transitions in a ***one-band*** model

Metal.
Density
$2 + p \cong p$

Mott insulator
Spin liquid
or AF order

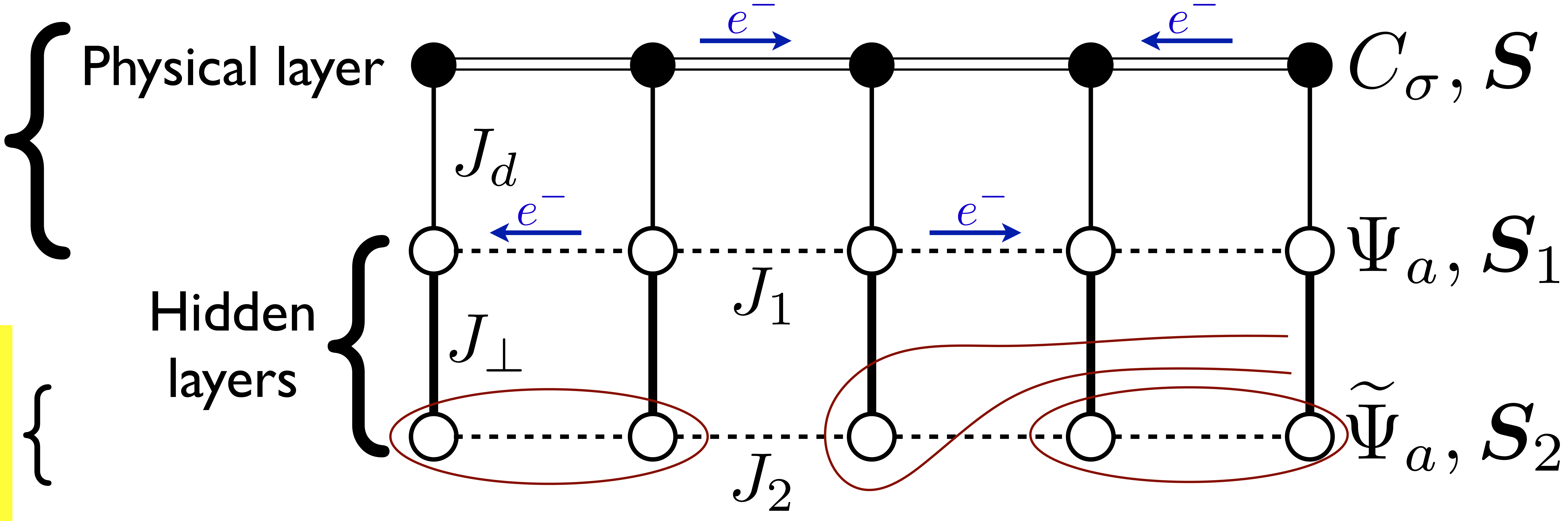

density
1+p

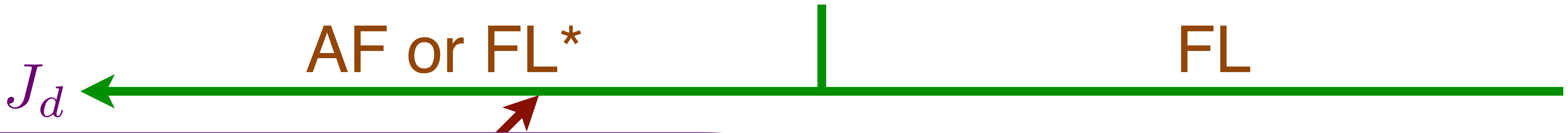

Small Fermi surface of size p

$$|\Phi\rangle = \left[\text{Projection onto rung singlets of } \Psi, \widetilde{\Psi}\right] \bowtie |\text{Slater determinant of } (C, \Psi)\rangle \otimes \left|\text{Spin liquid of } \widetilde{\Psi}\right\rangle$$

Ya-Hui Zhang

Ya-Hui Zhang, S. Sachdev, PRR **2**, 023172 (2020); arXiv:2006.01140.

Metal-metal transitions in a ***one-band*** model

Metal.
Density
$2 + p \cong p$

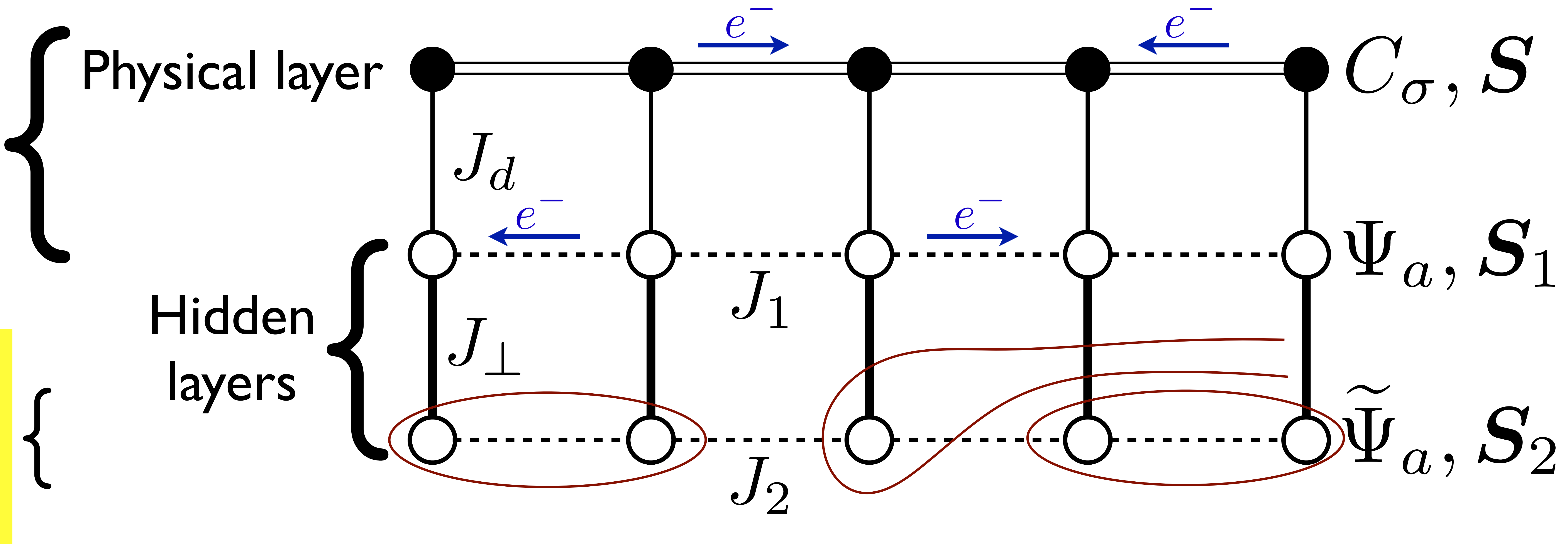

density
1+p

Mott insulator
Spin liquid
or AF order

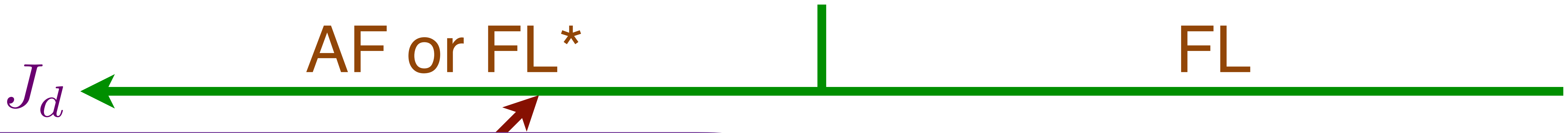

Small Fermi surface of size p

$$|\Phi\rangle = \left[\text{Projection onto rung singlets of } \Psi, \widetilde{\Psi}\right] \bowtie |\text{Slater determinant of } (C, \Psi)\rangle \otimes \left|\text{Spin liquid of } \widetilde{\Psi}\right\rangle$$

Luttinger Theorem
violated;
OK, because of
topological order of $\widetilde{\Psi}$

Ya-Hui Zhang

Ya-Hui Zhang, S. Sachdev, PRR **2**, 023172 (2020); arXiv:2006.01140.

Metal-metal transitions in a ***one-band*** model

Metal.
Density
$2 + p \cong p$

Mott insulator
Spin liquid
or AF order

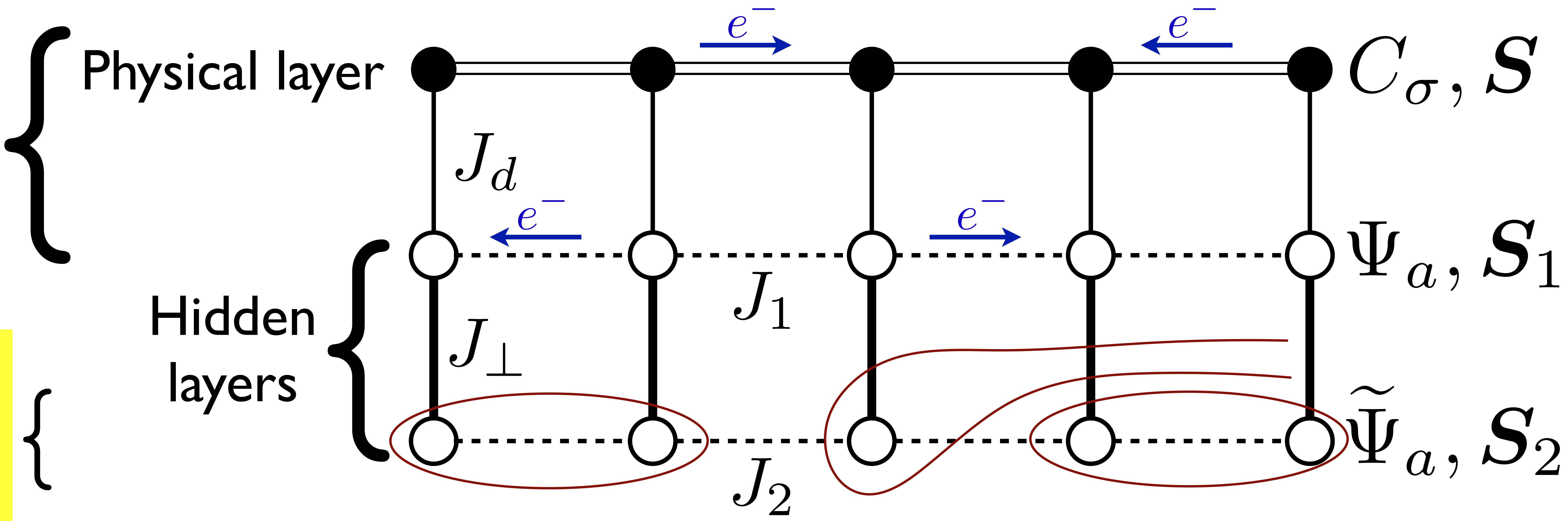

density
1+p

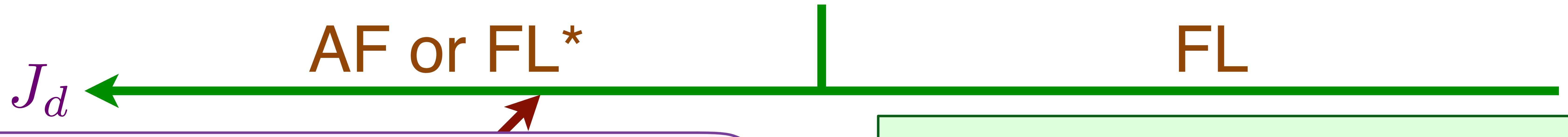

Small Fermi surface of size p

$$|\Phi\rangle = \left[\text{Projection onto rung singlets of } \Psi, \widetilde{\Psi}\right] \bowtie |\text{Slater determinant of } (C, \Psi)\rangle \otimes \left|\text{Spin liquid of } \widetilde{\Psi}\right\rangle$$

Similar to a selective Mott transition in hidden layer 1: Ψ fermions are insulating in FL phase, and metallic in FL* phase.

Ya-Hui Zhang

Ya-Hui Zhang, S. Sachdev, PRR **2**, 023172 (2020); arXiv:2006.01140.

Metal-metal transitions in a ***one-band*** model

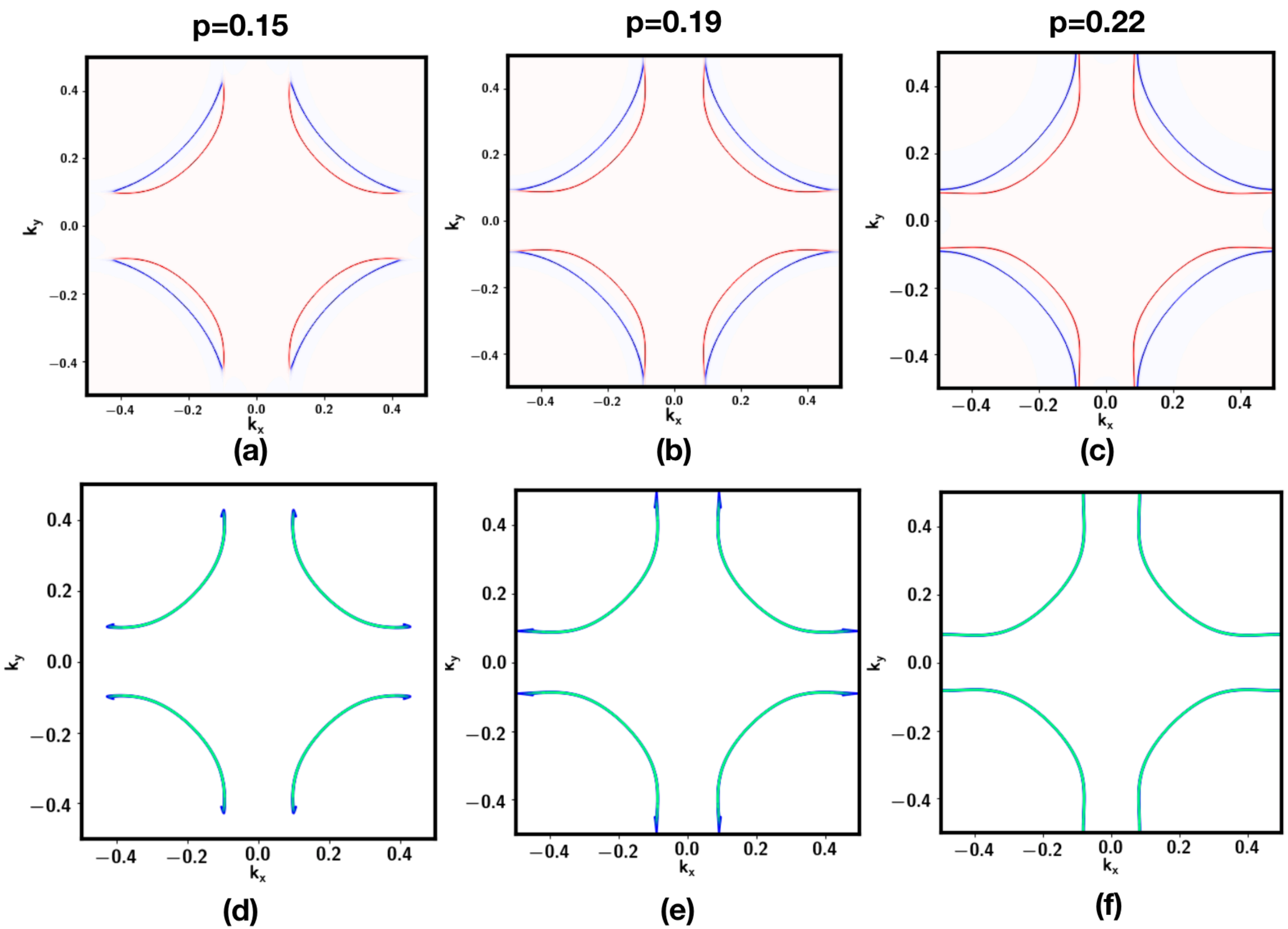

Zero frequency spectral density of electrons (red) and ghosts (blue)

"Fermi arc" spectral functions in the FL* phase

Ya-Hui Zhang

Ya-Hui Zhang, S. Sachdev, PRR **2**, 023172 (2020); arXiv:2006.01140.

Metal-metal transitions in a ***one-band*** model

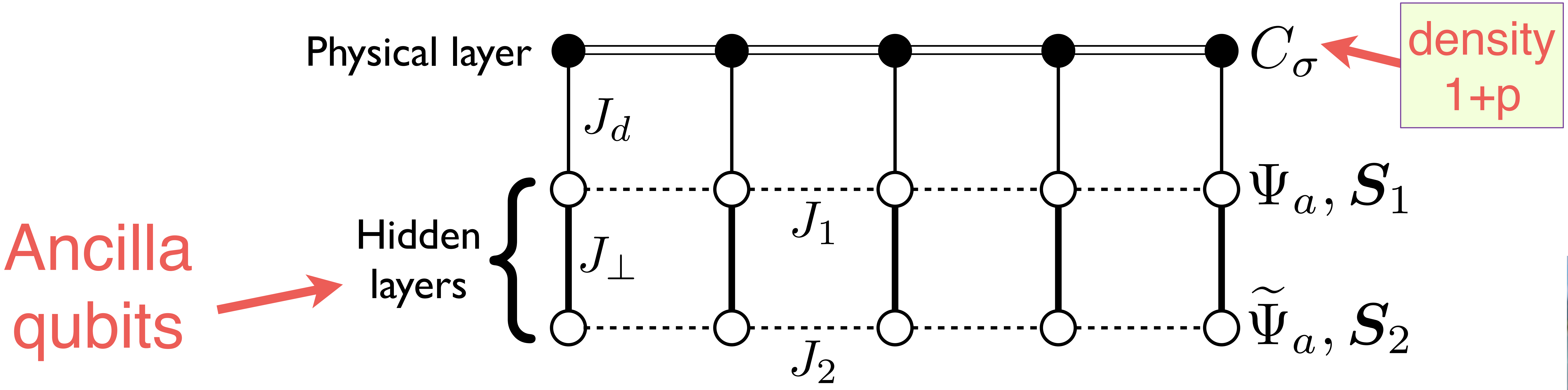


Yahui Zhang

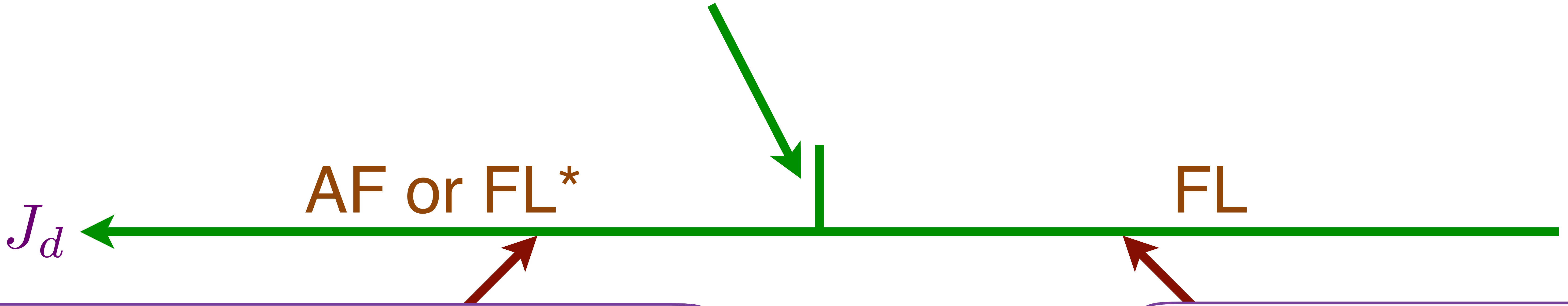

Small Fermi surface of size p

$$|\Phi\rangle = \left[\text{Projection onto rung singlets of } \Psi, \widetilde{\Psi}\right] \bowtie |\text{Slater determinant of } (C, \Psi)\rangle \otimes \left|\text{Slater determinant of } \widetilde{\Psi}\right\rangle$$

Large Fermi surface of size $1 + p$

$$|\Phi\rangle = \left|\text{Rung singlets of } \Psi, \widetilde{\Psi}\right\rangle \otimes |\text{Slater determinant of } C\rangle$$

Ya-Hui Zhang, S. Sachdev, PRR **2**, 023172 (2020); arXiv:2006.01140.

Metal-metal transitions in a ***one-band*** model

Write fermion operators as 2×2 matrices

$$\boldsymbol{\Psi} = \begin{pmatrix} \Psi_\uparrow & -\Psi_\downarrow^\dagger \\ \Psi_\downarrow & \Psi_\uparrow^\dagger \end{pmatrix} \quad , \quad \widetilde{\boldsymbol{\Psi}} = \begin{pmatrix} \widetilde{\Psi}_\uparrow & -\widetilde{\Psi}_\downarrow^\dagger \\ \widetilde{\Psi}_\downarrow & \widetilde{\Psi}_\uparrow^\dagger \end{pmatrix}$$

Single occupancy constraints of $\boldsymbol{\Psi}$, $\widetilde{\boldsymbol{\Psi}}$ leads to $\mathrm{SU}(2)_1 \times \mathrm{SU}(2)_2$ gauge symmetry:

$$\mathrm{SU}(2)_1 : \quad \boldsymbol{\Psi} \rightarrow \boldsymbol{\Psi} U_1 \quad , \quad \widetilde{\boldsymbol{\Psi}} \rightarrow \widetilde{\boldsymbol{\Psi}}$$
$$\mathrm{SU}(2)_2 : \quad \boldsymbol{\Psi} \rightarrow \boldsymbol{\Psi} \quad , \quad \widetilde{\boldsymbol{\Psi}} \rightarrow \widetilde{\boldsymbol{\Psi}} U_2$$

P.A. Lee, N. Nagaosa, and X.-G. Wen, RMP **78**, 17 (2006)

Local singlet formation ('antiferromagnetism') $\boldsymbol{S}_1 + \boldsymbol{S}_2 \approx 0$ leads to $\mathrm{SU}(2)_S$ gauge symmetry:

$$\mathrm{SU}(2)_S : \quad \boldsymbol{\Psi} \rightarrow U_S \boldsymbol{\Psi} \quad , \quad \widetilde{\boldsymbol{\Psi}} \rightarrow U_S \widetilde{\boldsymbol{\Psi}}$$

S. Sachdev, M.A. Metlitski, Yang Qi, and Cenke Xu, PRB **80**, 155129 (2009)
S. Sachdev, H. D. Scammell, M. S. Scheurer, and G. Tarnopolsky, PRB **99**, 054516 (2019)

Ya-Hui Zhang, S. Sachdev, PRR **2**, 023172 (2020); arXiv:2006.01140.

Metal-metal transitions in a ***one-band*** model

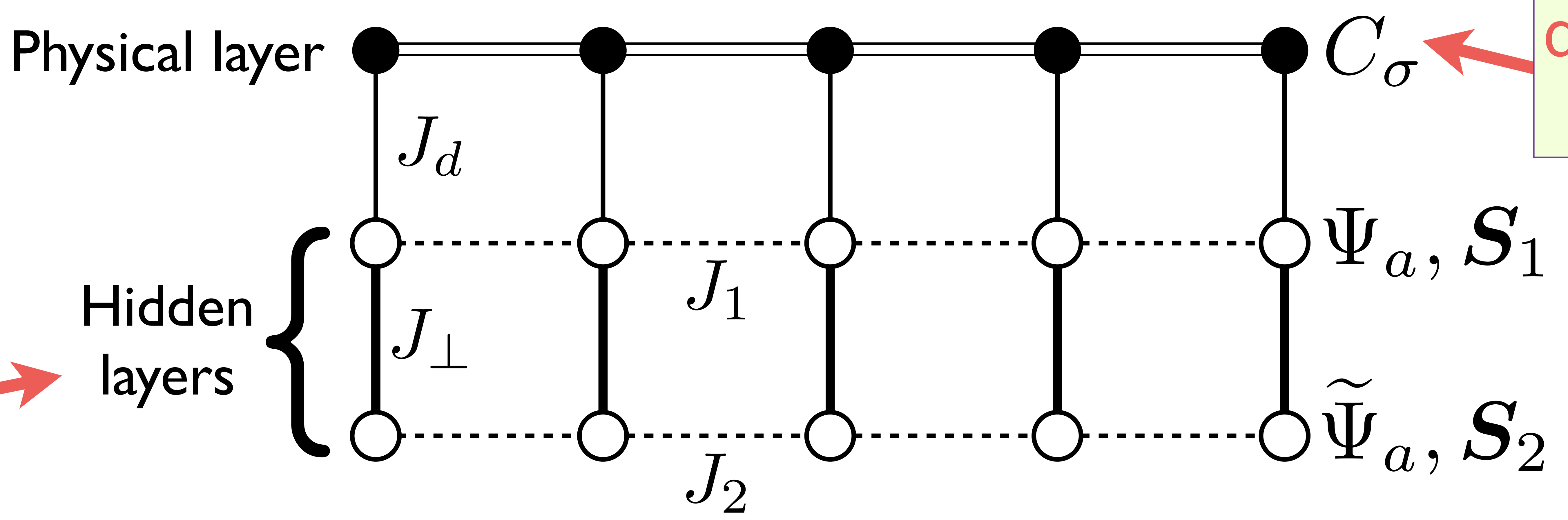

density 1+p

Ancilla qubits

Yahui Zhang

$(\mathrm{U}(1)_S \times \mathrm{U}(1)_1)/Z_2$ or $(\mathrm{SU}(2)_S \times \mathrm{U}(1)_1)/Z_2$ gauge theory of a Ψ ghost Fermi surface and a 'hybridization-Higgs' boson $\sim C_\sigma^\dagger \Psi_a$ which condenses on the 'Small Fermi surface' side.

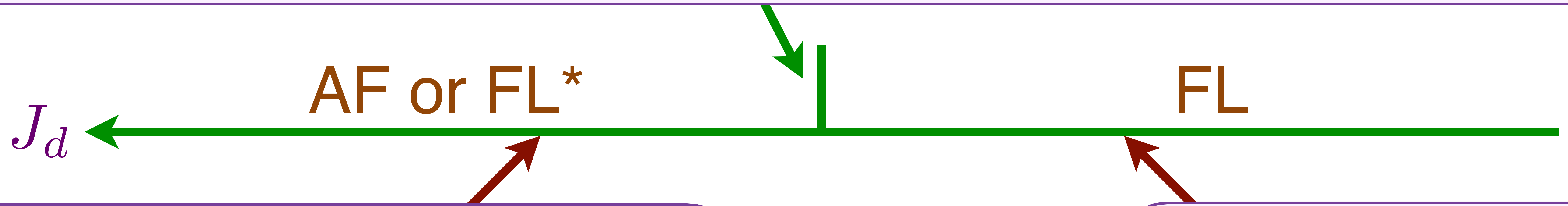

Small Fermi surface of size p

$$|\Phi\rangle = \left[\text{Projection onto rung singlets of } \Psi, \widetilde{\Psi}\right] \bowtie |\text{Slater determinant of } (C, \Psi)\rangle \otimes \left|\text{Slater determinant of } \widetilde{\Psi}\right\rangle$$

Large Fermi surface of size $1+p$

$$|\Phi\rangle = \left|\text{Rung singlets of } \Psi, \widetilde{\Psi}\right\rangle \otimes |\text{Slater determinant of } C\rangle$$

See also Liujun Zou, D. Chowdhury, PRR **2**, 023344 (2020) Ya-Hui Zhang, S. Sachdev, PRR **2**, 023172 (2020); arXiv:2006.01140.

Ancilla qubit theory of metal-metal quantum phase transitions

- FL* as the pseudogap metal with carrier density p. Variants of the theory can have broken symmetries (*e.g.* antiferromagnetism) without fractionalization in the pseudogap metal.

Ya-Hui Zhang, S. Sachdev, PRR **2**, 023172 (2020); arXiv:2006.01140.

Ancilla qubit theory of metal-metal quantum phase transitions

- FL* as the pseudogap metal with carrier density p. Variants of the theory can have broken symmetries (*e.g.* antiferromagnetism) without fractionalization in the pseudogap metal.

- Ghost fermions, carrying neither spin nor charge, emerge as additional low energy excitations near the critical point to the FL phase. While the ancilla qubits are gauged away as 'fake' in the UV theory, the ghost fermions are physical excitations in the IR theory, which can be detected by thermal probes.

Ya-Hui Zhang, S. Sachdev, PRR **2**, 023172 (2020); arXiv:2006.01140.

Ancilla qubit theory of metal-metal quantum phase transitions

- FL* as the pseudogap metal with carrier density p. Variants of the theory can have broken symmetries (*e.g.* antiferromagnetism) without fractionalization in the pseudogap metal.

- Ghost fermions, carrying neither spin nor charge, emerge as additional low energy excitations near the critical point to the FL phase. While the ancilla qubits are gauged away as 'fake' in the UV theory, the ghost fermions are physical excitations in the IR theory, which can be detected by thermal probes.

- The ghost fermions are coupled to 2 gauge fields: the first arising from the no double occupancy constraint, and the second from transforming to a rotating reference frame in spin space. These gauge fields lead respectively to repulsive and attractive interactions between the ghost fermions.

See also Liujun Zou, D. Chowdhury, PRR **2**, 023344 (2020) Ya-Hui Zhang, S. Sachdev, PRR **2**, 023172 (2020); arXiv:2006.01140.

1. Metal-metal transition in the Kondo Lattice

2. Metal-metal transition in a one-band model
    A. *FL* model of the pseudogap*
    B. *Ancilla qubits and ghost Fermi surfaces*

3. Random t-J model
    SYK criticality and Numerics

Hidden magnetism at the pseudogap critical point of a high temperature superconductor

Nature Physics doi: 10.1038/s41567-020-0950-5

Mehdi Frachet[1]†, Igor Vinograd[1]†, Rui Zhou[1,2], Siham Benhabib[1], Shangfei Wu[1], Hadrien Mayaffre[1], Steffen Krämer[1], Sanath K. Ramakrishna[3], Arneil P. Reyes[3], Jérôme Debray[4], Tohru Kurosawa[5], Naoki Momono[6], Migaku Oda[5], Seiki Komiya[7], Shimpei Ono[7], Masafumi Horio[8], Johan Chang[8], Cyril Proust[1], David LeBoeuf[1*], Marc-Henri Julien[1*]

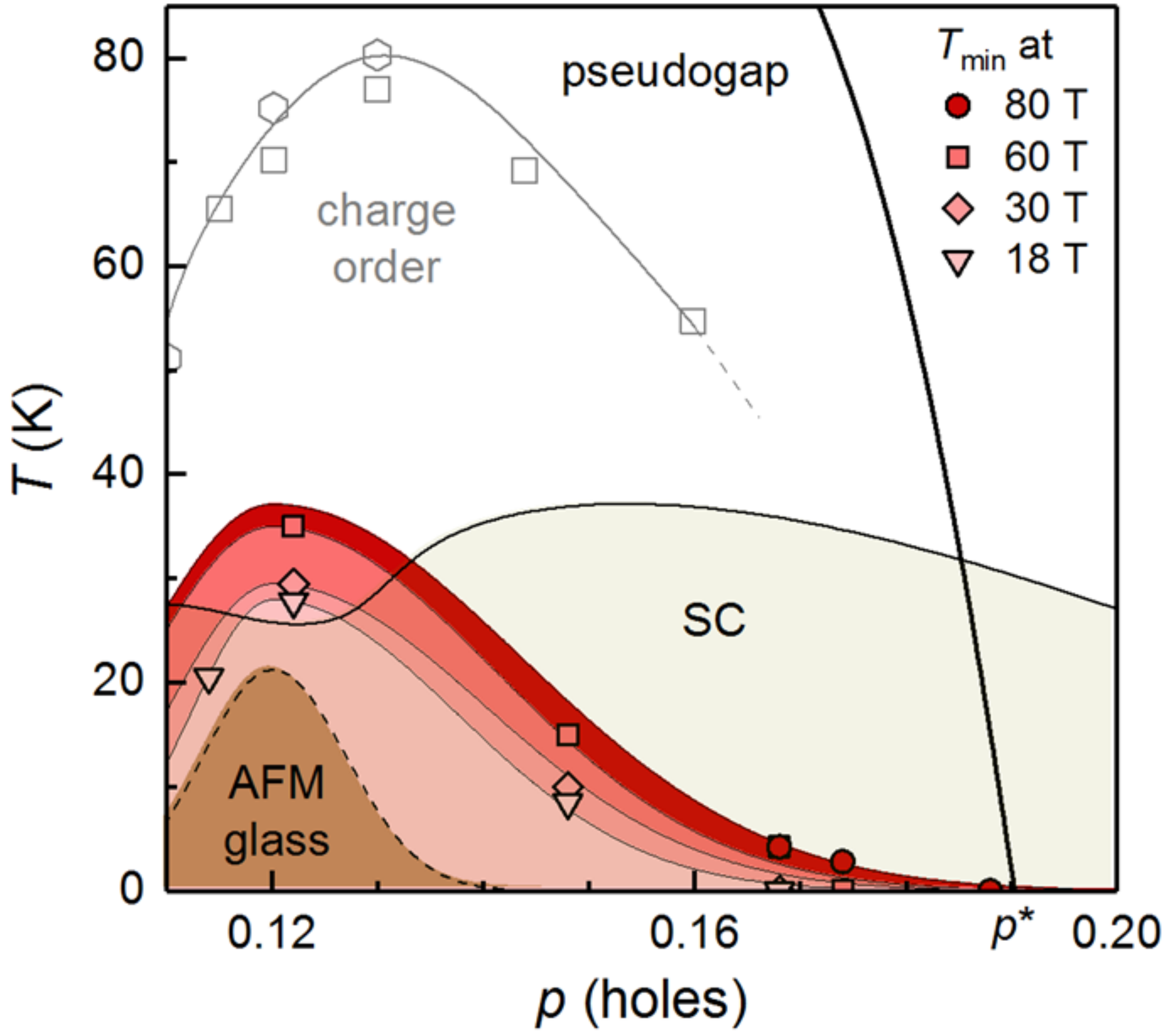

Quasi-static magnetism in the pseudogap state of La2-xSrxCuO4.

Temperature – doping phase diagram representing T_{min}, the temperature of the minimum in the sound velocity, at different fields. Since superconductivity precludes the observation of T_{min} in zero-field, the dashed line (brown area) represents the extrapolated $T_{min}(B=0)$. While not exactly equal to the freezing temperature T_f (see Fig. 2), T_{min} is closely tied to T_f and so is expected to have the same doping dependence, including a peak around $p = 0.12$ in zero/low fields (ref. 2). Onset temperatures of charge order are from ref. 33 (squares) and 35 (hexagons).

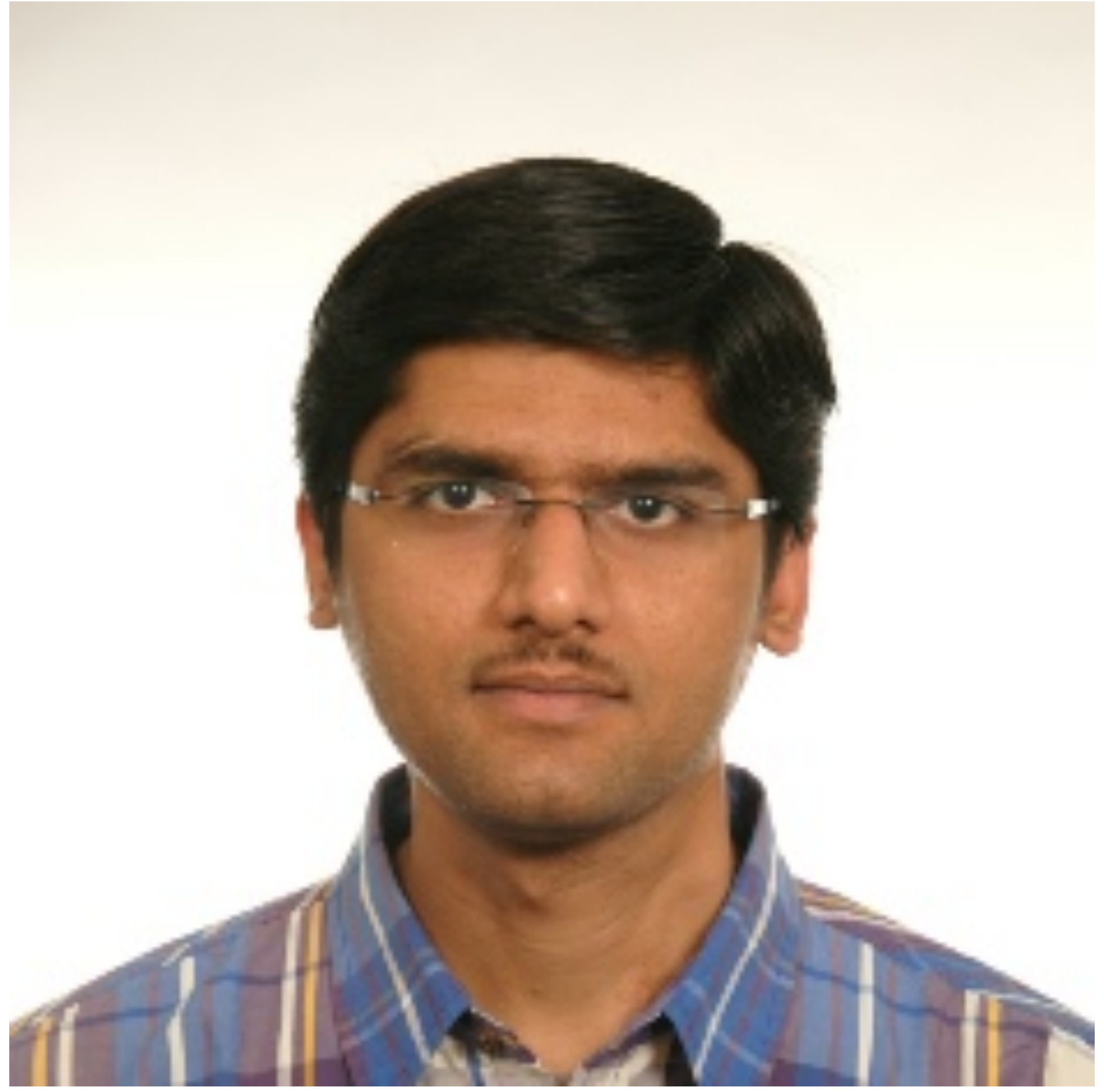

Darshan Joshi

Chenyuan Li

Physical Review X **10**, 021033 (2020)

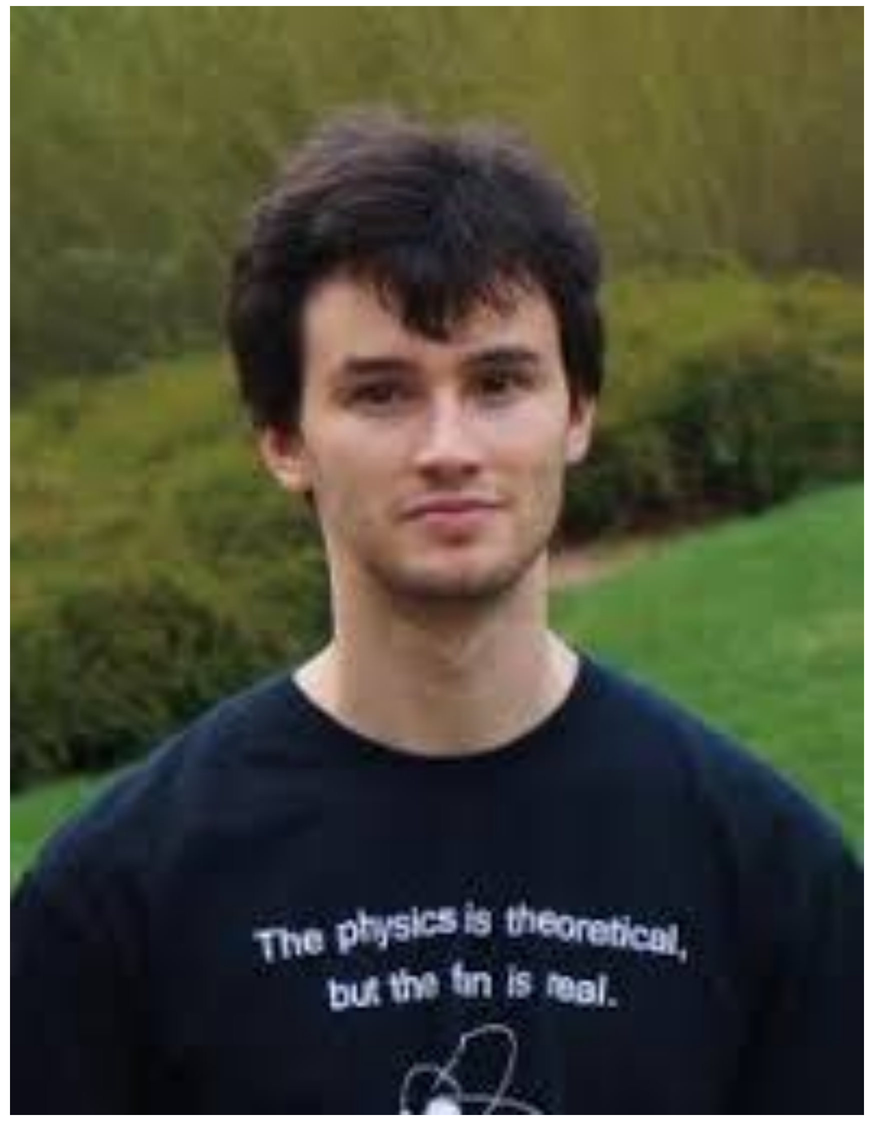

Grigory Tarnopolsky

Antoine Georges

Maria Tikhanovskaya

Haoyu Guo

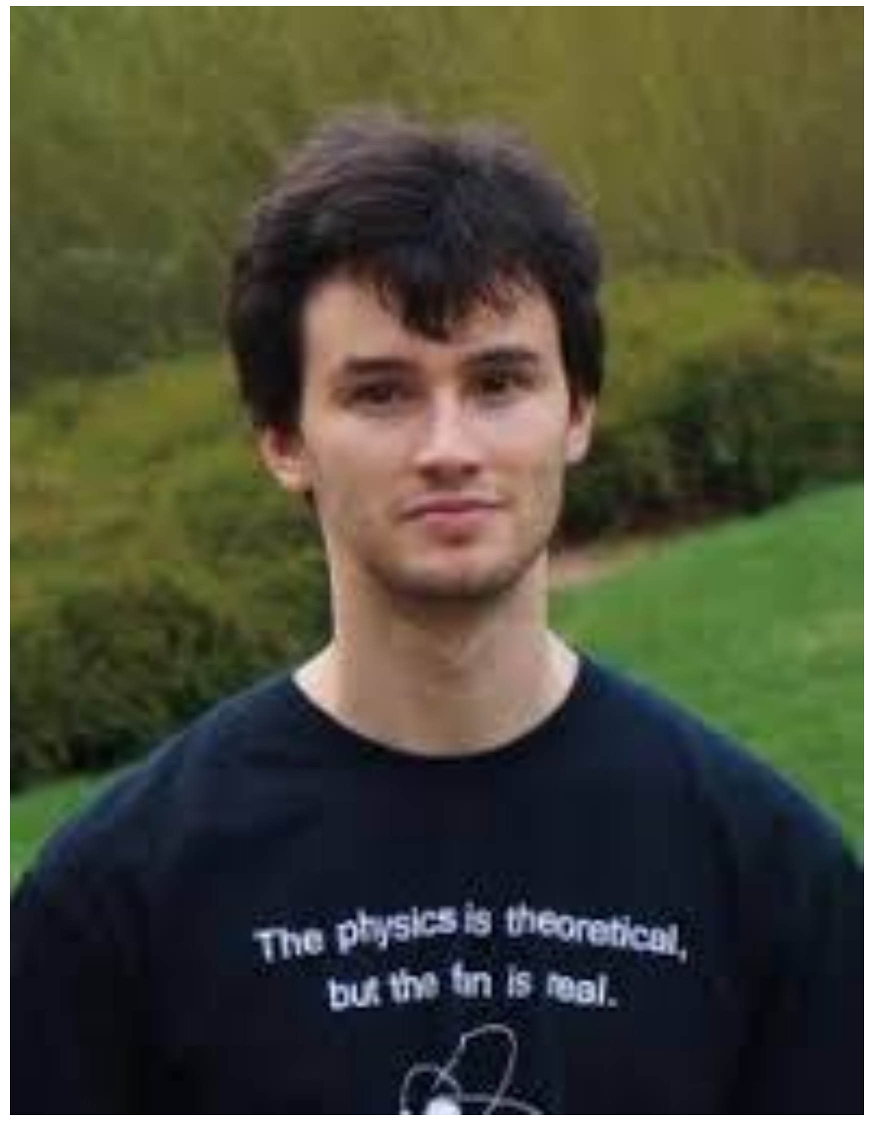

Grigory Tarnopolsky

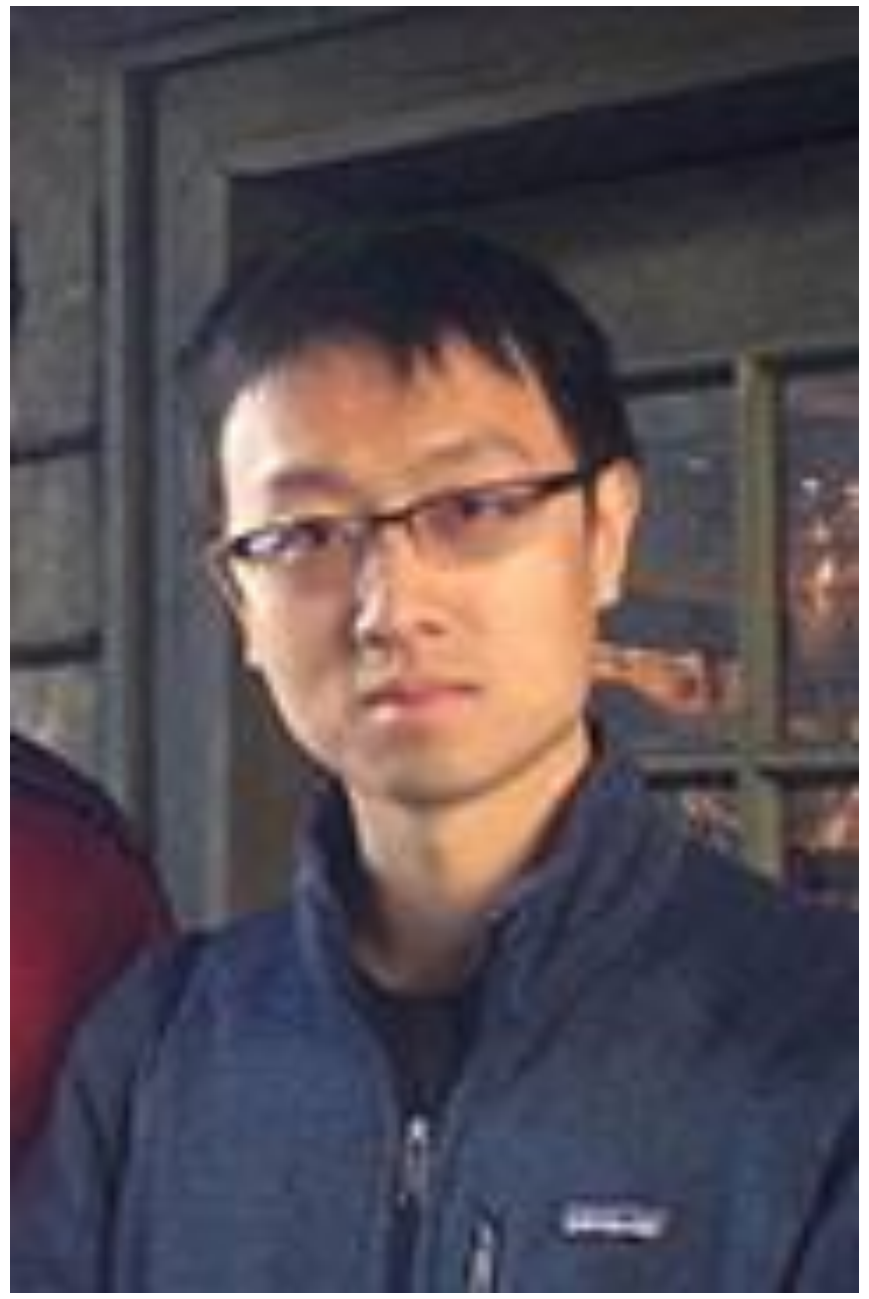

Yingfeu Gu

Random *t-J* model

$$H = -\frac{1}{\sqrt{N}} \sum_{i,j=1}^{N} t_{ij}\, c_{i\alpha}^{\dagger} c_{j\alpha} + \frac{1}{\sqrt{N}} \sum_{i<j=1}^{N} J_{ij}\, \vec{S}_i \cdot \vec{S}_j$$

We consider the hole-doped case, with no double occupancy.

$$\alpha = \uparrow, \downarrow, \quad \{c_{i\alpha}, c_{j\beta}^{\dagger}\} = \delta_{ij}\delta_{\alpha\beta}, \quad \{c_{i\alpha}, c_{j\beta}\} = 0$$

$$\vec{S}_i = \frac{1}{2} c_{i\alpha}^{\dagger} \vec{\sigma}_{\alpha\beta} c_{i\beta}, \quad \sum_{\alpha} c_{i\alpha}^{\dagger} c_{i\alpha} \leq 1, \quad \frac{1}{N} \sum_{i\alpha} c_{i\alpha}^{\dagger} c_{i\alpha} = 1 - p$$

$$J_{ij} \text{ random}, \ \overline{J_{ij}} = 0, \ \overline{J_{ij}^2} = J^2$$

$$t_{ij} \text{ random}, \ \overline{t_{ij}} = 0, \ \overline{t_{ij}^2} = t^2$$

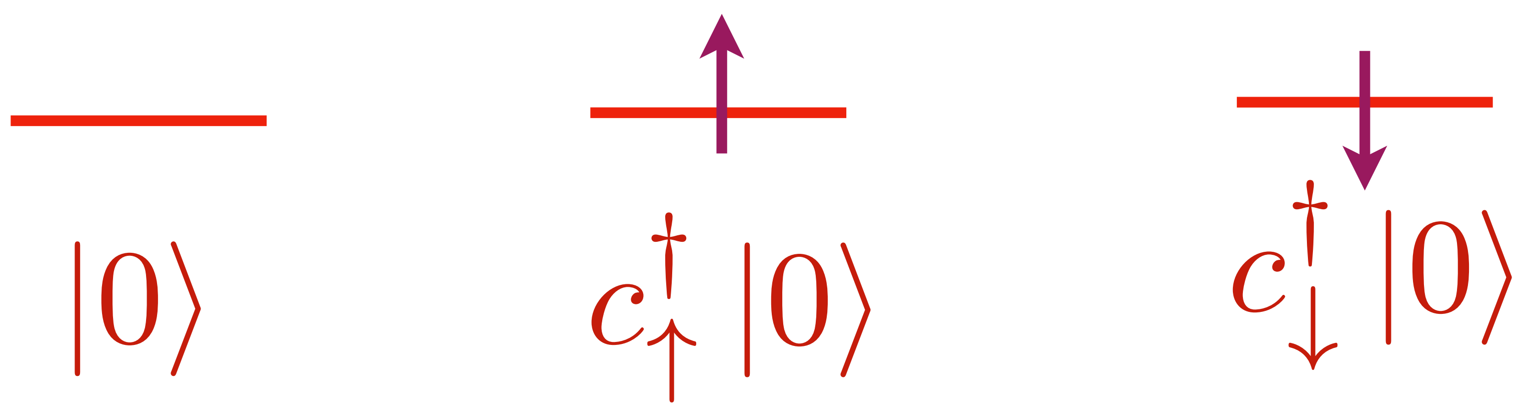

Random *t-J* model

$$H = -\frac{1}{\sqrt{N}} \sum_{i,j=1}^{N} t_{ij}\, c_{i\alpha}^{\dagger} c_{j\alpha} + \frac{1}{\sqrt{N}} \sum_{i<j=1}^{N} J_{ij}\, \vec{S}_i \cdot \vec{S}_j$$

We consider the hole-doped case, with no double occupancy.

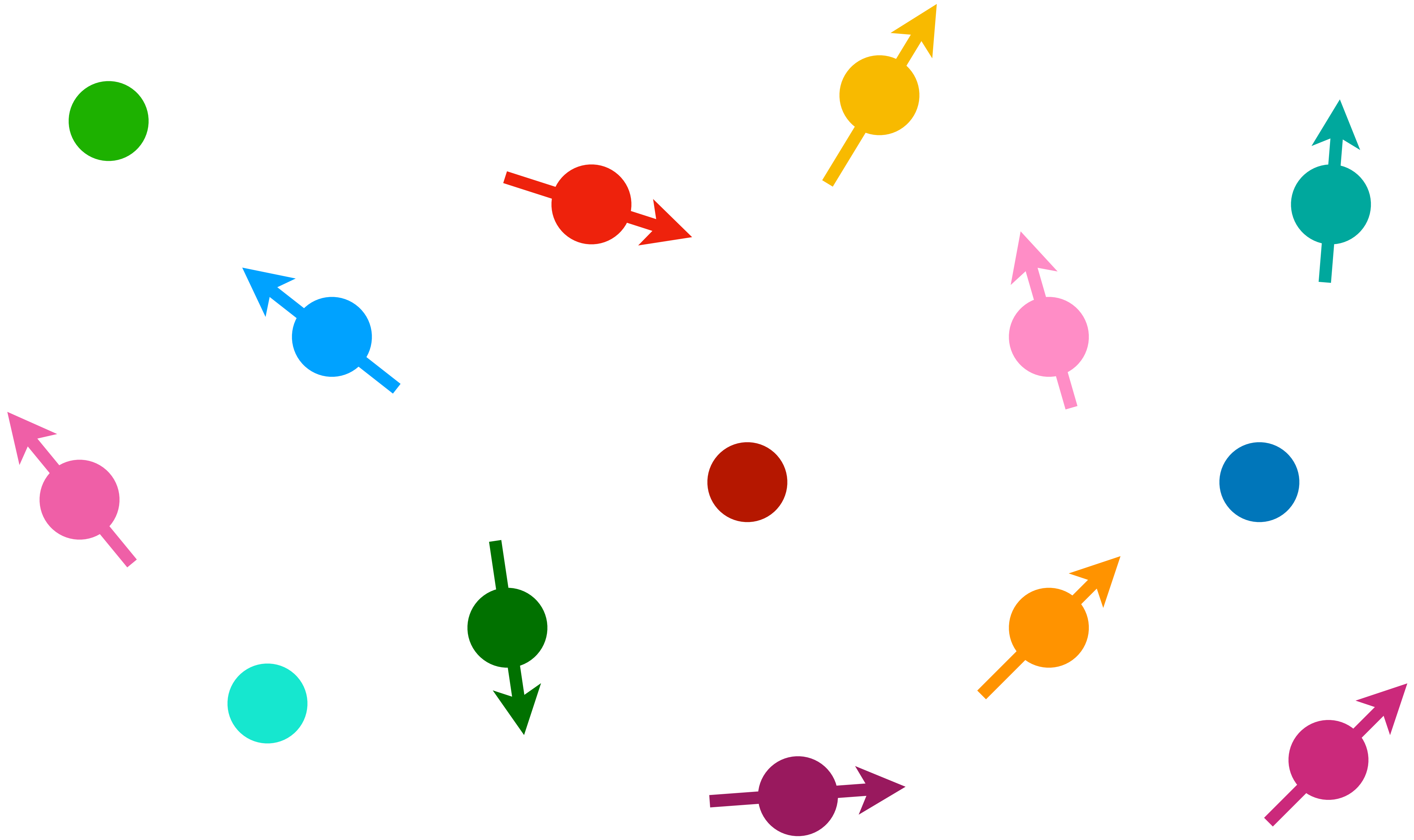

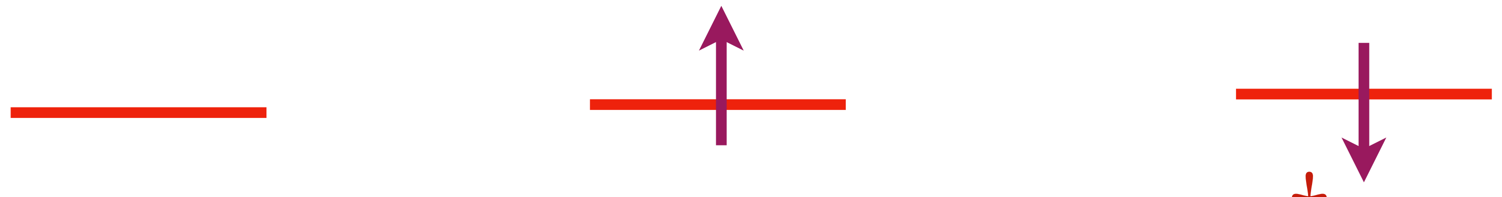

$|0\rangle$ $\qquad c_{\uparrow}^{\dagger}\,|0\rangle$ $\qquad c_{\downarrow}^{\dagger}\,|0\rangle$

Random *t-J* model

$$H = -\frac{1}{\sqrt{N}} \sum_{i,j=1}^{N} t_{ij}\, c_{i\alpha}^{\dagger} c_{j\alpha} + \frac{1}{\sqrt{N}} \sum_{i<j=1}^{N} J_{ij}\, \vec{S}_i \cdot \vec{S}_j$$

We consider the hole-doped case, with no double occupancy.

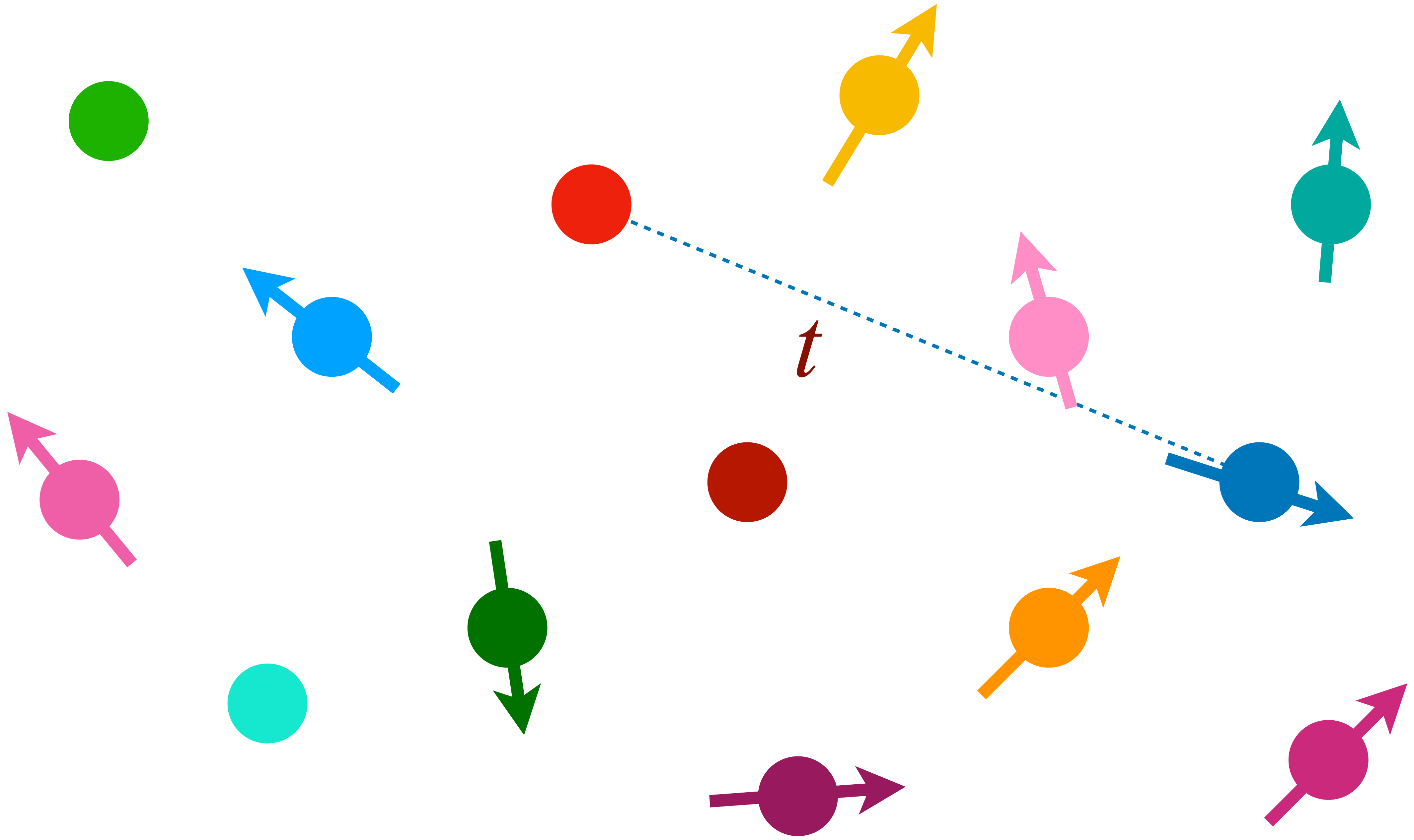

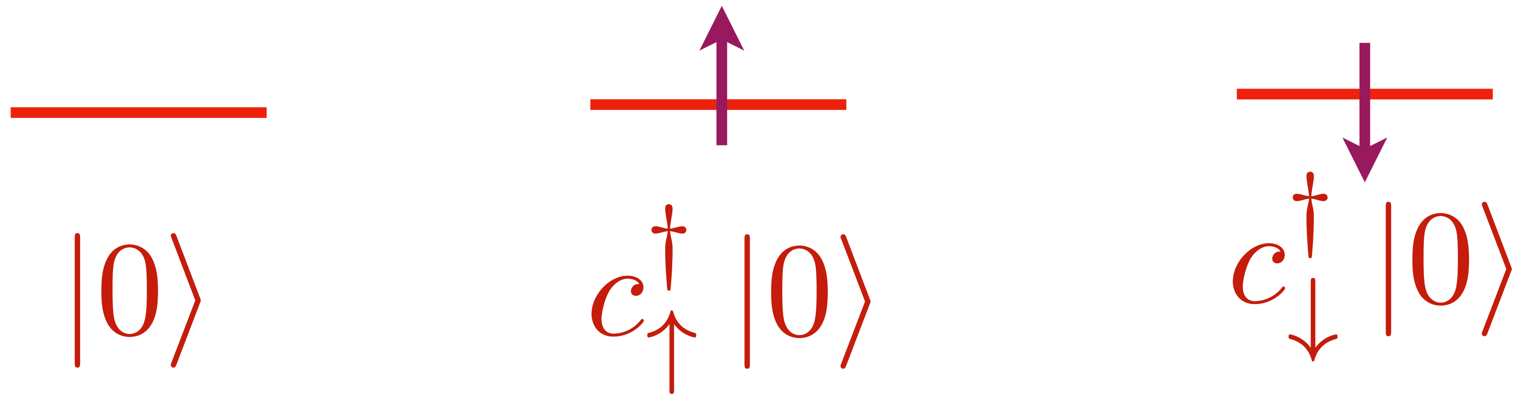

Random *t-J* model

$$H = -\frac{1}{\sqrt{N}} \sum_{i,j=1}^{N} t_{ij}\, c_{i\alpha}^{\dagger} c_{j\alpha} + \frac{1}{\sqrt{N}} \sum_{i<j=1}^{N} J_{ij}\, \vec{S}_i \cdot \vec{S}_j$$

We consider the hole-doped case, with no double occupancy.

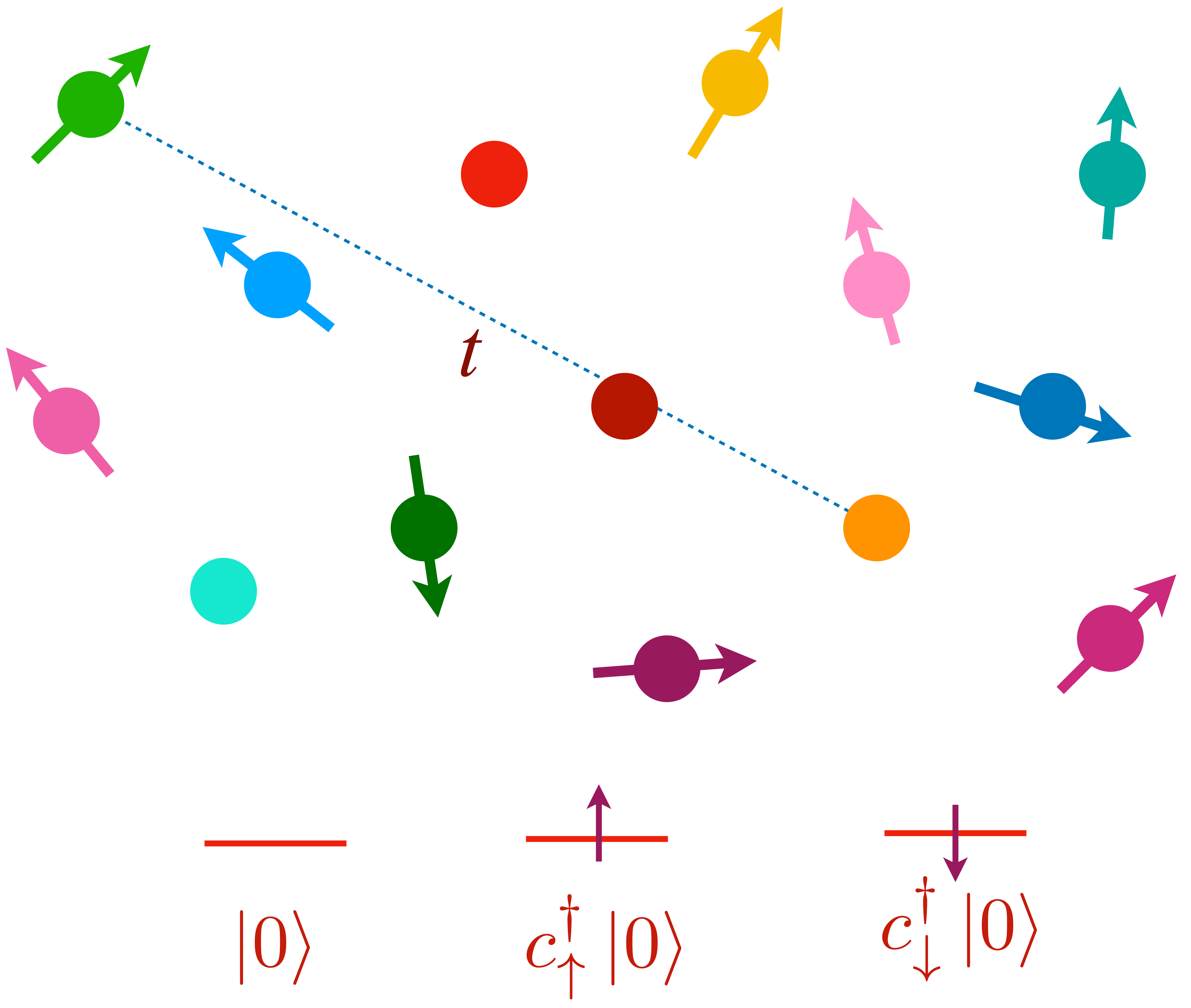

Random *t-J* model

$$H = -\frac{1}{\sqrt{N}} \sum_{i,j=1}^{N} t_{ij}\, c_{i\alpha}^{\dagger} c_{j\alpha} + \frac{1}{\sqrt{N}} \sum_{i<j=1}^{N} J_{ij}\, \vec{S}_i \cdot \vec{S}_j$$

We consider the hole-doped case, with no double occupancy.

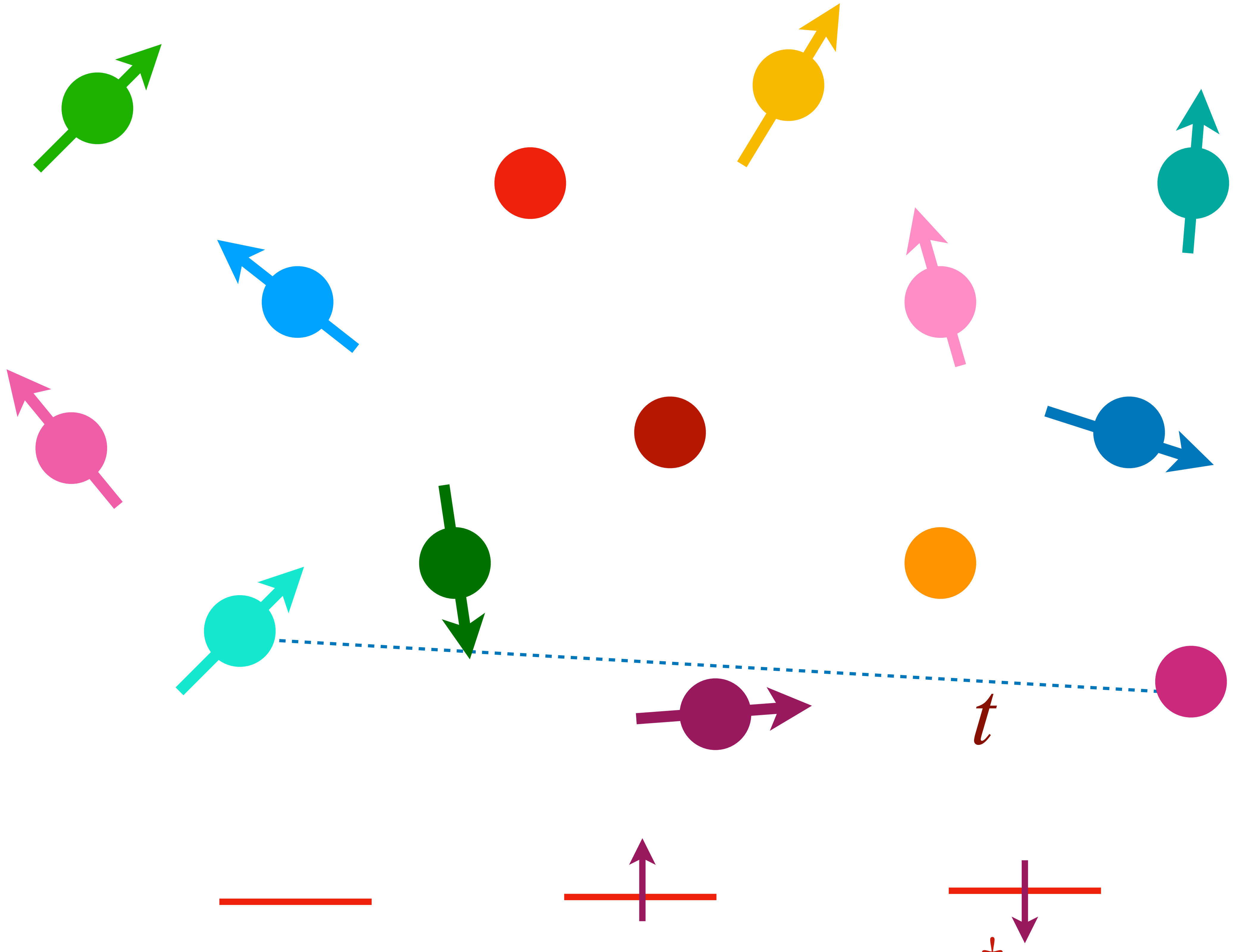

$|0\rangle$ $\quad c_{\uparrow}^{\dagger}|0\rangle$ $\quad c_{\downarrow}^{\dagger}|0\rangle$

Random *t-J* model

$$H = -\frac{1}{\sqrt{N}} \sum_{i,j=1}^{N} t_{ij}\, c_{i\alpha}^\dagger c_{j\alpha} + \frac{1}{\sqrt{N}} \sum_{i<j=1}^{N} J_{ij}\, \vec{S}_i \cdot \vec{S}_j$$

We consider the hole-doped case, with no double occupancy.

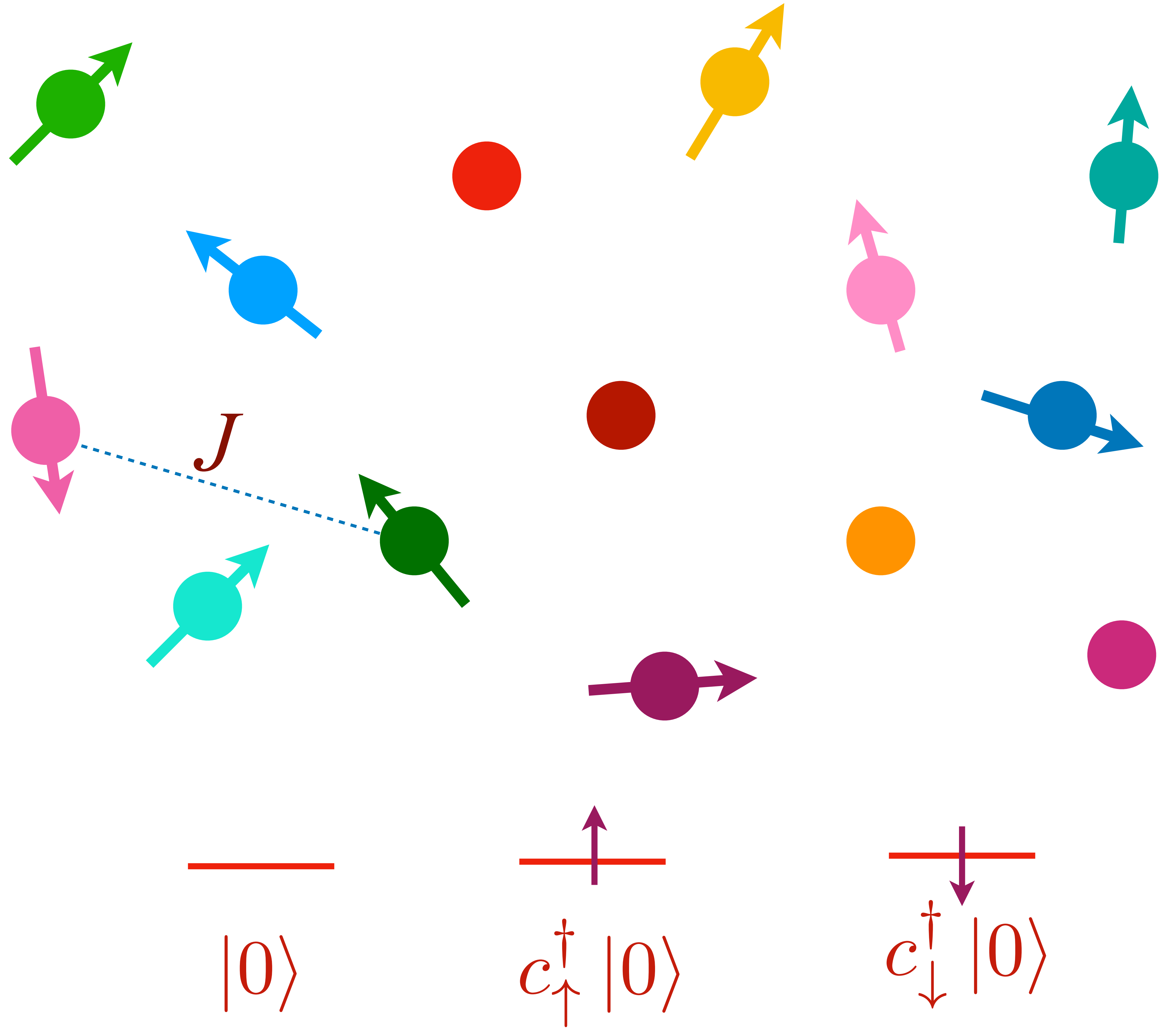

Random *t-J* model

$$H = -\frac{1}{\sqrt{N}} \sum_{i,j=1}^{N} t_{ij}\, c_{i\alpha}^{\dagger} c_{j\alpha} + \frac{1}{\sqrt{N}} \sum_{i<j=1}^{N} J_{ij}\, \vec{S}_i \cdot \vec{S}_j$$

We consider the hole-doped case, with no double occupancy.

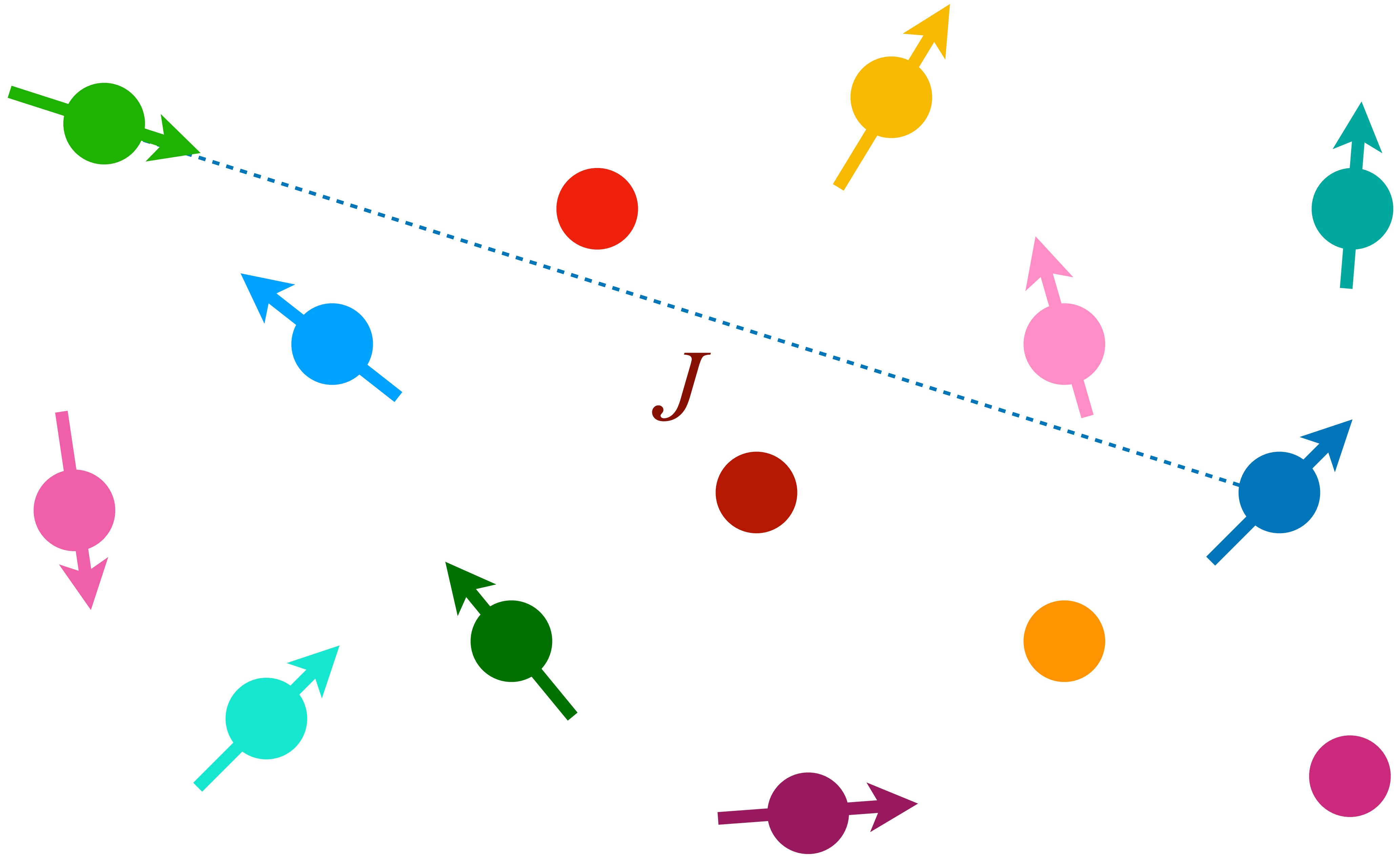

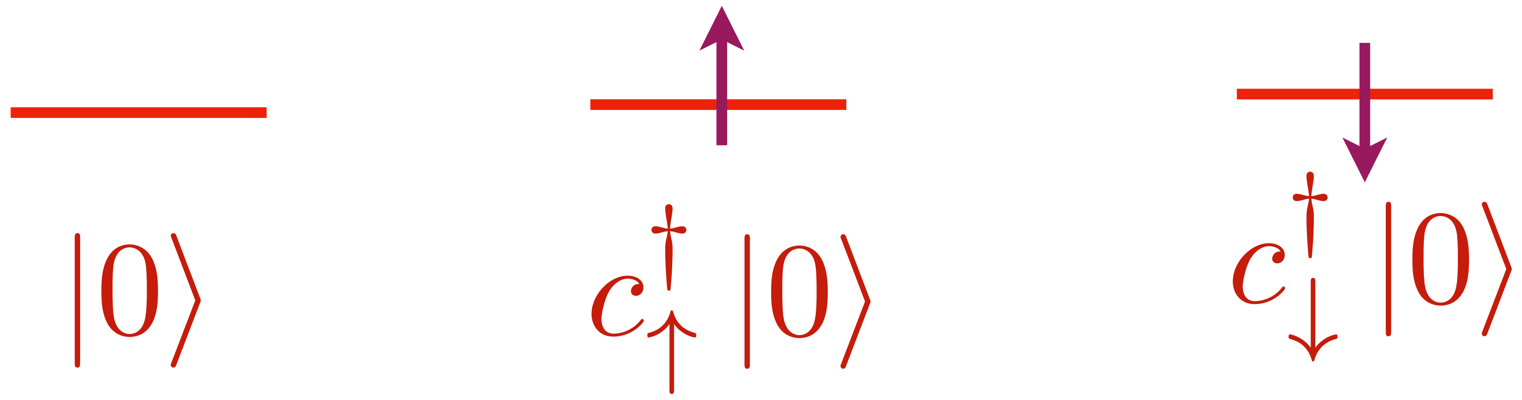

Random t-J model

$$H = -\frac{1}{\sqrt{N}} \sum_{i,j=1}^{N} t_{ij}\, c_{i\alpha}^\dagger c_{j\alpha} + \frac{1}{\sqrt{N}} \sum_{i<j=1}^{N} J_{ij}\, \vec{S}_i \cdot \vec{S}_j$$

We consider the hole-doped case, with no double occupancy.

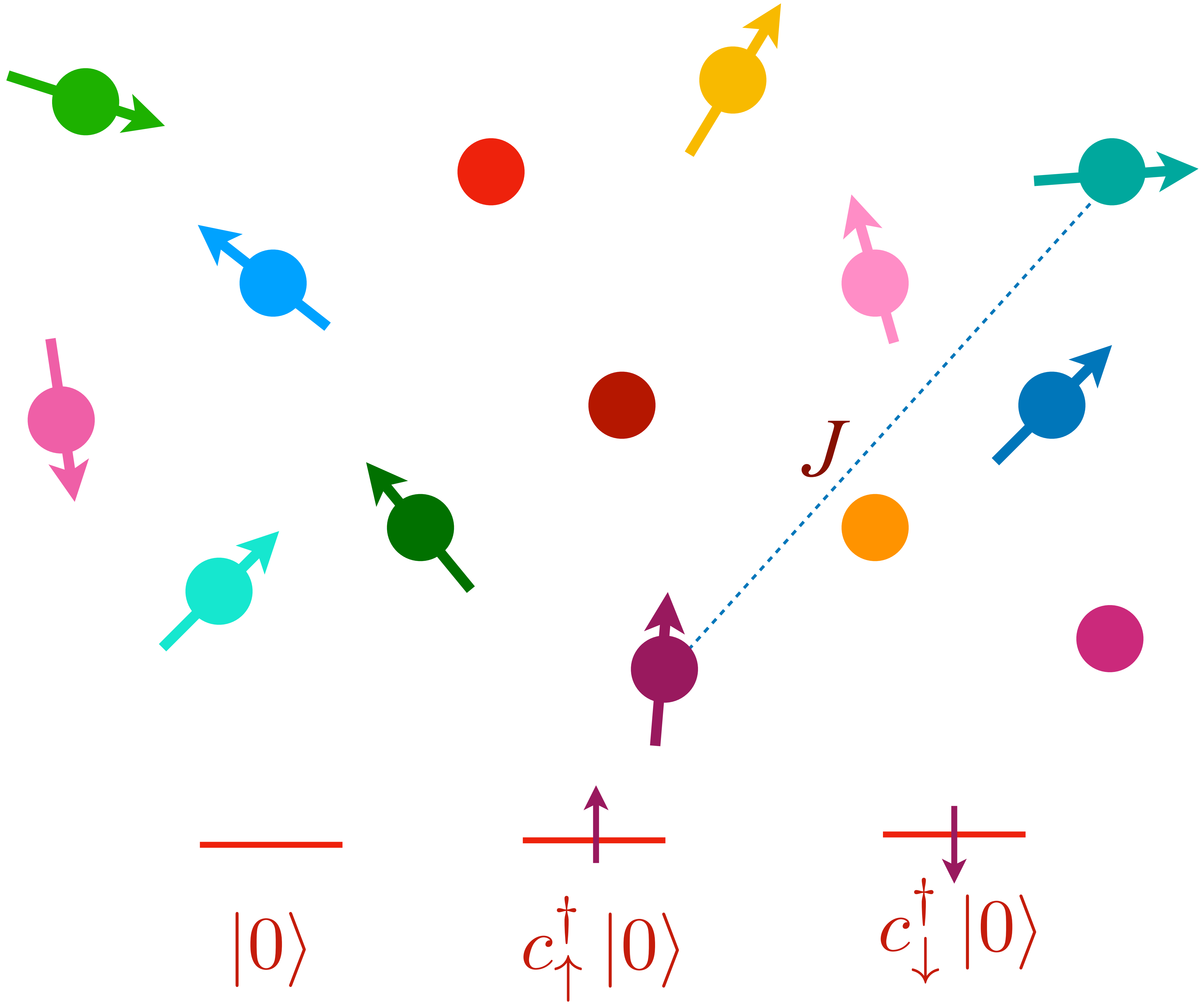

t-J phase diagram: RG

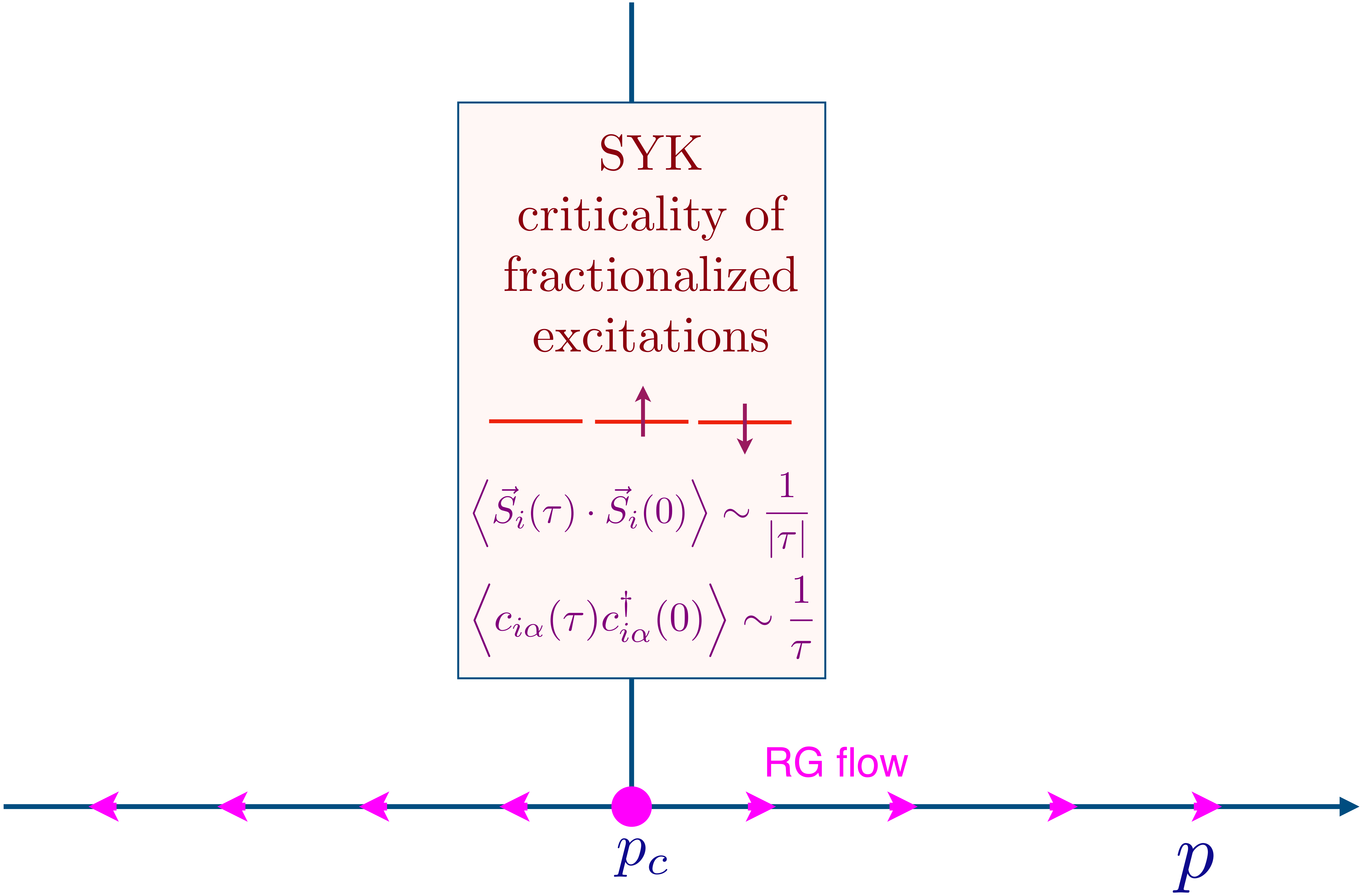

D. Joshi, Chenyuan Li, G. Tarnopolsky, A. Georges, S. Sachdev, PRX **10**, 021033 (2020)

t-J phase diagram: RG

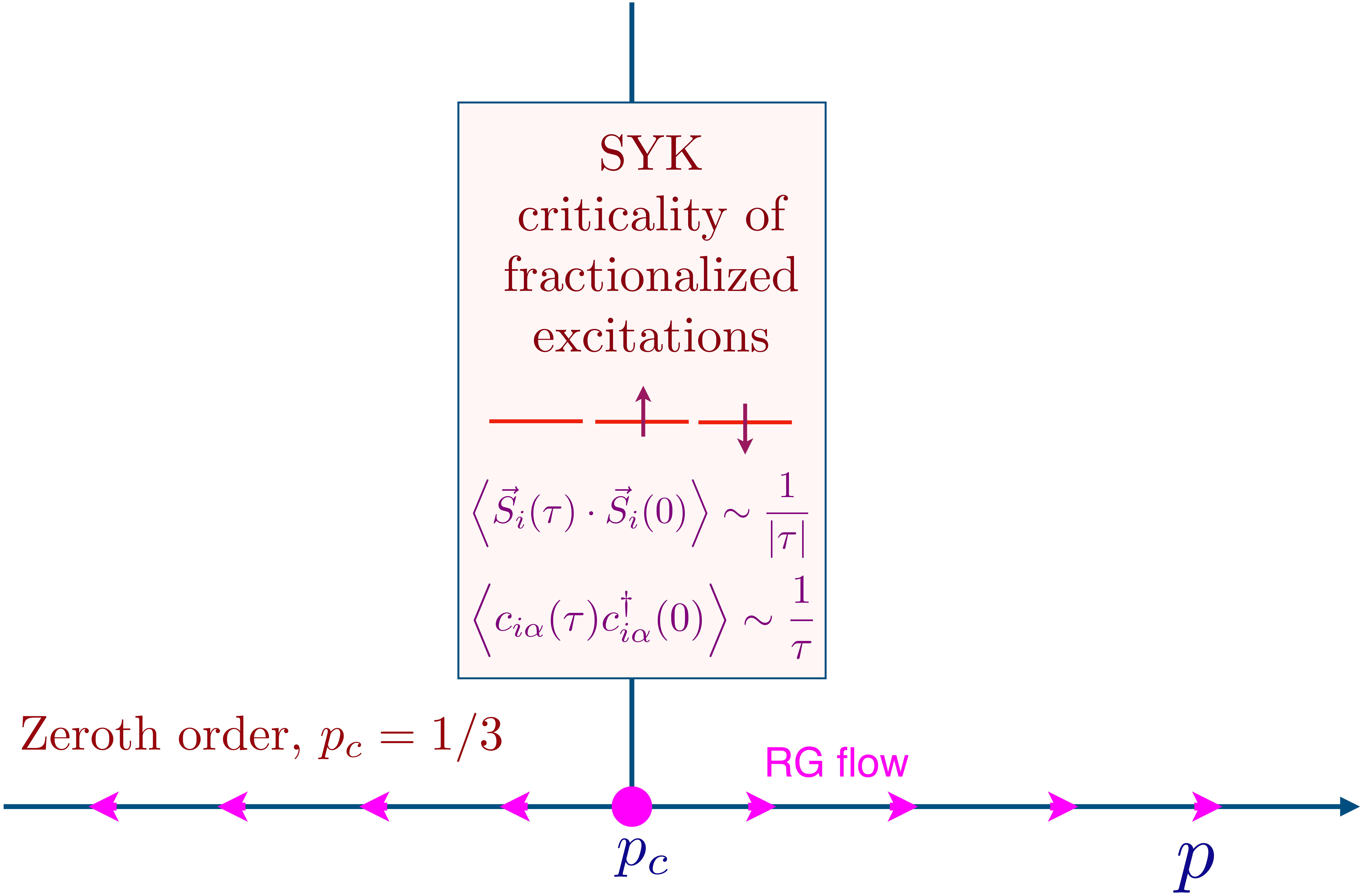

D. Joshi, Chenyuan Li, G. Tarnopolsky, A. Georges, S. Sachdev, PRX **10**, 021033 (2020)

t-J phase diagram: RG

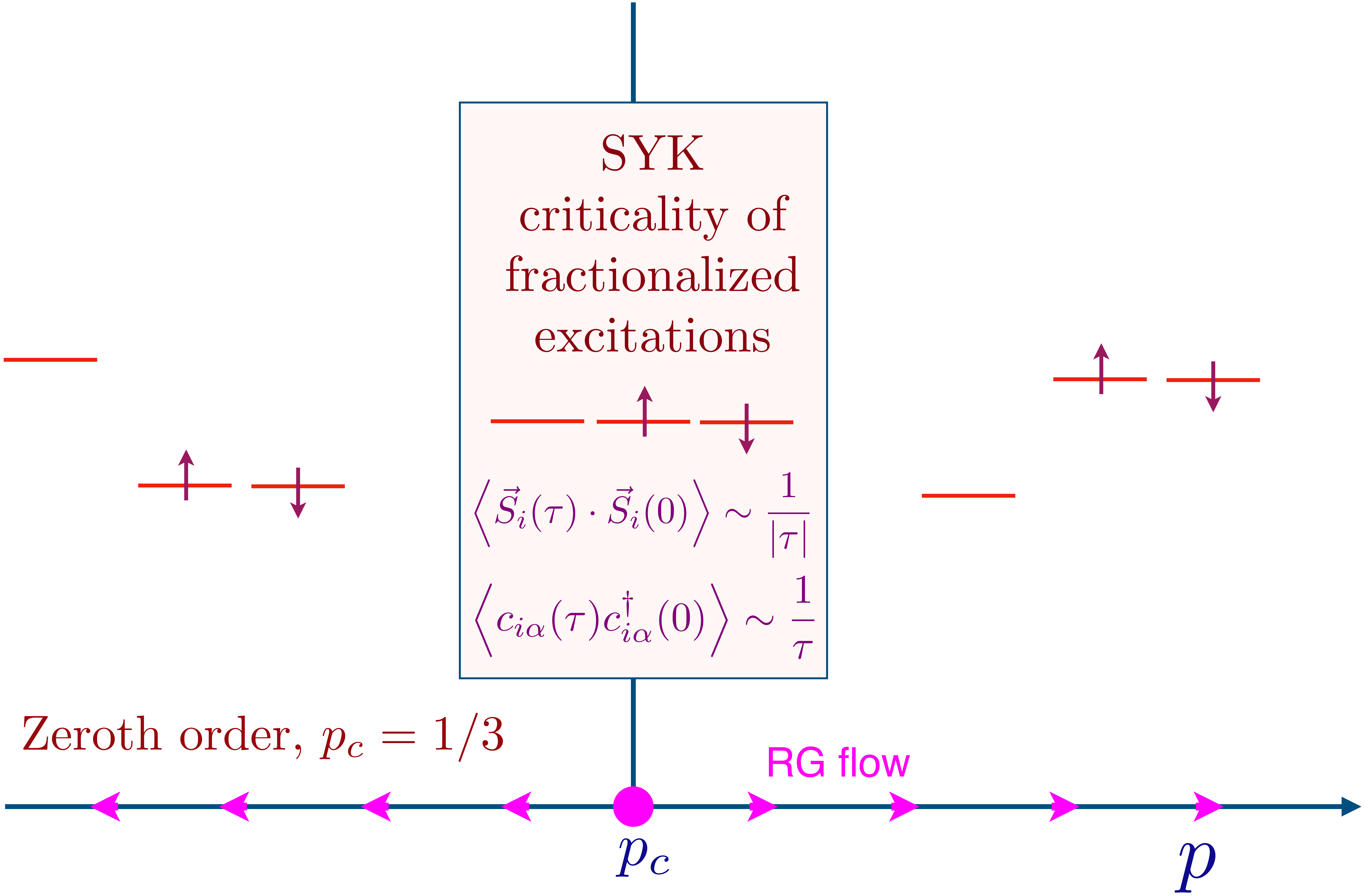

D. Joshi, Chenyuan Li, G. Tarnopolsky, A. Georges, S. Sachdev, PRX **10**, 021033 (2020)

t-J phase diagram: RG

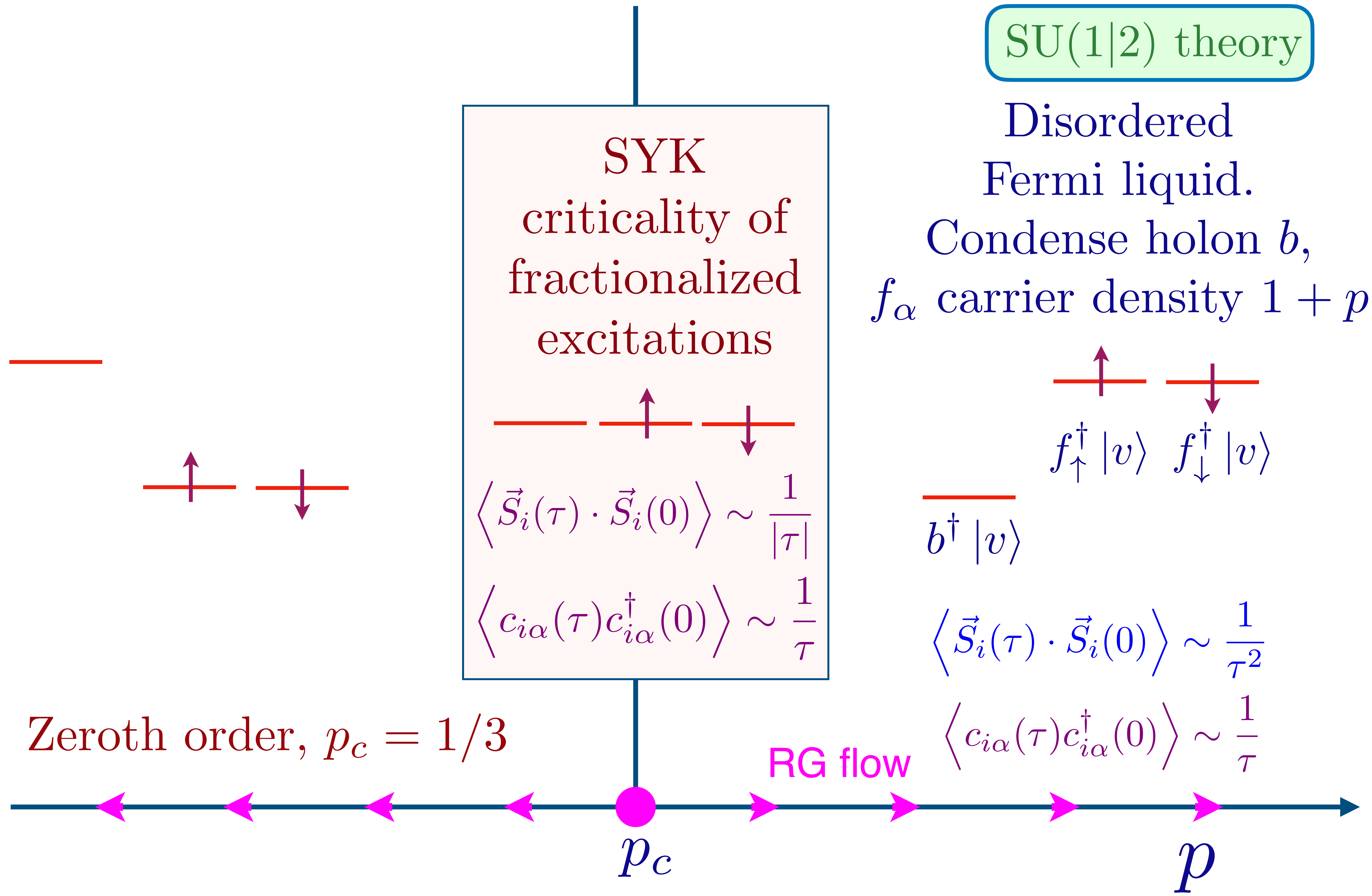

D. Joshi, Chenyuan Li, G. Tarnopolsky, A. Georges, S. Sachdev, PRX **10**, 021033 (2020)

t-J phase diagram: RG

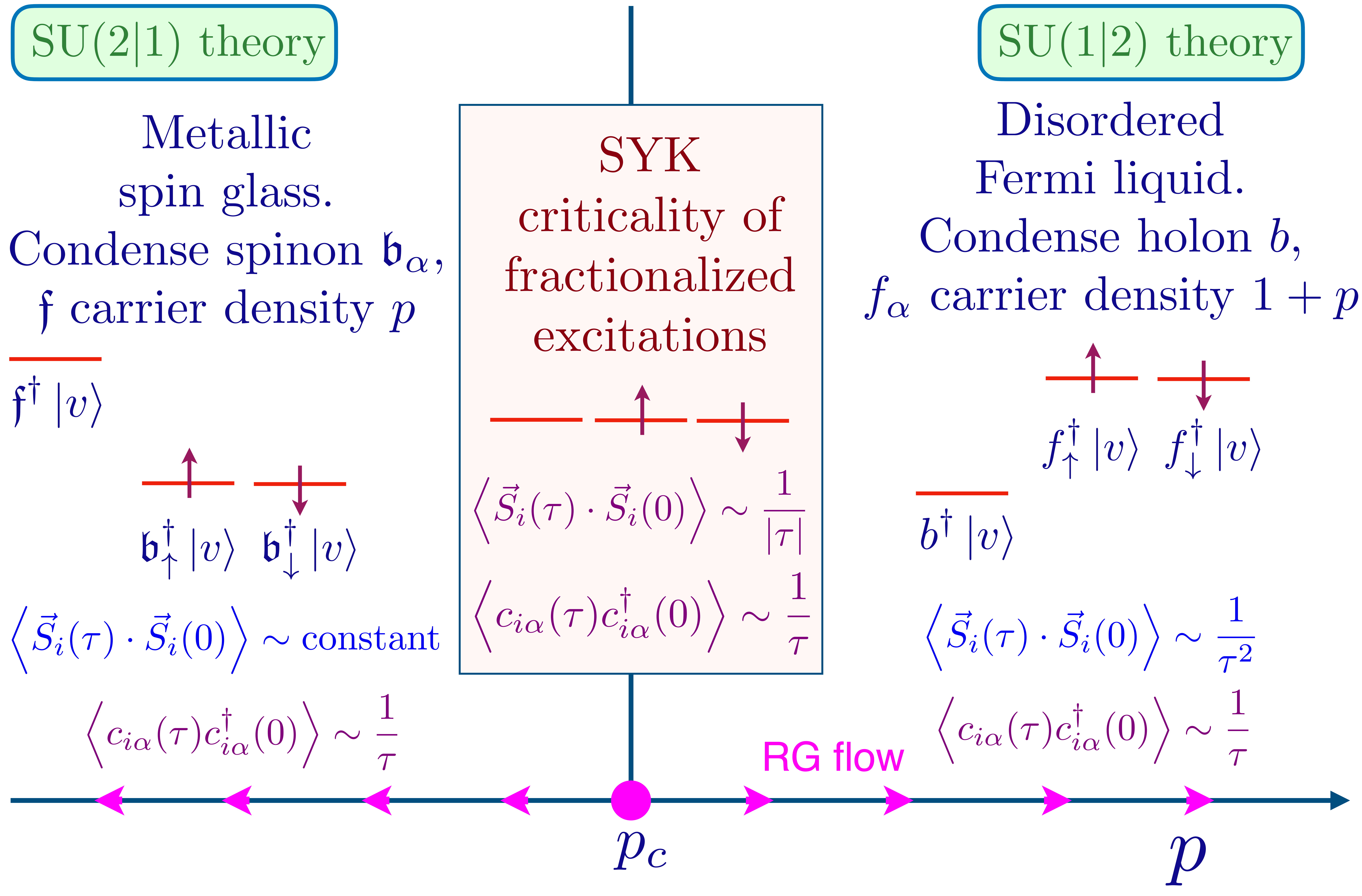

D. Joshi, Chenyuan Li, G. Tarnopolsky, A. Georges, S. Sachdev, PRX **10**, 021033 (2020)

SYK criticality

Key properties

1. The ground state is 'critical' and there are no quasiparticles.

S. Sachdev and J. Ye, PRL **70**, 3339 (1993)

SYK criticality

Key properties

1. The ground state is 'critical' and there are no quasiparticles.

2. There is an emergent time reparameterization symmetry which is softly broken at high energies.

A. Kitaev, KITP talk (2015)

J. Maldacena and D. Stanford, PRD **94**, 106002 (2016)

A. Kitaev and J. Suh, JHEP 183 (2018)

SYK criticality

Key properties

1. The ground state is ‘critical’ and there are no quasiparticles.

2. There is an emergent time reparameterization symmetry which is softly broken at high energies.

3. There is a non-zero extensive entropy as $T \to 0$

A. Georges, O. Parcollet, and S. Sachdev, PRB **63**, 134406 (2001)

$$\lim_{T \to 0} \lim_{N \to \infty} \frac{S}{N} = \mathcal{S}_0(\mathcal{Q}) \neq 0$$

This entropy is <u>*not*</u> due to an exponentially large ground degeneracy. Instead, it reflects an exponentially small many-body level spacing $\sim e^{-N\mathcal{S}_0}$ down to the ground state.

SYK criticality

Key properties

1. The ground state is 'critical' and there are no quasiparticles.

2. There is an emergent time reparameterization symmetry which is softly broken at high energies.

3. There is a non-zero extensive entropy as $T \to 0$

$$\lim_{T\to 0} \lim_{N\to\infty} \frac{S}{N} = \mathcal{S}_0(\mathcal{Q}) \neq 0$$

This entropy is *not* due to an exponentially large ground degeneracy. Instead, it reflects an exponentially small many-body level spacing $\sim e^{-N\mathcal{S}_0}$ down to the ground state.

4. Dynamic scaling of equilibrium and non-equilibrium properties in a universal time $\sim \hbar/(k_B T)$

A. Eberlein, V. Kasper, S. Sachdev, and J. Steinberg, PRB **96**, 205123 (2017)

SYK criticality

Key properties

5. The leading low temperature behavior of many observables is controlled by a time reparameterization soft mode. The action for this soft mode is controlled by an emergent SL(2,R) symmetry. Specifically, the entropy is $S(T)/N = \mathcal{S}_0(\mathcal{Q}) + \gamma T$, where γ propotional to the co-efficient of the Schwarzian.

A. Kitaev, KITP talk (2015)

J. Maldacena and D. Stanford, PRD **94**, 106002 (2016)

A. Kitaev and J. Suh, JHEP 183 (2018)

SYK criticality

Key properties

5. The leading low temperature behavior of many observables is controlled by a time reparameterization soft mode. The action for this soft mode is controlled by an emergent SL(2,R) symmetry. Specifically, the entropy is $S(T)/N = \mathcal{S}_0(\mathcal{Q}) + \gamma T$, where γ propotional to the co-efficient of the Schwarzian.

6. The time reparameterization mode leads to a frequency dependence in the spin susceptibility and a linear-in-T temperature dependence to the resistivity as $T \to 0$.

Haoyu Guo, Yingfei Guo, S. Sachdev, Annals of Physics **418**, 168202 (2020)
M. Tikhanovskaya, Haoyu Guo, S. Sachdev, and G. Tarnopolsky, to appear

Random J model (insulator): SU(M) symmetry

The local dynamic spin susceptibility, $\chi_L(i\omega_n) = \int_0^{1/T} d\tau \left\langle \vec{S}_i(\tau)\vec{S}i(0)\right\rangle e^{i\omega_n\tau}$, obeys

$$\mathrm{Im}\chi_L(\omega) \propto \tanh\left(\frac{\omega}{2T}\right)\left[1 - \alpha_S\,\omega\tanh\left(\frac{\omega}{2T}\right) + \ldots\right]$$

From the time reparameterization soft-mode

The ratio α_S/γ is a universal number, which we have computed in the large M limit

$$\frac{\alpha_S}{\gamma} = \frac{24}{\pi(2+3\pi)} \quad , \quad M \to \infty\,.$$

(Recall the specific heat is $C = \gamma T$ per site and spin component.)

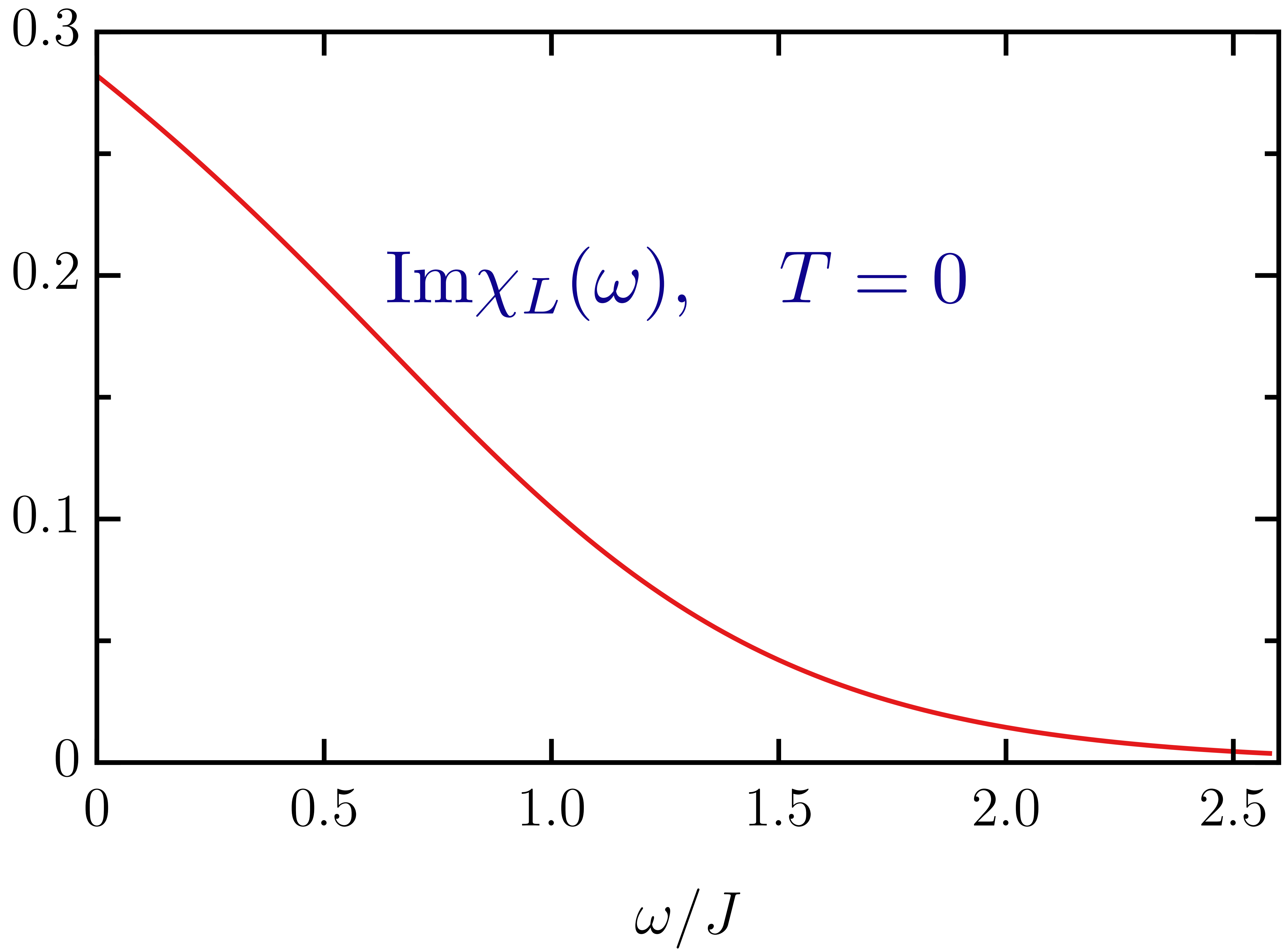

Henry Shackleton

Alexander Wietek

Antoine Georges

Random J model

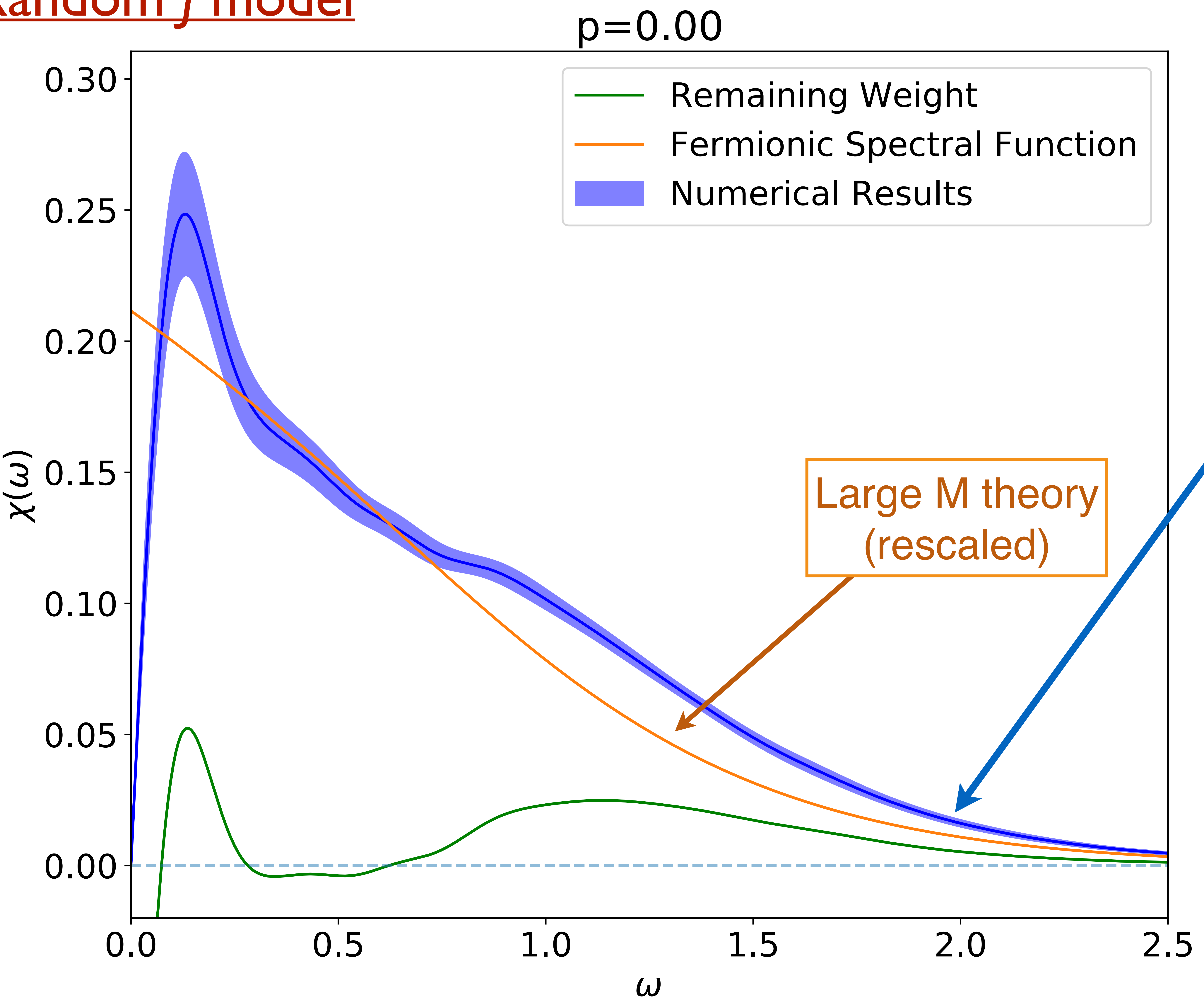

Exact diagonalization results of SU(2) random magnet
L. Arrachea and M. J. Rozenberg, PRB **65**, 224430 (2002)
(recomputed by Henry Shackleton)

Incoherent contribution similar to SY spin liquid !

Random J model

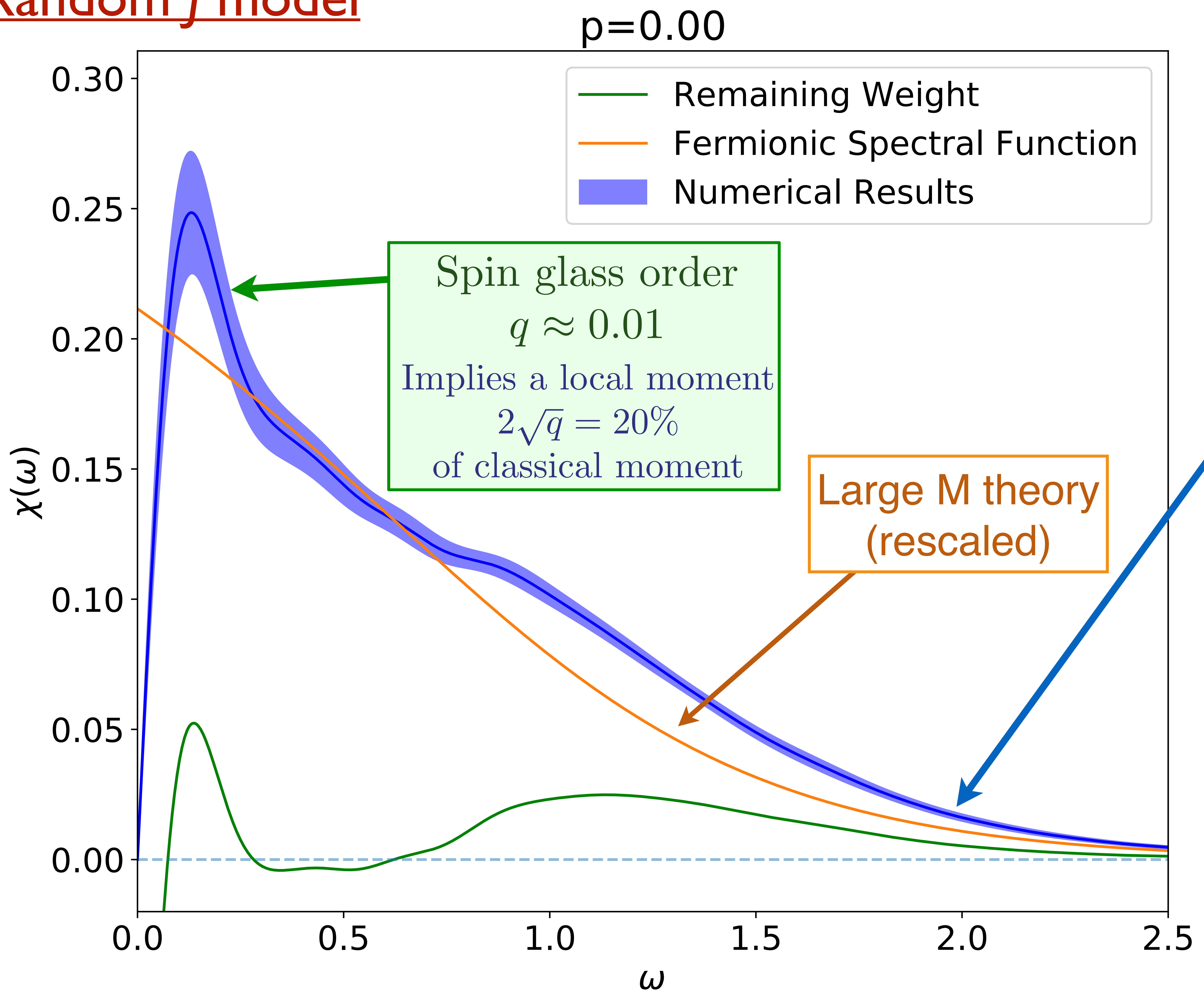

Exact diagonalization results of SU(2) random magnet L. Arrachea and M. J. Rozenberg, PRB **65**, 224430 (2002) (recomputed by Henry Shackleton)

Incoherent contribution similar to SY spin liquid !

Random *t-J* model

Exact diagonalization of clusters with N finite

Local dynamic spin susceptibility $\mathrm{Im}\chi_L(\omega)$

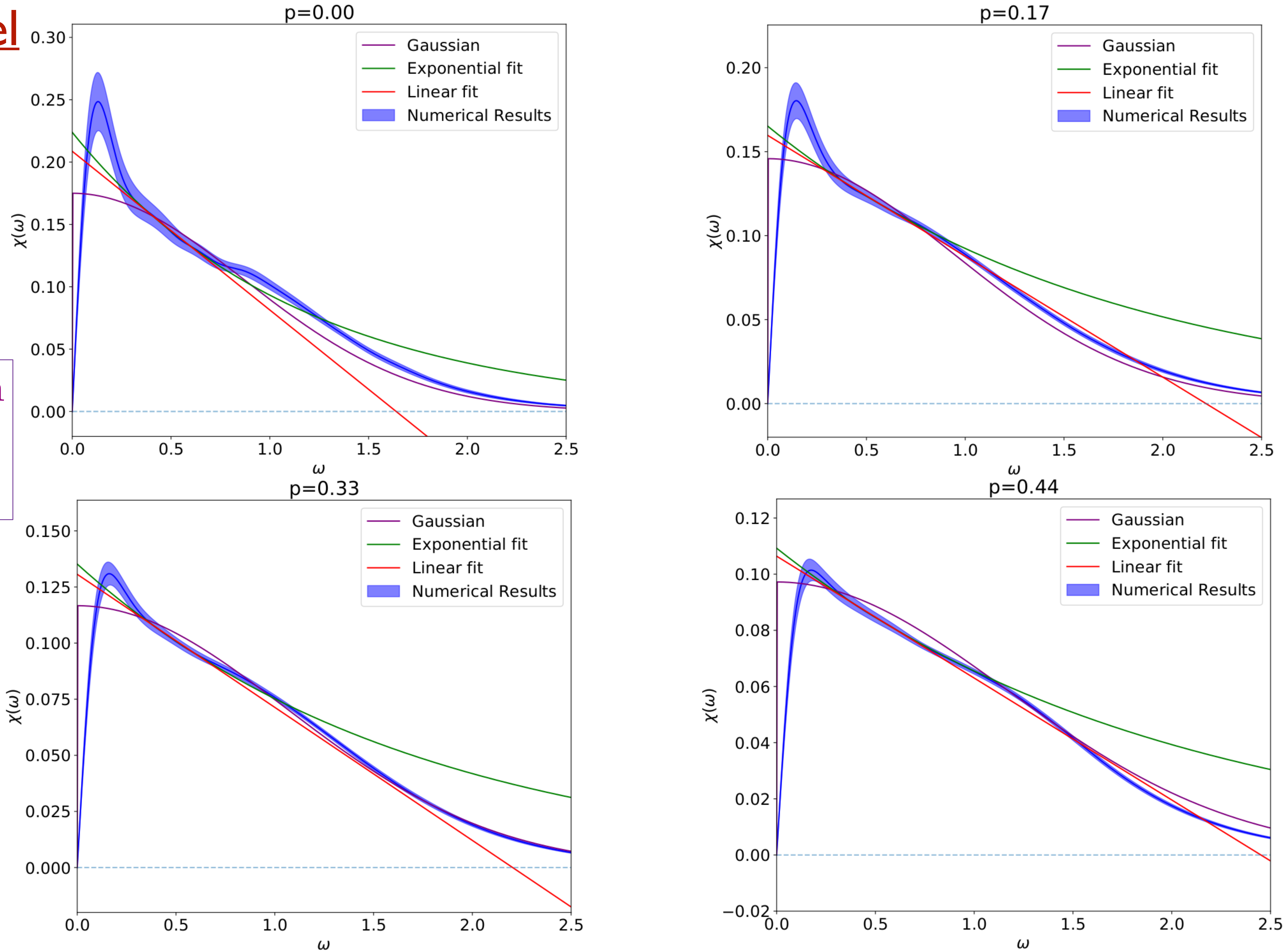

Random *t-J* model

Exact diagonalization of clusters with *N* finite

Local dynamic spin susceptibility $\mathrm{Im}\chi_L(\omega)$

Incoherent contribution similar to SY spin liquid !

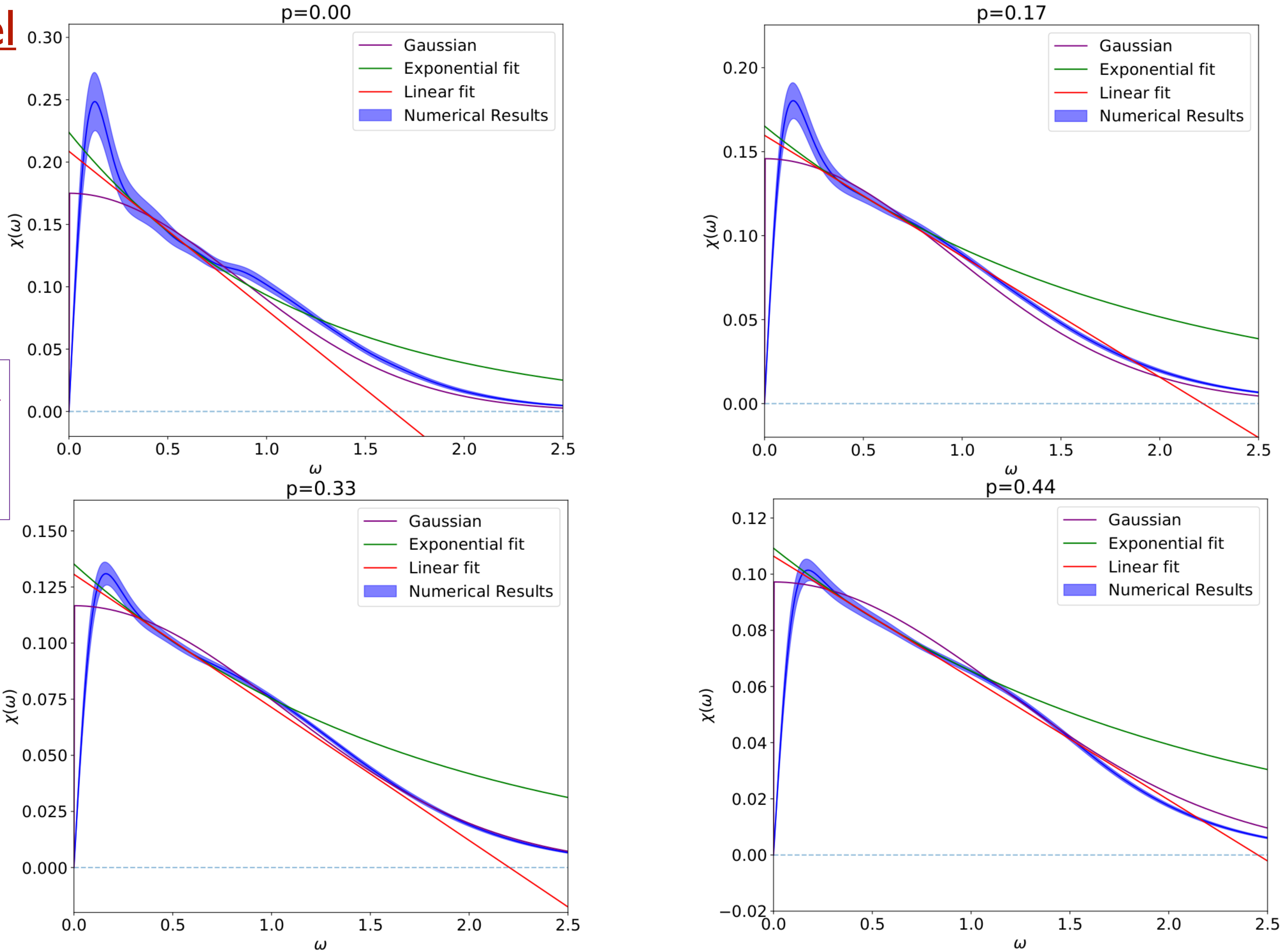

Random *t-J* model

Exact diagonalization of clusters with *N* finite

Local dynamic spin susceptibility $\mathrm{Im}\chi_L(\omega)$

Remaining low frequency weight integrates to the spin glass order parameter q

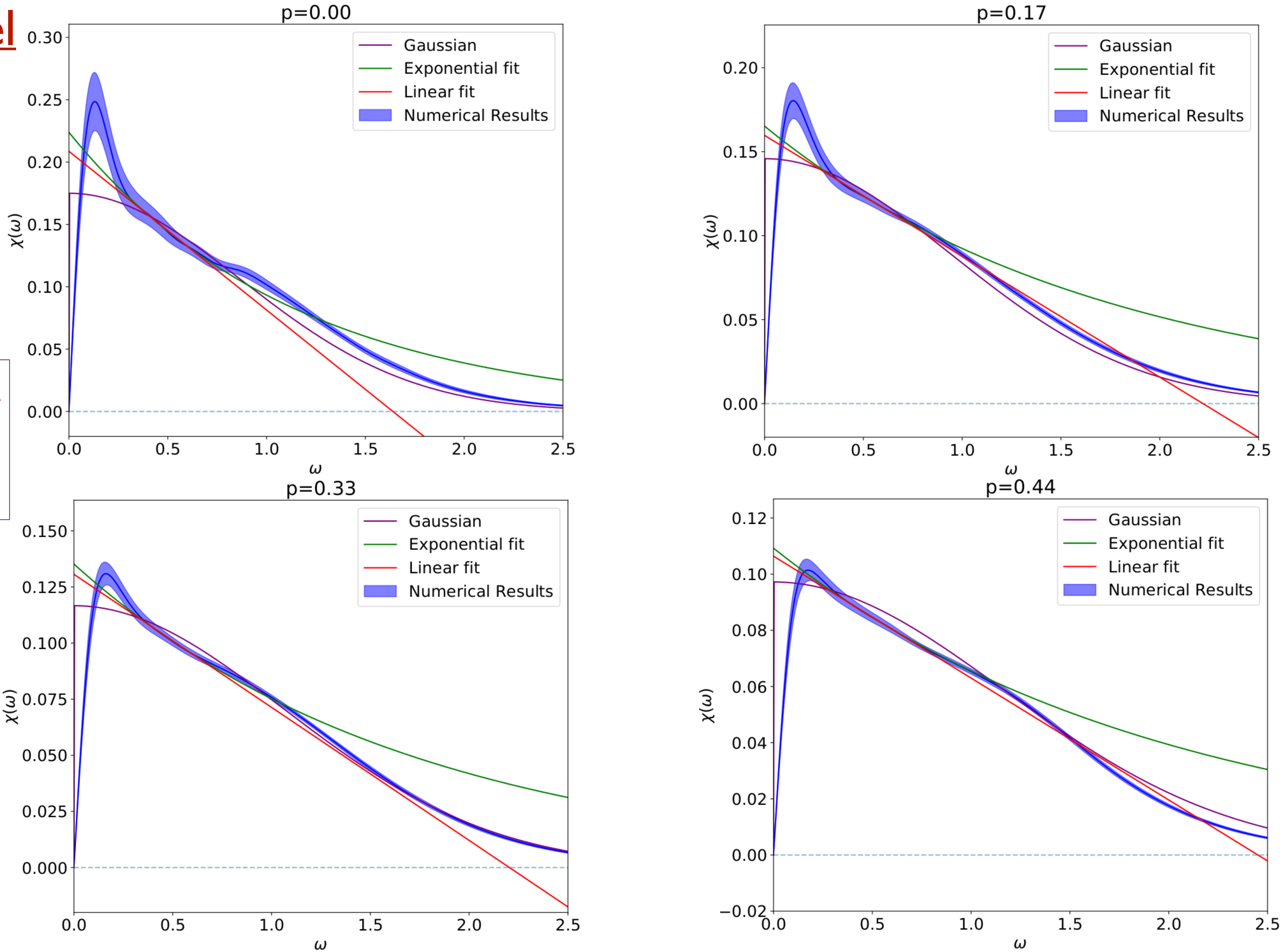

Entropy at $T \gg 1$ determined by $\dim(\mathcal{H})$

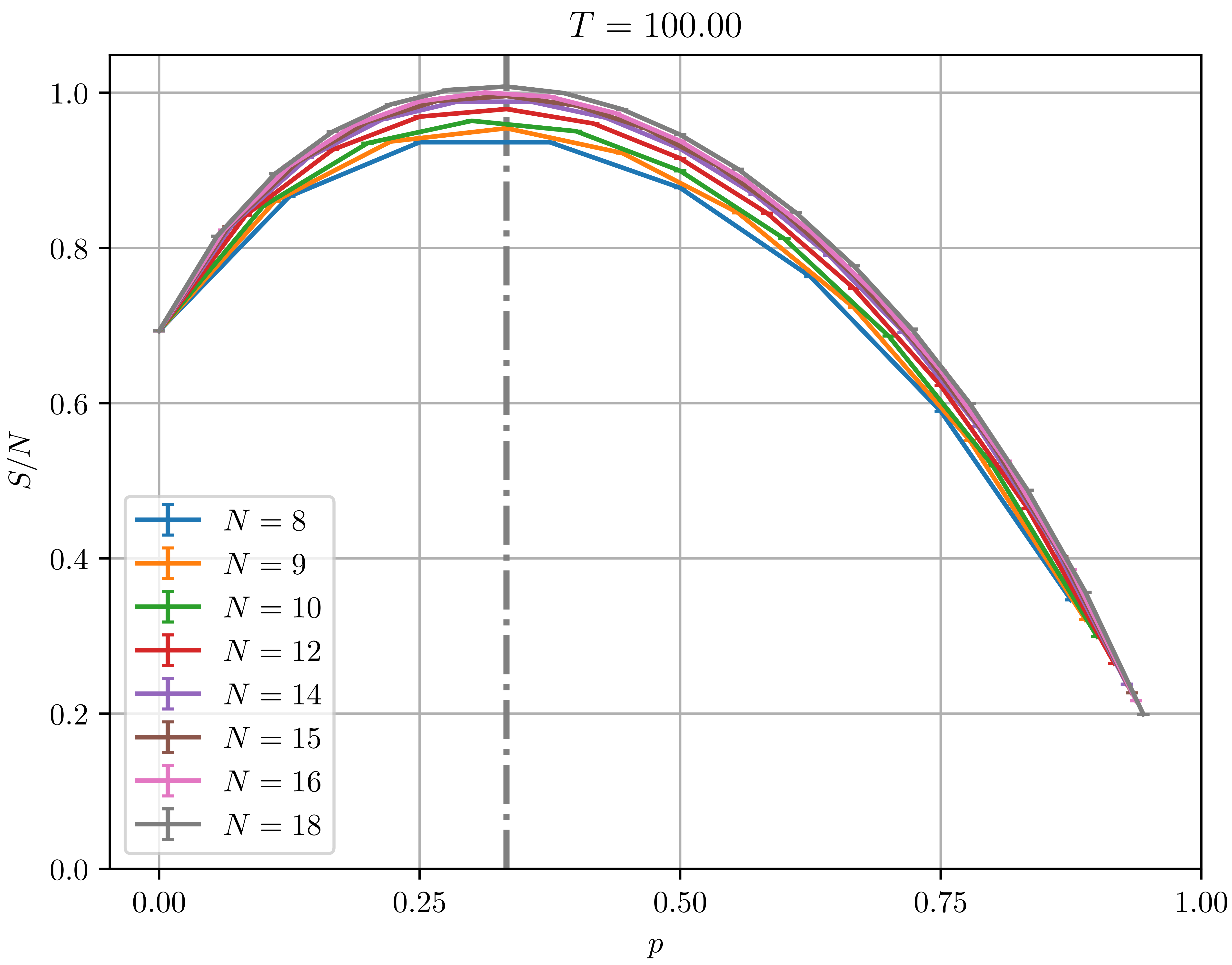

Maximum entropy shifts at lower temperature

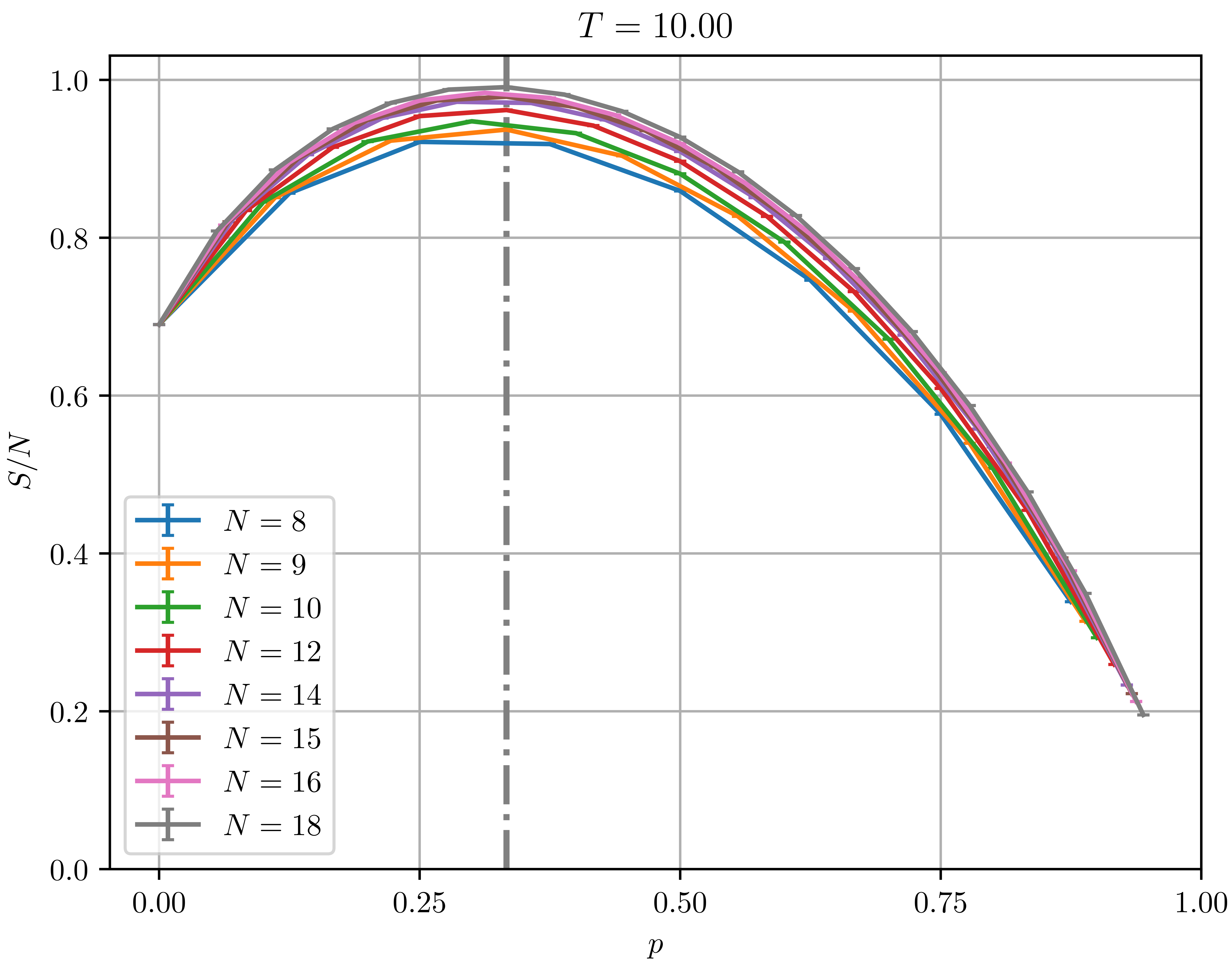

Maximum entropy shifts at lower temperature

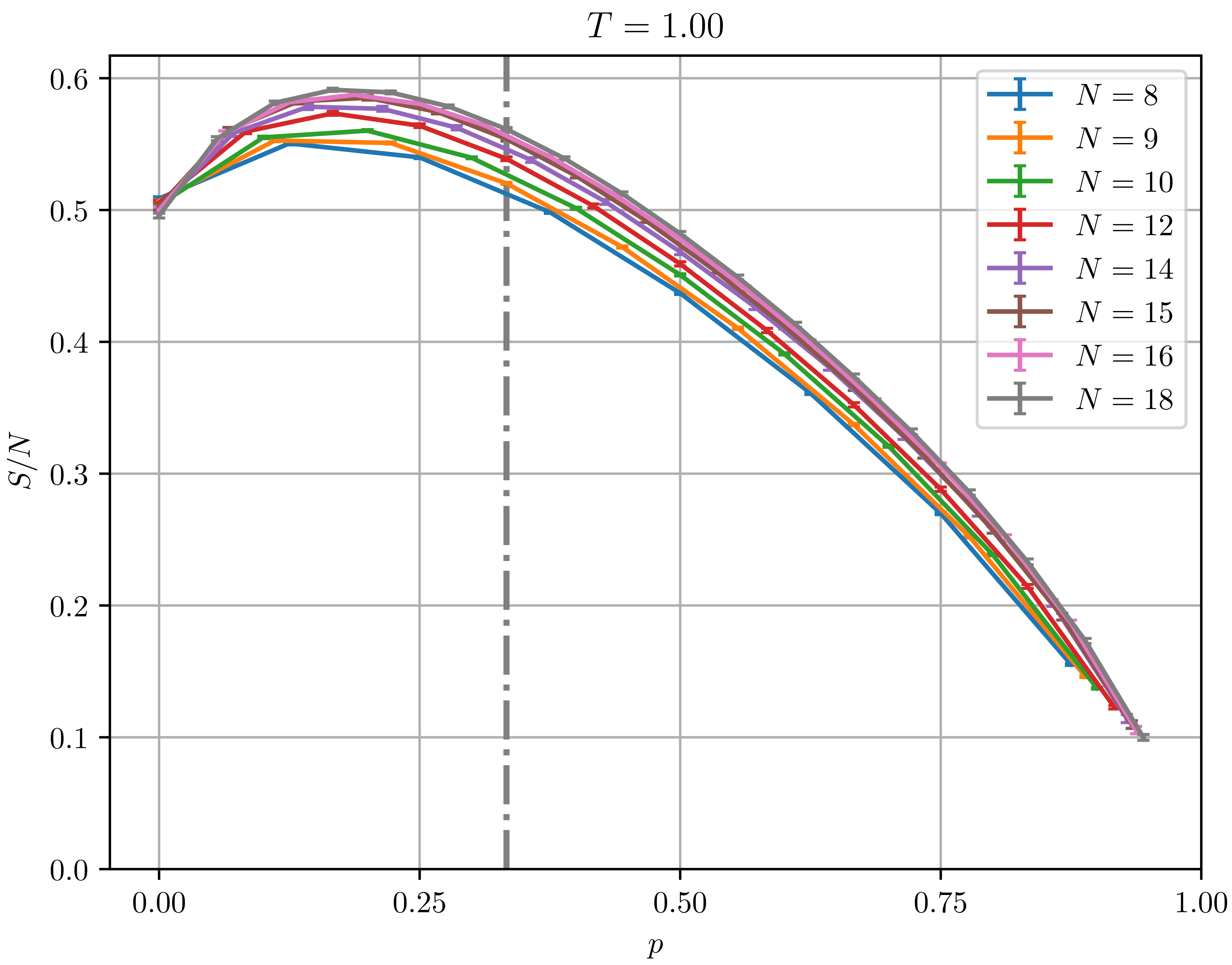

Maximum entropy shifts at lower temperature

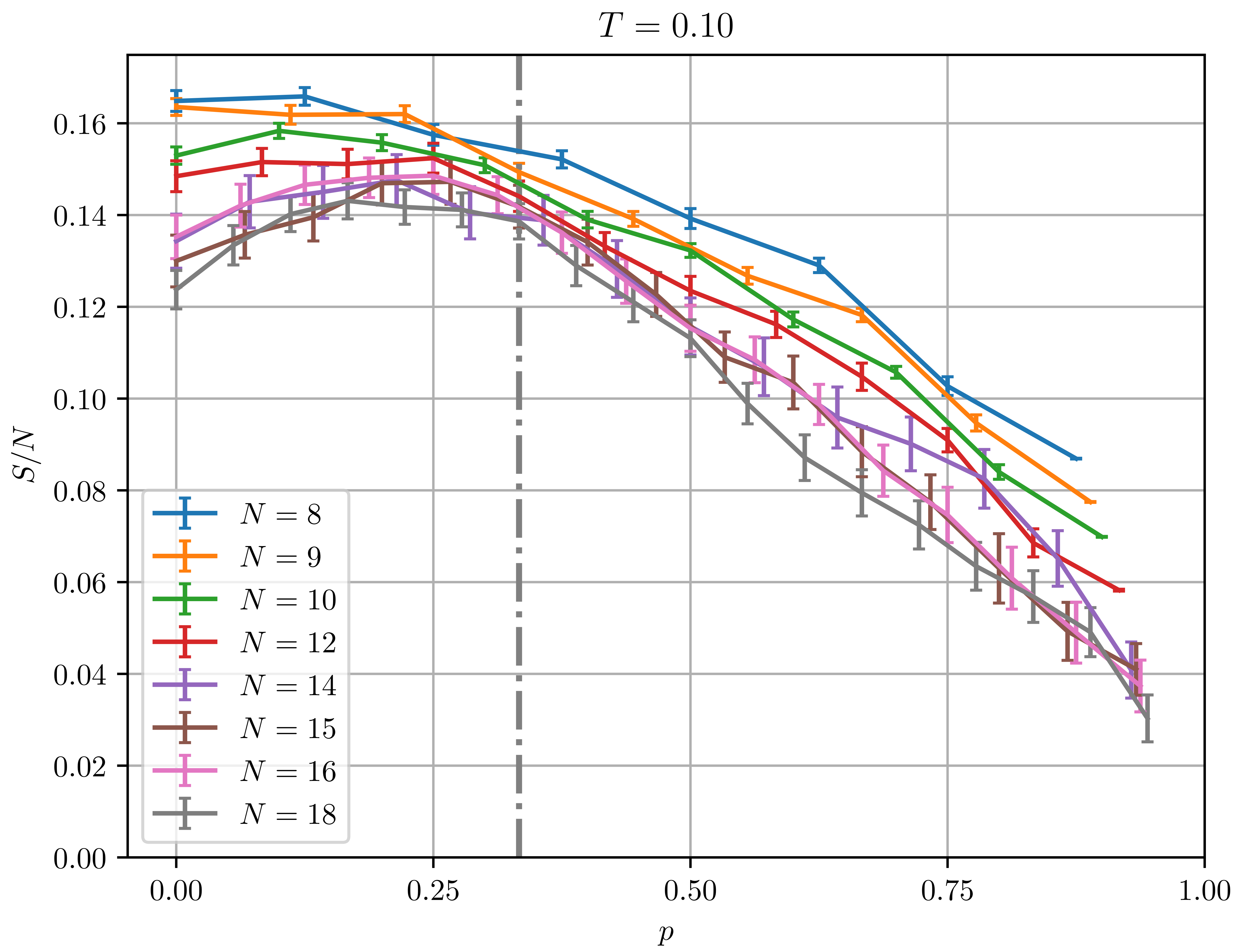

Large-N extrapolation of entropy density

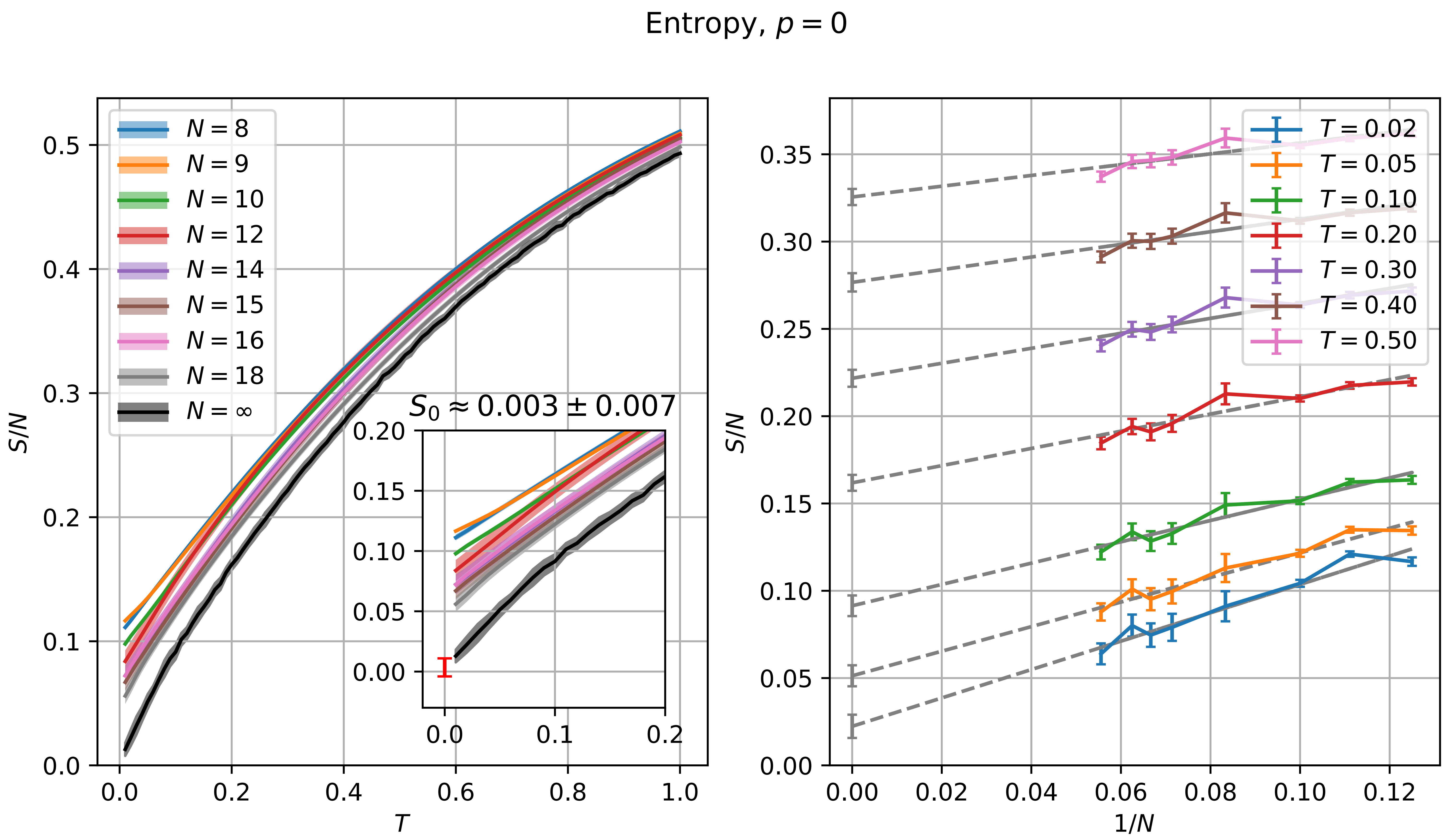

Large-N extrapolation of entropy density

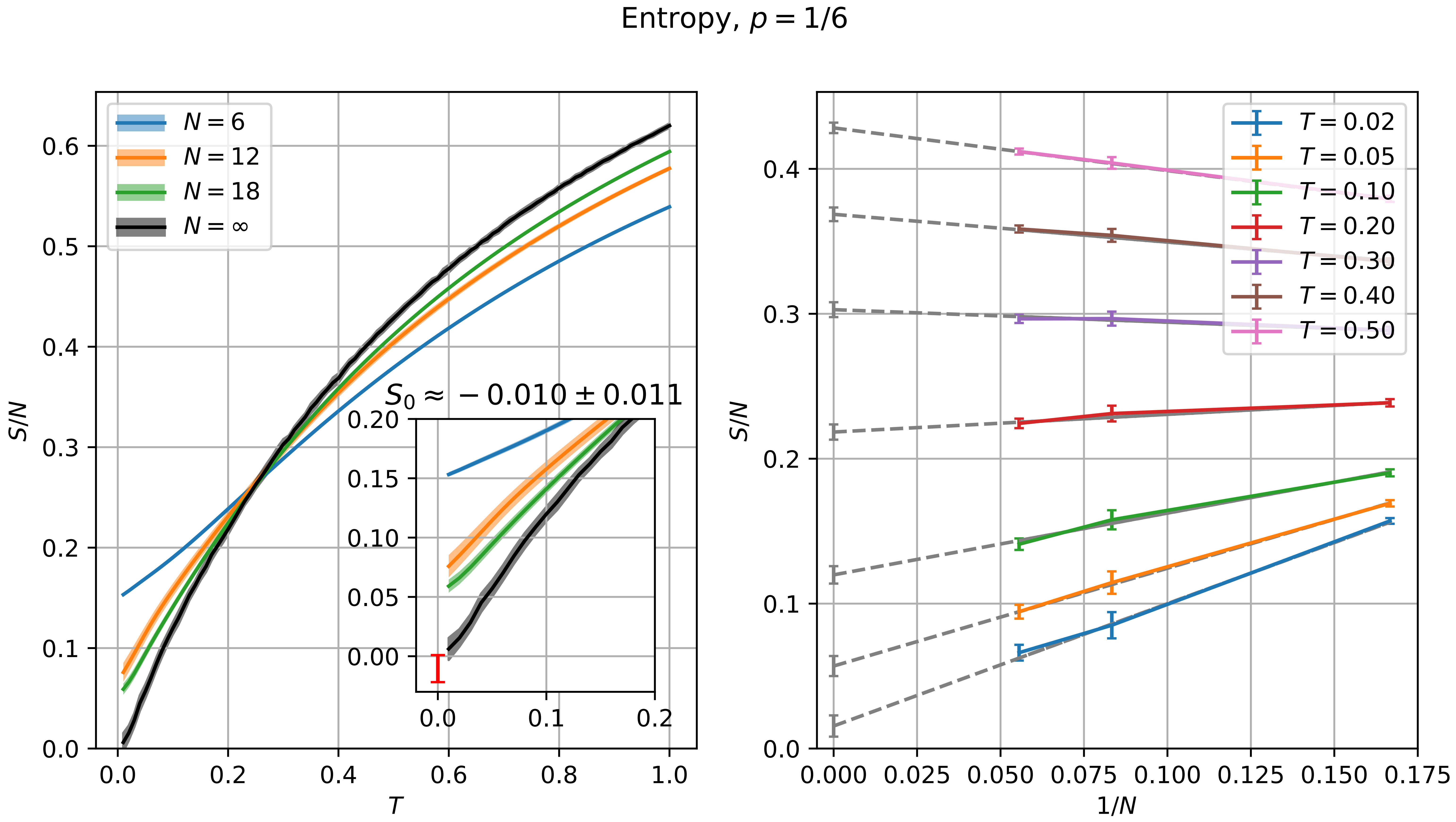

Large-N extrapolation of entropy density

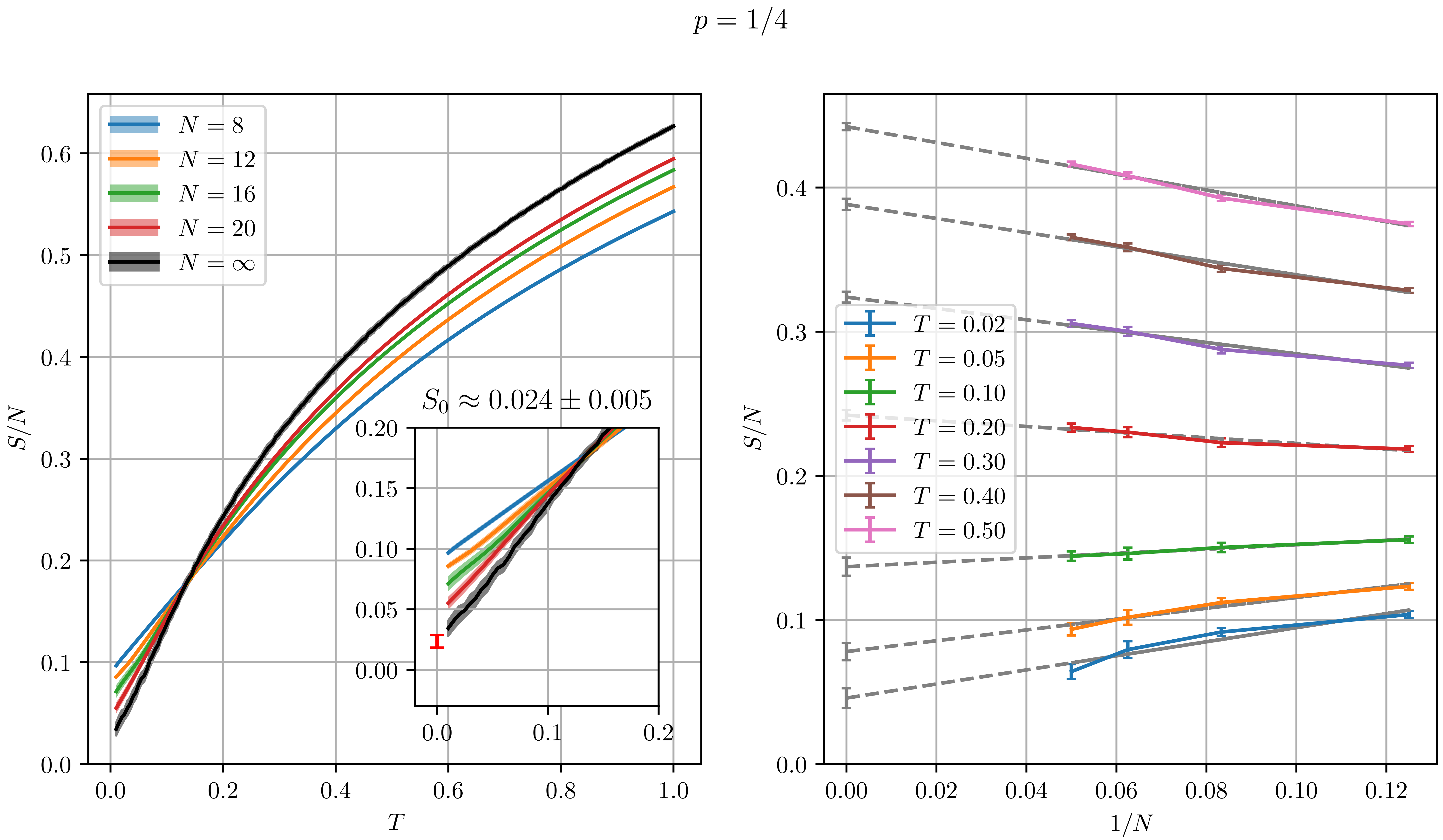

Large-N extrapolation of entropy density

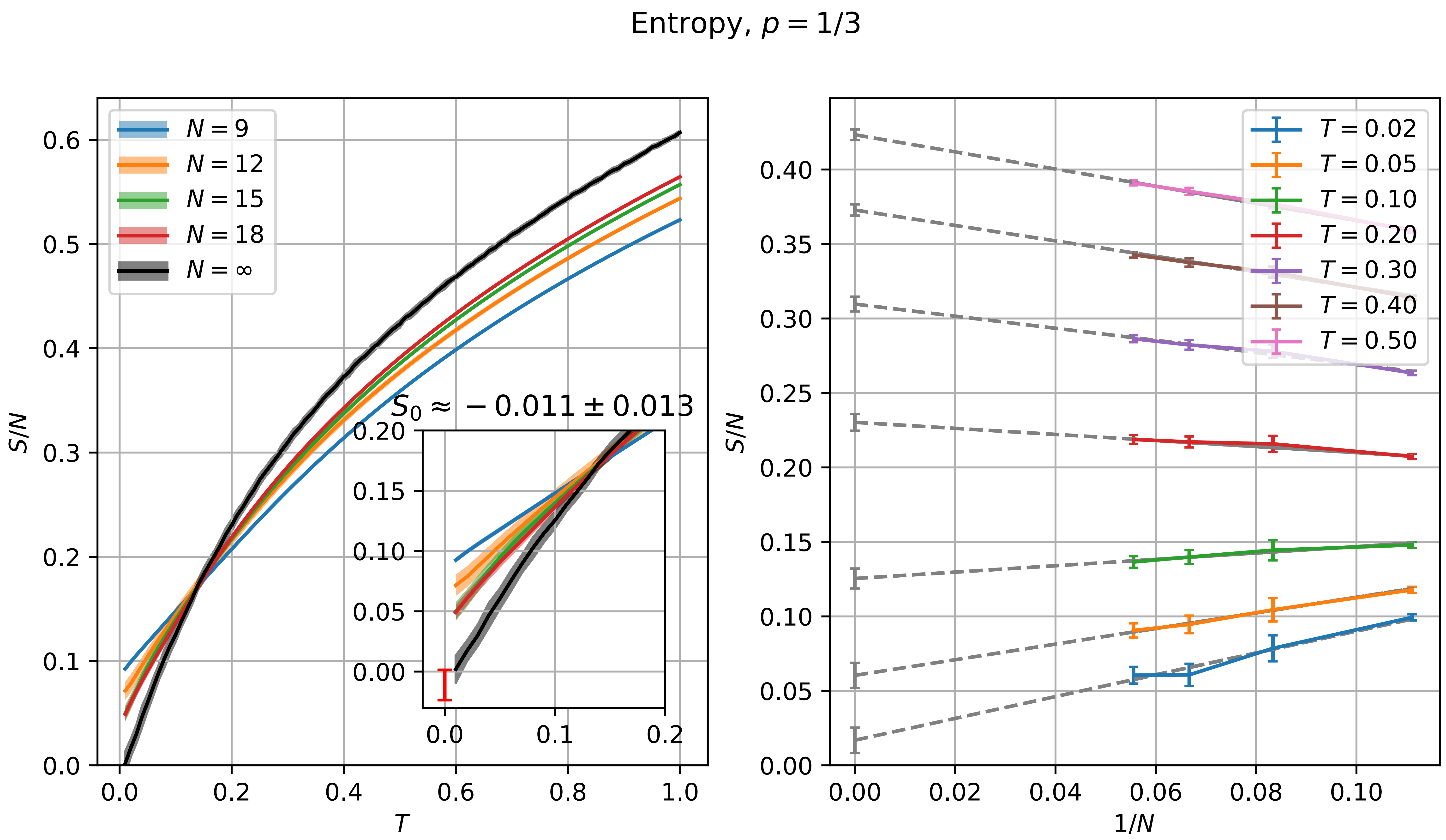

Large-N extrapolation of entropy density

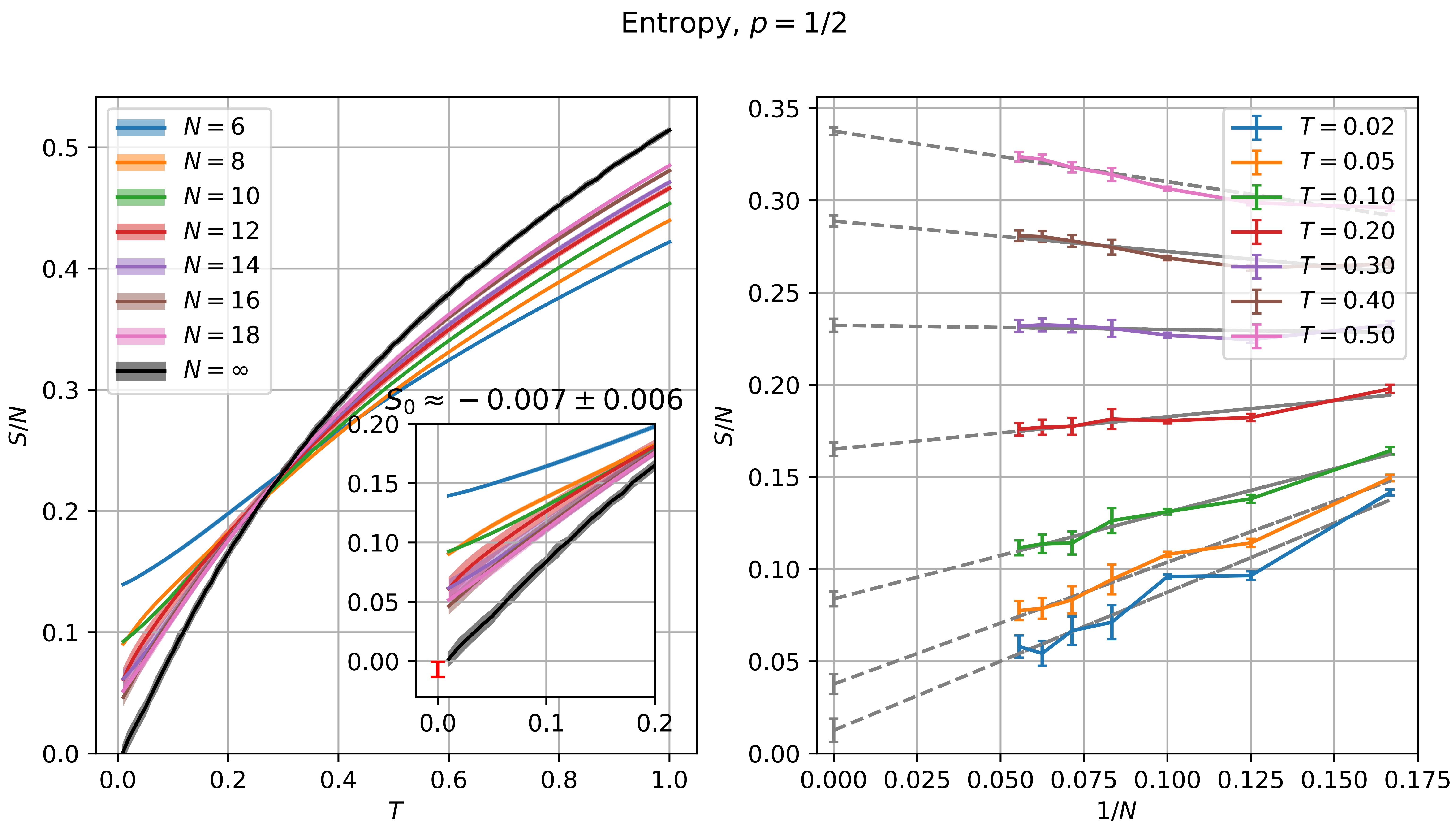

Non-zero s_0 at $p = 1/4$ is extrapolation-dependent

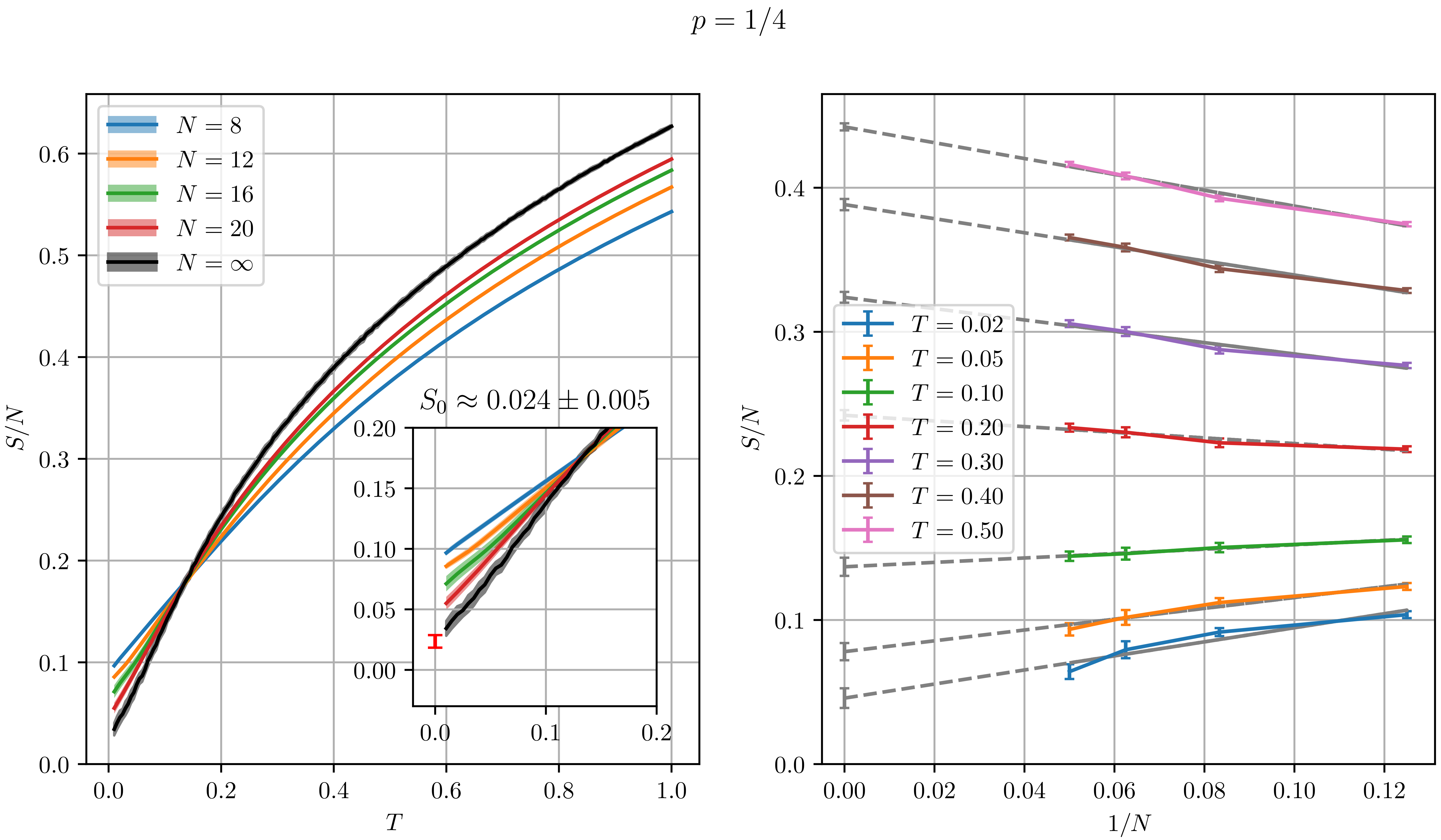

Non-zero s_0 at $p = 1/4$ is extrapolation-dependent

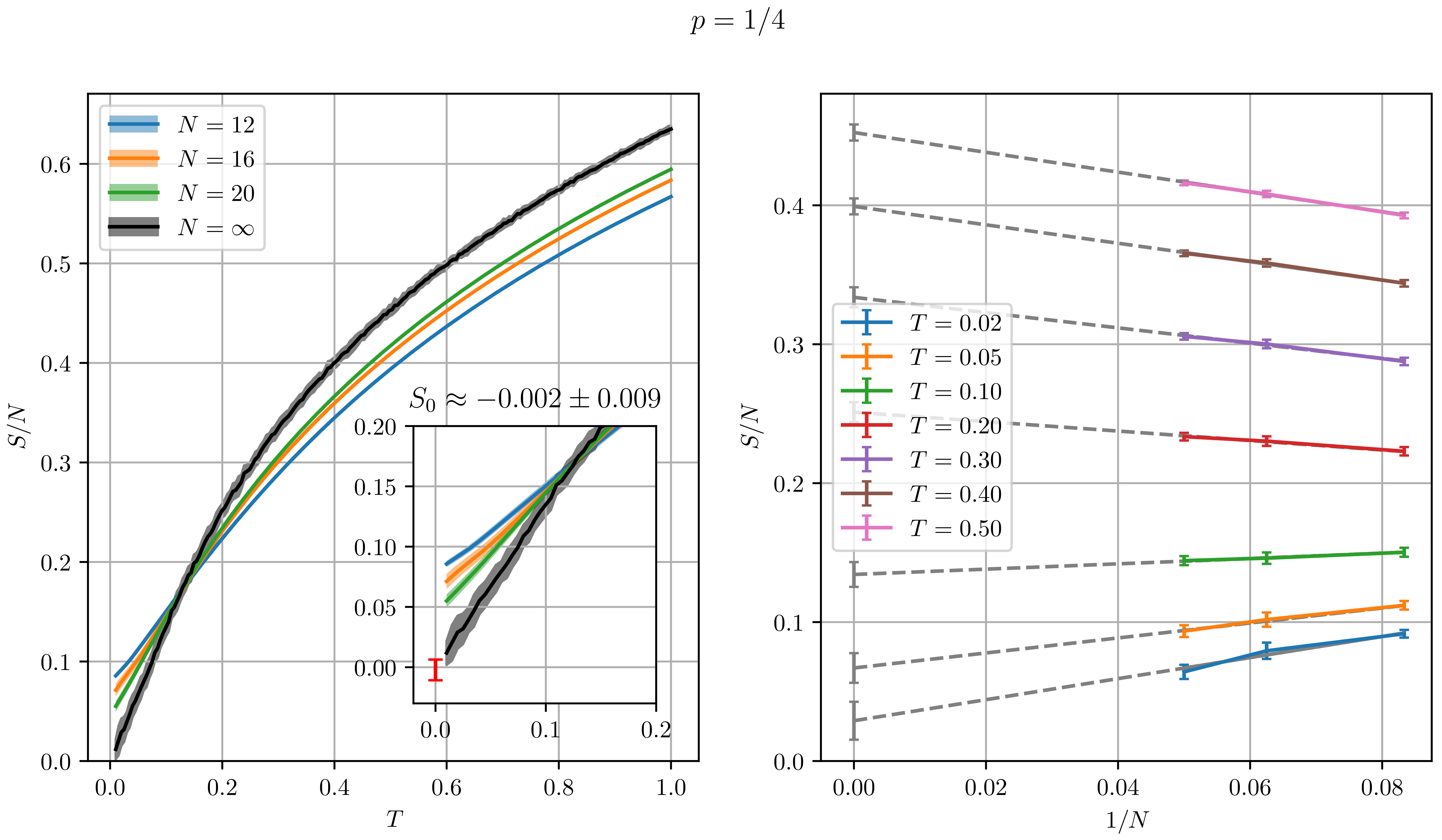

- The t-J model with random and all-to-all hopping and exchange displays a phase diagram which captures many of the key characteristics of the cuprate phase diagram.

- It has an optimal doping metal-metal transition with SYK criticality of fractionalized excitations which displays a linear-in-T resistivity.

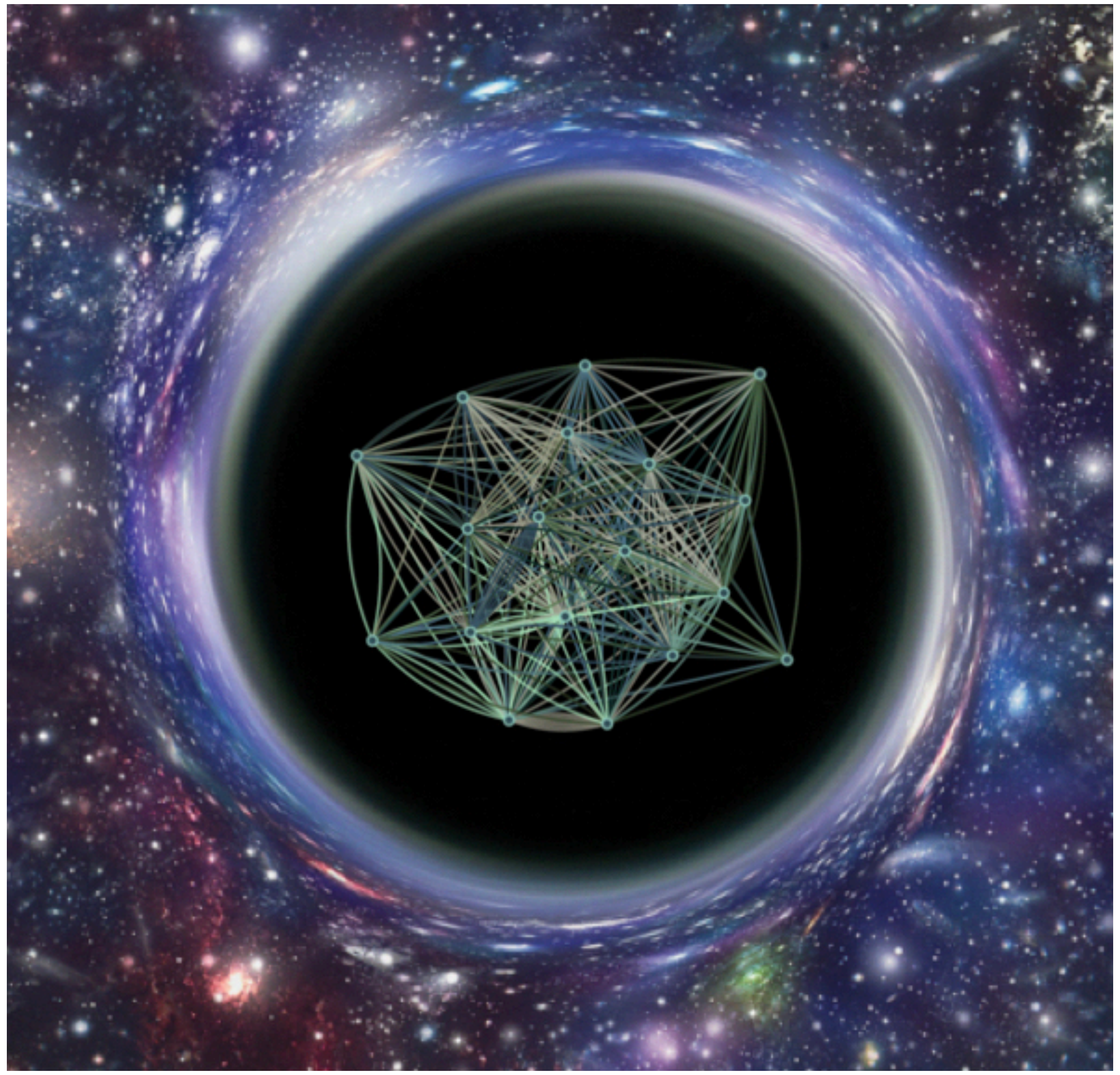

Metal-metal quantum phase transitions

The ancilla qubit approach for non-random t-J models, and the random t-J model, have in common

- A metal-metal quantum phase transition with a change in carrier density from p to $1+p$.
- Fractionalization of the electron in the critical regime
- Unexpectedly large low T entropy near the critical point (from ghost fermions, or the SYK black hole entropy).